A Generalization of Bivariate Splines Over Polygonal Partitions
and Applications

by

James M. Lanterman

(Under the Direction of Ming-Jun Lai)

Abstract

There has recently been interest in extending various finite element methods to
more arbitrary partitions, particularly unstructured partitions of various polygons.
Various methods aimed at this task have arisen, but of particular note, in a paper
published in 2016, Floater and Lai produced a method for numerical solution of Pois-
son equations using polygonal splines, which are extensions of bivariate splines. This
work first presents a method for numerical solution of partial differential equations
which extends the method of Floater and Lai to solve very general second-order ellip-
tic equations, but can also be used to approximate solutions of some mixed hyperbolic
and parabolic equations. Next, this work will address a features common to many
polygonal finite elements: a lack of global differentiability. This work provides a con-
struction of C^1 local basis functions, particularly over quadrangulations, with some
applications to function interpolation and smooth surface construction. The methods
used to construct these functions, while computationally difficult, can be extended to
higher regularity or to partitions of polygons with more vertices.

Index words: bivariate splines, partial differential equation, finite element
                 methods, local basis

A Generalization of Bivariate Splines Over Polygonal Partitions
and Applications

by

James M. Lanterman

B.S., Mercer University, 2013

A Dissertation Submitted to the Graduate Faculty

of The University of Georgia in Partial Fulfillment

of the

Requirements for the Degree

Doctor of Philosophy

Athens, Georgia

2018

A Generalization of Bivariate Splines Over Polygonal Partitions

and Applications

by

James M. Lanterman

Major Professor:	Ming-Jun Lai	
Committee:	Juan Gutierrez	
	Sa'ar Hersonsky	
	Jingzhi Tie	

Electronic Version Approved:

Suzanne Barbour
Dean of the Graduate School
The University of Georgia
May 2018

Acknowledgments

I thank my advisor Ming-Jun Lai, who has been supportive and patient, and has provided great insight and advice through the many difficulties encountered during my time in graduate school and in the development of this work. I am extremely fortunate to have had the opportunity to work under Dr. Lai's direction and to learn from him.

I thank the members of my committee for their patience and time, especially given the length of this work.

The challenges of graduate school have been difficult to say the least, but my friends have helped me through. I thank Eric Perkerson, the first friend I made in Athens, and one who has helped me on more occasions than I can count, both professionally and personally. I also thank Clay Mersmann, who has served as both a friend and a source of growth. I am lucky to have a friend and colleague with the same advisor, working in the same field, even in the same office. I especially thank my oldest friend Matt Holton, whose friendship has done more to maintain my sanity and keep up my spirits throughout graduate school than I can say.

Finally, I thank my beautiful wife Savannah. I could not have accomplished this enormous task without her constant encouragement and endless support. Despite all the challenges that graduate school has brought, you have stayed by my side and made these the best years of my life. I love you.

Contents

List of Figures

List of Tables

Chapter 1

Introduction

1.1 Motivation

The primary goal of this dissertation is to develop and apply novel generalizations of splines. Multivariate splines are a well-studied space of piecewise functions, defined over a polyhedral region of $\mathbb{R}^n$ which is partitioned into n-simplices. The results of this work will focus particularly on bivariate splines, the case in which the dimension $n = 2$.

In the bivariate case, then, splines are traditionally defined over partitions of 2-simplices; that is to say, triangulations. This dissertation aims to loosen this restriction by constructing analogous function spaces over more general partitions. This is not without motivation; oftentimes, a natural partition of a region may not be a triangulation, but perhaps a Voronoi diagram, or a grid. Moreover, this is not without precedent: in 2016, Floater and Lai [16] constructed the first polygonal splines in what might be called a "proof of concept," and they applied these functions toward numerical solutions of Poisson equations.

We'll extend on the kind of functions that Floater and Lai constructed: first, in the development of a deeper application toward numerical solutions of partial differential

equations; second, we will explore a weakness of the Floater-Lai polygonal spline construction: they are only continuous, and are not globally differentiable. We will first define the ambient space of polygonal splines of arbitrary degree d, and then, with a restriction to quadrilateral partitions, we will construct local polygonal spline basis functions whose span is contained in C^1 for a variety of degrees, along with finding some conditions which partitions must satisfy in order to allow construction of such bases.

1.2 Literature review

1.2.1 Numerical solution of PDEs

Numerical solution of partial differential equations (PDEs) is a field of mathematics which is not particularly old; many agree that the landmark paper by Courant, Friedrichs, and Lewy in 1928 [11], which specifically addressed using finite difference methods to approach some problems in mathematical physics, was the bridge between older, more traditional differential equations, which are now distinguished as ordinary differential equations (ODEs). While a variety of methods for numerical solution of PDEs have been created and studied over the past century, multivariate spline methods fall into a category known as Finite Element Methods (FEMs). A detailed and well-written history of the development of various methods for numerical solutions of PDEs can be found in an article written by Thomée (see [29]), with a more detailed study available in Evans' well-known textbook [12]. The remainder of this section is

A highly related new method for numerical solution of PDEs that has arisen in recent years is known as the Virtual Element Method (VEM), an evolution of a type of method known as the Mimetic Finite Differences (MFD). VEM was pioneered by Beirão da Veiga, Brezzi, Cangiani, Manzini, Marini, and Russo in 2013 (see [4]). VEM uses local functions spaces defined over polygons with a reasonably small number of

degrees of freedom; more than the spaces defined used in the Floater-Lai polygonal spline method (see Chapter 2 Section 2.1 of this dissertation). VEM is perhaps most interesting in that its local basis functions are never explicitly computed, and instead are defined by various degrees of freedom which allow for computation of local stiffness and mass matrices without ever needing to know the functions themselves. See [1], [4], [3], and [21] for more on VEM.

Quadratic serendipity finite elements are another related approach, with functions defined over polygons which are very similar to the Floater-Lai polygonal spline basis functions. Pioneered by Rand, Gillete, and Bajaj in 2014 (see [25]), quadratic serendipity finite elements are local functions which are based on generalized barycentric coordinates (GBCs), as are the polygonal splines which will be explored throughout this dissertation, including the Floater-Lai basis.

While not quite as closely related as the previous two methods, another recently-developed method is the Weak Galerkin method (WG), which was first introduced by Wang and Ye in 2011; see [30]. Perhaps the most noteworthy feature of this method is that the underlying finite elements are allowed to be totally discontinuous; in particular, there are separate functions defined on the boundaries and the interiors of each polygon. The Weak Galerkin method has been developed for many applications since its introduction; see [23], [22], [31].

1.2.2 Construction of differentiable functions over polygons using local basis functions

Solutions of higher-order PDEs usually must satisfy higher regularity conditions, so it is desirable to have numerical solutions which are similarly regular. From the perspective of FEMs, this means that we want to find a way to use our local basis functions to ensure some kind of regularity, or perhaps to find a more regular subspace of the local basis functions.

Another motivation for construction of more globally-differentiable local basis functions comes from geometric surface design, like aircraft and car body design, or in computer graphics. Over quadrilaterals, tensor-product B-splines are widely used to this end, but they are only defined over highly-restrictive partitions of quadrilaterals - most glaringly, the valence of every interior vertex of such a partition is exactly 4. Historically, it is difficult to manage the behavior of locally-defined functions around interior vertices with other valences, commonly known as *extraordinary points*. In computer graphics, different methods of subdivision of surfaces, most based on the well-known methods of Catmull and Clark (see [9]), are often used, as well as methods based on NURBS (non-uniform rational basis splines) or their successors, T-splines (see [8], [26], [27], [24]). Both methods, being based on subdivision, can result in meshes with many underlying patches. Of course, a minimal number of patches is preferable.

While the functions used in the aforementioned Virtual Element Method can be globally C^r for any arbitrary $r \geq 0$, recall that the basis functions themselves are not explicitly constructed. However, the quadratic serendipity finite elements can only ensure C^0 continuity, while the functions used in the Weak Galerkin method are generally not continuous at all.

Over triangulations, bivariate splines of sufficiently high degree can made be globally C^r by enforcing some constraints on its coefficients, but there are not yet any such methods established for polygonal splines; even the Floater-Lai construction is only continuous. For this reason, we aim to find various C^1 subspaces of polygonal splines in Chapters 3, 4, and 5 of this dissertation.

Chapter 2

Polygonal Spline Methods for Numerical Solution of General Second-Order Elliptic Equations

2.1 Previous results

In this chapter we extend the polygonal spline methods of Floater and Lai in [16] to solve a larger class of partial differential equations. That paper laid some foundational work, and served as proof of the viability of this type of numerical method, and focused on the solution of Poisson equations of the form

$$\begin{cases} -\Delta u = f; & \mathbf{x} \in \Omega \subset \mathbb{R}^2, \\ u = g; & \mathbf{x} \in \partial\Omega \end{cases}$$

for some polygonal region Ω.

We first give a brief overview of the Floater-Lai methods. Let us begin with the construction of what we'll call Floater-Lai polygonal splines.

2.1.1 Floater-Lai polygonal splines

Let $P = \langle v_1, v_2, ..., v_n \rangle$ be a convex n-gon for some natural number $n \geq 3$. We'll often refer to the vertices of P cyclically, so that $v_{n+j} = v_j$ for any natural number j. Any collection of n functions $\{\phi_i\}_{i=1}^n$ defined over P is called a set of *generalized barycentric coordinates* (GBCs) for P if, for all $\mathbf{x} \in P$ and $i = 1, 2, ..., n$,

$$\phi_i(\mathbf{x}) \geq 0, \ \sum_{j=1}^n \phi_j(\mathbf{x}) = 1, \text{ and } \sum_{j=1}^n v_j \phi_j(\mathbf{x}) = \mathbf{x}. \qquad (2.1.1)$$

A corollary property to those listed in (2.1.1) is that the GBCs of P are linear on its edges: where $\mathbf{x}_t = (1-t)v_j + tv_{j+1}$ for some $j \in \mathbb{N}$ and $t \in [0, 1]$,

$$\phi_i(\mathbf{x}_t) = (1-t)\phi_i(v_j) + t\phi_i(v_{j+1}). \qquad (2.1.2)$$

A variety of particular choices of GBCs can be reviewed in an excellent survey by Michael Floater; see [13]. For this work, though, we focus on perhaps the simplest-formulated and most-studied choice of GBCs, known as Wachspress coordinates.

While the usual barycentric coordinates over triangles are polynomials, Wachspress coordinates over convex polygons are generally rational functions. A variety of equivalent definitions of Wachspress coordinates have been used, but we will stick to one in this paper which is highly related to the usual definition of barycentric coordinates. First, we introduce some notation to express some geometric quantities.

For each i, denote by C_i the area of the subtriangle of P given by $\langle v_{i-1}, v_i, v_{i+1} \rangle$. Denote by $A_i(\mathbf{x})$ the signed area of the triangle $\langle \mathbf{x}, v_i, v_{i+1} \rangle$, positive for points $\mathbf{x}$ on the interior of P. Notice that, while C_i are constants for a given quadrilateral P for each i, A_i is a linear bivariate polynomial. It is worth noting that $A_i(v_{i-1}) = C_i$, $A_i(v_{i+2}) = C_{i+1}$, and $A_i(v_i) = A_i(v_{i+1}) = 0$. Both of these notations use cyclic indices, just as for the vertices. Figure 2.1 shows an illustration of C_2 and $A_3(\mathbf{x})$ for
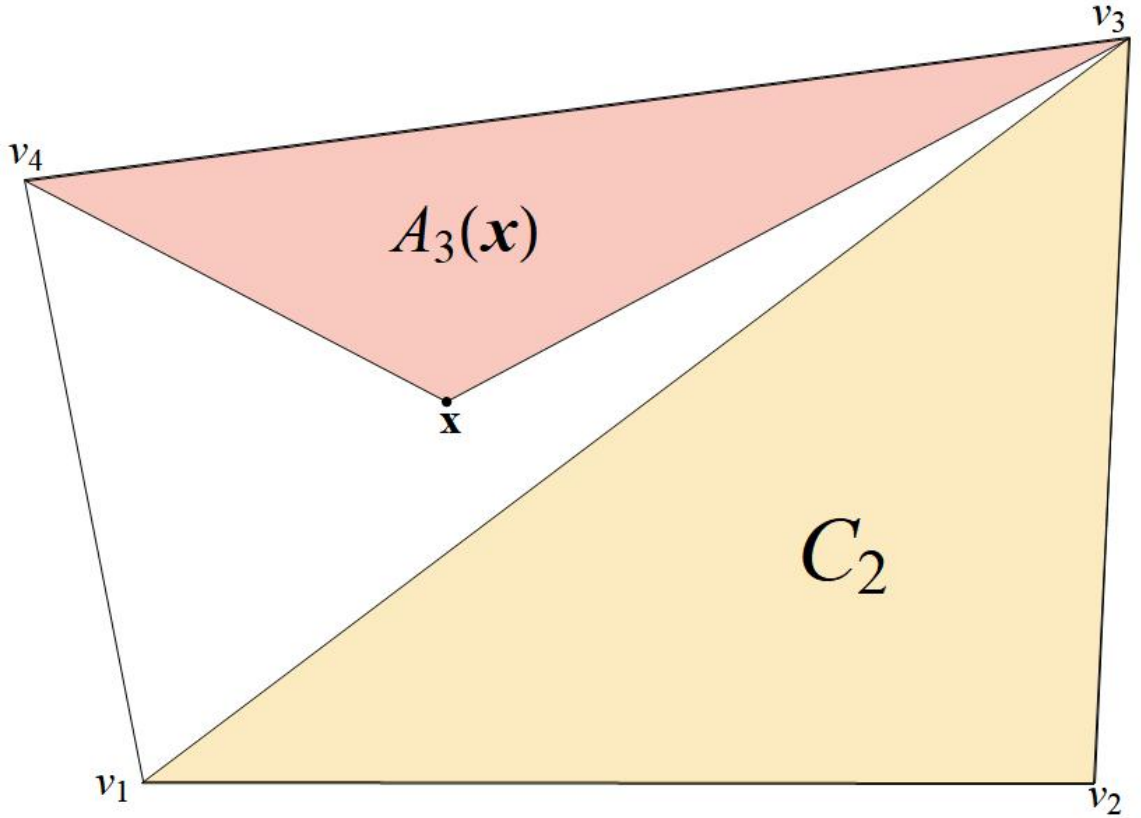
Figure 2.1: An illustration to show the areas C_2 and $A_3(\mathbf{x})$

a given quadrilateral.

Then the Wachspress coordinates of P are defined by

$$\phi_i(\mathbf{x}) = \frac{w_i(\mathbf{x})}{\sum\limits_{j=1}^{n} w_j(\mathbf{x})}, \quad \text{where} \quad w_i(\mathbf{x}) = C_i \prod_{\substack{j=1,\ldots,n \\ j \neq i, i-1}} A_j(\mathbf{x}).$$

Floater and Lai used Wachspress coordinates in the construction of spline functions over convex polygons in the same role as the usual barycentric coordinates, first by constructing Bernstein-Bézier functions. For a multi-index $\mathbf{j} = (j_1, j_2, \ldots j_n) \in \mathbb{N}_0^n$

with $|\mathbf{j}| := j_1 + ... + j_n = d \geq 0$, define

$$B_{\mathbf{j}}^{(d)}(\mathbf{x}) := \frac{d!}{j_1!...j_n!} \prod_{i=1}^{n} \phi_i^{j_i}(\mathbf{x})$$

for every point $\mathbf{x} \in P$. A function of this type is known as a degree-d Bernstein-Bézier function over P. Define a function space over P by the linear span of such functions:

$$\Phi_d(P) := \left\{ s : s(\mathbf{x}) = \sum_{|\mathbf{j}|=d} c_{\mathbf{j}} B_{\mathbf{j}}^{(d)}(\mathbf{x}) \right\}$$

where the $c_{\mathbf{j}}$ are real coefficients and $\mathbf{x} \in P$. Where Π_d is the space of polynomials of degree $\leq d$, one can directly show that $\Pi_d \subseteq \Phi_d(P)$ using (2.1.1).

It is unfortunate that, in general, the set of functions $\left\{ B_{\mathbf{j}}^{(d)} \right\}$ is not linearly independent, and hence is not a true basis for $\Phi_d(P)$. Floater and Lai constructed a basis for a subspace $\Psi_d(P) \subset \Phi_d(P)$, which is still robust enough to satisfy $\Pi_d \subset \Psi_d(P)$.

The remainder of this section will focus on the case $d = 2$: for $i = -1, 0, 1$ and $j = 1, ..., n$, denote by $\lambda_{i,j}$ the usual barycentric coordinate associated with vertex v_{i+j} with respect to the triangle $\langle v_{j-1}, v_j, v_{i+1} \rangle$, and define the $2n$ functions

$$F_i(\mathbf{x}) = \phi_i(\mathbf{x})\lambda_{i,0}(\mathbf{x}) \quad \text{and} \quad F_{i,1}(\mathbf{x}) = \phi_i(\mathbf{x})\lambda_{i,1}(\mathbf{x}) + \phi_{i+1}(\mathbf{x})\lambda_{i+1,-1}(\mathbf{x}) \qquad (2.1.3)$$

for each $i = 1, ..., n$, and let $\Psi_2(P)$ be the linear span of the functions F_i and $F_{i,1}$ over P. The reader can refer to [16] for some details which lead to the constructions of F_i and $F_{i,1}$, along with a more general construction of a basis for $\Psi_d(P)$ and a proof that $\Pi_d \subset \Psi_d(P)$, but it is clear to see that these functions are linearly independent: F_i is zero at every vertex except v_i, at which its value is 1, and $F_{i,1}$ is zero at every vertex and on every edge except the edge between v_i and v_{i+1}.

Now, for a polygonal region $\Omega \subset \mathbb{R}^2$, let $\mathcal{P}$ be a partition of Ω into convex polygons.

To divert from Floater and Lai's original notation a bit, we'll write

$$\mathcal{S}_d^{FL}(\mathcal{P}) = \left\{ s \in C^0(\Omega) : s|_P \in \Psi_d(P), \ \forall P \in \mathcal{P} \right\}.$$

We use this notation because, as we'll see in the later chapters, there are ways to construct a true basis for the full space which they've named $\Phi_d(P)$, with no need to search for a subspace. Therefore, we'll reserve the more general notation $\mathcal{S}_d(\mathcal{P})$ for

$$\mathcal{S}_d(\mathcal{P}) = \{s : s|_P \in \Phi_d(P), \ \forall P \in \mathcal{P}\}, \text{ and}$$

$$\mathcal{S}_d^r(\mathcal{P}) = \{s \in C^r(\Omega) : s|_P \in \Psi_d(P), \ \forall P \in \mathcal{P}\},$$

so $\mathcal{S}_d^{FL}(\mathcal{P}) \subseteq \mathcal{S}_d^0(\mathcal{P})$.

For a given polygon $P \in \mathcal{P}$, Floater and Lai built an alternative basis $\{L_{i,P}, L_{i,1,P}\}_{i=1}^n$ for $\Psi_2(P)$ which could be used to interpolate functions at the vertices v_i and the edge midpoints $v_{i,1} = \dfrac{v_i + v_{i+1}}{2}$ by the function $s_f \in \mathcal{S}_2^{FL}(\mathcal{P})$ defined by

$$s_f(\mathbf{x})|_P = \sum_{i=1}^n f(v_i) L_{i,P}(\mathbf{x}) + f(v_{i,1}) L_{i,1,P}(\mathbf{x}),$$

for each $P \in \mathcal{P}$. The function s_f satisfies $s_f(v_i) = f(v_i)$ and $s_f(v_{i,1}) = f(v_{i,1})$ for each vertex v_i and edge midpoint $v_{i,1}$ of each polygon $P \in \mathcal{P}$.

2.1.2 A Polygonal spline method for numerical solution of Poisson equations

We are now ready to discuss the method of numerical solution of the Poisson equation using Floater-Lai polygonal splines. We solve the weak form of the Poisson equation:

where

$$B(u, v) = \int_\Omega \nabla u \cdot \nabla v \, d\mathbf{x},$$

solve for a function $u_h \in \mathcal{S}_2^{FL}(\mathcal{P}) \cap H_0^1(\Omega)$ such that $B(u_h, v_h) = \langle f, v_h \rangle$ for all functions $v_h \in \mathcal{S}_2^{FL}(\mathcal{P}) \cap H_0^1(\Omega)$.

We mention that we can represent a spline by an ordered vector of its coefficients. Therefore, our solution will be a vector $\mathbf{c}$ which will represent a polygonal spline solution u.

The first step is to enforce continuity. Whenever two polygons share a common edge, we need that the coefficients of the 3 basis functions which are supported on the edge have the same value. Then we build a matrix H such that $H\mathbf{c} = 0$ represents this continuity condition.

Next we form mass and stiffness matrices M and K. Both of these matrices are block-diagonal; for example $M = \text{diag}(M_P, P \in \mathcal{P})$ where

$$M_{P,i,j} = \int_P \tilde{L}_i \tilde{L}_j d\mathbf{x}$$

for $L_{i,P} = \tilde{L}_{2i-1}$ and $L_{i,1,P} = \tilde{L}_{2i}$, $i = 1, ...n$. K is constructed similarly to form the stiffness matrix.

We then form the interpolatory spline s_f for the source function f, and approximate the right-hand side of the Poisson equation $\langle f, L_{i,P} \rangle$ by $\langle s_f, L_{i,P} \rangle$. Where the spline s_f can be represented by the vector of coefficients $\mathbf{c}_f$, we compute the vector $\langle s_f, L_{i,P} \rangle = M\mathbf{c}_f$.

We can use the same interpolation scheme to interpolate the boundary-value function g by a spline s_g with vector of coefficients $\mathbf{c}_g$. Denote by G the subvector of $\mathbf{c}_g$ which corresponds to coefficients of basis functions which are supported on the boundary of Ω by G. Construct a matrix B such that $B\mathbf{c}_g = G$, and enforce the condition

that $B\mathbf{c} = g$, where $\mathbf{c}$ is the solution vector.

Our goal, then, is to solve $K\mathbf{c} = M\mathbf{c}_f$ subject to the constraints $B\mathbf{c} = G$ and $H\mathbf{c} = 0$. This is solved by the constrained minimization

$$\min_{\mathbf{c}} \frac{1}{2}\mathbf{c}^T K \mathbf{c} - \mathbf{c}_f^T M \mathbf{c}; \quad H\mathbf{c} = 0, \ B\mathbf{c} = G.$$

An iterative approach to the above minimization is presented in [2]. Many numerical solutions of Poisson equations retrieved using this method are given in the paper [16]. We're now ready to go on to the original content presented in this chapter: an extension of this method to numerically solve more general second-order PDEs.

2.2 A Novel polygonal spline method for numerical solution of PDEs

2.2.1 Motivation

In this section we'll present an extension of the Floater-Lai method presented above to solve more general second-order partial differential equations, namely

$$\begin{cases} \mathcal{L}(u) = f; & \mathbf{x} \in \Omega \subset \mathbb{R}^2, \\ u = g; & \mathbf{x} \in \partial\Omega, \end{cases} \tag{2.2.1}$$

where $\mathcal{L}$ is a partial differential operator with the following form:

$$\mathcal{L}(u) := \sum_{i,j=1}^{2} \frac{\partial}{\partial x_j}\left(A_{ij}\frac{\partial}{\partial x_i}u\right) + \sum_{k=1}^{2} B_k \frac{\partial}{\partial x_k}u + Cu,$$

with $A_{ij} \in L^\infty(\Omega)$, $B_k \in L^\infty(\Omega)$, $C \in L^\infty(\Omega)$, f is a function in $L^2(\Omega)$, and $g \in L^\infty(\partial\Omega)$. These results were published in a work which I co-authored with my advisor, Ming-Jun Lai, in Approximation Theory XV: San Antonio 2016.

When the matrix $A = [A_{ij}]_{1 \leq i,j \leq 2}$ is symmetric and positive definite over Ω, the PDE in (2.2.1) is said to be elliptic. A typical PDE of this type can be given by defining the operator $\mathcal{L}$ with the following weight functions: Let

$$
\begin{bmatrix} A_{11} & A_{12} \\ A_{21} & A_{22} \end{bmatrix} = \begin{bmatrix} \epsilon + x & xy \\ xy & \epsilon + y \end{bmatrix}, \tag{2.2.2}
$$

with $\epsilon > 0$, $\mathbf{B} = (B_1, B_2) = (0,0)$, and $C = \exp(-x^2 - y^2)$. Then the corresponding PDE is elliptic in the first quadrant. Given the conditions listed above for A_{ij}, B_k, C, f, and g, we know that this type of PDE has a unique solution. See Theorem 2.2.1 in a later section.

There is a standard approach to use methods for solution of 2nd-order elliptic PDE to study hyperbolic equations, transport equations, and mixed parabolic and hyperbolic equations. Indeed, consider a singularly-perturbed elliptic PDE:

$$
-\epsilon \Delta u + (2 - y^2) D_x u + (2 - x) D_y u + (1 + (1+x)(1+y)^2) u = f, \quad (x,y) \in \Omega, \tag{2.2.3}
$$

where $\Omega = (0,1) \times (0,1)$, with $u|_{\partial \Omega} = g$, where f and g are any appropriate functions. When $\epsilon = 0$, this is a hyperbolic test problem considered in [5, 18, 19]. One can numerically solve (2.2.3) for $\epsilon > 0$ very small to approximate the solution of the hyperbolic problem with $\epsilon = 0$.

For another example, the following is a singularly perturbed advection-diffusion problem:

$$
-\epsilon \Delta u + D_x u + D_y u = f, \quad (x,y) \in \Omega = (0,1) \times (0,1), \tag{2.2.4}
$$

with $u|_{\partial \Omega} = g$, where f and g are appropriate functions. This example was studied in [19].

Yet another example: the following problem is parabolic for $y > 0$ and hyperbolic

for $y \leq 0$:

$$-\epsilon D_{yy}u + D_x u + c_1 u = 0, \quad (x, y) \in (-1, 1) \times (0, 1),$$

$$D_x u + c_2 u = 0, \quad (x, y) \in (-1, 1) \times (-1, 0], \tag{2.2.5}$$

with $u|_{\partial\Omega} = g$, for any constants $c_1 > 0$ and $c_2 > 0$. It was also studied in [19]. We can use the following general elliptic PDE to study the above problem by considering

$$-\eta D_{xx}u - \epsilon D_{yy}u + D_x u + c_1 u = f_1, \quad (x, y) \in (-1, 1) \times (0, 1),$$

$$-\eta \Delta u + D_x u + c_2 u = f_2, \quad (x, y) \in (-1, 1) \times (-1, 0], \tag{2.2.6}$$

with $u|_{\partial\Omega} = g$ and $\eta > 0$, where f_1, f_2 and g are appropriate functions. We can approximate the solution to (2.2.5) by letting $\eta > 0$ go to zero and use spline functions which are not necessarily continuous at $y = 0$.

These examples demonstrate that there is usefulness in a numerically solving the model problem (2.2.1).

2.2.2 Existence, uniqueness, and stability of solutions

We will review some sufficient conditions such that the elliptic PDE in (2.2.1) admits a unique weak solution with zero boundary condition; that is, $g = 0$ on $\partial\Omega$. Of course, it would be beneficial to find necessary conditions as well, but these can be hard to pinpoint. In particular, it must be required that the associated homogeneous PDE, where $f = g = 0$, has the unique solution $u = 0$; otherwise, when given a solution u^* of the PDE above, we would be able to build a distinct solution using $u^* + Ku$ for any constant K.

The weak formulation of this PDE is given by the following: for all $v \in H_0^1(\Omega)$,

$$\sum_{i,j=1}^{2} \int_{\Omega} A_{ij} \frac{\partial}{\partial x_i} u \frac{\partial}{\partial x_j} v + \sum_{k=1}^{2} \int_{\Omega} \left[B_k \frac{\partial}{\partial x_k} u \right] v + \int_{\Omega} Cuv = \int_{\Omega} fv \qquad (2.2.7)$$

We use the following norm and semi-norms on $H^1(\Omega)$ for convenience:

$$\|u\|_{2,\Omega} = \|u\|_{L^2(\Omega)}, \qquad\qquad |u|_{1,2,\Omega} = \|\nabla u\|_{L^2(\Omega)},$$

$$|u|_{2,2,\Omega} = |u|_{H^2(\Omega)}, \text{ and} \qquad\qquad |u|_{d+1,2,\Omega} = |u|_{H^{d+1}(\Omega)}.$$

Define by $a(u,v)$ the bilinear form in the left-hand side of the equation in (2.2.7). To find the weak solution in $H_0^1(\Omega)$, we must show that $a(u,v)$ is bounded above and coercive in order to use the Lax-Milgram theorem. Recall that the PDE in (2.2.1) is said to be *uniformly elliptic with ellipticity* α if the coefficient matrix A is symmetric and positive definite with smallest eigenvalue $\alpha > 0$ over Ω. Then we have the following theorem:

Theorem 2.2.1. *Suppose that the second order PDE in (2.2.1) is uniformly elliptic with ellipticity* $\alpha > 0$. *Let* $\beta := \|\mathbf{B}\|_{\infty,\Omega} < \infty$ *and* $C \geq \gamma > 0$. *Suppose that there exists a positive constant c such that*

$$\alpha > \frac{\beta}{2c} \text{ and } \gamma \geq \frac{c\beta}{2}. \qquad (2.2.8)$$

Then the PDE (2.2.1) has a unique weak solution u *in* $H_0^1(\Omega)$ *satisfying the weak formulation (2.2.7) for* $v \in H_0^1(\Omega)$.

Many standard finite element method textbooks provide a proof of Theorem 2.2.1; see, for example, [7] and [6].

When B_1 is a function of y and B_2 is a function of x, one can show that for all

14

$u \in H_0^1(\Omega)$,

$$\int_\Omega B_1 \left(\frac{\partial}{\partial x_1} u \right) u \; dxdy = - \int_\Omega B_1 \left(\frac{\partial}{\partial x_1} u \right) u \; dxdy$$

using integration by parts and the zero boundary condition. Thus, $\int_\Omega B_1(\frac{\partial}{\partial x_1} u) u dxdy = 0$. Similarly, $\int_\Omega B_2(\frac{\partial}{\partial x_2} u) u dxdy = 0$. Hence, the terms involving first order derivatives in $a(u, u)$ are zero and

$$a(u, u) = \int_\Omega \left[\sum_{i,j=1}^2 A_{ij} \frac{\partial}{\partial x_i} u \frac{\partial}{\partial x_j} u + Cu^2 \right] dxdy$$

$$\geq \alpha |u|_{1,2,\Omega}^2 + \gamma \|u\|_{2,\Omega}^2$$

which implies that $a(u, u)$ is coercive. Thus, we have established the following:

Corollary 2.2.1. *Suppose that the second order PDE in (2.2.1) is uniformly elliptic with ellipticity $\alpha > 0$. Suppose that B_1 is a function of y and B_2 is a function of x. If $C \geq 0$, then the PDE (2.2.1) has a unique weak solution u in $H_0^1(\Omega)$ satisfying the weak formulation (2.2.7) for $v \in H_0^1(\Omega)$.*

By applying Theorem 2.2.1 and Corollary 2.2.1, we can establish the following result:

Corollary 2.2.2. *Suppose that the second order PDE in (2.2.1) is uniformly elliptic with ellipticity $\alpha > 0$. Suppose that $B_1(x, y) = \hat{B}_1(x, y) + B_1'(y)$ and $B_2(x, y) = \hat{B}_2(x, y) + B_2'(x)$, where $B_1'(y)$ is a function of y and B_2' is a function of x. Let $\hat{\beta} := \max\{\|\hat{B}_1\|_{\infty,\Omega}, \|\hat{B}_2\|_{\infty,\Omega}\} < \infty$ and $C \geq \gamma > 0$. Suppose that there exists a positive constant c such that*

$$\alpha > \frac{\hat{\beta}}{2c} \text{ and } \gamma \geq \frac{c\hat{\beta}}{2}. \tag{2.2.9}$$

Then the PDE (2.2.1) has a unique weak solution u in $H_0^1(\Omega)$ satisfying the weak

15

formulation (2.2.7) for $v \in H_0^1(\Omega)$.

In particular, when $B_1 = B_2 \equiv 0$, the PDE in (2.2.1) has a unique weak solution according to Theorem 2.2.1 and Corollary 2.2.2. In fact, we can establish the existence, uniqueness and stability of the solution of (2.2.1) without using Lax-Milgram theorem. Indeed, in this case, it is easy to see that the weak form $a(u, v) = \langle f, v \rangle$ is the Euler-Langrange equation of the following minimization:

$$\min_{\substack{u \in H^1(\Omega) \\ u|_{\partial\Omega} = g}} J_f(u), \tag{2.2.10}$$

where $J_f(u) = \dfrac{1}{2} a(u, u) - \langle f, u \rangle$. To approximate the exact solution $u \in H^1(\Omega)$ with $u|_{\partial\Omega} = 0$, we can instead find the minimum among $u \in H_0^1(\Omega)$. To numerically solve the PDE, we can instead search for u in $S_d := H_0^1(\Omega) \cap \mathcal{S}_d^{FL}(\mathcal{P})$, where $\mathcal{S}_d^{FL}(\mathcal{P})$ is the space of degree-d Floater-Lai polygonal splines which are defined over a polygonal partition $\mathcal{P}$ of Ω as explained in the previous section. In the following analysis, we will consider the minimization (2.2.10) for $u \in S_d$.

Using a standard convex analysis, one can show

Theorem 2.2.2. *Suppose that A is symmetric and positive definite. Suppose that $B_1 = B_2 \equiv 0$. If $C \geq \gamma \geq 0$, then J_f is strongly convex with convexity coefficient μ which is independent of f; therefore J_f has a unique minimizer u_f. Hence, there exists a unique weak solution u_f satisfying (2.2.7).*

Using another standard strong-convexity argument, one can further derive the following result regarding the stability of the minimizer of J_f with respect to the source function f:

Theorem 2.2.3. *Suppose that the PDE in (2.2.1) satisfies the uniform ellipticity conditions in the hypotheses of Theorem 2.2.1. For two functions f and g, denote*

the minimizer of J_f by u_f and the minimizer of J_g by u_g. Then $||u_f - u_g||_{L^2(\Omega)} \leq \mu^{-1}||f - g||_{L^2(\Omega)}$.

2.2.3 Convergence of polygonal spline solutions

Finally we discuss convergence of the numerical solutions. The discussion is divided into two parts. The first part shows the approximation power of $\mathcal{S}_d^{FL}(\mathcal{P})$. The second part is to apply the approximation property to establish the convergence of polygonal splines to the weak solution.

Approximation power of interpolatory polygonal splines

Proving the approximation power of this space is more complicated than in the cases of finite elements and splines over triangulations due to difficulties in bounding the gradients of the Wachspress coordinates. Fortunately, it has been shown in [15] and [13] that

$$\sup_{\mathbf{x} \in P} \sum_{j=1}^{n} ||\nabla \phi_j(\mathbf{x})||_2 \leq \frac{4}{h_*}, \tag{2.2.11}$$

where h^* is the shortest perpendicular distance from any vertex of a convex polygon $P \in \mathcal{P}$ to a non-incident edge of P. To control this quantity, we'll have to assume that $\mathcal{P}$ satisfies

$$0 < \alpha_1 < \theta_{P,i} < \alpha_2 < \pi, \quad i = 1, \cdots, n(P), \forall P \in \mathcal{P} \tag{2.2.12}$$

for two given positive constants α_1 and α_2, where $\theta_{P,i}$ is the interior angle of P at its ith vertex, and $n(P)$ stands for the number of sides of P.

We shall assume that there exists a positive integer n_0 such that $n(P) \leq n_0$ for all $P \in \mathcal{P}$. For each $P \in \mathcal{P}$, let $|P|$ be the diameter of P (that is, the diameter of the smallest circle containing P) and ρ_P be the radius of the largest circle contained in P. We denote by $\kappa_P = \frac{|P|}{\rho_P}$ the shape parameter, also known as the chunkiness, of P

17

(see [20] and [7]). We define $|\mathcal{P}| := \max\limits_{P \in \mathcal{P}} |P|$; this is in contrast to the usual use of this notation to mean the longest edge in the partition $\mathcal{P}$. Where $e(P)$ is the length of the shortest edge of P, let $e(\mathcal{P}) = \min\limits_{P \in \mathcal{P}} e(P)$. Finally, we will assume that the global shape parameter $\gamma_{\mathcal{P}}$ satisfies

$$\gamma_{\mathcal{P}} = \frac{|\mathcal{P}|}{e(\mathcal{P})} \leq \gamma < \infty \tag{2.2.13}$$

for a given $\gamma > 0$.

As $\mathcal{S}_d^{FL}(\mathcal{P})$ is a space of continuous functions over Ω, we can not simply apply the Bramble-Hilbert lemma to establish the approximation property of $\mathcal{S}_d(\mathcal{P})$. Instead, we follow the ideas in [20]. For simplicity, let us focus ourselves to the case $d = 2$; the case $d \geq 3$ can be done similarly.

First we prove the following lemma:

Lemma 2.2.1. *Let P be a convex n-gon in $\mathcal{P}$. Let L_j be one of the Floater-Lai interpolatory basis functions which is supported on P. Then*

$$||L_j||_{2,P} \leq C_{n,\alpha_2,\gamma} |P| \tag{2.2.14}$$

and

$$|L_j|_{1,2,P} \leq C_{n,\alpha_1,\alpha_2,\gamma} \tag{2.2.15}$$

for two positive constants $C_{n,\alpha_2,\gamma}$ and $C_{n,\alpha_1,\alpha_2,\gamma}$.

Proof. Since the functions L_j are built from linear combinations of the functions F_k and $F_{k,1}$ given in (2.1.3), we have for some constant C_n which depends only on n

$$||L_j||_{2,P} \leq C_n \max\limits_{k=1,\dots,n} \{||F_k||_{2,P}, ||F_{k,1}||_{2,P}\}.$$

Thus we really need to bound $||F_k||_{2,P}$ and $||F_{k,1}||_{2,P}$. By the definition of F_k,

$$||F_k||_{2,P} \leq ||\phi_i\lambda_{i,0}||_{2,P} \leq ||\lambda_{i,0}||_{\infty,P}||\phi_i||_{2,P} \leq |P|||\lambda_{i,0}||_{\infty,P}$$

To estimate $||\lambda_{i,0}||_{\infty,P}$, let $h_{\perp,i}$ be the perpendicular distance from v_i to the line connecting v_{i-1} to v_{i+1}, and denote by m_i the point on this line which is a distance $h_{\perp,i}$ from v_i. Then since $\lambda_{i,0}$ is a linear function, we have $||\nabla\lambda_{i,0}||_2 = h_{\perp,i}^{-1}$.

Let $|e_{i-1}|$ be the length of the edge between v_{i-1} and v_i, and similarly define $|e_i|$. Without loss of generality, suppose that $|e_i| \leq |e_{i-1}|$. If we draw the triangle $\tau = \langle v_i, v_{i+1}, m_i \rangle$ (see Figure 2.2), we can see that $h_{\perp,i} = |e_i|\cos(\eta)$, where η is the interior angle of τ at v_i. Since $|e_i| \leq |e_{i-1}|$, we have that $\eta < \frac{1}{2}\theta_{P,i}$. By (2.2.12), $0 < \frac{1}{2}\theta_{P,i} < \frac{\pi}{2}$, so

$$\cos(\eta) \geq \cos\left(\frac{\theta_{P,i}}{2}\right) = \sqrt{\frac{1 + \cos(\theta_{P,i})}{2}} \geq \sqrt{\frac{1 + \cos(\alpha_2)}{2}} = C_{\alpha_2} \qquad (2.2.16)$$

for a constant C_{α_2} which depends on α_2.
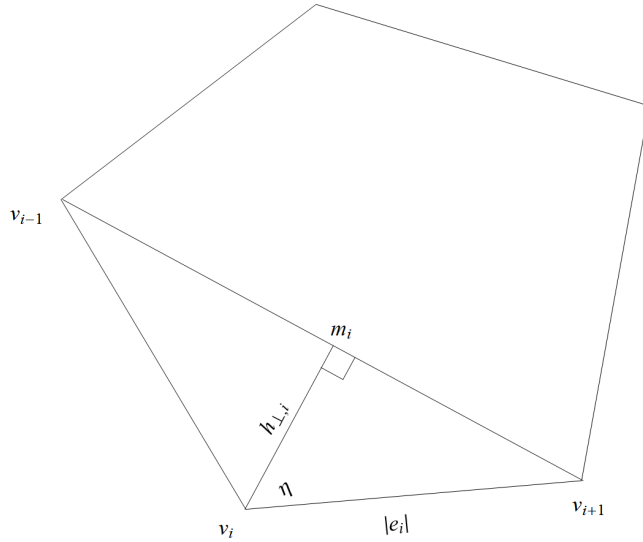
Figure 2.2: An illustration to clarify the geometry used to show (2.2.16)

19

Therefore we have that

$$h_{\perp,i} \geq C_{\alpha_2}|e_i| \geq C_{\alpha_2}e(P). \tag{2.2.17}$$

Now $||\lambda_{i,0}||_{\infty,P}$ will be achieved by $\lambda_{i,0}$ at the point in P which has the largest perpendicular distance from the line connecting v_{i-1} and v_{i+1}, which is of course a distance at most $|P|$ from this line. Since $\lambda_{i,0}$ is linear, we have that

$$||\lambda_{i,0}||_{\infty,P} \leq \frac{|P|}{h_{\perp,i}} \leq \frac{|P|}{C_{\alpha_2}e(P)} \leq C_{\alpha_2}\gamma. \tag{2.2.18}$$

Therefore we have $||F_k||_{2,P} \leq C_{n(P),\alpha_2,\gamma}|P|$. A similar argument shows that

$$||F_{k,1}||_{2,P} \leq \frac{2|P|^2}{C_{\alpha_2}e(P)} \leq C_{n,\alpha_2,\gamma}|P|,$$

which completes the proof of (2.2.14).

To prove (2.2.15), we will follow a similar strategy. As

$$|L_j|_{1,2,P} \leq C_n \max_{k=1,\ldots,n} \{|F_k|_{1,2,P}, |F_{k,1}|_{1,2,P}\},$$

we need to bound $|F_k|_{1,2,P}$ and $|F_{k,1}|_{1,2,P}$. We compute the following using (2.2.11) and (2.2.17):

$$\begin{aligned}
|F_k|_{1,2,P}^2 &= \int_P (\lambda_{i,0}D_x\phi_i + \phi_i D_x\lambda_{i,0})^2 + (\lambda_{i,0}D_y\phi_i + \phi_i D_y\lambda_{i,0})^2 \; dx \; dy \\
&\leq 2\sup_{\mathbf{x}\in P} ||\nabla\phi_i(\mathbf{x})||_2^2 \int_P \lambda_{i,0}^2 \; dx \; dy + 2\sup_{\mathbf{x}\in P} ||\nabla\lambda_{i,0}(\mathbf{x})||_2^2 \int_P \phi_i^2 \; dx \; dy \\
&\leq 2\sup_{\mathbf{x}\in P} ||\nabla\phi_i(\mathbf{x})||_2^2 (||\lambda_{i,0}||_{\infty,P}^2)|P|^2 + \frac{2}{h_{\perp,i}^2}|P|^2 \\
&\leq C_{n(P)}\sup_{\mathbf{x}\in P} ||\nabla\phi_i(\mathbf{x})||_2^2 \left(\frac{|P|}{h_{\perp,i}}\right)^2 |P|^2 + C_{n(P)}\left(\frac{|P|}{h_{\perp,i}}\right)^2 \\
&\leq C_{n(P)}\frac{16|P|^2}{h_*^2}\left(\frac{|P|}{h_{\perp,i}}\right)^2 + C_{n(P)}\left(\frac{|P|}{h_{\perp,i}}\right)^2 = C_{n(P),\alpha_2}\left(\frac{|P|}{e(P)}\right)^2 (1 + \frac{16|P|^2}{h_*^2}).
\end{aligned}$$

Now we will show that h_* is comparable to $e(P)$. In particular, since P is convex,

h_* ought to be realized by a line drawn from a vertex of P, say v_k, to an edge to an edge which is a graph-distance of 2 from v_k, say the edge between v_{k+1} and v_{k+2}. If we draw in this line (see Figure 2.3), a right triangle is formed which shows that

$$h_* = \sin\theta_{k+1}|e_k| \geq \min_{\mathbf{x}}\{\sin\alpha_1, \sin\alpha_2\}e(P). \tag{2.2.19}$$
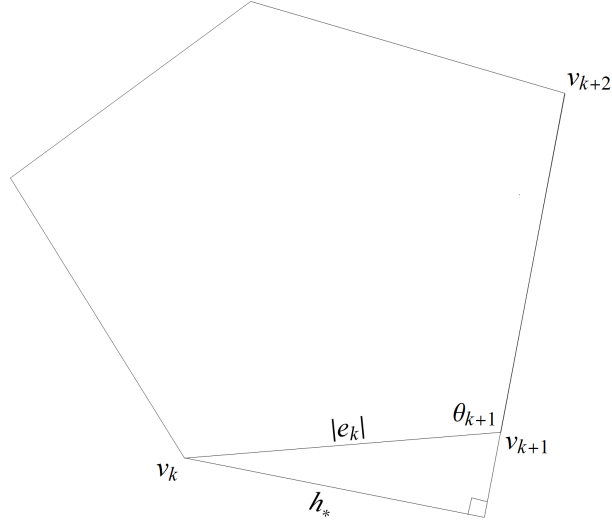
Figure 2.3: An illustration of the geometry used to show (2.2.19)

Therefore we can say

$$\sup_{\mathbf{x}\in P}||\nabla\phi_i(\mathbf{x})||_2^2 \leq \frac{16}{h_*^2} \leq \frac{C_{\alpha_1,\alpha_2}}{e(P)^2}. \tag{2.2.20}$$

Combining (2.2.20) and our above analysis shows that

$$|F_k|_{1,2,P}^2 \leq C_{n(P)}\frac{|P|^2}{e(P)^2}(1 + 16C_{\alpha_1,\alpha_2}\frac{|P|^2}{e(P)^2})$$
$$\Rightarrow |F_k|_{1,2,P} \leq C_{\alpha_1,\alpha_2}\frac{|P|}{e(P)}(1 + \frac{|P|}{e(P)})C_{\alpha_1,\alpha_2,\gamma}.$$

A similar argument will show that $|F_{k,1}|_{1,2,P} \leq C_{\alpha_1,\alpha_2,\gamma}$, so we have that $|L_j|_{1,2,P} \leq C_{n,\alpha_1,\alpha_2,\gamma}$ as desired in (2.2.15). $\qquad\square$

We are nearly ready to establish the approximation power of $\mathcal{S}_d(\mathcal{P})$. Our main

result is the following theorem:

Theorem 2.2.4. *Suppose that $\mathcal{P}$ satisfies four assumptions: $\gamma_{\mathcal{P}} \leq \gamma$, $0 < \alpha_1 \leq \theta_{P,i} \leq \alpha_2 < \pi$, $\kappa_P \leq \kappa < \infty$ and $n(\mathcal{P}) \leq n_0$. Then for any $u \in H^{d+1}(\Omega)$, there exists a polygonal spline $Q(u) \in \mathcal{S}_d(\mathcal{P})$ such that*

$$\|u - Q(u)\|_{2,\Omega} \leq C_{n_0,\alpha_1,\alpha_2,\kappa,\gamma}|\mathcal{P}|^{d+1}|u|_{d+1,2,\Omega} \tag{2.2.21}$$

and

$$|u - Q(u)|_{1,2,\Omega} \leq C_{n_0,\alpha_1,\alpha_2,\kappa,\gamma}|\mathcal{P}|^{d}|u|_{d+1,2,\Omega} \tag{2.2.22}$$

for constant $C(n_0, \alpha_1, \alpha_2, \kappa, \gamma)$ which is independent of u, but may be dependent the Lipschitz constant of the boundary of Ω if Ω is nonconvex.

We will require bit more discussion, along with another lemma, to prove this theorem. For convenience, we focus on the case $d = 2$. We will construct a quasi-interpolatory spline $Q(u) \in \mathcal{S}_2^{FL}(\mathcal{P})$.

We first extend any $u \in H^3(\Omega)$ to a function in $H^3(\mathbb{R}^2)$ with the property $\|u\|_{H^3(\mathbb{R}^2)} \leq E\|u\|_{H^3(\Omega)}$ with a positive constant E dependent only on the Lipschitz constant of the boundary of Ω (cf. [28] Chapter 6§3) and call it u again for convenience.

For each vertex v, let Ω_v be the collection of all polygons in $\mathcal{P}$ sharing the vertex v. Let B_v be largest disk contained in Ω_v if v is an interior vertex. If **v** is a boundary vertex, we let B_v be the largest disk contained in the convex hull of Ω_v. Let $F_v(u)$ be the averaged Taylor polynomial of degree 2 associated with u based in the disk B_v (cf. [20]). Define by

$$c_v(u) = F_v(u)|_v. \tag{2.2.23}$$

Let $T_v \in \Omega_v$ be a triangle with vertex v. We simply use the polynomial property $\|p\|_{\infty,T} \leq \frac{1}{\sqrt{A_T}}\|p\|_{2,T}$ for any triangle T along with the property that $\|F_v(u)\|_{2,\Omega_v} \leq$

$K_1\|u\|_{2,\Omega_v}$ (cf. [20]) to have

$$|c_v(u)| \le \|F_v(u)\|_{\infty,T_v} \le \frac{1}{\sqrt{A_{T_v}}}\|F_v(u)\|_{2,T_v} \le \frac{K_1}{\sqrt{A_{T_v}}}\|u\|_{2,\Omega_v} \tag{2.2.24}$$

for a constant K_1 independent of u and T_v.

The triangle T_v is contained within some polygon $\in \mathcal{P}$, and in particular two of its edges are edges of P; say e_1 and e_2. Then $A_{T_v} = |e_1||e_2|\sin(\theta)$ where θ is the interior angle of P at the vertex joining e_1 and e_2. Then

$$A_{T_v} \ge e(P)^2 \sin(\theta) \Rightarrow \sqrt{A_{T_v}} \ge K_2\, e(P) \ge K_2\, e(\mathcal{P})$$

for a constant K_2 depending only on α_1 and α_2, so we have

$$|c_{\mathbf{v}}(u)| \le \frac{K_1 K_2}{e(\mathcal{P})}\|u\|_{2,\Omega_{\mathbf{v}}}. \tag{2.2.25}$$

Similarly, for edges $e \in \mathcal{P}$, let Ω_e be the union of the two polygons sharing e in $\mathcal{P}$ if e is an interior edge. Let B_e be a largest disk contained in Ω_e. If e is a boundary edge, we can choose a disk B_e contained in the polygon with edge e. Then we let $F_e(u)$ be the averaged Taylor polynomial of degree d based on B_e. Choose c_e to be the value at $F_e(u)$ evaluated at the midpoint w_e of e. Choose a good triangle T_e containing w_e. Then $c_e(u)$ will satisfy a similar property in (2.2.25). Our quasi-interpolatory spline is defined by

$$Q(u) = \sum_{v \in \mathcal{P}} c_v(u)L_v + \sum_{e \in \mathcal{P}} c_e(u)L_e. \tag{2.2.26}$$

Let us show that $Q(u)$ is a bounded operator on $L^2(\Omega)$. That is,

Lemma 2.2.2. *For any $u \in L^2(\Omega)$, we have*

$$\|Q(u)\|_{2,\Omega} \le K_3\|u\|_{2,\Omega} \tag{2.2.27}$$

23

for a positive constant K_3 independent of u, depending only on $n_0, \alpha_1, \alpha_2, \gamma$, and the Lipschitz constant of the boundary of Ω. In addition, for nonnegative integers α, β with $\alpha + \beta = 1$,

$$\|D_x^\alpha D_y^\beta Q(u)\|_{2,\Omega} \leq \frac{K_4}{e(\mathcal{P})}\|u\|_{2,\Omega} \tag{2.2.28}$$

for another positive constant K_4 independent of u, depending only on the same quantities as K_3.

Proof. For each polygon $P \in \mathcal{P}$, denote by Ω_P the union of polygons which share an edge or a vertex of P. Note that $L_v|_P$ is just L_j for some j and so is $L_e|_P$. Then, we use Lemma 2.2.1 to have

$$
\begin{aligned}
\|Q(u)\|_{2,P} &= \left[\int_P |\sum_{v\in P} c_v(u)L_v + \sum_{e\in P} c_e(u)L_e|^2 dx\ dy\right]^{1/2}\\
&\leq \sum_{v\in P} |c_v(u)| \left(\int_P |L_v|^2 dx\ dy\right)^{1/2} + \sum_{e\in P} |c_e(u)| \left(\int_P |L_e|^2 dx\ dy\right)^{1/2}\\
&\leq \sum_{v\in P} \frac{K_1 K_2}{e(\mathcal{P})}\|u\|_{2,\Omega_v}\|L_v\|_{2,P} + \sum_{e\in P} \frac{K_1 K_2}{e(\mathcal{P})}\|u\|_{2,\Omega_e}\|L_e\|_{2,P}\\
&\leq C_{n(P),\alpha_1,\alpha_2,\gamma} \frac{|P|}{e(\mathcal{P})}\|u\|_{2,\Omega_P}\\
&\leq C_{n_0,\alpha_1,\alpha_2,\gamma} \frac{|\mathcal{P}|}{e(\mathcal{P})}\|u\|_{2,\Omega_P} \leq C_{n_0,\alpha_1,\alpha_2,\gamma}\|u\|_{2,\Omega_P} \tag{2.2.29}
\end{aligned}
$$

for a constant $C_{n_0,\alpha_1,\alpha_2,\gamma}$. Hence,

$$
\begin{aligned}
\|Q(u)\|_{2,\Omega}^2 &= \sum_{P\in\mathcal{P}} \|Q(u)\|_{2,P}^2 \leq C_{n_0,\alpha_1,\alpha_2,\gamma}^2 \sum_{P\in\mathcal{P}} \|u\|_{2,\Omega_P}^2\\
&\leq C_{n_0,\alpha_1,\alpha_2,\gamma}^2 \sum_{P\in\mathcal{P}} \|u\|_{2,P}^2 = C_{n_0,\alpha_1,\alpha_2,\gamma}^2\|u\|_{2,\Omega}^2, \tag{2.2.30}
\end{aligned}
$$

where we have used the fact that $\sum_{P\in\mathcal{P}} \|u\|_{2,\Omega_P}^2 \leq C_{n_0,\alpha_1} \sum_{P\in\mathcal{P}} \|u\|_{2,P}^2$ for a positive constant C_{n_0,α_1} since each polygon $q \in \mathcal{P}$, $q \in \Omega_P$ for at most $n_0 2\pi/\alpha_1$ polygons $P \in \mathcal{P}$.

Similarly, for nonnegative integers α and β such that $\alpha + \beta = 1$, we have

$$\|D_x^\alpha D_y^\beta Q(u)\|_{2,P} = \left[\int_P |\sum_{v \in P} c_v(u) D_x^\alpha D_y^\beta L_v + \sum_{e \in P} c_e(u) D_x^\alpha D_y^\beta L_e|^2 dx\ dy \right]^{1/2}$$

$$\leq \sum_{v \in P} |c_v(u)| \left(\int_P |D_x^\alpha D_y^\beta L_v|^2 \right)^{1/2} + \sum_{e \in P} |c_e(u)| \left(\int_P |D_x^\alpha D_y^\beta L_e|^2 dx\ dy \right)^{1/2}$$

$$\leq \sum_{v \in P} \frac{K_1 K_2}{e(\mathcal{P})} \|u\|_{2,\Omega_v} |L_v|_{1,2,\Omega_v} + \sum_{e \in P} \frac{K_1 K_2}{e(\mathcal{P})} \|u\|_{2,\Omega_e} |L_e|_{1,2,\Omega_e}$$

$$\leq C_{n_0,\alpha_1,\alpha_2,\gamma} \frac{\|u\|_{2,\Omega_P}}{e(\mathcal{P})}.$$

Hence, we have

$$\|D_x^\alpha D_y^\beta Q(u)\|_{2,\Omega}^2 = \sum_{P \in \mathcal{P}} \|D_x^\alpha D_y^\beta Q(u)\|_{2,P}^2$$

$$\leq C_{n_0,\alpha_2,\gamma}^2 \sum_{P \in \mathcal{P}} \|u\|_{2,\Omega_P}^2 \frac{1}{e(\mathcal{P})^2} = \frac{C_{n_0,\alpha_1,\alpha_2,\gamma}^2}{e(\mathcal{P})^2} \|u\|_{2,\Omega}^2. \quad (2.2.31)$$

By taking the square root of both sides, we finish the proof of (2.2.28). $\qquad\square$

Now we are ready to prove the main result:

Proof (of Theorem 2.2.4). For simplicity, let us consider the approximation in $L^2(\Omega)$ first. It is easy to see

$$\|u - Q(u)\|_{L^2(\Omega)}^2 = \sum_{P \in \mathcal{P}} \|u - Q(u)\|_{L^2(P)}^2$$

$$\leq 2 \sum_{P \in \mathcal{P}} \|u - F_{P,2}(u)\|_{L^2(P)}^2 + \|F_{P,2}(u) - Q(u)\|_{L^2(P)}^2, \qquad (2.2.32)$$

where $F_{P,2}(u)$ is the averaged Taylor polynomial of degree 2 associated with u based on the largest disk B_P inside P. We know from [20] that

$$\|u - F_{P,2}(u)\|_{2,P} \leq C_{\kappa_P} |P|^3 |u|_{3,2,P}. \qquad (2.2.33)$$

For $v \in P$, $F_v(F_{P,2}(u)) = F_{P,2}(u)$ and for $e \in P$, $F_e(F_{P,2}(u)) = F_{P,2}(u)$. We have $Q(F_{P,2}(u)) = F_{P,2}(u)$ and hence, by Lemma 2.2.2,

$$\|F_{P,2}(u) - Q(u)\|_{2,P} = \|Q(F_{P,2}(u) - u)\|_{2,P}$$
$$\leq K_3 \|u - F_{P,2}(u)\|_{2,\Omega_P} \leq K_3 C_{\kappa_P} |\Omega_P|^3 |u|_{3,2,\Omega_P}.$$

Combining this with (2.2.32) and (2.2.33), we have the following:

$$\|u - Q(u)\|_{2,\Omega}^2 \leq 2 \sum_{P \in \mathcal{P}} \|u - F_{P,2}(u)\|_{2,P}^2 + \|F_{P,2}(u) - Q(u)\|_{2,P}^2$$
$$\leq \sum_{P \in \mathcal{P}} C_{\kappa_P}^2 |P|^6 |u|_{3,2,P}^2 + K^2 C_{\kappa_P}^2 |\Omega_P|^6 |u|_{3,2,\Omega_P}^2$$
$$\leq K_3^2(1 + C_\kappa^2) \sum_{P \in \mathcal{P}} |\Omega_P|^6 |u|_{3,2,\Omega}^2 \leq K_3^2(1 + C_\kappa^2) |\mathcal{P}|^6 |u|_{3,2,\Omega}^2,$$

where we have noted that the number of polygons containing each vertex is bounded by $2\pi/\alpha_1$, and hence the number of polygons $P \in \mathcal{P}$ such that $P \subset \Omega_P$ is bounded by $n_0 2\pi/\alpha_1$, and that $|\Omega_P| \leq 3|\mathcal{P}|$. Therefore

$$\|u - Q(u)\|_{2,\Omega} \leq C_\kappa |\mathcal{P}|^3 |u|_{3,2,\Omega}.$$

Now we consider $|u - Q(u)|_{1,2,\Omega}$. Recall that the averaged Taylor polynomial has the property that $D_x^\alpha D_y^\beta F_{P,d}(u) = F_{P,d-\alpha-\beta}(D_x^\alpha D_y^\beta u)$, so we use Lemma 2.2.2,

particularly (2.2.28), to have

$$
|u - Q(u)|^2_{1,2,\Omega} = \sum_{\alpha+\beta=1} ||D_x^\alpha D_y^\beta(u - Q(u))||^2_{2,\Omega}
$$

$$
= \sum_{P\in\mathcal{P}} \sum_{\alpha+\beta=1} ||D_x^\alpha D_y^\beta(u - Q(u))||^2_{2,P}
$$

$$
\leq 2 \sum_{P\in\mathcal{P}} \sum_{\alpha+\beta=1} ||D_x^\alpha D_y^\beta u - F_{P,1}(D_x^\alpha D_y^\beta u)||^2_{2,P} + ||D_x^\alpha D_y^\beta(F_{P,1}(u) - Q(u))||^2_{2,P}
$$

$$
= 2 \sum_{P\in\mathcal{P}} \sum_{\alpha+\beta=1} ||D_x^\alpha D_y^\beta u - F_{P,1}(D_x^\alpha D_y^\beta u)||^2_{2,P} + \frac{K_4^2}{e(\mathcal{P})^2}||F_{P,2}(u) - u||^2_{2,\Omega_P}
$$

$$
\leq 2 \sum_{P\in\mathcal{P}} \sum_{\alpha+\beta=1} C_{\kappa_P}|P|^4|D_x^\alpha D_y^\beta u|^2_{2,2,\Omega_P} + \frac{K_4^2}{e(\mathcal{P})^2}C_{\kappa_P}|P|^6|u|^2_{3,\Omega_P}
$$

which completes the proof of (2.2.22). $\qquad\qquad\qquad\qquad\qquad\qquad\square$

Convergence of polygonal splines to weak solutions

We are now ready to prove the convergence of polygonal splines toward the weak solution of (2.2.1).

Theorem 2.2.5. *Suppose that the PDE in (2.2.1) satisfies the assumptions in Theorem 2.2.1 and $\mathcal{P}$ satisfies (2.2.13) and (2.2.12). Suppose that the weak solution u of the PDE in (2.2.1) is in $H^{d+1}(\Omega)$. Let $u_S \in S_d$ be the weak solution satisfying $a(u_S, v) = \langle f, v \rangle$ for all $v \in S_d$. Then*

$$
|u - u_S|_{1,2,\Omega} \leq K|u|_{d+1,2,\Omega}|\mathcal{P}|^d, \tag{2.2.34}
$$

where here, we denote by $|\mathcal{P}|$ is the length of the longest edge in $\mathcal{P}$, and K is a positive constant depending on $\beta, ||C||_{\infty,\Omega}, |\Omega|, \mu, n_0, \alpha_1, \alpha_2, \kappa, \gamma$, the smallest and largest eigenvalues of A, and the Lipschitz constant of the boundary of Ω.

Proof. We must prove some preliminary results in order to prove the results in this

Theorem. First, notice that in the proof of Theorem 2.2.1, we actually have

$$a(v,v) \geq \mu|v|_{1,2,\Omega}^2, \tag{2.2.35}$$

where $\mu = \alpha - \dfrac{c\beta}{2}$ for $c > 0$ such that $\gamma - \dfrac{\beta}{2c} \geq 0$. In addition, we can show that $a(u,v)$ is bounded. Indeed,

$$
\begin{aligned}
a(u,v) &= \int_\Omega \sum_{i,j=1}^2 A_{ij} \frac{\partial u}{\partial x_i} \frac{\partial v}{\partial x_j} + \int_\Omega \sum_{k=1}^2 B_k \frac{\partial u}{\partial x_k} v + \int_\Omega Cuv \\
&\leq \Lambda ||\nabla u||_{L^2} ||\nabla v||_{L^2} + \beta ||\nabla u||_{L^2} ||v||_{L^2} + ||C||_\infty ||u||_{L^2} ||v||_{L^2} \\
&\leq M_1 \left(||\nabla u||_{L^2} ||\nabla v||_{L^2} + ||\nabla u||_{L^2} ||v||_{L^2} + ||u||_{L^2} ||v||_{L^2} \right) \\
&\leq M_1 \left(|u|_{1,2,\Omega} |v|_{1,2,\Omega} + |u|_{1,2,\Omega}(K_1 |v|_{1,2,\Omega}) + (K_1 |u|_{1,2,\Omega})(K_1 |v|_{1,2,\Omega}) \right) \\
&\leq 3 \max\{M_1, M_1 K_1, M_1 K_1^2\} |u|_{1,2,\Omega} |v|_{1,2,\Omega}
\end{aligned}
$$

where $\Lambda > 0$ is the largest eigenvalue of $[A_{ij}]_{1\leq i,j\leq 2}$, $M_1 = \max\{\Lambda, \beta, ||C||_{\infty,\Omega}\}$, and K_1 is the constant given by Poincaré's inequality, which depends only on $|\Omega|$. That is,

$$a(u,v) \leq M|u|_{1,2,\Omega} |v|_{1,2,\Omega}. \tag{2.2.36}$$

for another positive constant M. By definition of weak solution, we know that for all $v \in H_0^1(\Omega)$, $a(u,v) = \langle f, v \rangle$, and for all $v \in S_d$, $a(u_S, v) = \langle f, v \rangle$. Since $S_d \subset H_0^1(\Omega)$, we can say that for all $v \in S_d$,

$$a(u - u_S, v) = 0, \quad \forall v \in S_d. \tag{2.2.37}$$

Now, define $u_{best} := \arg\min_{s \in S_d} |u - s|_{1,2,\Omega}$. Then we have

$$
\begin{aligned}
\mu|u_{best} - u_S|_{1,2,\Omega}^2 &\leq a(u_{best} - u_S, u_{best} - u_S) \\
&= a(u_{best} - u, u_{best} - u_S) \\
&\leq M|u_{best} - u|_{1,2,\Omega}\,|u_{best} - u_S|_{1,2,\Omega} \\
\Rightarrow \quad \mu|u_{best} - u_S|_{1,2,\Omega} &\leq M|u_{best} - u|_{1,2,\Omega} \\
\mu|u - u_S|_{1,2,\Omega} &\leq \mu|u - u_{best}|_{1,2,\Omega} + \mu|u_{best} - u_S|_{1,2,\Omega} \\
&\leq \mu|u - u_{best}|_{1,2,\Omega} + M|u_{best} - u|_{1,2,\Omega} \\
\Rightarrow \quad |u - u_S|_{1,2,\Omega} &\leq \frac{\mu + M}{\mu}|u - u_{best}|_{1,2,\Omega} \\
&\leq \frac{\mu + M}{\mu} C_{n_0,\alpha_1,\alpha_2,\kappa,\gamma}|u|_{d+1,2,\Omega}|\mathcal{P}|^d.
\end{aligned}
$$

This completes the proof. $\qquad\qquad\square$

We next show convergence in the L^2 norm. When Ω is a convex domain, the convergence rate $\|u - u_{best}\|_{L_2(\Omega)}$ should be optimal based on a generalization of the well-known Aubin-Nitsche technique (see [10]) for Poisson equation. That is, we have

Theorem 2.2.6. *Suppose that the conditions of Theorem 2.2.5 are satisfied, and further suppose that the underlying Lipschitz domain Ω is convex. Let u_S be the weak solution of (2.2.1). Then for $d \geq 1$,*

$$
\|u - u_S\|_{L_2(\Omega)} \leq C|\mathcal{P}|^{d+1}|u|_{d+1,2,\Omega} \tag{2.2.38}
$$

for a constant C depending on the same quantities as the constant K from Theorem 2.2.5.

Proof. For $u - u_S \in L_2(\Omega)$, we can find the weak solution $w \in H_0^1(\Omega)$ satisfying

$$
a(v, w) = \langle u - u_S, v \rangle, \quad \forall v \in H_0^1(\Omega). \tag{2.2.39}
$$

29

Indeed, let $\hat{a}(u, v) = a(v, u)$ be a new bilinear form. By using the same proof of Theorem 2.2.1, we can show $\hat{a}(u, v)$ is a bounded bilinear form and $\hat{a}(u, u)$ is coercive since $\hat{a}(u, u) = a(u, u)$. By the Lax-Milgram theorem, there exists a weak solution w satisfying (2.2.39). It is known that $w \in H^2(\Omega)$ when Ω is convex (cf. [17]) and satisfies $|w|_{2,2,\Omega} \leq C\|u - u_S\|_{L^2(\Omega)}$ for a positive constant $C > 0$ independent of u and u_S.

Thus, we use (2.2.36) and (2.2.37) with an appropriate $v \in S_d$,

$$
\begin{aligned}
\|u - u_S\|_{L_2(\Omega)}^2 &= \langle u - u_S, u - u_S \rangle = a(u - u_S, w) \\
&= a(u - u_S, w - v) \leq M|u - u_S|_{1,2,\Omega} \, |w - v|_{1,2,\Omega} \\
&\leq MK|\mathcal{P}|^d|u|_{d+1,2,\Omega}C_{n_0,\alpha_1,\alpha_2,\kappa,\gamma}|\mathcal{P}||w|_{2,2,\Omega} \\
&\leq C|\mathcal{P}|^{d+1}|u|_{d+1,2,\Omega}\|u - u_S\|_{L_2(\Omega)},
\end{aligned}
$$

where the constant K is the one in the statement of Theorem 2.2.5, and M is the one from the proof of the same Theorem; therefore the final constant C has the same dependence as K from Theorem 2.2.5.

It now follows that

$$
\|u - u_S\|_{L_2(\Omega)} \leq C|\mathcal{P}|^{d+1}|u|_{d+1,2,\Omega}
$$

for another positive constant C with the same dependence. This completes the proof. $\square$

2.2.4 Description of our numerical method

In this section we explain our implementation to numerically solve general second-order elliptic PDEs.

Our goal will be to solve for a vector of coefficients $\mathbf{u}$. We can begin in the same

place as in [16], first constructing a matrix H to determine continuity conditions by $H\mathbf{u} = 0$. We can similarly represent our boundary conditions by a linear system $B\mathbf{u} = G$.

An important difference arises from here: we will need to form a different "stiffness" matrix than in the simpler Poisson case. In particular, in $\mathbb{R}^D$, using degree d polygonal splines, the new left-hand side of the weak form of the problem can be simplified to the following:

$$\sum_{P_n \in \mathcal{P}} \sum_{k=1}^{dn} u_k \left[\sum_{i,j=1}^{D} \int_{P_n} A_{ij} \frac{\partial v}{\partial x_i} \frac{\partial L_k}{\partial x_j} + \int_{P_n} cv L_k \right]$$

where we have expressed $u \approx u_S = \sum_{k=1}^{dn} u_k L_k$ for some coefficients u_k, where L_k is an ordering of the interpolatory basis of $\mathcal{S}_d^{FL}(\mathcal{P})$ (which, when restricted to an n-gon P_n, is simply $\Psi_d(P_n)$). Similarly write $f \approx s_f = \sum_{k=1}^{dn} f_k L_k$ and notice that the right-hand side of the weak form will be equal to $\sum_{P_n \in \mathcal{P}} \sum_{k=1}^{dn} f_k \int_{P_n} v L_k$ for any $v \in \mathcal{S}_d^{FL}(\mathcal{P}) \cap H_0^1(\Omega)$. Hence, it must be true for $v = L_m$ for $m = 1, 2, ..., dn$. We can thus construct the following matrices:

$$M = [M_{P_n}]_{P_n \in \mathcal{P}}, \text{ where } M_{P_n} = (M_{P_n,p,q})_{p,q=1}^{D}, \text{ and } M_{P_n,p,q} = \int_{P_n} L_p L_q ;$$

$$\mathcal{K} = [\mathcal{K}_{P_n}]_{P_n \in \mathcal{P}}, \text{ where } \mathcal{K}_{P_n} = \sum_{i,j=1}^{D} \mathcal{K}_{P_n}^{i,j} \text{ and}$$

$$\mathcal{K}_{P_n}^{i,j} = \left(\mathcal{K}_{P_n,p,q}^{i,j}\right)_{p,q=1}^{D} \text{ where } \mathcal{K}_{P_n,p,q}^{i,j} = \int_{P_n} A_{ij} \frac{\partial L_p}{\partial x_i} \frac{\partial L_q}{\partial x_j} ;$$

$$\mathcal{M}_{P_n} = (\mathcal{M}_{P_n,p,q})_{p,q=1}^{D} \text{ where } \mathcal{M}_{P_n,p,q} = \int_{P_n} C L_p L_q ;$$

$$K = [\mathcal{K}_{P_n}]_{P_n \in \mathcal{P}} + [\mathcal{M}_{P_n}]_{P_n \in \mathcal{P}}; \quad \mathbf{u} = (u_k)_{k=1}^{D} ; \quad \mathbf{f} = (f_k)_{k=1}^{D} ;$$

where the integrals are numerically computed by first decomposing each polygon into

quadrilaterals, and then using the tensor product of the Gauss quadrature formula of high order, say order 5×5, on each quadrilateral, with some modified weights determined by the inverse of a rational bilinear map of the quadrilateral to the unit square (see [14]). This type of quadrature was used in [16] to compute the integrals associated with numerically solving Poisson equations using polygonal splines.

Then notice that we can rewrite our weak formulation as

$$K\mathbf{u} = M\mathbf{f}.$$

Our minimization in (2.2.10) can be recast in terms of polygonal splines as

$$\min_{\substack{\mathbf{u} \\ H\mathbf{u}=0, B\mathbf{u}=\mathbf{g}}} \frac{1}{2}\mathbf{u}^T K\mathbf{u} - \mathbf{f}^T M\mathbf{u}$$

which is a constrained minimization problem which can be solved using the iterative method described in [2]. We have implemented the computational scheme in MATLAB and experimented with many second order elliptic PDEs. Some numerical results will be shown in the next section. Some of these results also involve first derivatives; these are implemented as another stiffness matrix added to K: first we define

$$\mathcal{J}_{P_n} = \sum_{k=1}^{2} \mathcal{J}_{P_n}^k$$

where $\mathcal{J}_{P_n}^k = \left(\mathcal{J}_{P_n,p,q}^k\right)_{p,q=1}^{D}$ and $\mathcal{J}_{P_n,p,q}^k = \int_{P_n} B_k L_p \frac{\partial L_q}{\partial x_k}$, where B_k is the appropriate coefficient function. Then we instead use $K = [\mathcal{K}_{P_n}]_{P_n \in \mathcal{P}} + [\mathcal{J}_{P_n}]_{P_n \in \mathcal{P}} + [\mathcal{M}_{P_n}]_{P_n \in \mathcal{P}}$.

It is worth mentioning that other finite element methods accommodate continuity conditions directly rather than solving a linear system, which saves computational power and time. However, our approach is designed conveniently to implement more complex continuity conditions; see Example 2.2.6.

2.2.5 Numerical results of our method on elliptic PDEs

In all the following examples, we denote by u_S the spline solution, and by u the exact solution. To approximate the L^2 error, we report the root mean squared (RMS) error $E_{RMS} = ||u - u_S||_{RMS}$ of the spline solution based on 1001×1001 equally-spaced points over Ω. Since $\nabla(u - u_S) = \left(\frac{\partial}{\partial x}(u - u_S), \frac{\partial}{\partial y}(u - u_S) \right)$, we report the RMS error $\nabla E_{RMS} = ||\nabla(u - u_S)||_{RMS}$, which is the average of the RMS error of $\frac{\partial}{\partial x}(u - u_S)$ and $\frac{\partial}{\partial y}(u - u_S)$. We also report the mesh size (that is, the longest edge length) of the partition at each iteration, and the computed rate of convergence in reference to the mesh size - in light of Theorems 2.2.5 and 2.2.6, we expect the rates to be 4 for degree 3 in the L^2 norm, 3 for degree 2 in the L^2 norm and degree 3 in the H^1 norm, and 2 for degree 2 in the H^1 norm.

Let us begin with numerical solutions of some standard second-order elliptic PDEs.

Example 2.2.1. We return to example (2.2.2) on the unit square $\Omega = (0,1) \times (0,1)$ to demonstrate convergence of the method. We'll set $\epsilon = 10^{-5}$ and choose f and g so that

$$u(x,y) = \frac{(1+x)^2}{4} \sin(2\pi xy) \tag{2.2.40}$$

is the exact solution. We use the polygonal partition shown in Figure 2.4.

We employ our polygonal spline method to solve (2.2.1) with exact solution in (2.2.40). Our numerical results are shown below in Tables 2.1 and 2.2.

The numerical results in Tables 2.1 and 2.2 show that the polygonal spline method works very well. We compare with the solution retrieved using degree-2 and degree-3 bivariate splines over a triangulation of the same domain. We chose a grid-based initial triangulation with close to the same number of elements as our initial polygonal partition; see these results in Tables 2.3 and 2.4.
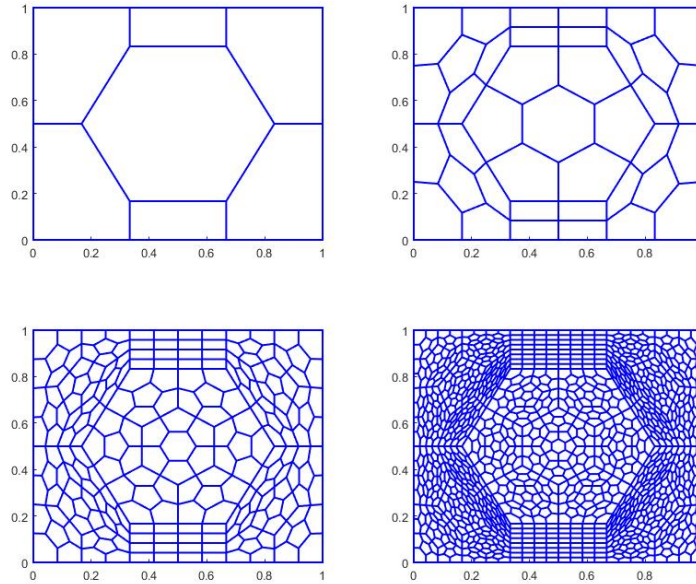
Figure 2.4: A partition of the unit square and a few refinements

Table 2.1: Degree-2 Polygonal spline approximation of solution to Example 2.2.1 with exact solution in (2.2.40)

# P	mesh	E_{RMS}	rate	∇E_{RMS}	rate
39	2.50e-01	5.47e-03	0.00	1.34e-01	0.00
219	1.25e-01	4.16e-04	3.72	2.60e-02	2.36
1251	6.25e-02	3.68e-05	3.50	5.17e-03	2.33
7251	3.13e-02	3.29e-06	3.48	1.03e-03	2.33

Table 2.2: Degree-3 Polygonal spline approximation of solution to Example 2.2.1 with exact solution in (2.2.40)

# P	mesh	E_{RMS}	rate	∇E_{RMS}	rate
39	2.50e-01	9.01e-04	0.00	1.61e-02	0.00
219	1.25e-01	2.74e-05	5.04	1.41e-03	3.52
1251	6.25e-02	1.25e-06	4.45	1.31e-04	3.43
7251	3.13e-02	6.92e-08	4.18	1.22e-05	3.43

Table 2.3: Degree-2 Bivariate spline approximation of solution to (2.2.1) with exact solution in (2.2.40)

# T	mesh	E_{RMS}	rate	∇E_{RMS}	rate
40	3.54e-01	6.94e-03	0.00	2.09e-01	0.00
160	1.77e-01	8.29e-04	3.06	5.38e-02	1.96
640	8.84e-02	1.00e-04	3.05	1.34e-02	2.00
2560	4.42e-02	1.22e-05	3.03	3.32e-03	2.01

Table 2.4: Degree-3 Bivariate spline approximation of solution to (2.2.1) with exact solution in (2.2.40)

# T	mesh	E_{RMS}	rate	∇E_{RMS}	rate
40	3.54e-01	7.16e-04	0.00	3.15e-02	0.00
160	1.77e-01	4.43e-05	4.01	3.96e-03	2.99
640	8.84e-02	5.33e-06	3.06	4.96e-04	3.00
2560	4.42e-02	5.52e-06	-0.05	7.22e-05	2.78

From Tables 2.1, 2.2, 2.3, and 2.4, we can see that polygonal splines can produce a more accurate solution on polygonal partitions containing a similar number of polygons as a triangulation of the same domain.

It is worth noting the difference in degrees of freedom in this example. In particular, the polygonal splines have significantly more degrees of freedom than each iteration of triangular spline. However, this doesn't seem representative in general, and is simply an artifact of the convenient triangulation we chose for our numerical trials. For example, one could imagine retrieving a triangulation from a polygonal partition by adding some diagonals to triangulate each polygon; however, this would substantially increase the number of degrees of freedom in this case. Regardless, there is no doubt that our polygonal spline methods are more numerically taxing than traditional bivariate spline methods. At each iteration we have the following numbers of degrees of freedom:

Table 2.5: Polygonal splines' degrees of freedom

# P	DoF ($d = 2$)	DoF ($d = 3$)
39	179	313
219	886	1657
1251	4958	9313
7251	28654	53857

Table 2.6: Bivariate splines' degrees of freedom

# T	DoF ($d = 2$)	DoF ($d = 3$)
40	97	205
160	353	769
640	1345	2977
2560	5249	11713

As we'll use the same partitions for each example in this paper, the reader can refer back to these tables.

Example 2.2.2. Here is another example of an elliptic second order PDE: let

$$\begin{bmatrix} A_{11} & A_{12} \\ A_{21} & A_{22} \end{bmatrix} = \begin{bmatrix} 1 + \epsilon & 1 \\ 1 & 1 + \epsilon \end{bmatrix}$$

for some $\epsilon > 0$, and let $C = 1$, and solve the PDE given by

$$-\sum_{i,j=1}^{2} \frac{\partial}{\partial x_j}\left(A_{ij}\frac{\partial u}{\partial x_i}\right) + \frac{\partial u}{\partial x_1} + \frac{\partial u}{\partial x_2} + Cu = \quad f \text{ in } \Omega;$$

$$u = \quad g \text{ on } \partial\Omega. \tag{2.2.41}$$

To test our method, we choose f and g so that

$$u = (1 + x^2 + y^2)^{-1} \tag{2.2.42}$$

is the exact solution.

According to Corollary 2.2.1, this elliptic PDE has a unique weak solution. In fact, we can even use $\epsilon = 0$, which makes this PDE non-elliptic, and still produce good solutions. We use the same partition as in Example 2.2.1 to solve this PDE. Tables 2.7 and 2.8 show the results of our minimization, using the non-elliptic condition $\epsilon = 0$:

Table 2.7: Degree-2 Polygonal spline approximation of solution to Example 2.2.2 with exact solution (2.2.42)

Table 2.8: Degree-3 Polygonal spline approximation of solution to Example 2.2.2 with exact solution (2.2.42)

# P	mesh	E_{RMS}	rate	∇E_{RMS}	rate
39	2.50e-01	1.30e-04	0.00	3.82e-03	0.00
219	1.25e-01	1.08e-05	3.59	7.47e-04	2.35
1251	6.25e-02	1.09e-06	3.30	1.54e-04	2.28
7251	3.13e-02	1.57e-07	2.80	3.40e-05	2.18

# P	mesh	E_{RMS}	rate	∇E_{RMS}	rate
39	2.50e-01	7.64e-06	0.00	2.41e-04	0.00
219	1.25e-01	3.70e-07	4.37	2.41e-05	3.32
1251	6.25e-02	1.99e-08	4.21	2.36e-06	3.35
7251	3.13e-02	1.25e-09	4.00	2.41e-07	3.29

Similarly, the minimization (2.2.10) with first-order derivatives based on bivariate splines can also produce good numerical results. For comparison, Tables 2.9 and 2.10 tabulate the results of the same computation using bivariate splines of degree 2 and degree 3 over grid-based right triangulations of the same domain.

Table 2.9: Degree-2 Bivariate spline approximation of solution to Example 2.2.2 with exact solution in (2.2.42)

# T	mesh	E_{RMS}	rate	∇E_{RMS}	rate
40	3.54e-01	4.80e-04	0.00	1.14e-02	0.00
160	1.77e-01	5.23e-05	3.20	2.70e-03	2.07
640	8.84e-02	6.21e-06	3.07	7.14e-04	1.92
2560	4.42e-02	8.53e-07	2.86	2.29e-04	1.64

Table 2.10: Degree-3 Bivariate spline approximation of solution to Example 2.2.2 with exact solution in (2.2.42)

# T	mesh	E_{RMS}	rate	∇E_{RMS}	rate
40	3.54e-01	2.43e-05	0.00	9.87e-04	0.00
160	1.77e-01	1.81e-06	3.75	1.44e-04	2.77
640	8.84e-02	1.29e-07	3.81	2.01e-05	2.84
2560	4.42e-02	9.69e-09	3.74	2.97e-06	2.76

2.2.6 Numerical results of our method on parabolic and hyperbolic PDEs

Example 2.2.3. We return again to example (2.2.2) on the unit square $\Omega = (0, 1) \times (0, 1)$, but this time with $\epsilon = 0$. We'll choose f and g so that

$$u(x, y) = \frac{(1 + x)^2}{4} \sin(2\pi x y) \tag{2.2.43}$$

is the exact solution. Notice that, in this case, the PDE is not elliptic. However, our method still approximates the true solution quite well. We'll show the convergence of our approximations for decreasing values of ϵ; see Tables 2.11, 2.12, 2.13, 2.14, 2.15, and 2.16.

For comparison, we'll also show the results of the same PDE using bivariate splines over a triangulation of the same domain instead; see Tables 2.17, 2.18, 2.19, 2.20, 2.21, and 2.22. These numerical results show that the polygonal spline method is efficient in approximating the solutions of non-elliptic PDEs.

Table 2.11: Degree-2 Polygonal spline approximation of solution to Example 2.2.3 with exact solution in (2.2.43) and $\epsilon = 10^{-3}$

# P	mesh	E_{RMS}	rate	∇E_{RMS}	rate
39	2.50e-01	5.27e-03	0.00	1.33e-01	0.00
219	1.25e-01	6.41e-04	3.04	2.61e-02	2.35
1251	6.25e-02	5.54e-04	0.21	6.14e-03	2.09
7251	3.13e-02	5.56e-04	-0.00	3.71e-03	0.73

Table 2.12: Degree-3 Polygonal spline approximation of solution to Example 2.2.3 with exact solution in (2.2.43) and $\epsilon = 10^{-3}$

# P	mesh	E_{RMS}	rate	∇E_{RMS}	rate
39	2.50e-01	1.39e-03	0.00	1.71e-02	0.00
219	1.25e-01	5.71e-04	1.29	3.70e-03	2.21
1251	6.25e-02	5.56e-04	0.04	3.55e-03	0.06
7251	3.13e-02	5.56e-04	-0.00	3.65e-03	-0.04

Table 2.13: Degree-2 Polygonal spline approximation of solution to Example 2.2.3 with exact solution in (2.2.43) and $\epsilon = 10^{-5}$

# P	mesh	E_{RMS}	rate	∇E_{RMS}	rate
39	2.50e-01	5.47e-03	0.00	1.34e-01	0.00
219	1.25e-01	4.15e-04	3.72	2.60e-02	2.36
1251	6.25e-02	3.69e-05	3.49	5.17e-03	2.33
7251	3.13e-02	6.45e-06	2.52	1.03e-03	2.33

Table 2.14: Degree-3 Polygonal spline approximation of solution to Example 2.2.3 with exact solution in (2.2.43) and $\epsilon = 10^{-5}$

# P	mesh	E_{RMS}	rate	∇E_{RMS}	rate
39	2.50e-01	9.06e-04	0.00	1.61e-02	0.00
219	1.25e-01	3.11e-05	4.86	1.41e-03	3.52
1251	6.25e-02	6.10e-06	2.35	1.37e-04	3.37
7251	3.13e-02	5.62e-06	0.12	4.29e-05	1.67

Table 2.15: Degree-2 Polygonal spline approximation of solution to Example 2.2.3 with exact solution in (2.2.43) and $\epsilon = 10^{-10}$

# P	mesh	E_{RMS}	rate	∇E_{RMS}	rate
39	2.50e-01	5.47e-03	0.00	1.34e-01	0.00
219	1.25e-01	4.16e-04	3.72	2.60e-02	2.36
1251	6.25e-02	3.68e-05	3.50	5.17e-03	2.33
7251	3.13e-02	3.29e-06	3.48	1.03e-03	2.33

Table 2.16: Degree-3 Polygonal spline approximation of solution to Example 2.2.3 with exact solution in (2.2.43) and $\epsilon = 10^{-10}$

# P	mesh	E_{RMS}	rate	∇E_{RMS}	rate
39	2.50e-01	9.01e-04	0.00	1.61e-02	0.00
219	1.25e-01	2.74e-05	5.04	1.41e-03	3.52
1251	6.25e-02	1.25e-06	4.45	1.31e-04	3.43
7251	3.13e-02	6.92e-08	4.18	1.22e-05	3.43

Table 2.17: Degree-2 Bivariate spline approximation of solution to Example 2.2.3 with exact solution in (2.2.43) and $\epsilon = 10^{-3}$

# T	mesh	E_{RMS}	rate	∇E_{RMS}	rate
40	3.54e-01	6.91e-03	0.00	2.09e-01	0.00
160	1.77e-01	9.63e-04	2.84	5.38e-02	1.96
640	8.84e-02	5.55e-04	0.80	1.37e-02	1.97
2560	4.42e-02	5.53e-04	0.00	4.68e-03	1.55

Table 2.18: Degree-3 Bivariate spline approximation of solution to Example 2.2.3 with exact solution in (2.2.43) and $\epsilon = 10^{-3}$

# T	mesh	E_{RMS}	rate	∇E_{RMS}	rate
40	3.54e-01	7.40e-04	0.00	3.14e-02	0.00
160	1.77e-01	5.37e-04	0.46	4.99e-03	2.66
640	8.84e-02	5.52e-04	-0.04	3.36e-03	0.57
2560	4.42e-02	5.55e-04	-0.01	3.60e-03	-0.10

Table 2.19: Degree-2 Bivariate spline approximation of solution to Example 2.2.3 with exact solution in (2.2.43) and $\epsilon = 10^{-5}$

# T	mesh	E_{RMS}	rate	∇E_{RMS}	rate
40	3.54e-01	6.94e-03	0.00	2.09e-01	0.00
160	1.77e-01	8.29e-04	3.06	5.38e-02	1.96
640	8.84e-02	1.00e-04	3.05	1.34e-02	2.00
2560	4.42e-02	1.32e-05	2.92	3.32e-03	2.01

Table 2.20: Degree-3 Bivariate spline approximation of solution to Example 2.2.3 with exact solution in (2.2.43) and $\epsilon = 10^{-5}$

# T	mesh	E_{RMS}	rate	∇E_{RMS}	rate
40	3.54e-01	7.16e-04	0.00	3.15e-02	0.00
160	1.77e-01	4.43e-05	4.01	3.96e-03	2.99
640	8.84e-02	5.33e-06	3.06	4.96e-04	3.00
2560	4.42e-02	5.52e-06	-0.05	7.22e-05	2.78

Table 2.21: Degree-2 Bivariate spline approximation of solution to Example 2.2.3 with exact solution in (2.2.43) and $\epsilon = 10^{-10}$

# T	mesh	E_{RMS}	rate	∇E_{RMS}	rate
40	3.54e-01	6.94e-03	0.00	2.09e-01	0.00
160	1.77e-01	8.29e-04	3.06	5.38e-02	1.96
640	8.84e-02	1.00e-04	3.05	1.34e-02	2.00
2560	4.42e-02	1.22e-05	3.03	3.32e-03	2.01

Table 2.22: Degree-3 Bivariate spline approximation of solution to Example 2.2.3 with exact solution in (2.2.43) and $\epsilon = 10^{-10}$

# T	mesh	E_{RMS}	rate	∇E_{RMS}	rate
40	3.54e-01	7.18e-04	0.00	3.15e-02	0.00
160	1.77e-01	4.59e-05	3.97	3.96e-03	2.99
640	8.84e-02	2.93e-06	3.97	4.95e-04	3.00
2560	4.42e-02	1.85e-07	3.98	6.19e-05	3.00

Example 2.2.4. Let

$$\begin{bmatrix} A_{11} & A_{12} \\ A_{21} & A_{22} \end{bmatrix} = \begin{bmatrix} xy & 0 \\ 0 & xy \end{bmatrix}$$

and $C = 0$. Choose f and g so that

$$u = x(1-x)y(1-y) \qquad (2.2.44)$$

is the exact solution. This was studied in [23]. As in Example 2.2.3, this is a "nearly-elliptic" PDE, but with some degeneracy at the origin. We shall use a different partition of the unit square this time, simply using a uniform grid of squares, as was the case in the original paper [23]. The Weak Galerkin method presented in this paper retrieved the following results:

Table 2.23: Weak Galerkin approximation of solution to Example 2.2.4

# Poly's	mesh	$||u - u_{WG}||_{L^2}$	rate	$||\nabla u - \nabla u_{WG}||_{H^1}$	rate
64	1.25e-01	1.46e-03	0.00	2.52e-02	0.00
256	6.25e-02	3.74e-04	1.96	1.23e-02	9.98e-01
1024	3.13e-02	9.47e-05	1.98	6.31e-03	9.98e-01
4096	1.56e-02	2.39e-05	1.99	3.16e-03	9.98e-01

We use our method with polygonal splines to solve the PDE above and find that our method can produce much better results.

Table 2.24: Degree-2 Polygonal spline approximation of solution to Example 2.2.4

# P	mesh	E_{RMS}	rate	∇E_{RMS}	rate
64	1.25e-01	1.83e-06	0.00	1.39e-04	0.00
256	6.25e-02	9.85e-08	4.22	1.60e-05	3.12
1024	3.13e-02	5.65e-09	4.12	1.91e-06	3.07
4096	1.56e-02	3.42e-10	4.05	2.33e-07	3.04

Table 2.25: Degree-3 Polygonal spline approximation of solution to Example 2.2.4

# P	mesh	E_{RMS}	rate	∇E_{RMS}	rate
64	2.50e-01	3.59e-12	0.00	5.63e-11	0.00
256	1.25e-01	1.40e-11	-1.96	2.07e-10	-1.88
1024	6.25e-02	2.34e-11	-0.74	2.71e-10	-0.39
4096	3.13e-02	4.47e-11	-0.93	5.61e-10	-1.05

Comparison of Tables 2.23, 2.24, and 2.25 shows that our polygonal spline method

produces a much more accurate solution. These results call for some remarks. First, it is worth pointing out that our MATLAB code can only achieve 1e-11 accuracy. In Table 2.25, the rates of convergence become negative due to round-off errors. That is, polygonal splines of degree-3 converged to the solution *virtually instantly*. Similarly, the degree-2 splines also appear to have an increased order of convergence $O(h^4)$. Of course, we are interested in why the convergence rate of polygonal splines is often better than triangular splines. Although we know that the degree-2 GBC functions contain more than quadratic polynomials and the degree-3 GBC functions contain more than cubic polynomials, our investigation shows that the partition also plays a significant role. If we run a few iterations to solve the same problem over the unit square based on the partition from Example 2, we retrieve the following standard convergence results:

Table 2.26: Degree-2 Polygonal spline approximation of solution to Example 2.2.4 over non-grid partition

# P	mesh	E_{RMS}	rate	∇E_{RMS}	rate
39	2.50e-01	3.66e-05	0.00	1.19e-03	0.00
219	1.25e-01	3.09e-06	3.57	2.29e-04	2.38
1251	6.25e-02	2.75e-07	3.49	4.59e-05	2.32

Table 2.27: Degree-3 Polygonal spline approximation of solution to Example 2.2.4 over non-grid partition

# P	mesh	E_{RMS}	rate	∇E_{RMS}	rate
39	2.50e-01	3.10e-06	0.00	9.17e-05	0.00
219	1.25e-01	1.22e-07	4.66	7.07e-06	3.70
1251	6.25e-02	4.59e-09	4.74	5.96e-07	3.57

We can see that this time the numerical solutions are closer to the expected rate of convergence. Thus, the grid partition plays a role in the solution of this problem. In particular, while triangulation-based degree-d bivariate splines have a span of exactly Π_d over a triangle, degree-d polygonal spline space over an n-gon has a dimension higher than Π_d, and hence has a greater span. It would be interesting to know how one can exert any control over these additional degrees of freedom by choosing a good partition.

Example 2.2.5. Consider the following example:

$$- \epsilon \Delta u + (2 - y^2)D_x u + (2 - x)D_y u + (1 + (1 + x)(1 + y)^2)u = f, (x, y) \in \Omega \quad (2.2.45)$$

with $\Omega = (0, 1)^2$, and $u|_{\partial\Omega} = g$. The function f is so chosen that the exact solution is

$$u(x, y) = 1 + \sin(\pi(1 + x)(1 + y)^2/8).$$

When $\epsilon = 0$, this is a hyperbolic test problem considered in [5, 18, 19]. However, for positive values of ϵ, this is an elliptic PDE. We can well-approximate a solution to the hyperbolic problem by using very small positive values of ϵ:

Table 2.28: Degree-2 Polygonal spline approximation of solution to Example 2.2.5 with $\epsilon = 10^{-3}$

# P	mesh	E_{RMS}	rate	∇E_{RMS}	rate
39	2.50e-01	1.28e-03	0.00	5.58e-02	0.00
219	1.25e-01	4.22e-04	1.60	2.38e-02	1.23
1251	6.25e-02	4.04e-04	0.07	2.28e-02	0.06
7251	3.13e-02	3.99e-04	0.02	2.15e-02	0.09

Table 2.29: Degree-3 Polygonal spline approximation of solution to Example 2.2.5 with $\epsilon = 10^{-3}$

# P	mesh	E_{RMS}	rate	∇E_{RMS}	rate
39	2.50e-01	4.62e-04	0.00	2.02e-02	0.00
219	1.25e-01	4.07e-04	0.18	2.24e-02	-0.15
1251	6.25e-02	4.00e-04	0.02	2.18e-02	0.04
7251	3.13e-02	3.99e-04	0.01	1.81e-02	0.26

Table 2.30: Degree-2 Polygonal spline approximation of solution to Example 2.2.5 with $\epsilon = 10^{-5}$

# P	mesh	E_{RMS}	rate	∇E_{RMS}	rate
39	2.50e-01	1.83e-03	0.00	7.70e-02	0.00
219	1.25e-01	2.97e-04	2.62	3.03e-02	1.35
1251	6.25e-02	4.51e-05	2.72	1.25e-02	1.28
7251	3.13e-02	6.32e-06	2.84	3.67e-03	1.77

Table 2.31: Degree-3 Polygonal spline approximation of solution to Example 2.2.5 with $\epsilon = 10^{-5}$

# P	mesh	E_{RMS}	rate	∇E_{RMS}	rate
39	2.50e-01	3.71e-05	0.00	2.50e-03	0.00
219	1.25e-01	6.66e-06	2.48	8.58e-04	1.54
1251	6.25e-02	5.19e-06	0.36	1.42e-03	-0.72
7251	3.13e-02	4.36e-06	0.25	2.02e-03	-0.51

Table 2.32: Degree-2 Polygonal spline approximation of solution to Example 2.2.5 with $\epsilon = 10^{-10}$

# P	mesh	E_{RMS}	rate	∇E_{RMS}	rate
39	2.50e-01	1.84e-03	0.00	7.73e-02	0.00
219	1.25e-01	3.05e-04	2.59	3.10e-02	1.32
1251	6.25e-02	5.26e-05	2.54	1.43e-02	1.12
7251	3.13e-02	8.46e-06	2.63	5.60e-03	1.35

Table 2.33: Degree-3 Polygonal spline approximation of solution to Example 2.2.5 with $\epsilon = 10^{-10}$

# P	mesh	E_{RMS}	rate	∇E_{RMS}	rate
39	2.50e-01	3.49e-05	0.00	2.37e-03	0.00
219	1.25e-01	2.00e-06	4.13	3.46e-04	2.78
1251	6.25e-02	1.24e-07	4.01	5.26e-05	2.72
7251	3.13e-02	1.84e-08	2.75	1.88e-05	1.49

For comparison, here are the results of the same computation using bivariate splines over a triangulation of the same domain:

Table 2.34: Degree-2 Bivariate spline approximation of solution to Example 2.2.5 with $\epsilon = 10^{-3}$

# T	mesh	E_{RMS}	rate	∇E_{RMS}	rate
40	3.54e-01	1.52e-04	0.00	4.07e-03	0.00
160	1.77e-01	4.58e-05	1.73	1.70e-03	1.26
640	8.84e-02	2.87e-05	0.67	1.13e-03	0.58
2560	4.42e-02	2.67e-05	0.10	1.13e-03	-0.00

Table 2.35: Degree-3 Bivariate spline approximation of solution to Example 2.2.5 with $\epsilon = 10^{-3}$

# T	mesh	E_{RMS}	rate	∇E_{RMS}	rate
40	3.54e-01	3.08e-05	0.00	7.95e-04	0.00
160	1.77e-01	2.82e-05	0.13	1.03e-03	-0.37
640	8.84e-02	2.69e-05	0.07	1.13e-03	-0.13
2560	4.42e-02	2.66e-05	0.02	1.21e-03	-0.10

Table 2.36: Degree-2 Bivariate spline approximation of solution to Example 2.2.5 with $\epsilon = 10^{-5}$

# T	mesh	E_{RMS}	rate	∇E_{RMS}	rate
40	3.54e-01	1.58e-04	0.00	4.64e-03	0.00
160	1.77e-01	3.93e-05	2.01	2.21e-03	1.07
640	8.84e-02	9.81e-06	2.00	1.08e-03	1.04
2560	4.42e-02	2.40e-06	2.03	5.04e-04	1.09

Table 2.37: Degree-3 Bivariate spline approximation of solution to Example 2.2.5 with $\epsilon = 10^{-5}$

# T	mesh	E_{RMS}	rate	∇E_{RMS}	rate
40	3.54e-01	5.36e-06	0.00	2.65e-04	0.00
160	1.77e-01	6.10e-07	3.13	5.66e-05	2.23
640	8.84e-02	3.13e-07	0.96	3.86e-05	0.55
2560	4.42e-02	2.99e-07	0.07	6.72e-05	-0.80

Table 2.38: Degree-2 Bivariate spline approximation of solution to Example 2.2.5 with $\epsilon = 10^{-10}$

# T	mesh	E_{RMS}	rate	∇E_{RMS}	rate
40	3.54e-01	1.58e-04	0.00	4.65e-03	0.00
160	1.77e-01	3.94e-05	2.01	2.22e-03	1.06
640	8.84e-02	9.90e-06	1.99	1.10e-03	1.01
2560	4.42e-02	2.46e-06	2.01	5.48e-04	1.01

Table 2.39: Degree-3 Bivariate spline approximation of solution to Example 2.2.5 with $\epsilon = 10^{-10}$

# T	mesh	E_{RMS}	rate	∇E_{RMS}	rate
40	3.54e-01	5.43e-06	0.00	2.67e-04	0.00
160	1.77e-01	5.68e-07	3.26	5.57e-05	2.26
640	8.84e-02	6.93e-08	3.03	1.42e-05	1.97
2560	4.42e-02	8.55e-09	3.02	3.40e-06	2.06

We can see that the polygonal spline solutions approximate the exact solution very well. However, as in (2.2.43), we see that this PDE has a unique weak solution, but does not satisfy the assumptions of Theorem 2.2.3. Nevertheless, our method works well as shown in Tables 2.36 and 2.37.

Example 2.2.6. For another example, the following problem is parabolic for $y > 0$ and hyperbolic for $y \leq 0$:

$$-\epsilon D_{yy} u + D_x u + c_1 u = 0, \quad (x, y) \in (-1, 1) \times (0, 1)$$
$$D_x u + c_2 u = 0, \quad (x, y) \in (-1, 1) \times (-1, 0] \qquad (2.2.46)$$

with $u|_{\partial\Omega} = g$, for any constants $c_1 > 0$ and $c_2 > 0$. This PDE was studied in [19]. Note that the solution is discontinuous at $y = 0$. We can solve the following general elliptic PDE to estimate the solution to this problem:

$$-\eta D_{xx} u - \epsilon D_{yy} u + D_x u + c_1 u = 0, \quad (x, y) \in (-1, 1) \times (0, 1)$$
$$-\eta \Delta u + D_x u + c_2 u = 0, \quad (x, y) \in (-1, 1) \times (-1, 0] \qquad (2.2.47)$$

with $u|_{\partial\Omega} = g$ and $\eta > 0$. We can approximate the solution to (2.2.5) by letting $\eta > 0$ go to zero and use spline functions which are not necessarily continuous at $y = 0$. Let

44

the exact solution, $u(x, y)$, of (2.2.5) be the following piecewise function:

$$\begin{array}{ll} \sin(\pi(1+y)/2)\exp(-(c_1 + \epsilon\pi^2/4)(1+x)), & -1 \le x \le 1, 0 \le y \le 1 \\ \sin(\pi(1+y)/2)\exp(-c_2(1+x)), & -1 \le x \le 1, -1 < y \le 0. \end{array} \quad (2.2.48)$$

We set $\epsilon = 0.05$ and use a similar partition to the one from Example 2.2.1, scaled to cover the domain $\Omega = [-1, 1]^2$ and with an added edge to account for the discontinuity at $y = 0$:
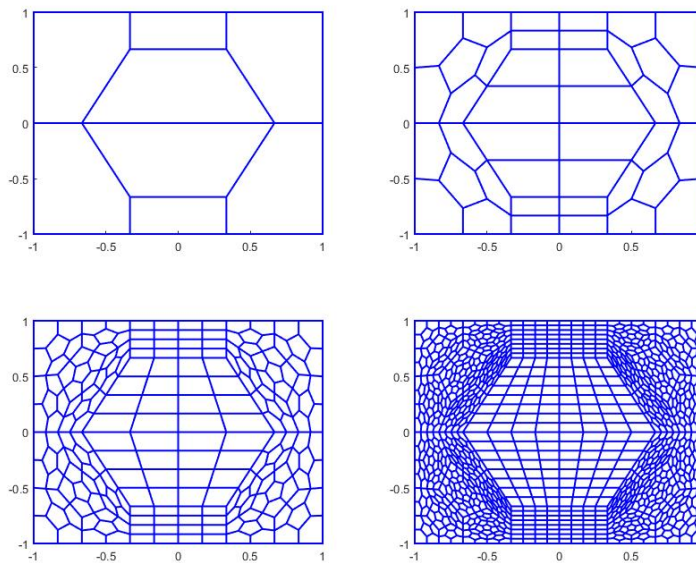
Figure 2.5: A partition of $\Omega = [-1, 1]^2$ and a few refinements

This extra edge will allow us to conveniently control the continuity (or lack thereof) of our solution across the line $y = 0$. In particular, the solution to this PDE is generally discontinuous across this line, and so to find a continuous solution is undesirable. Instead, we can very easily modify the continuity matrix H (see section 4.1) by changing the elements of H which are associated with this edge to zeros, and then we solve the same minimization problem as always. This allows us to avoid any difficulties which arise in deciding which elements affect continuity across this edge; by using

$H\mathbf{c} = 0$ as a side constraint, modifying H allows for a quick adjustment in this way.

While adjusting continuity across one line is not the most complex of conditions, one could consider controlling a discontinuous solution's jump across an edge, or even controlling various continuity conditions across many edges in the partition. Being able to adjust H allows us to make changes like this more readily, without having to heavily modify our code.

Numerical results for the solution of (2.2.48) using degree-2 polygonal splines are shown in Table 2.40.

Table 2.40: Degree-2 Polygonal spline approximation of solution to (2.2.5) with exact solution (2.2.48) when $\eta = 10^{-10}, c_1 = c_2 = 0.1$

# P	mesh	E_{RMS}	rate	∇E_{RMS}	rate
40	6.67e-01	6.80e-03	0.00	2.13e-01	0.00
208	3.33e-01	2.45e-03	1.46	2.10e-01	0.02
1120	1.67e-01	1.15e-03	1.10	2.03e-01	0.05
6208	8.33e-02	4.98e-04	1.21	1.76e-01	0.20

If we change the value of c_2 to $0.1 + \epsilon \pi^2 / 4$, so that the solution is continuous, we retrieve the results in Table 2.41 (without forcing continuity over the line $y = 0$). Enforcing continuity over the line $y = 0$ leads to the results in Table 2.42. We can see that the computational results in Tables 2.41 and 2.42 are very similar.

Table 2.41: Degree-2 Polygonal spline approximation of solution to (2.2.5) with exact solution (2.2.48) when $\eta = 10^{-10}, C_1 = 0.1, c_2 = c_1 + \epsilon \pi^2 / 4$

# P	mesh	E_{RMS}	rate	∇E_{RMS}	rate
40	6.67e-01	1.64e-03	0.00	2.82e-02	0.00
208	3.33e-01	2.61e-04	2.65	1.03e-02	1.45
1120	1.67e-01	3.86e-05	2.76	3.60e-03	1.52
6208	8.33e-02	5.68e-06	2.76	1.23e-03	1.55

Table 2.42: Degree-2 Polygonal spline approximation of solution to (2.2.5) with exact solution (2.2.48) when $\eta = 10^{-10}, C_1 = 0.1, c_2 = c_1 + \epsilon \pi^2 / 4$

# P	mesh	E_{RMS}	rate	∇E_{RMS}	rate
40	6.67e-01	1.65e-03	0.00	2.62e-02	0.00
208	3.33e-01	2.48e-04	2.73	8.87e-03	1.56
1120	1.67e-01	3.80e-05	2.71	3.33e-03	1.42
6208	8.33e-02	5.65e-06	2.75	1.20e-03	1.47

Chapter 3

A Degree-3 Construction of C^1 Polygonal Vertex Splines on Skewed-Grids

3.1   Preliminaries on vertex splines

While the Floater-Lai polygonal splines are clearly useful for PDE applications, the particular spline spaces they use are poorly suited for differentiability. Multivariate splines are well-known for their ability to ensure C^r smoothness for any $r \geq 0$, at least given sufficiently large degree d relative to r, so an analogous function space over polygons should at least have some analogous feature. We focus the remainder of this dissertation, then, on constructions of C^1 polygonal splines as a first venture toward the overall goal of arbitrarily smooth polygonal splines.

The reader will see that the computations involved are extremely complex and lengthy, and that makes this work slow and difficult. To at least slightly reduce these issues, we will make a simplifying assumption for now: we'll assume that we work over a quadrangulation; that is, a partition of only quadrilaterals.

Our constructions will depend on a variety of geometric features of the underlying quadrilaterals. We introduce some notation for this geometry now. Let $P = \langle v_1, v_2, v_3, v_4 \rangle$ be a quadrilateral with vertices v_1, v_2, v_3, v_4, listed in counterclockwise order. We will refer to its vertices cyclically; that is, $v_i = v_j$ whenever $j \equiv i \mod 4$. Oftentimes, we'll implicitly choose a value i, and consider $P = \langle v_i, v_{i+1}, v_{i+2}, v_{i-1} \rangle$. This will allow us to focus on a single arbitrary vertex, and to make conclusions for all vertices by simply shifting indices.

We'll often abuse some notation and consider each vertex v_i as a Cartesian point $v_i = (v_{i,x}, v_{i,y})$ or as a vector $\langle v_{i,x}, v_{i,y} \rangle$. We write e_i to mean the ith edge of P, which is between v_i and v_{i+1}, and write $\vec{e_i} = \langle e_{i,x}, e_{i,y} \rangle := v_{i+1} - v_i = \langle v_{i+1,x} - v_{i,x}, v_{i+1,y} - v_{i,y} \rangle$ to represent e_i as a vector quantity. We'll write $|e_i|$ to represent the length of the ith edge, and denote by $\vec{n_i}$ the outward unit normal to $\vec{e_i}$; that is, $\vec{n_i} = |\vec{e_i}|^{-1} \langle e_{i,y}, -e_{i,x} \rangle$.

For each i, denote by C_i the area of the subtriangle of P given by $\langle v_{i-1}, v_i, v_{i+1} \rangle$, and denote by θ_i the interior angle of P at v_i. Finally, define $A_i(\mathbf{x})$ to be the signed area of the triangle $\langle \mathbf{x}, v_i, v_{i+1} \rangle$, positive for points $\mathbf{x}$ on the interior of P. Notice that, while C_i, θ_i, e_i, and n_i are constants for a given quadrilateral P for each i, A_i is a linear bivariate polynomial. It is worth noting that $A_i(v_{i-1}) = C_i$, $A_i(v_{i+2}) = C_{i+1}$, and $A_i(v_i) = A_i(v_{i+1}) = 0$. All of these notations use cyclic indices, just as for the vertices. Please refer back to Figure 2.1 for an illustration of C_2 and $A_3(\mathbf{x})$ for a given quadrilateral.

As in the Floater-Lai case, we'll construct our polygonal splines from Wachspress coordinates. We first analyze the behavior of these coordinates. For a quadrilateral P, recall that the Wachspress coordinate with respect to the vertex v_i is given by the rational function

$$\phi_i(\mathbf{x}) = \frac{w_i(\mathbf{x})}{\sum\limits_{j=1}^{4} w_j(\mathbf{x})}, \qquad (3.1.1)$$

where w_i is the bivariate quadratic polynomial

$$w_i(\mathbf{x}) = C_i A_{i+1}(\mathbf{x}) A_{i+2}(\mathbf{x}). \tag{3.1.2}$$

As we are interested in construction of functions which are globally C^1, we should pay special attention to the gradients of the Wachspress coordinates on the edges of each quadrilateral. Since Wachspress coordinates are linear on edges, the edge direction derivatives are easy to compute. Where we suppress the arguments of the functions ϕ_j and write $\tilde{e}_i = \dfrac{\vec{e}_i}{|\vec{e}_i|}$, we have the following derivatives:

$$\left.\frac{\partial \phi_i}{\partial \tilde{e}_i}\right|_{e_i} = |e_i|^{-1}, \tag{3.1.3}$$

$$\left.\frac{\partial \phi_i}{\partial \tilde{e}_{i-1}}\right|_{e_{i-1}} = -|e_{i-1}|^{-1}, \tag{3.1.4}$$

$$\left.\frac{\partial \phi_i}{\partial \tilde{e}_{i+1}}\right|_{e_{i+1}} = \left.\frac{\partial \phi_i}{\partial \tilde{e}_{i+2}}\right|_{e_{i+2}} = 0, \tag{3.1.5}$$

$$\left.\frac{\partial^n \phi_i}{\partial \tilde{e}_j{}^n}\right|_{e_j} = 0, \tag{3.1.6}$$

where (3.1.6) holds for any j whenever $n > 1$.

We'll also be interested in the outward normal derivatives of Wachspress coordinates on the edges of each quadrilateral. This will require more work than the edge-direction derivatives.

Lemma 3.1.1. *Given a quadrilateral* $P = \langle v_1, v_2, v_3, v_4 \rangle$, *then the outward normal*

derivatives of the Wachspress coordinates of P on edge e_i are given by

$$\frac{\partial \phi_i}{\partial \vec{n_i}}\bigg|_{e_i} = \phi_{i+1}|_{e_i}\left(\frac{|e_{i+1}|\cos(\theta_{i+1})}{2C_{i+1}}\right) - \phi_i|_{e_i}\left(\frac{|e_{i-1}|\cos(\theta_i)}{2C_i}\right)$$
$$+ \left(\frac{|e_i|}{2A_{i+2}}\right)\left(\phi_i^2|_{e_i}\left(\frac{C_{i-1}}{C_i}\right) + \phi_i\phi_{i+1}|_{e_i}\left(\frac{C_{i+2}}{C_{i+1}}\right)\right),$$

$$\frac{\partial \phi_{i+1}}{\partial \vec{n_i}}\bigg|_{e_i} = \phi_i|_{e_i}\left(\frac{|e_{i-1}|\cos(\theta_i)}{2C_i}\right) - \phi_{i+1}|_{e_i}\left(\frac{|e_{i+1}|\cos(\theta_{i+1})}{2C_{i+1}}\right)$$
$$+ \left(\frac{|e_i|}{2A_{i+2}}\right)\left(\phi_{i+1}^2|_{e_i}\left(\frac{C_{i+2}}{C_{i+1}}\right) + \phi_i\phi_{i+1}|_{e_i}\left(\frac{C_{i-1}}{C_i}\right)\right),$$

$$\frac{\partial \phi_{i-1}}{\partial \vec{n_i}}\bigg|_{e_i} = -\left(\frac{C_{i-1}}{C_i}\right)\left(\frac{|e_i|}{2A_{i+2}}\right)\phi_i|_{e_i},$$

$$\frac{\partial \phi_{i+2}}{\partial \vec{n_i}}\bigg|_{e_i} = -\left(\frac{C_{i+2}}{C_{i+1}}\right)\left(\frac{|e_i|}{2A_{i+2}}\right)\phi_{i+1}|_{e_i}.$$

Proof. We first compute

$$\nabla \phi_i = \frac{\nabla w_i \sum_{k=1}^{4} w_k - w_i \sum_{k=1}^{4} \nabla w_k}{\left(\sum_{j=1}^{4} w_j\right)^2} = \frac{\nabla w_i}{\sum_{j=1}^{4} w_j} - \frac{w_i}{\sum_{j=1}^{4} w_j}\left(\sum_{k=1}^{4}\frac{\nabla w_k}{\sum_{j=1}^{4} w_j}\right).$$

Then we write

$$\nabla \phi_i = R_i - \phi_i \sum_{k=1}^{4} R_k, \tag{3.1.7}$$

where

$$R_i := \frac{\nabla w_i}{\sum_{j=1}^{4} w_j}.$$

It is worth mentioning that this notation is inspired by that found in the gradient analysis of Wachspress coordinates in [13], but is not quite the same. In particular, this expression of the gradient is well-defined on the boundary of the polygon, which is where we are most concerned.

The gradients ∇w_i are fairly simple:

$$\nabla w_i = C_i \left(\nabla A_{i+1} A_{i+2} + \nabla A_{i+2} A_{i+1} \right). \qquad (3.1.8)$$

Moreover, when we are on an edge, we can simplify the sums in the denominators by exploiting the behavior of the area functions on the edges. Since the area functions are linear polynomials, we note that an arbitrary point on edge e_i can be expressed as $(1-t)v_i + tv_{i+1}$ for some $t \in [0,1]$, and so we can see that

$$A_i\big|_{e_i} = 0,$$

$$A_{i+1}\big|_{e_i} = (1-t)C_{i+1},$$

$$A_{i-1}\big|_{e_i} = tC_i,$$

Using the properties above, we can see that

$$\sum_{j=1}^{4} w_j\Big|_{e_k} = w_k + w_{k+1} = A_{k+2}(C_k A_{k+1} + C_{k+1} A_{k-1}) = C_k C_{k+1} A_{k+2}. \qquad (3.1.9)$$

Then we have the following expressions for R_i on each edge:

$$
\begin{aligned}
R_i|_{e_i} &= \frac{C_i \left(\nabla A_{i+1} A_{i+2} + \nabla A_{i+2} A_{i+1} \right)}{C_i C_{i+1} A_{i+2}} \\
&= \frac{\nabla A_{i+1}}{C_{i+1}} + \left(\frac{A_{i+1}}{C_{i+1}} \right) \left(\frac{\nabla A_{i+2}}{A_{i+2}} \right) \quad = \frac{\nabla A_{i+1}}{C_{i+1}} + \phi_i|_{e_i} \left(\frac{\nabla A_{i+2}}{A_{i+2}} \right) \qquad (3.1.10)
\end{aligned}
$$

$$
\begin{aligned}
R_i|_{e_{i-1}} &= \frac{C_i \left(\nabla A_{i+1} A_{i+2} + \nabla A_{i+2} A_{i+1} \right)}{C_{i-1} C_i A_{i+1}} \\
&= \frac{\nabla A_{i+2}}{C_{i-1}} + \left(\frac{A_{i+2}}{C_{i-1}} \right) \left(\frac{\nabla A_{i+1}}{A_{i+1}} \right) \quad = \frac{\nabla A_{i+2}}{C_{i-1}} + \phi_i|_{e_{i-1}} \left(\frac{\nabla A_{i+1}}{A_{i+1}} \right) \qquad (3.1.11)
\end{aligned}
$$

$$
\begin{aligned}
R_i|_{e_{i+1}} &= \frac{C_i \left(\nabla A_{i+1} A_{i+2} + \nabla A_{i+2} A_{i+1} \right)}{C_{i+1} C_{i+2} A_{i-1}} \quad = \frac{C_i \left(\nabla A_{i+1} A_{i+2} \right)}{C_{i+1} C_{i+2} A_{i-1}} \\
&= \left(\frac{C_i}{C_{i+1}} \right) \left(\frac{A_{i+2}}{C_{i+2}} \right) \left(\frac{\nabla A_{i+1}}{A_{i-1}} \right) \quad = \left(\frac{C_i}{C_{i+1}} \right) \left(\frac{\nabla A_{i+1}}{A_{i-1}} \right) \phi_{i+1}|_{e_{i+1}} \qquad (3.1.12)
\end{aligned}
$$

$$
\begin{aligned}
R_i|_{e_{i+2}} &= \frac{C_i \left(\nabla A_{i+1} A_{i+2} + \nabla A_{i+2} A_{i+1} \right)}{C_{i+2} C_{i-1} A_i} \quad = \frac{C_i \left(\nabla A_{i+2} A_{i+1} \right)}{C_{i+2} C_{i-1} A_i} \\
&= \left(\frac{C_i}{C_{i-1}} \right) \left(\frac{A_{i+1}}{C_{i+2}} \right) \left(\frac{\nabla A_{i+2}}{A_i} \right) \quad = \left(\frac{C_i}{C_{i-1}} \right) \left(\frac{\nabla A_{i+2}}{A_i} \right) \phi_{i-1}|_{e_{i+2}} . \quad (3.1.13)
\end{aligned}
$$

We will also need to know values of $\sum_{k=1}^{4} R_k$ on each edge. Using (3.1.10)-(3.1.13), along with the fact that $(\phi_i + \phi_{i+1})|_{e_i} = 1$, we see that

$$
\begin{aligned}
\sum_{k=1}^{4} R_k \Big|_{e_j} &= \frac{\nabla A_{j+1}}{C_{j+1}} + \frac{\nabla A_{j-1}}{C_j} + \frac{\nabla A_{j+2}}{A_{j+2}} \\
&\quad + \left(\frac{\nabla A_i}{A_{i+2}} \right) \left(\left(\frac{C_{i-1}}{C_i} \right) \phi_i|_{e_i} + \left(\frac{C_{i+2}}{C_{i+1}} \right) \phi_{i+1}|_{e_i} \right). \qquad (3.1.14)
\end{aligned}
$$

It is easy to see that $\nabla A_j = -\frac{1}{2} |e_j| n_j$. Moreover, note that

$n_{j-1}.n_j = \cos(\pi - \theta_j) = -\cos(\theta_j)$. Using these two observations, along with (3.1.10)-

52

(3.1.14), we compute the outward normal derivatives:

$$
\begin{aligned}
\left.\frac{\partial \phi_i}{\partial \vec{n_i}}\right|_{e_i} &= \left.R_i.\vec{n_i}\right|_{e_i} - \phi_i \sum_{k=1}^{4} \left.R_k.\vec{n_i}\right|_{e_i} \\
&= \frac{|e_{i+1}|\cos(\theta_{i+1})}{2C_{i+1}} + \phi_i|_{e_i} \left(\frac{\nabla A_{i+2}.\vec{n_i}}{A_{i+2}}\right) - \phi_i \sum_{k=1}^{4} \left.R_k.\vec{n_i}\right|_{e_i} \\
&= \frac{|e_{i+1}|\cos(\theta_{i+1})}{2C_{i+1}} - \phi_i \left(\frac{|e_{i+1}|\cos(\theta_{i+1})}{2C_{i+1}} + \frac{|e_{i-1}|\cos(\theta_i)}{2C_i}\right. \\
&\qquad \left. - \left(\frac{|e_i|}{2A_{i+2}}\right)\left(\left(\frac{C_{i-1}}{C_i}\right)\phi_i|_{e_i} + \left(\frac{C_{i+2}}{C_{i+1}}\right)\phi_{i+1}|_{e_i}\right)\right) \\
&= \phi_{i+1}|_{e_i}\left(\frac{|e_{i+1}|\cos(\theta_{i+1})}{2C_{i+1}}\right) - \phi_i|_{e_i}\left(\frac{|e_{i-1}|\cos(\theta_i)}{2C_i}\right) \\
&\qquad + \left(\frac{|e_i|}{2A_{i+2}}\right)\left(\phi_i^2|_{e_i}\left(\frac{C_{i-1}}{C_i}\right) + \phi_i\phi_{i+1}|_{e_i}\left(\frac{C_{i+2}}{C_{i+1}}\right)\right),
\end{aligned}
$$

$$
\begin{aligned}
\left.\frac{\partial \phi_{i+1}}{\partial \vec{n_i}}\right|_{e_i} &= \left.R_{i+1}.\vec{n_i}\right|_{e_i} - \phi_{i+1} \sum_{k=1}^{4} \left.R_k.\vec{n_i}\right|_{e_i} \\
&= \frac{|e_{i-1}|\cos(\theta_i)}{2C_i} + \phi_{i+1}|_{e_i}\left(\frac{\nabla A_{i+2}.\vec{n_i}}{A_{i+2}}\right) - \phi_{i+1} \sum_{k=1}^{4} \left.R_k.n_k\right|_{e_i} \\
&= \frac{|e_{i-1}|\cos(\theta_i)}{2C_i} - \phi_{i+1}\left(\frac{|e_{i+1}|\cos(\theta_{i+1})}{2C_{i+1}} + \frac{|e_{i-1}|\cos(\theta_i)}{2C_i}\right. \\
&\qquad \left. - \left(\frac{|e_i|}{2A_{i+2}}\right)\left(\left(\frac{C_{i-1}}{C_i}\right)\phi_i|_{e_i} + \left(\frac{C_{i+2}}{C_{i+1}}\right)\phi_{i+1}|_{e_i}\right)\right) \\
&= \phi_i|_{e_i}\left(\frac{|e_{i-1}|\cos(\theta_i)}{2C_i}\right) - \phi_{i+1}|_{e_i}\left(\frac{|e_{i+1}|\cos(\theta_{i+1})}{2C_{i+1}}\right) \\
&\qquad + \left(\frac{|e_i|}{2A_{i+2}}\right)\left(\phi_{i+1}^2|_{e_i}\left(\frac{C_{i+2}}{C_{i+1}}\right) + \phi_i\phi_{i+1}|_{e_i}\left(\frac{C_{i-1}}{C_i}\right)\right),
\end{aligned}
$$

$$
\begin{aligned}
\left.\frac{\partial \phi_{i-1}}{\partial \vec{n_i}}\right|_{e_i} &= \left.R_{i-1}.\vec{n_i}\right|_{e_i} + \phi_{i-1} \sum_{k=1}^{4} \left.R_k.\vec{n_i}\right|_{e_i} \\
&= -\left(\frac{C_{i-1}}{C_i}\right)\left(\frac{|e_i|}{2A_{i+2}}\right)\phi_i|_{e_i},
\end{aligned}
$$

$$\frac{\partial \phi_{i+2}}{\partial \vec{n_i}}\bigg|_{e_i} = R_{i+2}.\vec{n_i}\big|_{e_i} + \phi_{i+2} \sum_{k=1}^{4} R_k.\vec{n_i}\big|_{e_i}$$

$$= -\left(\frac{C_{i+2}}{C_{i+1}}\right)\left(\frac{|e_i|}{2A_{i+2}}\right)\phi_{i+1}\big|_{e_i}.$$

$\square$

We mention one more brief lemma, which is trivial to prove, but has important consequences.

Lemma 3.1.2.

$$\frac{\phi_i \phi_{i+2}}{C_i C_{i+2}} = \frac{\phi_{i+1}\phi_{i-1}}{C_{i+1}C_{i-1}}.$$

Proof.

$$\phi_{i+1}\phi_{i-1} = \frac{C_{i+1}A_{i+2}A_{i-1}C_{i-1}A_iA_{i+1}}{\left(\sum_{j=1}^{4} w_j\right)^2}$$

$$= \frac{C_{i+1}C_{i-1}}{C_iC_{i+2}}\frac{C_iA_{i+1}A_{i+2}C_{i+2}A_{i-1}A_i}{\left(\sum_{j=1}^{4} w_j\right)^2}$$

$$= \frac{C_{i+1}C_{i-1}}{C_iC_{i+2}}\phi_i\phi_{i+2}.$$

Division by $C_{i+1}C_{i-1}$ completes the proof. $\square$

The implications of this lemma are important: using this relationship, we can determine which monomials of Wachspress coordinates are linearly independent. Because of its connection with the bubble function $\prod_{j=1}^{4} A_j$, we often write

$$B = \frac{\phi_i\phi_{i+2}}{C_iC_{i+2}} = \frac{\phi_{i+1}\phi_{i-1}}{C_{i+1}C_{i-1}}.$$

Using the Lemma 3.1.2, we can now say with certainty that the full space of

ϕ_4^4 $\phi_3\phi_4^3$ $\phi_3^2\phi_4^2$ $\phi_3^3\phi_4$ ϕ_3^4

$\phi_1\phi_4^3$ $B\phi_4^2$ $B\phi_3\phi_4$ $B\phi_3^2$ $\phi_2\phi_3^3$

$\phi_1^2\phi_4^2$ $B\phi_1\phi_4$ B^2 $B\phi_2\phi_3$ $\phi_2^2\phi_3^2$

$\phi_1^3\phi_4$ $B\phi_1^2$ $B\phi_1\phi_2$ $B\phi_2^2$ $\phi_2^3\phi_3$

ϕ_1^4 $\phi_1^3\phi_2$ $\phi_1^2\phi_2^2$ $\phi_1\phi_2^3$ ϕ_2^4

Figure 3.1: An illustration of the degree-4 polygonal spline basis functions with the associated domain points over a rectangle

degree-d polygonal splines over a single quadrilateral P, $\mathcal{S}_d(P)$, has as a basis

$$\mathcal{B}_d(P) = \bigcup_{i=1}^{4}\{B^a\phi_i^b\phi_{i+1}^c : a, b, c \geq 0; 2a + b + c = d\}. \qquad (3.1.15)$$

This particular basis is convenient in that it permits an identification to domain points in an analogous way to the case of bivariate splines over triangles; in particular, Figure 3.1 shows how to lay out the degree-4 polygonal spline basis functions with their associated domain points over a rectangle with v_1 at its lower-left corner.

Now we discuss our overall strategy. For a given partition of convex quadrilaterals $\mathcal{P}$, define

$$\mathcal{S}_d(\mathcal{P}) := \{s : s|_{P \in \mathcal{P}} \in \text{span}\{\mathcal{B}_d(P)\} \} \qquad (3.1.16)$$

How can we construct a polygonal spline s in such a way to ensure that it is C^1? While some coefficient conditions to ensure C^1 smoothness might be desirable, as are available in the traditional triangular case, after some initial investigation we deemed

55

Figure 3.2: A partition of quadrilaterals $\mathcal{P}$

this problem too difficult to tackle at the outset of this project. Instead, we opted for a different approach: to construct a basis for a C^1 subspace of $\mathcal{S}_d(\mathcal{P})$. In doing so, we opted to make this basis as locally-supported as possible; in fact, along the way we will create a basis for a C^1 polygonal vertex spline space, where a *vertex spline* is defined as one which is a linear combination of splines which are supported only in the ring of polygons Ω_v containing a single vertex v.

Consider the following partition of quadrilaterals $\mathcal{P}$:

We wish to construct a C^1 polygonal spline ψ_v over this partition which can interpolate values at the vertex v, while having value 0 at the other vertices (i.e. $\psi_v(w) = \delta_{v,w}$ for vertices w). Since we'll be doing this piecewise across each quadrilateral, we'll need to ensure that both the values and gradients match on shared edges and vertices. In particular, we'll enforce that $\nabla \psi_v(v) = 0$ for some simplicity. Moreover, to maintain some locality, we'd like ψ_v to be 0 outside Ω_v; that is, since v is not included in the quadrilateral Q, we would like $\psi_v|_Q \equiv 0$. Notice that this implies that $\nabla \psi_v|_{\partial Q} \equiv 0$; we can summarize this by saying that we want $\text{supp}(\psi_v) \subseteq \Omega_v$, $\psi_v|_{\partial \Omega_v} = 0$, and $\nabla \psi_v|_{\partial \Omega_v} = 0$.

Now, where $P = \langle v_1, v_2, v_3, v_4 \rangle$, let $v = v_i$ be the ith vertex of P. Consider

56

$\psi_{i,P} := \psi_v|_P$. While we restrict our attention to only the quadrilateral P, we will suppress the additional subscript and merely refer to this function as ψ_i. Then we want

$$\psi_i(v_j) = \delta_{ij}, \tag{3.1.17}$$

$$\nabla \psi_i(v_j) = 0, \tag{3.1.18}$$

$$\psi_i|_{e_{i+1}} = \psi_i|_{e_{i+2}} \equiv 0, \text{ and} \tag{3.1.19}$$

$$\nabla \psi_i|_{e_{i+1}} = \nabla \psi_i|_{e_{i+2}} \equiv 0. \tag{3.1.20}$$

We can enforce properties (3.1.19) and (3.1.20) by simply requiring that ψ_i has a factor of ϕ_i^2, since $\phi_i|_{e_{i+1}} = \phi_i|_{e_{i+2}} \equiv 0$. This will also ensure that properties (3.1.17) and (3.1.18) are satisfied for all vertices except v_i.

Now consider the values of ψ_i on edges e_i and e_{i-1}. Since the Wachspress coordinates of P are linear on its edges, if we build ψ_i as a polynomial of Wachspress coordinates then it will have polynomial values on the edges of P.

Write $p(t) = \psi_i(v_i + t(v_{i+1} - v_i))$ for $t \in [0,1]$. Then we want p to satisfy the following:

$$p(0) = 1, \tag{3.1.21}$$

$$p(1) = 0, \tag{3.1.22}$$

$$p'(0) = 0, \text{ and} \tag{3.1.23}$$

$$p'(1) = 0. \tag{3.1.24}$$

Given that ψ_i interpolates values at a single vertex, it can be used not entirely unlike a GBC, so we might wish to enforce a new property

$$\sum_{j=1}^{4} \psi_j \equiv 1, \tag{3.1.25}$$

which will in turn yield a new property for p:

$$p(t) + p(1 - t) = 1. \tag{3.1.26}$$

As p is a univariate polynomial, properties (3.1.21)-(3.1.24) imply that we need p to be at least degree 3. A natural question is whether we can accomplish our goals with p being precisely degree 3.

3.2 Degree-3 C^1 polygonal spline construction

3.2.1 Construction of $\psi_v^{(3)}$

Using the basis $\mathcal{B}_3(P)$ and the knowledge that we desire a factor of ϕ_i^2 by properties (3.1.19) and (3.1.20), we can form a template for $\psi_i^{(3)}$, where the superscript is merely used to distinguish the degree:

$$\psi_i^{(3)} = \phi_i^2(J_{0,i}\phi_i + J_{1,i}\phi_{i+1} + J_{2,i}\phi_{i-1} + K_{0,i}\phi_{i+2}), \tag{3.2.1}$$

where $J_{0,i}, J_{1,i}, J_{2,i}, K_{0,i}$ are constants.

There is a unique univariate polynomial p of degree 3 satisfying properties (3.1.21)-(3.1.24), namely $p(t) = (1 - t)^2(1 + 2t) = (1 - t)^2((1 - t) + 3t)$. Recall that $p(t)$ is defined as $\psi_i(v_i + t(v_{i+1} - v_i))$. We have that $\phi_i(v_i + t(v_{i+1} - v_i)) = 1 - t$, and $\phi_{i+1}(v_i + t(v_{i+1} - v_i)) = t$, so we'll say $\psi_i|_{e_i} = \phi_i^2(\phi_i + 3\phi_{i+1})$. Similarly, we can say $\psi_i|_{e_{i-1}} = \phi_i^2(\phi_i + 3\phi_{i-1})$. This is enough to inform us that $J_{0,i} = 1, J_{1,i} = J_{2,i} = 3$.

We will be able to solve for $K_{0,i}$ by enforcing property (3.1.25). First, we strategically express 1 as a cubic polynomial of Wachspress coordinates, using the fact that

58

$\sum_{k=1}^{4} \phi_k = 1$:

$$1 = \left(\sum_{k=1}^{4} \phi_k \right)^3$$

$$= \phi_1^3 + 3\phi_1^2\phi_2 + 3\phi_1^2\phi_3 + 3\phi_1^2\phi_4 + 3\phi_1\phi_2^2 + 6\phi_1\phi_2\phi_3 + 6\phi_1\phi_2\phi_4 + 3\phi_1\phi_3^2$$

$$+ 6\phi_1\phi_3\phi_4 + 3\phi_1\phi_4^2 + \phi_2^3 + 3\phi_2^2\phi_3 + 3\phi_2^2\phi_4 + 3\phi_2\phi_3^2 + 6\phi_2\phi_3\phi_4 + 3\phi_2\phi_4^2$$

$$+ \phi_3^3 + 3\phi_3^2\phi_4 + 3\phi_3\phi_4^2 + \phi_4^3.$$

We can simplify this using our prior notation B, from Lemma 3.1.2:

$$1 = \phi_1^3 + 3\phi_1^2\phi_2 + 3\phi_1^2\phi_4 + 3\phi_1\phi_2^2 + 3\phi_1\phi_4^2 + \phi_2^3$$

$$+ 3\phi_2^2\phi_3 + 3\phi_2\phi_3^2 + \phi_3^3 + 3\phi_3^2\phi_4 + 3\phi_3\phi_4^2 + \phi_4^3$$

$$+ B((3C_1C_3 + 6C_2C_4)\phi_1 + (6C_1C_3 + 3C_2C_4)\phi_2$$

$$+ (3C_1C_3 + 6C_2C_4)\phi_3 + (6C_1C_3 + 3C_2C_4)\phi_4). \qquad (3.2.2)$$

We can rewrite $\psi_i^{(3)}$ as

$$\psi_i^{(3)} = \phi_i^3 + 3\phi_i^2\phi_{i+1} + 3\phi_i^2\phi_{i-1} + K_{0,i}C_iC_{i+2}B\phi_i,$$

so it's easy enough to see that

$$1 - \sum_{j=1}^{4} \psi_i = B \sum_{k=1}^{4} ((3 - K_{0,i})C_iC_{i+2} + 6C_{i+1}C_{i-1})\phi_i. \qquad (3.2.3)$$

Then we'll set $K_{0,i} = 3 + 6\dfrac{C_{i+1}C_{i-1}}{C_iC_{i+2}}$, so we'll have

$$\psi_i^{(3)} = \phi_i^2 \left(\phi_i + 3(\phi_{i+1} + \phi_{i-1}) + 3 \left(1 + 2\frac{C_{i+1}C_{i-1}}{C_iC_{i+2}} \right) \phi_{i+2} \right). \qquad (3.2.4)$$

While this satisfies our initial set of conditions, it remains to see whether this definition will ensure that the piecewise function f is C^1 over $\mathcal{P}$.

Suppose we have the following subpartition, where $v = v_{i,P} = v_{i,R}$:
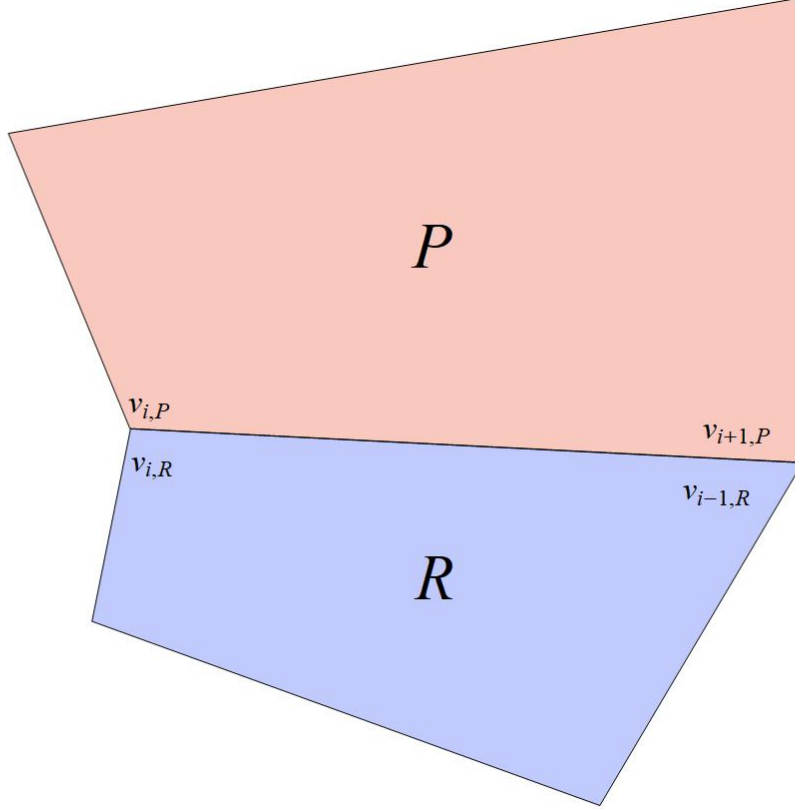
Figure 3.3: A pair of adjacent quadrilaterals P and R

We require that the function ψ_v is C^1 over the union of P and R, and since Wachspress coordinates are smooth on the interior of the polygon over which they are defined, then we need only check the shared edge $e_{i,P} = e_{i-1,R}$. In particular, we'll check the outward normal derivatives on this edge $\dfrac{\partial \psi_{i,P}^{(3)}}{\partial \vec{n_{i,P}}}$ and $\dfrac{\partial \psi_{i,R}^{(3)}}{\partial \vec{n_{i-1,R}}}$. Since $\vec{n}_{i-1,R} = -\vec{n}_{i,P}$, then we will need to enforce

$$\frac{\partial \psi_{i,P}^{(3)}}{\partial \vec{n}_{i,P}} + \frac{\partial \psi_{i,R}^{(3)}}{\partial \vec{n}_{i-1,R}} = 0. \tag{3.2.5}$$

Let us take the relevant derivatives. We suppress the specific quadrilateral subscripts.

$$\left.\frac{\partial \psi_i^{(3)}}{\partial \vec{n}_i}\right|_{e_i} = 2\phi_i \frac{\partial \phi_i}{\partial \vec{n}_i}(\phi_i + 3\phi_{i+1})$$

$$+ \phi_i^2 \left(\frac{\partial \phi_i}{\partial \vec{n}_i} + 3\frac{\partial}{\partial \vec{n}_i}(\phi_{i+1} + \phi_{i-1} + \phi_{i+2}) + 6\frac{C_{i+1}C_{i-1}}{C_i C_{i+2}}\frac{\partial \phi_{i+2}}{\partial \vec{n}_i}\right)$$

$$= (3\phi_i^2 + 6\phi_i\phi_{i+1})\frac{\partial \phi_i}{\partial \vec{n}_i} + 3\phi_i^2\frac{\partial}{\partial \vec{n}_i}(1-\phi_i) + 6\frac{C_{i+1}C_{i-1}}{C_i C_{i+2}}\phi_i^2\frac{\partial \phi_{i+2}}{\partial \vec{n}_i}$$

$$= 6\phi_i\left(\phi_{i+1}\frac{\partial \phi_i}{\partial \vec{n}_i} + \frac{C_{i+1}C_{i-1}}{C_i C_{i+2}}\phi_i\frac{\partial \phi_{i+2}}{\partial \vec{n}_i}\right)$$

$$= 6\phi_i\left(\phi_{i+1}^2\frac{|e_{i+1}|\cos(\theta_{i+1})}{2C_{i+1}} - \phi_i\phi_{i+1}\frac{|e_{i-1}|\cos(\theta_i)}{2C_i}\right.$$

$$\left. + \left(\frac{|e_i|}{2A_{i+2}}\right)\left(\frac{C_{i-1}}{C_i}\phi_i^2\phi_{i+1} + \frac{C_{i+2}}{C_{i+1}}\phi_i\phi_{i+1}^2 - \frac{C_{i-1}}{C_i}\phi_i\phi_{i+1}\right)\right)$$

$$= 6\phi_i\phi_{i+1}\left(\phi_{i+1}\frac{|e_{i+1}|\cos(\theta_{i+1})}{2C_{i+1}} - \phi_i\frac{|e_{i-1}|\cos(\theta_i)}{2C_i}\right.$$

$$\left. + \left(\frac{|e_i|}{2A_{i+2}}\right)\left(\frac{C_{i+2}}{C_{i+1}} - \frac{C_{i-1}}{C_i}\right)\phi_i\phi_{i+1}\right); \tag{3.2.6}$$

$$\left.\frac{\partial \psi_i^{(3)}}{\partial \vec{n}_{i-1}}\right|_{e_{i-1}} = 2\phi_i \frac{\partial \phi_i}{\partial \vec{n}_{i-1}}(\phi_i + 3\phi_{i-1})$$

$$+ \phi_i^2 \left(\frac{\partial \phi_i}{\partial \vec{n}_{i-1}} + 3\frac{\partial}{\partial \vec{n}_{i-1}}(\phi_{i+1} + \phi_{i-1} + \phi_{i+2}) + 6\frac{C_{i+1}C_{i-1}}{C_i C_{i+2}}\frac{\partial \phi_{i+2}}{\partial \vec{n}_{i-1}}\right)$$

$$= 6\phi_i\left(\phi_{i-1}\frac{\partial \phi_i}{\partial \vec{n}_{i-1}} + \frac{C_{i+1}C_{i-1}}{C_i C_{i+2}}\phi_i\frac{\partial \phi_{i+2}}{\partial \vec{n}_{i-1}}\right)$$

$$= 6\phi_i\phi_{i-1}\left(\phi_{i-1}\frac{|e_{i+2}|\cos(\theta_{i-1})}{2C_{i-1}} - \phi_i\frac{|e_i|\cos(\theta_i)}{2C_i}\right.$$

$$\left. + \left(\frac{|e_{i-1}|}{2A_{i+1}}\right)\left(\frac{C_{i+2}}{C_{i-1}} - \frac{C_{i+1}}{C_i}\right)\phi_i\phi_{i-1}\right). \tag{3.2.7}$$

Keeping in mind that $\phi_{i,R}|_{e_{i-1,R}} = \phi_{i,P}|_{e_{i,P}}$ and $\phi_{i-1,R}|_{e_{i-1,R}} = \phi_{i+1,P}|_{e_{i,P}}$, we have

$$\left.\frac{\partial\psi_{i,P}^{(3)}}{\partial\vec{n}_{i,P}}\right|_{e_{i,P}} + \left.\frac{\partial\psi_{i,R}^{(3)}}{\partial\vec{n}_{i-1,R}}\right|_{e_{i-1,R}} =$$

$$6\phi_{i,P}\phi_{i+1,P}\left(\phi_{i+1,P}\left(\frac{|e_{i+1,P}|\cos(\theta_{i+1,P})}{2C_{i+1,P}} + \frac{|e_{i+2,R}|\cos(\theta_{i-1,R})}{2C_{i-1,R}}\right)\right.$$

$$-\phi_{i,P}\left(\frac{|e_{i-1,P}|\cos(\theta_{i,P})}{2C_{i,P}} + \frac{|e_{i,R}|\cos(\theta_{i,R})}{2C_{i,R}}\right)$$

$$+\phi_{i,P}\phi_{i+1,P}\left(\frac{|e_{i,P}|}{2A_{i+2,P}}\left(\frac{C_{i+2,P}}{C_{i+1,P}} - \frac{C_{i-1,P}}{C_{i,P}}\right)\right.$$

$$\left.\left.+\frac{|e_{i-1,R}|}{2A_{i+1,R}}\left(\frac{C_{i+2,R}}{C_{i-1,R}} - \frac{C_{i+1,R}}{C_{i,R}}\right)\right)\right). \tag{3.2.8}$$

In the special case that P is a rectangle, $\left.\dfrac{\partial\psi_{i,P}^{(3)}}{\partial\vec{n}_{i,P}}\right|_{e_{i,P}} = 0$, so to ensure C^1 smoothness

we would need $\left.\dfrac{\partial\psi_{i,R}^{(3)}}{\partial\vec{n}_{i-1,R}}\right|_{e_{i-1,R}} = 0$. However, this is easily checked numerically on an

arbitrary quadrilateral R, and we see that this is not generally the case. In order to force (3.2.8) to be zero, we'll need to enforce some particular geometry on the partition $\mathcal{P}$.

First of all, note that $\phi_{i,P}$ and $\phi_{i+1,P}$ are linearly independent polynomials on the shared edge. Then we need each coefficient in (3.2.8) to be zero. Then we must have

$$\frac{|e_{i+1,P}|\cos(\theta_{i+1,P})}{2C_{i+1,P}} = -\frac{|e_{i+2,R}|\cos(\theta_{i-1,R})}{2C_{i-1,R}}.$$

We can rewrite this by noting that $|e_{i,P}| = |e_{i-1,R}|$ and $C_j = \frac{1}{2}|e_{j-1}||e_j|\sin(\theta_j)$:

$$\cot(\theta_{i+1,P}) = -\cot(\theta_{i-1,R}). \tag{3.2.9}$$

Since we require that P and R are convex quadrilaterals, $0 < \theta_{i+1,P}, \theta_{i-1,R} < \pi$. Then (3.2.9) is only true whenever $\theta_{i+1,P} = \pi - \theta_{i-1,R}$ which is equivalent to the condition that $e_{i+1,P}$ and $e_{i+2,R}$ are collinear. Similarly, we'll require that $e_{i-1,P}$ and $e_{i+1,R}$ are

collinear - equivalently, $\theta_{i,P} = \pi - \theta_{i,R}$ - to make the second term of (3.2.8) have a coefficient of zero.

The last term is harder.

$$\left(\frac{1}{2A_{i+2,P}}\right)\left(\frac{|e_{i+2,P}|}{|e_{i,P}|}\right)\left(\frac{\sin(\theta_{i+2,P})}{\sin(\theta_{i+1,P})} - \frac{\sin(\theta_{i-1,P})}{\sin(\theta_{i,P})}\right)$$
$$+ \left(\frac{1}{2A_{i+1,R}}\right)\left(\frac{|e_{i+1,R}|}{|e_{i-1,R}|}\right)\left(\frac{\sin(\theta_{i+2,R})}{\sin(\theta_{i-1,R})} - \frac{\sin(\theta_{i+1,R})}{\sin(\theta_{i,R})}\right) \qquad (3.2.10)$$

Since we've enforced that $\theta_{i,P} = \pi - \theta_{i,R}$ and $\theta_{i+1,P} = \pi - \theta_{i-1,R}$, which implies that $\sin(\theta_{i,P}) = \sin(\theta_{i,R})$ and $\sin(\theta_{i+1,P}) = \sin(\theta_{i-1,R})$, so we can rewrite (3.2.10) as

$$\left(\frac{1}{|e_{i,P}|}\right)\left[\left(\frac{|e_{i+2,P}|}{2A_{i+2,P}}\right)\left(\frac{\sin(\theta_{i+2,P})}{\sin(\theta_{i+1,P})} - \frac{\sin(\theta_{i-1,P})}{\sin(\theta_{i,P})}\right)\right.$$
$$\left. + \left(\frac{|e_{i+1,R}|}{2A_{i+1,R}}\right)\left(\frac{\sin(\theta_{i+2,R})}{\sin(\theta_{i+1,P})} - \frac{\sin(\theta_{i+1,R})}{\sin(\theta_{i,P})}\right)\right]. \qquad (3.2.11)$$

Now this should be zero for every point on the shared edge, so consider the point $x_t := (1-t)v_{i,P} + tv_{i+1,P} = (1-t)v_{i,R} + tv_{i-1,R}$ for some $t \in [0,1]$. Then

$$2A_{i+2,P}(x_t) = (1-t)2C_{i-1,P} + t2C_{i+2,P}$$
$$= |e_{i+2,P}|((1-t)|e_{i-1,P}|\sin(\theta_{i-1,P}) + t|e_{i+1,P}|\sin(\theta_{i+2,P})), \qquad (3.2.12)$$

and

$$2A_{i+1,R}(x_t) = (1-t)2C_{i+1,R} + t2C_{i+2,R}$$
$$= |e_{i+1,R}|((1-t)|e_{i,R}|\sin(\theta_{i+1,R}) + t|e_{i+2,R}|\sin(\theta_{i+2,R})). \qquad (3.2.13)$$

Denote by $p_{1,1}$ the univariate polynomial given in (3.2.12) divided by $|e_{i+2,P}|$, and by $p_{1,2}$ the univariate polynomial given in (3.2.13) divided by $|e_{i+1,R}|$, so we can further

simplify (3.2.11) evaluated at the point x_t as

$$\left(\frac{1}{|e_{i,P}|}\right)\left[\left(\frac{1}{p_{1,1}}\right)\left(\frac{\sin(\theta_{i+2,P})}{\sin(\theta_{i+1,P})} - \frac{\sin(\theta_{i-1,P})}{\sin(\theta_{i,P})}\right)\right.$$
$$\left.+ \left(\frac{1}{p_{1,2}}\right)\left(\frac{\sin(\theta_{i+2,R})}{\sin(\theta_{i+1,P_1})} - \frac{\sin(\theta_{i+1,R})}{\sin(\theta_{i,P})}\right)\right]$$
$$= \left(\frac{1}{|e_{i,P}|p_{1,1}p_{1,2}}\right)\left[p_{1,2}\left(\frac{\sin(\theta_{i+2,P})}{\sin(\theta_{i+1,P})} - \frac{\sin(\theta_{i-1,P})}{\sin(\theta_{i,P})}\right)\right.$$
$$\left.+p_{1,1}\left(\frac{\sin(\theta_{i+2,R})}{\sin(\theta_{i+1,P})} - \frac{\sin(\theta_{i+1,R})}{\sin(\theta_{i,P})}\right)\right].$$

Define a vector V by

$$V := \left\langle \frac{\sin(\theta_{i+2,P})}{\sin(\theta_{i+1,P})} - \frac{\sin(\theta_{i-1,P})}{\sin(\theta_{i,P})}, \frac{\sin(\theta_{i+2,R})}{\sin(\theta_{i+1,P})} - \frac{\sin(\theta_{i+1,R})}{\sin(\theta_{i,P})} \right\rangle,$$

and rewrite (3.2.11) as

$$\left(\frac{1}{|e_{i,P}|p_{1,1}p_{1,2}}\right)\left((1-t)V \cdot \langle|e_{i,R}|\sin(\theta_{i+1,R}), |e_{i-1,P}|\sin(\theta_{i-1,P})\rangle\right.$$
$$\left. +t\, V \cdot \langle|e_{i+2,R}|\sin(\theta_{i+2,R}), |e_{i+1,P}|\sin(\theta_{i+2,P})\rangle\right).$$

We require this to be equal to 0 for every $t \in [0,1]$. Since t and $1-t$ are independent linear polynomials, this implies that we must have

$$V \cdot \langle|e_{i,R}|\sin(\theta_{i+1,R}), |e_{i-1,P}|\sin(\theta_{i-1,P})\rangle = 0 \tag{3.2.14}$$

$$\text{and } V \cdot \langle|e_{i+2,R}|\sin(\theta_{i+2,R}), |e_{i+1,P}|\sin(\theta_{i+2,P})\rangle = 0. \tag{3.2.15}$$

Then both of the right-hand vectors must be orthogonal to V, and hence are parallel to each other. Then we must have

$$|e_{i,R}|\sin(\theta_{i+1,R}) = K|e_{i+2,R}|\sin(\theta_{i+2,R})$$

$$\text{and } |e_{i-1,P}|\sin(\theta_{i-1,P}) = K|e_{i+1,P}|\sin(\theta_{i+2,P}),$$

64

for the same positive constant K, or, equivalently,

$$\frac{|e_{i,R}|\sin(\theta_{i+1,R})}{|e_{i+2,R}|\sin(\theta_{i+2,R})} = \frac{|e_{i-1,P}|\sin(\theta_{i-1,P})}{|e_{i+1,P}|\sin(\theta_{i+2,P})}. \tag{3.2.16}$$

These terms are heights of each quadrilateral. We use the updated Figure 3.4 to make some new notation:
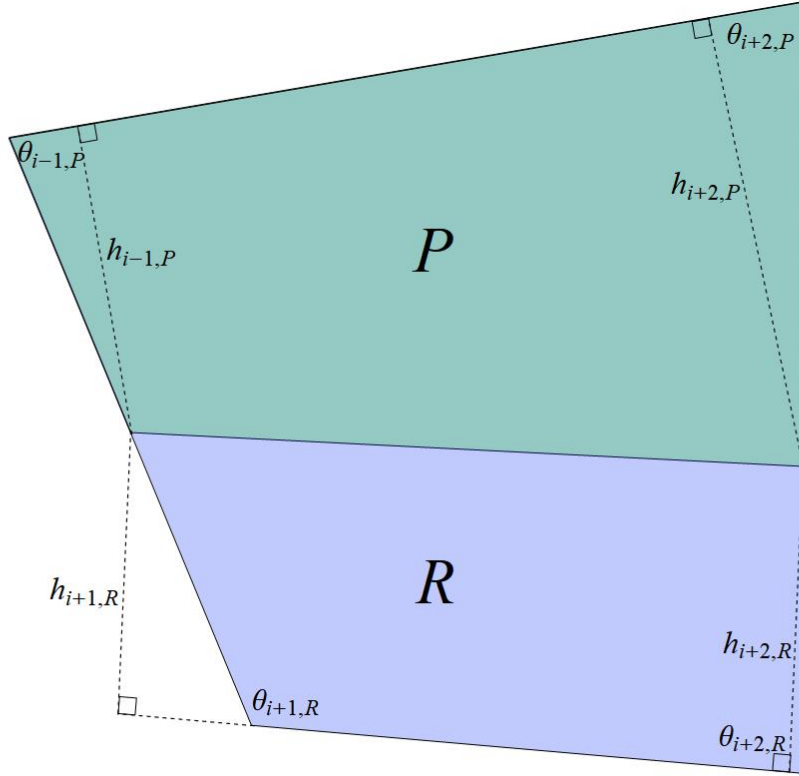
Figure 3.4: An updated figure which shows heights of each quadrilateral as dashed lines

Then we can rewrite (3.2.16) as the following:

$$\frac{h_{i+1,R}}{h_{i+2,R}} = \frac{h_{i-1,P}}{h_{i+2,P}}. \tag{3.2.17}$$

This is a hard condition to enforce across an entire partition. In particular, the
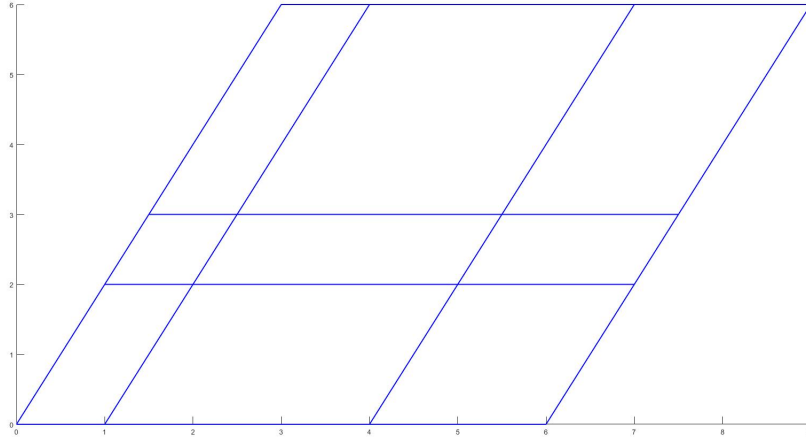
Figure 3.5: A skewed grid

other edges of P and R will generally be shared with other quadrilaterals as well, which means that more edges must remain collinear and more heights must have a common ratio.

However, consider the case $K = 1$. When applied to all heights of each quadrilateral, this implies that each quadrilateral is a parallelogram. Combined with the fact that the edges adjacent to shared edges must be collinear, this implies that an admissible partition must be a subpartition of a skewed grid, which is quite easy to enforce.

Within parallelograms, the areas C_j are all equal, so we may simplify the expression of $\psi_i^{(3)}$ in (3.2.4) as follows:

$$\psi_i^{(3)} = \phi_i^2 \left(\phi_i + 3(\phi_{i+1} + \phi_{i-1} + 3\phi_{i+2}) \right). \tag{3.2.18}$$

For each vertex v in $\mathcal{P}$, we define the basis spline $\psi_v^{(3)}$ by $\psi_{i,P}^{(3)}$ for each $P \in \Omega_v$, where $v = v_i$ in P, and 0 otherwise, and by construction, $\psi_v^{(3)}$ is globally C^1. The discussion in this section serves as a proof of the following:

Theorem 3.2.1. *Let Ω be a polygonal region in $\mathbb{R}^2$ which permits a skewed-grid partition as in Figure 3.5, and let $\mathcal{P}$ be such a skewed-grid partition of Ω. For every vertex v in the partition $\mathcal{P}$, define a polygonal spline $\psi_v^{(3)}$ over Ω_v by*

$$
\psi_v^{(3)}(\mathbf{x}) := \begin{cases} \psi_{i,P}^{(3)}(\mathbf{x}) & \mathbf{x} \in P \subseteq \Omega_v; v = v_{i,P} \\ 0 & \mathbf{x} \notin \Omega_v \end{cases},
$$

where $\psi_{i,P}^{(3)}$ is the function in (3.2.18).

Then $\psi_v^{(3)}$ satisfies the following properties:

(1) $\psi_v^{(3)}(w) = \delta_{v,w}$ for any vertex w of $\mathcal{P}$;

(2) $\nabla\psi_v^{(3)}(w) = 0$ for any vertex w of $\mathcal{P}$;

(3) $\psi_v^{(3)} \in C^1(\Omega)$; and

(4) $\sum_{v \in \mathcal{P}} \psi_v^{(3)} = 1$.

Figure 3.6 shows the plot of the function $\psi_v^{(3)}$ which smoothly interpolates values at a single vertex v over the partition shown in Figure 3.5.

3.2.2   Construction of $\psi_{x,v}^{(3)}$ and $\psi_{y,v}^{(3)}$

We'd like to have a greater span than just that of the functions $\psi_v^{(3)}$. While the condition (3.1.25) ensures that constant functions are in $\text{span}\{\psi_v^{(3)}\}$, we can be sure that even linear functions are not. In particular, the gradient of any linear combination of the functions $\psi_v^{(3)}$ vanishes at every vertex, a behavior which is both unusual and, possibly, undesirable. To augment our function space, it seems reasonable to give ourselves a tool with which to adjust the gradient at the vertices. To that end, we'll
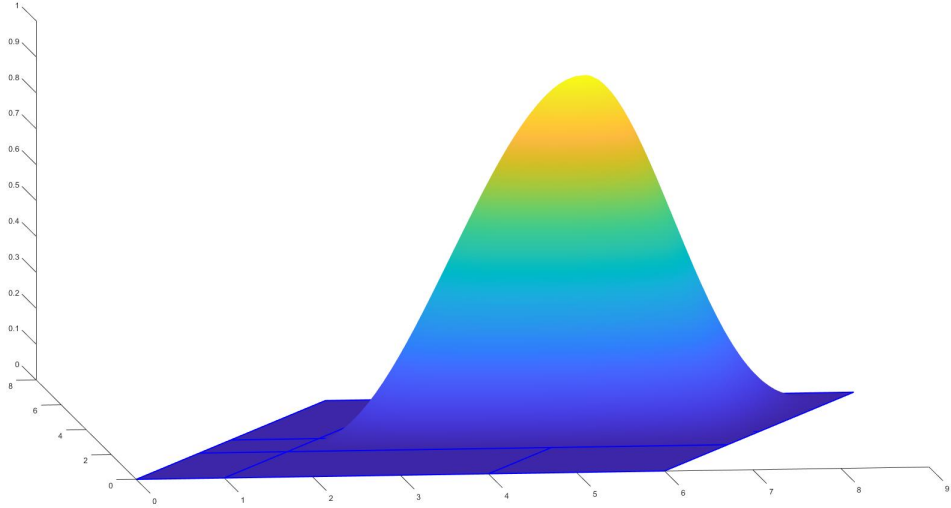
Figure 3.6: The plot of a function $\psi_v^{(3)}$

design functions $\psi_{x,v}^{(3)}$ and $\psi_{y,v}^{(3)}$ which satisfy the following for every vertex w:

$$\psi_{x,v}^{(3)}\big|_w = 0, \qquad\qquad \psi_{y,v}^{(3)}\big|_w = 0,$$

$$\nabla\psi_{x,v}^{(3)}\big|_w = \langle \delta_{v,w}, 0\rangle, \qquad\qquad \nabla\psi_{y,v}^{(3)}\big|_w = \langle 0, \delta_{v,w}\rangle.$$

We'll first focus on the construction of the function $\psi_{x,v}^{(3)}$; the $\psi_{y,v}^{(3)}$ case is very similar.

As in the previous section, we'll first focus our attention on a single quadrilateral $P \in \Omega_v$ such that $v = v_i$ in P. Let $\psi_{x,i,P}^{(3)} := \psi_{x,v}^{(3)}\big|_P$; again, we'll suppress the subscript P while we are focused on solely this quadrilateral. In terms of the geometry of P, we need $\psi_{x,i}^{(3)}$ to satisfy

$$\psi_{x,i}^{(3)}\big|_{v_j} = 0, \tag{3.2.19}$$

$$\nabla\psi_{x,i}^{(3)}\big|_{v_j} = \langle \delta_{ij}, 0\rangle. \tag{3.2.20}$$

First, to ensure locality, we will again require that ϕ_i^2 is a factor of $\psi_{x,i}$. Then we

have the same template as in (3.2.1):

$$\psi_{x,i}^{(3)} = \phi_i^2(J_{0,i}\phi_i + J_{1,i}\phi_{i+1} + J_{2,i}\phi_{i-1} + K_{0,i}\phi_{i+2}), \tag{3.2.21}$$

where the notation $J_{0,i}$, $J_{1,i}$, $J_{2,i}$, and $K_{0,i}$ is reused to represent the constant coefficients of $\psi_{x,i}^{(3)}$.

Since $\psi_{x,i}^{(3)}\big|_{v_i} = J_{0,i}$, the condition (3.2.19) is enough to inform us that $J_{0,i} = 0$. We use (3.2.20) to determine $J_{1,i}$ and $J_{2,i}$ by taking edge-direction derivatives at v_i. We require that

$$\frac{\partial \psi_{x,i}}{\partial \tilde{e}_i}\bigg|_{v_i} = \frac{e_{i,x}}{|e_i|}, \text{ and} \tag{3.2.22}$$

$$\frac{\partial \psi_{x_i}}{\partial \tilde{e}_{i-1}}\bigg|_{v_i} = \frac{e_{i-1,x}}{|e_{i-1}|}. \tag{3.2.23}$$

We take these edge-direction derivatives from (3.2.21):

$$\frac{\partial \psi_{x,i}}{\partial \tilde{e}_i}\bigg|_{v_i} = J_{1,i}\frac{\partial \phi_{i+1}}{\partial \tilde{e}_i} = \frac{J_{1,i}}{|e_i|}, \text{ and}$$

$$\frac{\partial \psi_{x,i}}{\partial \tilde{e}_{i-1}}\bigg|_{v_i} = J_{2,i}\frac{\partial \phi_{i-1}}{\partial \tilde{e}_{i-1}} = \frac{-J_{2,i}}{|e_{i-1}|}.$$

Thus we set $J_{1,i} = e_{i,x}$ and $J_{2,i} = -e_{i-1,x}$.

We can find $K_{0,i}$ by considering the same scenario as is illustrated in Figure 3.3, but using the new requirements we set at the end of the previous section - especially that both P and R are parallelograms. In this case, we can substantially simplify the normal derivatives computed in Lemma 3.1.1. In particular, we take advantage

of the following geometric conveniences of parallelograms:

$$\vec{e}_i = -\vec{e}_{i+2}; \ \vec{e}_{i+1} = \vec{e}_{i-1};$$

$$\theta_i = \pi - \theta_{i+1} = \theta_{i+2} = \pi - \theta_{i-1};$$

$$C := C_i = C_{i+1} = C_{i+2} = C_{i-1}.$$

Then we can see that

$$A_{i+2}\big|_{e_i} = C_{i-1}\phi_i + C_{i+2}\phi_{i+1} = C(\phi_i + \phi_{i+1}) = C,$$

and finally we see that

$$\frac{\partial \phi_i}{\partial \vec{n}_i}\bigg|_{e_i} = \phi_i \frac{|e_i|}{2C} - \frac{|e_{i-1}|\cos(\theta_i)}{2C},$$

$$\frac{\partial \phi_{i+1}}{\partial \vec{n}_i}\bigg|_{e_i} = \phi_{i+1}\frac{|e_i|}{2C} + \frac{|e_{i-1}|\cos(\theta_i)}{2C},$$

$$\frac{\partial \phi_{i-1}}{\partial \vec{n}_i}\bigg|_{e_i} = -\phi_i \frac{|e_i|}{2C},$$

$$\frac{\partial \phi_{i+2}}{\partial \vec{n}_i}\bigg|_{e_i} = -\phi_{i+1}\frac{|e_i|}{2C}. \tag{3.2.24}$$

Now we use (3.2.24) along with the fact that $(\phi_i + \phi_{i+1})|_{e_i} = 1$ to compute the outward normal derivatives of $\psi_{x,i}^{(3)}$:

$$\frac{\partial \psi_{x,i}^{(3)}}{\partial \vec{n}_i}\bigg|_{e_i} = \frac{\partial \phi_i}{\partial \vec{n}_i}(2e_{i,x}\phi_i\phi_{i+1}) + \frac{\partial \phi_{i+1}}{\partial \vec{n}_i}(e_{i,x}\phi_i^2) + \frac{\partial \phi_{i-1}}{\partial \vec{n}_i}(-e_{i-1,x}\phi_i^2) + \frac{\partial \phi_{i+2}}{\partial \vec{n}_i}(K_{0,i}\phi_i^2)$$

$$= \phi_i^3\left(e_{i-1,x}\frac{|e_i|}{2C} + e_{i,x}\frac{|e_{i-1}|\cos(\theta_i)}{2C}\right)$$

$$+ \phi_i^2\phi_{i+1}\left((3e_{i,x} - K_{0,i})\frac{|e_i|}{2C} - e_{i,x}\frac{|e_{i-1}|\cos(\theta_i)}{2C}\right) +$$

$$+ \phi_i\phi_{i+1}^2\left(-2e_{i,x}\frac{|e_{i-1}|\cos(\theta_i)}{2C}\right).$$

70

We ought to have $\left.\dfrac{\partial \psi_{x,i}^{(3)}}{\partial \vec{n}_i}\right|_{v_i} = n_{i,x} = \dfrac{e_{i,y}}{|e_i|}$, since $\nabla \psi_{x,i}^{(3)} = \langle 1, 0 \rangle$. In fact, that's exactly what we have. If we consider the unit vectors $\tilde{e}_i$ and $\tilde{e}_{i-1}$, we see we can rotate one to the other by the angle $\pi - \theta_i$, which informs us that

$$
\begin{aligned}
\frac{e_{i-1}}{|e_{i-1}|} &= \begin{pmatrix} -\cos(\theta_i) & \sin(\theta_i) \\ -\sin(\theta_i) & -\cos(\theta_i) \end{pmatrix} \frac{e_i}{|e_i|} \\
&= \frac{1}{|e_i|} \begin{pmatrix} -e_{i,x} \cos(\theta_i) + e_{i,y} \sin(\theta_i) \\ -e_{i,x} \sin(\theta_i) - e_{i,y} \cos(\theta_i) \end{pmatrix},
\end{aligned} \tag{3.2.25}
$$

and, similarly,

$$
\frac{e_i}{|e_i|} = \frac{1}{|e_{i-1}|} \begin{pmatrix} -e_{i-1,x} \cos(\theta_i) - e_{i-1,y} \sin(\theta_i) \\ e_{i-1,x} \sin(\theta_i) - e_{i-1,y} \cos(\theta_i) \end{pmatrix}.
$$

Then we have

$$
\begin{aligned}
\left.\frac{\partial \psi_{x,i}^{(3)}}{\partial \vec{n}_i}\right|_{e_i} &= \phi_i^3 \left(\frac{e_{i,y}}{|e_i|} \right) \\
&\quad + \phi_i^2 \phi_{i+1} \left((3e_{i,x} - K_{0,i}) \frac{|e_i|}{2C} - e_{i,x} \frac{|e_{i-1}| \cos(\theta_i)}{2C} \right) + \\
&\quad + \phi_i \phi_{i+1}^2 \left(-2e_{i,x} \frac{|e_{i-1}| \cos(\theta_i)}{2C} \right).
\end{aligned} \tag{3.2.26}
$$

Similarly, we compute

$$
\begin{aligned}
\left.\frac{\partial \psi_{x,i}^{(3)}}{\partial \vec{n}_{i-1}}\right|_{e_{i-1}} &= \phi_i^3 \left(\frac{e_{i-1,y}}{|e_{i-1}|} \right) \\
&\quad + \phi_i^2 \phi_{i-1} \left((-3e_{i-1,x} - K_{0,i}) \frac{|e_{i-1}|}{2C} + e_{i-1,x} \frac{|e_i| \cos(\theta_i)}{2C} \right) \\
&\quad + \phi_i \phi_{i-1}^2 \left(2e_{i-1,x} \frac{|e_i| \cos(\theta_i)}{2C} \right),
\end{aligned} \tag{3.2.27}
$$

71

so in terms of the quadrilaterals P and R from Figure 3.3, we have

$$
\left.\frac{\partial \psi^{(3)}_{x,i,P}}{\partial \vec{n}_{i,P}}\right|_{e_{i,P}} + \left.\frac{\partial \psi^{(3)}_{x,i,R}}{\partial \vec{n}_{i-1,R}}\right|_{e_{i-1,R}} =
$$

$$
\phi^3_{i,P}\left(\frac{e_{i,y,P}}{|e_{i,P}|} + \frac{e_{i-1,y,R}}{|e_{i-1,R}|}\right)
$$

$$
+ \phi^2_{i,P}\phi_{i+1,P}\left((3e_{i,x,P} - K_{0,i,P})\frac{|e_{i,P}|}{2C_P} - e_{i,x,P}\frac{|e_{i-1,P}|\cos(\theta_{i,P})}{2C_P}\right.
$$

$$
\left. +(-3e_{i-1,x,R} - K_{0,i,R})\frac{|e_{i-1,R}|}{2C_R} + e_{i-1,x,R}\frac{|e_{i,R}|\cos(\theta_{i,R})}{2C_R}\right)
$$

$$
+ \phi_{i,P}\phi^2_{i+1,P}\left(-2e_{i,x,P}\frac{|e_{i-1,P}|\cos(\theta_{i,P})}{2C_P} + 2e_{i-1,x,R}\frac{|e_{i,R}|\cos(\theta_{i,R})}{2C_R}\right)
$$

$$
= \frac{\phi^2_{i,P}\phi_{i+1,P}}{\sin(\theta_{i,P})}\left(\frac{3e_{i,x,P} - K_{0,i,P}}{|e_{i-1,P}|} + \frac{-3e_{i-1,x,R} - K_{0,i,R}}{|e_{i,R}|}\right).
$$

There's not a unique solution for $K_{0,i}$, but in the interest of having each function defined only by the geometry of the quadrilateral it's defined over, we'll set $K_{0,i} = 3(e_{i,x} - e_{i-1,x})$ to have

$$
\left.\frac{\partial \psi^{(3)}_{x,i,P}}{\partial \vec{n}_{i,P}}\right|_{e_{i,P}} + \left.\frac{\partial \psi^{(3)}_{x,i,R}}{\partial \vec{n}_{i-1,R}}\right|_{e_{i-1,R}}
$$

$$
= \frac{\phi^2_{i,P}\phi_{i+1,P}}{\sin(\theta_{i,P})}\left(\frac{3e_{i-1,x,P}}{|e_{i-1,P}|} - \frac{3e_{i,x,R}}{|e_{i,R}|}\right)
$$

$$
= \frac{3\phi^2_{i,P}\phi_{i+1,P}}{\sin(\theta_{i,P})}\left(\tilde{e}_{i-1,x,P} - \tilde{e}_{i,x,R}\right).
$$

Since we required that $\vec{e}_{i-1,P}$ and $\vec{e}_{i,R}$ are collinear, then their unit vectors are parallel, and based on the counter-clockwise orientation of P and R, in fact we have $\tilde{e}_{i-1,P} = \tilde{e}_{i,R}$, so that

$$
\left.\frac{\partial \psi^{(3)}_{x,i,P}}{\partial \vec{n}_{i,P}}\right|_{e_{i,P}} + \left.\frac{\partial \psi^{(3)}_{x,i,R}}{\partial \vec{n}_{i-1,R}}\right|_{e_{i-1,R}} = 0.
$$

Conveniently, this choice of $K_{0,i}$ also satisfies

$$\sum_{i=1}^{4} v_{i,x}\psi_i^{(3)} + \psi_{x,i}^{(3)} = x, \tag{3.2.28}$$

which we can check using similar steps as we took in (3.2.2) and (3.2.3). First we compute x as a cubic Wachspress function:

$$x = \left(\sum_{j=1}^{4} v_{j,x}\phi_j\right)\left(\sum_{k=1}^{4} \phi_k\right)^2$$

$$= \sum_{j=1}^{4} v_{j,x}\phi_j^3 + (2v_{j,x} + v_{j+1,x})\phi_j^2\phi_{j+1} + (2v_{j,x} + v_{j-1,x})\phi_j^2\phi_{j-1}$$

$$+ (4v_{j,x} + 2(v_{j+1,x} + v_{j-1,x}) + v_{j+2,x})B\phi_j. \tag{3.2.29}$$

Expanding the sum on the left-hand side of (3.2.28) will reveal the same expression as (3.2.29).

Therefore, we conclude

$$\psi_{x,i}^{(3)} = \phi_i^2(e_{i,x}\phi_{i+1} - e_{i-1,x}\phi_{i-1} + 3(e_{i,x} - e_{i-1,x})\phi_{i+2}). \tag{3.2.30}$$

A nearly identical analysis will yield

$$\psi_{y,i}^{(3)} = \phi_i^2(e_{i,y}\phi_{i+1} - e_{i-1,y}\phi_{i-1} + 3(e_{i,y} - e_{i-1,y})\phi_{i+2}), \tag{3.2.31}$$

which has the analogous property that

$$\sum_{i=1}^{4} v_{i,y}\psi_i^{(3)} + \psi_{y,i}^{(3)} = y. \tag{3.2.32}$$

As in the previous section, for each vertex v in $\mathcal{P}$, we define the C^1 basis splines $\psi_{x,v}^{(3)}$ and $\psi_{y,v}^{(3)}$ by $\psi_{x,i,P}^{(3)}$ and $\psi_{y,i,P}^{(3)}$, respectively, in each $P \in \Omega_v$ where $v = v_i$ in P, and

0 otherwise. Then by construction, we have the following:

Theorem 3.2.2. *Let Ω be a polygonal region in $\mathbb{R}^2$ which permits a skewed-grid partition as in Figure 3.5, and let $\mathcal{P}$ be such a skewed-grid partition of Ω. For every vertex v in the partition $\mathcal{P}$, define polygonal splines $\psi_{x,v}^{(3)}$ and $\psi_{y,v}^{(3)}$ over Ω_v by*

$$\psi_{x,v}^{(3)}(\mathbf{x}) := \begin{cases} \psi_{x,i,P}^{(3)}(\mathbf{x}) & \mathbf{x} \in P \subseteq \Omega_v; v = v_{i,P} \\ 0 & \mathbf{x} \notin \Omega_v \end{cases}$$

$$\text{and } \psi_{y,v}^{(3)}(\mathbf{x}) := \begin{cases} \psi_{y,i,P}^{(3)}(\mathbf{x}) & \mathbf{x} \in P \subseteq \Omega_v; v = v_{i,P} \\ 0 & \mathbf{x} \notin \Omega_v \end{cases}$$

where $\psi_{x,i,P}^{(3)}$ is the function given in (3.2.30) and $\psi_{y,i,P}^{(3)}$ is the function given in (3.2.31).

Then $\psi_{x,v}^{(3)}$ and $\psi_{y,v}^{(3)}$ satisfy the following properties:

(1) $\psi_{x,v}^{(3)}(w) = \psi_{y,v}^{(3)}(w) = 0$ for any vertex w of $\mathcal{P}$;

(2) $\nabla\psi_{x,v}^{(3)}(w) = \langle \delta_{v,w}, 0 \rangle$ and $\nabla\psi_{y,v}^{(3)}(w) = \langle 0, \delta_{v,w} \rangle$ for any vertex w of $\mathcal{P}$;

(3) $\psi_{x,v}^{(3)}, \psi_{y,v}^{(3)} \in C^1(\Omega)$; and

(4) $\sum\limits_{v \in \mathcal{P}} v_x \psi_v^{(3)} + \psi_{x,v}^{(3)} = x$ and $\sum\limits_{v \in \mathcal{P}} v_y \psi_v^{(3)} + \psi_{y,v}^{(3)} = y$.

Figures 3.7a and 3.7b show plots of the functions $\psi_{x,v}^{(3)}$ and $\psi_{y,v}^{(3)}$ at the same vertex v of the same partition used in Figure 3.6.

3.2.3 Construction of $\psi_{x^2,v}^{(3)}$, $\psi_{y^2,v}^{(3)}$, and $\psi_{xy,v}^{(3)}$

It's reasonable to expect to be able to extend further. After all, the full span of all degree-3 Wachspress functions over a polygon P contains all degree-3 bivariate polynomials over P, so it is at least plausible that we could extend our span to contain this polynomial subspace as well. In fact, we can do just that.
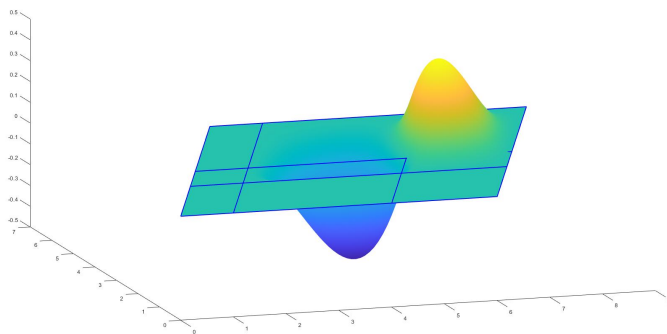
(a) The plot of a function $\psi_{x,v}^{(3)}$
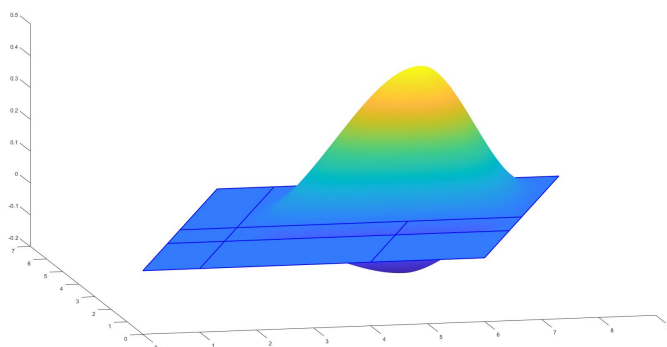
(b) The plot of a function $\psi_{y,v}^{(3)}$

Figure 3.7: Plots of degree-3 gradient-adjustment basis splines

We'll start by extending our span to include x^2. Again, let's first restrict our attention to a single quadrilateral P.

As things stand, the most natural approximation of the function x^2 over P using our current basis functions is

$$I_{x^2}^{(3)} := \sum_{i=1}^{4} v_{i,x}^2 \psi_i^{(3)} + 2 v_{i,x} \psi_{x,i}^{(3)}.$$

It is simple to check that $I_{x^2}^{(3)}$ is not equal to x^2; we can express x^2 as a cubic Wachspress function as we did for the constant function 1 in (3.2.2) and for the function x

in (3.2.29), and then evaluate the difference $x^2 - I_{x^2}^{(3)}$:

$$x^2 - I_{x^2}^{(3)} = \sum_{i=1}^{4} -2e_{i,x}e_{i-1,x}\phi_i^2\phi_{i+2}.$$

The obvious choice to make is to define a function

$$\psi_{x^2,i}^{(3)} = -e_{i,x}e_{i-1,x}\phi_i^2\phi_{i+2}, \tag{3.2.33}$$

so that $x^2 = \sum_{i=1}^{4} v_{i,x}^2\psi_i^{(3)} + 2v_{i,x}\psi_{x,i}^{(3)} + 2\psi_{x^2,i}^{(3)}$. Similar analyses of xy and y^2 produce functions

$$\psi_{y^2,i}^{(3)} = -e_{i,y}e_{i-1,y}\phi_i^2\phi_{i+2} \tag{3.2.34}$$

$$\text{and } \psi_{xy,i}^{(3)} = -(e_{i,x}e_{i-1,y} + e_{i,y}e_{i-1,x})\phi_i^2\phi_{i+2}. \tag{3.2.35}$$

These functions disappear on the boundary of the quadrilateral, so they will certainly join continuously across shared edges. In fact, they join C^1-smoothly. We'll check $\psi_{x^2,i}^{(3)}$.

$$\left.\frac{\partial\psi_{x^2,i}^{(3)}}{\partial\vec{n}_i}\right|_{e_i} = -e_{i,x}e_{i-1,x}\phi_i^2\frac{\partial\phi_{i+2}}{\partial\vec{n}_i}$$

$$= \frac{|e_i|}{2C}e_{i,x}e_{i-1,x}\phi_i^2$$

$$= \frac{e_{i-1,x}}{|e_{i-1}|}\frac{e_{i,x}}{\sin(\theta_i)}\phi_i^2;$$

$$\left.\frac{\partial\psi_{x^2,i}^{(3)}}{\partial\vec{n}_{i-1}}\right|_{e_{i-1}} = -e_{i,x}e_{i-1,x}\phi_i^2\frac{\partial\phi_{i+2}}{\partial\vec{n}_{i-1}}$$

$$= \frac{|e_{i-1}|}{2C}e_{i,x}e_{i-1,x}\phi_i^2$$

$$= \frac{e_{i,x}}{|e_i|}\frac{e_{i-1,x}}{\sin(\theta_i)}\phi_i^2.$$

Then, if we return to the adjacent quadrilaterals P and R in Figure 3.3, we use the facts that $\theta_{i,P} = \pi - \theta_{i,R}$, $\vec{e}_{i,P} = -\vec{e}_{i-1,R}$, and $\tilde{e}_{i-1,P} = \tilde{e}_{i,R}$ to show

$$\left.\frac{\partial \psi^{(3)}_{x^2,i,P}}{\partial \vec{n}_{i,P}}\right|_{e_{i,P}} + \left.\frac{\partial \psi^{(3)}_{x^2,i,R}}{\partial \vec{n}_{i-1,R}}\right|_{e_{i-1,R}} = \phi^2_{i,P} \left(\frac{e_{i-1,x,P}}{|e_{i-1,P}|}\frac{e_{i,x,P}}{\sin(\theta_{i,P})} + \frac{e_{i,x,R}}{|e_{i,R}|}\frac{e_{i-1,x,R}}{\sin(\theta_{i,R})}\right)$$

$$= \phi^2_{i,P}\frac{e_{i,x,P}}{|e_{i,P}|}\left(\tilde{e}_{i-1,x,P} - \tilde{e}_{i,x,R}\right)$$

$$= 0.$$

We can similarly show that $\psi^{(3)}_{y^2,i}$ and $\psi^{(3)}_{xy,i}$ join smoothly over shared edges.

Hence, for each vertex v in $\mathcal{P}$, we define C^1 splines $\psi^{(3)}_{x^2,v}$, $\psi^{(3)}_{y^2,v}$, and $\psi^{(3)}_{xy,v}$ as we did for $\psi^{(3)}_v$, $\psi^{(3)}_{x,v}$, and $\psi^{(3)}_{y,v}$. Figure 3.8 shows a plot of the function $\psi^{(3)}_{x^2,v}$ at the same vertex v of the same partition $\mathcal{P}$ used for the plots in Figures 3.6 and 3.7. However, we can't add each of these as basis splines, because they are in fact constant multiples of each other, so we simply include one of them.
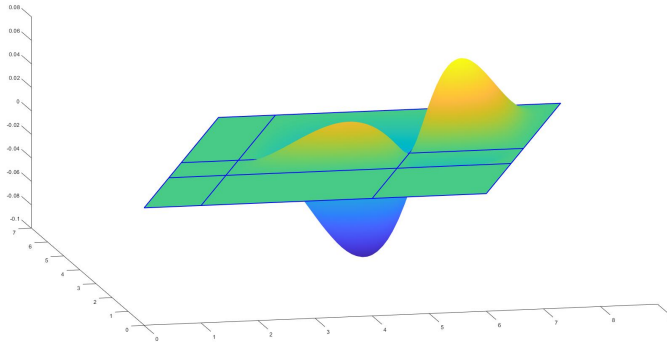
Figure 3.8: The plot of a function $\psi^{(3)}_{x^2,v}$

Note that it's possible one or more of these functions may be zero. In fact, on rectangular grid partitions which are aligned with the x and y axes, all three of them will be zero. For convenience, we'll still use the distinct notation for each of the 3 functions, but keep in mind that the total dimension of our space is only 4 times the number of vertices - or 3 times the number of vertices for rectangular grid partitions

which are aligned with the x and y axes.

By construction, we can use our previously built vertex splines along with these functions $\psi_{x^2,v}^{(3)}$, $\psi_{y^2,v}^{(3)}$, and $\psi_{xy,v}^{(3)}$ to recover degree-2 polynomials, but we can actually use them to recover degree-3 polynomials as well. It's not difficult to show the following:

$$x^3 = \sum_v v_x^3 \psi_v^{(3)} + 3v_x^2 \psi_{x,v}^{(3)} + 6v_x \psi_{x^2,v}^{(3)},$$

$$y^3 = \sum_v v_y^3 \psi_v^{(3)} + 3v_y^2 \psi_{y,v}^{(3)} + 6v_y \psi_{y^2,v}^{(3)},$$

$$x^2 y = \sum_v v_x^2 v_y \psi_v^{(3)} + 2v_x v_y \psi_{x,v}^{(3)} + v_x^2 \psi_{y,v}^{(3)} + 2v_y \psi_{x^2,v}^{(3)} + 2v_x \psi_{xy,v}^{(3)}, \text{ and}$$

$$xy^2 = \sum_v v_x v_y^2 \psi_v^{(3)} + v_y^2 \psi_{x,v}^{(3)} + 2v_x v_y \psi_{y,v}^{(3)} + 2v_x \psi_{y^2,v}^{(3)} + 2v_y \psi_{xy,v}^{(3)}.$$

The discussions in this section, along with the rest of this chapter, serves as a proof of the following:

Theorem 3.2.3. *Let Ω be a polygonal region in $\mathbb{R}^2$ which permits a skewed-grid partition as in Figure 3.5, and let $\mathcal{P}$ be such a skewed-grid partition of Ω. For every vertex v in the partition $\mathcal{P}$, define polygonal splines $\psi_{x^2,v}^{(3)}$, $\psi_{y^2,v}^{(3)}$, and $\psi_{xy,v}^{(3)}$ over Ω_v by*

$$\psi_{x^2,v}^{(3)}(\mathbf{x}) := \begin{cases} \psi_{x^2,i,P}^{(3)}(\mathbf{x}) & \mathbf{x} \in P \subseteq \Omega_v; \ v = v_{i,P} \\ 0 & \mathbf{x} \notin \Omega_v \end{cases}$$

$$\psi_{y^2,v}^{(3)}(\mathbf{x}) := \begin{cases} \psi_{y^2,i,P}^{(3)}(\mathbf{x}) & \mathbf{x} \in P \subseteq \Omega_v; \ v = v_{i,P} \\ 0 & \mathbf{x} \notin \Omega_v \end{cases}$$

$$\text{and } \psi_{xy,v}^{(3)}(\mathbf{x}) := \begin{cases} \psi_{xy,i,P}^{(3)}(\mathbf{x}) & \mathbf{x} \in P \subseteq \Omega_v; \ v = v_{i,P} \\ 0 & \mathbf{x} \notin \Omega_v \end{cases}$$

where $\psi_{x^2,i,P}^{(3)}$, $\psi_{y^2,i,P}^{(3)}$, and $\psi_{xy,i,P}^{(3)}$ are the functions defined in (3.2.33), (3.2.34), and (3.2.35).

Then $\psi_{x^2,v}^{(3)}$, $\psi_{y^2,v}^{(3)}$, *and* $\psi_{xy,v}^{(3)}$ *satisfy the following properties:*

(1) $\psi_{x^2,v}^{(3)}(w) = \psi_{y^2,v}^{(3)}(w) = \psi_{xy,v}^{(3)}(w) = 0$ *for any vertex* w *of* $\mathcal{P}$;

(2) $\nabla\psi_{x^2,v}^{(3)}(w) = \nabla\psi_{y^2,v}^{(3)}(w) = \nabla\psi_{xy,v}^{(3)}(w) = 0$ *for any vertex* w *of* $\mathcal{P}$;

(3) $\psi_{x^2,v}^{(3)}, \psi_{y^2,v}^{(3)}, \psi_{xy,v}^{(3)} \in C^1(\Omega)$;

(4) $\sum\limits_{v\in\mathcal{P}} v_x^2\psi_v^{(3)} + 2v_x\psi_{x,v}^{(3)} + 2\psi_{x^2,v}^{(3)} = x^2, \ \sum\limits_{v\in\mathcal{P}} v_y^2\psi_v^{(3)} + 2v_y\psi_{y,v}^{(3)} + 2\psi_{y^2,v}^{(3)} = y^2$

$\sum\limits_{v\in\mathcal{P}} v_xv_y\psi_v^{(3)} + v_y\psi_{x,v}^{(3)} + v_y\psi_{y,v}^{(3)} + \psi_{xy,v}^{(3)} = xy$,

(5) *The functions* $\psi_{x^2,v}^{(3)}$, $\psi_{y^2,v}^{(3)}$, *and* $\psi_{xy,v}^{(3)}$ *are constant multiples of each other, with the exception that some of them may be zero depending on the geometry of* $\mathcal{P}$;

(6) *Where* $\Psi_3^1(\mathcal{P}) := span\{\psi_v^{(3)}, \psi_{x,v}^{(3)}, \psi_{y,v}^{(3)}, \psi_{x^2,v}^{(3)}, \psi_{y^2,v}^{(3)}, \psi_{xy,v}^{(3)}\}_{v\in\mathcal{P}}$, $dim(\Psi_3(\mathcal{P})) = c|V|$, *where* $c = 3$ *if* $\mathcal{P}$ *is a rectangular grid aligned with the* x *and* y *axes, and* $c = 4$ *otherwise;*

(7) $\Pi_3 \subseteq \Psi_3^1(\mathcal{P})$.

Over parallelograms, an interesting phenomenon arises:

Theorem 3.2.4. *Let* P *be a parallelogram. Then the Wachspress coordinates of* P *are not rational functions, but in fact are degree-2 polynomials.*

Proof. Since all areas C_j of a parallelogram P are equal, we may as well label them all C. This, combined with the facts that e_i and e_{i+2} are parallel and the functions

A_j are linear and zero on the edge e_j, makes it easy to see that $A_{i+2} = C - A_i$. Then

$$
\begin{aligned}
\phi_i &= \frac{C_i A_{i+1} A_{i+2}}{\sum\limits_{j=1}^{4} C_j A_{j+1} A_{j+2}} \\
&= \frac{A_{i+1} A_{i+2}}{A_i A_{i+1} + A_{i+1} A_{i+2} + A_{i+2} A_{i-1} + A_{i-1} A_i} \\
&= \frac{A_{i+1} A_{i+2}}{(A_i + A_{i+2})(A_{i+1} + A_{i-1})} \\
&= \frac{A_{i+1} A_{i+2}}{C^2}.
\end{aligned}
\tag{3.2.36}
$$

$\square$

Therefore, our space $\Psi_3(\mathcal{P})$ is actually the same space as the space of tensor-product C^1 bicubic splines over $\mathcal{P}$. While it would be nice if this were a truly new space, this work so far has two main benefits. First, $\Psi_3(\Omega)$ has a nice basis which eases some of the workload when using tensor-product C^1 bicubic splines. Second, the techniques we used will be useful in the upcoming cases, where we use higher-degree polynomials of Wachspress coordinates to allow ourselves the flexibility to extend which partitions are admissible, along with increasing polynomial approximation power.

3.3 Approximation properties of $\Psi_3^1(\mathcal{P})$

Let $\Omega \subset \mathbb{R}^2$ be a polygonal region which admits a skewed-grid partition, and let $\mathcal{P}$ be such a skewed-grid partition of Ω. We consider a series of uniform refinements of $\mathcal{P}$; denote by $\mathcal{P}_k$ the kth uniform refinement of $\mathcal{P}$.

Using techniques from [20] and Chapter 2, we can show the following:

Theorem 3.3.1. *For any function $f \in C^3(\Omega)$, there exists a polygonal spline $s_{f,k}^{(3)} \in \Psi_3^1(\mathcal{P}_k)$ such that*

$$
||f - s_{f,k}^{(3)}||_{\infty,\Omega} \leq C|f|_{3,\infty,\Omega} 2^{-3k}
$$

where C is a positive constant independent of f.

Theorem 3.3.2. *For any function $f \in C^3(\Omega)$, there exists a polygonal spline $s_{f,k}^{(3)} \in \Psi_3^1(\mathcal{P}_k)$ such that*

$$||f - s_{f,k}^{(3)}||_{2,\Omega} \leq C|f|_{3,2,\Omega} 2^{-3k}$$

and

$$|f - s_{f,k}^{(3)}|_{1,2,\Omega} \leq C|f|_{3,2,\Omega} 2^{-2k}$$

for a constant C which is independent of u, but may be dependent on the boundary of Ω if Ω is nonconvex.

See Chapter 4 Section 4.3 for some numerical results using an improvement of the polygonal spline space detailed in this Chapter.

3.4   Increasing to degree 4

Let us now consider building a similar space, this time using degree-4 Wachspress functions. We'd start by building functions $\psi_v^{(4)}$ functions from the previous section. The natural next step would be to build $\psi_{x,v}^{(4)}, \psi_{y,v}^{(4)}$ and the like to construct a new function space $\Psi_4(\mathcal{P})$. However, it happens that $\Psi_4(\mathcal{P})$ is not a C^1 linear space over any more general partitions than our already-constructed space $\Psi_3(\mathcal{P})$ - the interested reader is welcome to complete the similar calculations, and will see that, while $\psi_v^{(4)}$ does permit more general partitions, adding analogous functions $\psi_{x,v}^{(4)}$ and $\psi_{y,v}^{(4)}$ will force us to resort to the same partition restrictions as in the degree-3 case. However, $\Psi_4(\mathcal{P})$ could allow us to extend our span to contain all degree-4 polynomials. We'll skip the details of this case and move on to the more interesting case of $\Psi_5(\mathcal{P})$, which permits more general partitions.

Chapter 4

A Degree-5 Construction of C^1 Polygonal Splines on Parallelogram Partitions

4.1 Degree-5 C^1 polygonal vertex splines

4.1.1 Construction of $\psi_v^{(5)}$

We'll build a degree-5 polygonal spline function which is analogous to $\psi_v^{(3)}$. As before, we start by first focusing on a single quadrilateral P where $v = v_i$ in P, and let $\psi_v^{(5)}\big|_P = \psi_{i,P}^{(5)}$, with the requirement that ϕ_i^2 divides $\psi_i^{(5)}$ to ensure locality. A template for our function, then, can be given by

$$
\begin{aligned}
\psi_i^{(5)} = \phi_i^2 \big(& J_{0,i}\phi_i^3 + \phi_i^2(J_{1,i}\phi_{i+1} + J_{2,i}\phi_{i-1}) \\
& + \phi_i(J_{3,i}\phi_{i+1}^2 + J_{4,i}\phi_{i-1}^2) + J_{5,i}\phi_{i+1}^3 + J_{6,i}\phi_{i-1}^3 \\
& + \phi_{i+2}\big(K_{0,i}\phi_i^2 + \phi_i(K_{1,i}\phi_{i+1} + K_{2,i}\phi_{i-1}) + K_{3,i}\phi_{i+1}^2 + K_{4,i}\phi_{i-1}^2\big) \\
& + \phi_{i+2}^2\big(S_{0,i}\phi_i + S_{1,i}\phi_{i+1} + S_{2,i}\phi_{i-1} + S_{3,i}\phi_{i+2}\big)\big).
\end{aligned} \tag{4.1.1}
$$

We choose different letters to name coefficients of terms which are divisible by different powers B. In particular, terms which have no factors of B are given coefficients J; these terms affect values on the edge, and thus are used to enforce continuity and to manipulate edge-direction derivatives at vertices. Terms which have a single factor of B are given coefficients K; these terms affect C^1 smoothness on edges. Terms which have two factors of B (the maximum possible using degree 5) are given coefficients S; these terms are more or less free, but we'll be able to determine them (at least to some extent) by sum conditions.

To remind the reader, we wish for our function $\psi_i^{(5)}$ to satisfy the following properties:

$$\psi_i^{(5)}\Big|_{v_j} = \delta_{ij}, \tag{4.1.2}$$

$$\nabla \psi_i^{(5)}\Big|_{v_j} = 0, \tag{4.1.3}$$

$$\sum_{j=1}^{4} \psi_j^{(5)} = 1. \tag{4.1.4}$$

Since $\psi_i^{(5)}\big|_{v_i} = J_{0,i}$, property (4.1.2) informs us that $J_{0,i} = 1$. To determine $J_{1,i}$ and $J_{2,i}$, we take edge-direction derivatives at v_i:

$$\frac{\partial \psi_i^{(5)}}{\partial \tilde{e}_i}\Big|_{v_i} = \frac{J_{1,i} - 5}{|e_i|} \text{ and}$$

$$\frac{\partial \psi_i^{(5)}}{\partial \tilde{e}_{i-1}}\Big|_{v_i} = \frac{J_{2,i} - 5}{|e_{i-1}|},$$

By property (4.1.3), both these derivatives should be equal to zero. Therefore, we'll set $J_{1,i} = J_{2,i} = 5$.

Skipping a bit of experimentation which was required in the development of these functions, we simply mention that the additional flexibility which comes with increasing the degree to 5 affords us the ability to control the Hessian at the vertices

with a C^1 basis. With this in mind, we anticipate the construction of some functions $\psi_{x^2,i}^{(5)}, \psi_{y^2,i}^{(5)}$, and $\psi_{xy,i}^{(5)}$ which will allow us to control second derivatives at a vertex. To make the implementation of these functions easier, we will include an additional property for $\psi_i^{(5)}$:

$$\nabla^2 \psi_i^{(5)}\big|_{v_j} = 0. \tag{4.1.5}$$

To satisfy this additional property, we will check some second derivatives of $\psi_i^{(5)}$. The second derivatives in each edge direction are easy to compute, since Wachspress coordinates are linear on the edges:

$$\begin{aligned}
\frac{\partial^2 \psi_i^{(5)}}{\partial \tilde{e}_i^2}\bigg|_{e_i} &= \frac{\partial}{\partial \tilde{e}_i}\left(\frac{\partial \phi_i}{\partial \tilde{e}_i}\left(5\phi_i^4 + 20\phi_i^3\phi_{i+1} + 3J_{3,i}\phi_i^2\phi_{i+1}^2 + 2J_{5,i}\phi_i\phi_{i+1}^3\right)\right.\\
&\qquad\left. + \frac{\partial \phi_{i+1}}{\partial \tilde{e}_i}\left(5\phi_i^4 + 2J_{3,i}\phi_i^3\phi_{i+1} + 3J_{5,i}\phi_i^2\phi_{i+1}^2\right)\right)\\
&= \left(\frac{\partial \phi_i}{\partial \tilde{e}_i}\right)^2\left(20\phi_i^3 + 60\phi_i^2\phi_{i+1} + 6J_{3,i}\phi_i\phi_{i+1}^2 + 2J_{5,i}\phi_{i+1}^3\right)\\
&\qquad + \frac{\partial \phi_i}{\partial \tilde{e}_i}\frac{\partial \phi_{i+1}}{\partial \tilde{e}_i}\left(40\phi_i^3 + 12J_{3,i}\phi_i^2\phi_{i+1} + 12J_{5,i}\phi_i\phi_{i+1}^2\right)\\
&\qquad + \left(\frac{\partial \phi_{i+1}}{\partial \tilde{e}_i}\right)^2\left(2J_{3,i}\phi_i^3 + 6J_{5,i}\phi_i^2\phi_{i+1}\right)\\
\Rightarrow \frac{\partial^2 \psi_i^{(5)}}{\partial \tilde{e}_i^2}\bigg|_{v_i} &= \frac{2J_{3,i} - 20}{|e_i|^2};\\
\frac{\partial^2 \psi_i^{(5)}}{\partial \tilde{e}_i^2}\bigg|_{v_{i+1}} &= \frac{2J_{5,i}}{|e_i|^2}.
\end{aligned}$$

This informs us that we should set $J_{3,i} = 10$ and $J_{5,i} = 0$. A similar computation in the direction $\tilde{e}_{i-1}$ informs us that $J_{4,i} = 10$ and $J_{6,i} = 0$.

There remains the computation of the mixed-direction derivative, $\dfrac{\partial^2 \psi_i^{(5)}}{\partial \tilde{e}_i \partial \tilde{e}_{i-1}}$. This computation is not particularly difficult either, but it does require that we know the mixed-direction derivatives of the Wachspress coordinates at the vertices. We compute these now, starting with the edge-direction derivatives of the functions w_j

84

given in (3.1.2):

$$\frac{\partial w_i}{\partial e_i}\bigg|_{v_i} = \frac{C_i C_{i+1}}{|e_i|}(C_{i+2} - 2C_{i-1}); \qquad \frac{\partial w_i}{\partial e_{i-1}}\bigg|_{v_i} = \frac{C_i C_{i-1}}{|e_{i-1}|}(2C_{i+1} - C_{i+2});$$

$$\frac{\partial w_{i+1}}{\partial e_i}\bigg|_{v_i} = \frac{C_i C_{i+1}}{|e_i|}C_{i-1}; \qquad \frac{\partial w_{i+1}}{\partial e_{i-1}}\bigg|_{v_i} = 0;$$

$$\frac{\partial w_{i-1}}{\partial e_i}\bigg|_{v_i} = 0; \qquad \frac{\partial w_{i-1}}{\partial e_{i-1}}\bigg|_{v_i} = \frac{C_i C_{i-1}}{|e_{i-1}|}(-C_{i+1});$$

$$\frac{\partial w_{i+2}}{\partial e_i}\bigg|_{v_i} = 0; \qquad \frac{\partial w_{i+2}}{\partial e_{i-1}}\bigg|_{v_i} = 0;$$

$$\sum_{j=1}^{4} \frac{\partial w_j}{\partial e_i}\bigg|_{v_i} = \frac{C_i C_{i+1}}{|e_i|}(C_{i+2} - C_{i-1}); \qquad \sum_{j=1}^{4} \frac{\partial w_j}{\partial e_{i-1}}\bigg|_{v_i} = \frac{C_i C_{i-1}}{|e_{i-1}|}(C_{i+1} - C_{i+2});$$

$$\frac{\partial^2 w_i}{\partial e_i \partial e_{i-1}}\bigg|_{v_i} = \frac{C_i}{|e_i||e_{i-1}|}(C_i C_{i+2} - 2C_{i+1} C_{i-1});$$

$$\frac{\partial^2 w_{i+1}}{\partial e_i \partial e_{i-1}}\bigg|_{v_i} = \frac{C_i}{|e_i||e_{i-1}|}C_{i-1} C_{i+1};$$

$$\frac{\partial^2 w_{i-1}}{\partial e_i \partial e_{i-1}}\bigg|_{v_i} = \frac{C_i}{|e_i||e_{i-1}|}C_{i-1} C_{i+1};$$

$$\frac{\partial^2 w_{i+2}}{\partial e_i \partial e_{i-1}}\bigg|_{v_i} = \frac{C_i}{|e_i||e_{i-1}|}(-C_i C_{i+2});$$

$$\sum_{j=1}^{4} \frac{\partial^2 w_j}{\partial e_i \partial e_{i-1}}\bigg|_{v_i} = 0.$$

We use the above to compute the following mixed-direction derivatives of the Wachspress coordinates at the vertices:

$$\frac{\partial^2 \phi_i}{\partial e_i \partial e_{i-1}}\bigg|_{v_i} = \frac{-C_{i+2}^2}{|e_i||e_{i-1}|C_{i+1}C_{i-1}};$$

$$\frac{\partial^2 \phi_{i+1}}{\partial e_i \partial e_{i-1}}\bigg|_{v_i} = \frac{C_{i+2}}{|e_i||e_{i-1}|C_{i+1}};$$

$$\frac{\partial^2 \phi_{i-1}}{\partial e_i \partial e_{i-1}}\bigg|_{v_i} = \frac{C_{i+2}}{|e_i||e_{i-1}|C_{i-1}};$$

$$\frac{\partial^2 \phi_{i+2}}{\partial e_i \partial e_{i-1}}\bigg|_{v_i} = \frac{-C_i C_{i+2}}{|e_i||e_{i-1}|C_{i+1}C_{i-1}}. \tag{4.1.6}$$

Using (4.1.6), we can compute the mixed-direction derivatives in edge directions. We can save ourselves some work by noting that, since $\phi_i\big|_{e_{i+1}} = \phi_i\big|_{e_{i+2}} = 0$ and ϕ_i^2 is a factor of $\psi_i^{(5)}$, then the following derivatives are all zero:

$$\frac{\partial^2 \psi_i^{(5)}}{\partial \tilde{e}_{i-1} \partial \tilde{e}_{i+2}}\bigg|_{v_{i-1}}, \quad \frac{\partial^2 \psi_i^{(5)}}{\partial \tilde{e}_i \partial \tilde{e}_{i+1}}\bigg|_{v_{i+1}}, \quad \frac{\partial^2 \psi_i^{(5)}}{\partial \tilde{e}_{i+1} \partial \tilde{e}_{i+2}}\bigg|_{v_{i+2}}$$

It remains to compute the mixed-direction derivative at v_i - this will involve the coefficient $K_{0,i}$.

$$\begin{aligned}
\frac{\partial^2 \psi_i^{(5)}}{\partial \tilde{e}_i \partial \tilde{e}_{i-1}}\bigg|_{v_i} &= \frac{\partial}{\partial \tilde{e}_i}\left(\frac{\partial \phi_i}{\partial \tilde{e}_{i-1}}\left(5\phi_i^4 + 20\phi_i^3\phi_{i+1} + 20\phi_i^3\phi_{i-1}\right)\right.\\
&\quad\left. + \frac{\partial \phi_{i+1}}{\partial \tilde{e}_{i-1}}\left(5\phi_i^4\right) + \frac{\partial \phi_{i-1}}{\partial \tilde{e}_{i-1}}\left(5\phi_i^4\right) + \frac{\partial \phi_{i+2}}{\partial \tilde{e}_{i-1}}\left(K_{0,i}\phi_i^4\right)\right)\\
&= 5\frac{\partial^2 \phi_i}{\partial \tilde{e}_i \partial \tilde{e}_{i-1}} + 20\frac{\partial \phi_i}{\partial \tilde{e}_i}\frac{\partial \phi_i}{\partial \tilde{e}_{i-1}} + 20\frac{\partial \phi_i}{\partial \tilde{e}_{i-1}}\frac{\partial \phi_{i+1}}{\partial \tilde{e}_i} + 5\frac{\partial^2 \phi_{i+1}}{\partial \tilde{e}_i \partial \tilde{e}_{i-1}}\\
&\quad + 20\frac{\partial \phi_i}{\partial \tilde{e}_i}\frac{\partial \phi_{i-1}}{\partial \tilde{e}_{i-1}} + 5\frac{\partial^2 \phi_{i-1}}{\partial \tilde{e}_i \partial \tilde{e}_{i-1}} + K_{0,i}\frac{\partial^2 \phi_{i+2}}{\partial \tilde{e}_i \partial \tilde{e}_{i-1}}\\
&= \frac{20}{|e_i||e_{i-1}|} + \frac{5C_{i+2}(C_{i-1} + C_{i+1} - C_{i+2}) - K_{0,i}C_iC_{i+2}}{C_{i+1}C_{i-1}|e_i||e_{i-1}|}.
\end{aligned}$$

It is clear that the full area of the quadrilateral P is given by $C_i + C_{i+2} = C_{i+1} - C_{i-1}$, so we note that $C_{i+1} + C_{i-1} - C_{i+2} = C_i$. Then we have

$$\frac{\partial^2 \psi_i^{(5)}}{\partial \tilde{e}_i \partial \tilde{e}_{i-1}}\bigg|_{v_i} = \frac{20C_{i+1}C_{i-1} + (5 - K_{0,i})C_iC_{i+2}}{C_{i+1}C_{i-1}|e_i||e_{i-1}|}.$$

Thus, in order to satisfy (4.1.5), we set $K_{0,i} = 5 + 20\dfrac{C_{i+1}C_{i-1}}{C_iC_{i+2}}$. Our results so far

have yielded the following:

$$\psi_i^{(5)} = \phi_i^2 \bigg(\phi_i^3 + 5\phi_i^2(\phi_{i+1} + \phi_{i-1}) + 10\phi_i(\phi_{i+1}^2 + \phi_{i-1}^2)$$

$$+ \phi_{i+2}\bigg(\bigg(5 + 20\frac{C_{i+1}C_{i-1}}{C_iC_{i+2}}\bigg)\phi_i^2 + \phi_i(K_{1,i}\phi_{i+1} + K_{2,i}\phi_{i-1})$$

$$+ K_{3,i}\phi_{i+1}^2 + K_{4,i}\phi_{i-1}^2 \bigg)$$

$$+ \phi_{i+2}^2\left(S_{0,i}\phi_i + S_{1,i}\phi_{i+1} + S_{2,i}\phi_{i-1} + S_{3,i}\phi_{i+2}\right) \bigg). \tag{4.1.7}$$

The remainder of the K coefficients will be determined by C^1 smoothness over shared edges. We start by taking the usual outward normal derivatives $\left.\dfrac{\partial \psi_i^{(5)}}{\partial \vec{n}_i}\right|_{e_i}$ and $\left.\dfrac{\partial \psi_i^{(5)}}{\partial \vec{n}_{i-1}}\right|_{e_{i-1}}$; after substantial simplification, we retrieve

$$\left.\frac{\partial \psi_i^{(5)}}{\partial \vec{n}_i}\right|_{e_i} = \phi_i^3\phi_{i+1}^2\bigg(30\bigg(\frac{|e_i|}{2C_i} - \frac{|e_{i-1}|\cos(\theta_i)}{2C_i}\bigg) + (20 - K_{1,i})\frac{|e_i|C_{i+2}}{2C_{i-1}C_{i+1}}\bigg)$$

$$+ \phi_i^2\phi_{i+1}^3\bigg(30\frac{|e_{i+1}|\cos(\theta_{i+1})}{2C_{i+1}} - K_{3,i}\frac{|e_i|}{2C_{i+1}}\bigg)$$

$$+ \bigg(\frac{C_{i-1} - C_{i+2}}{C_{i+1}}\bigg)\frac{|e_i|}{2A_{i+2}}\phi_i^3\phi_{i+1}^3\bigg(K_{3,i} + C_{i+2}\bigg(\frac{30}{C_i} + \frac{20 - K_{1,i}}{C_{i-1}}\bigg)\bigg);$$

$$\left.\frac{\partial \psi_i^{(5)}}{\partial \vec{n}_{i-1}}\right|_{e_{i-1}} = \phi_i^3\phi_{i-1}^2\bigg(30\bigg(\frac{|e_{i-1}|}{2C_i} - \frac{|e_i|\cos(\theta_i)}{2C_i}\bigg) + (20 - K_{2,i})\frac{|e_{i-1}|C_{i+2}}{2C_{i-1}C_{i+1}}\bigg)$$

$$+ \phi_i^2\phi_{i-1}^3\bigg(30\frac{|e_{i+2}|\cos(\theta_{i-1})}{2C_{i-1}} - K_{4,i}\frac{|e_{i-1}|}{2C_{i-1}}\bigg)$$

$$+ \bigg(\frac{C_{i+1} - C_{i+2}}{C_{i-1}}\bigg)\frac{|e_{i-1}|}{2A_{i+1}}\phi_i^3\phi_{i-1}^3\bigg(K_{4,i} + C_{i+2}\bigg(\frac{30}{C_i} + \frac{20 - K_{2,i}}{C_{i+1}}\bigg)\bigg).$$

Considering two adjacent quadrilaterals P and R as before, we'll want the following

sum to be zero:

$$
\left.\frac{\partial \psi_{i,P}^{(5)}}{\partial \vec{n}_{i,P}}\right|_{e_{i,P}} + \left.\frac{\partial \psi_{i,R}^{(5)}}{\partial \vec{n}_{i-1,R}}\right|_{e_{i-1,R}} = \tag{4.1.8}
$$

$$
\phi_{i,P}^3 \phi_{i+1,P}^2 \left(30 \left(\frac{|e_{i,P}|}{2C_{i,P}} - \frac{|e_{i-1,P}| \cos(\theta_{i,P})}{2C_{i,P}} + \frac{|e_{i-1,R}|}{2C_{i,R}} - \frac{|e_{i,R}| \cos(\theta_{i,R})}{2C_{i,R}} \right) \right.
$$

$$
\left. + (20 - K_{1,i,P}) \frac{|e_{i,P}| C_{i+2,P}}{2C_{i-1,P} C_{i+1,P}} + (20 - K_{2,i,R}) \frac{|e_{i-1,R}| C_{i+2,R}}{2C_{i-1,R} C_{i+1,R}} \right)
$$

$$
+ \phi_{i,P}^2 \phi_{i+1,P}^3 \left(30 \left(\frac{|e_{i+1,P}| \cos(\theta_{i+1,P})}{2C_{i+1,P}} + \frac{|e_{i+2,R}| \cos(\theta_{i-1,R})}{2C_{i-1,R}} \right) \right.
$$

$$
\left. - K_{3,i,P} \frac{|e_{i,P}|}{2C_{i+1,P}} - K_{4,i,R} \frac{|e_{i-1,R}|}{2C_{i-1,R}} \right)
$$

$$
+ \left(\frac{C_{i-1,P} - C_{i+2,P}}{C_{i+1,P}} \right) \frac{|e_{i,P}|}{2A_{i+2,P}} \phi_{i,P}^3 \phi_{i+1,P}^3 \left(K_{3,i,P} + C_{i+2,P} \left(\frac{30}{C_{i,P}} + \frac{20 - K_{1,i,P}}{C_{i-1,P}} \right) \right)
$$

$$
+ \left(\frac{C_{i+1,R} - C_{i+2,R}}{C_{i-1,R}} \right) \frac{|e_{i-1,R}|}{2A_{i+1,R}} \phi_{i,P}^3 \phi_{i+1,P}^3 \left(K_{4,i,R} + C_{i+2,R} \left(\frac{30}{C_{i,R}} + \frac{20 - K_{2,i,R}}{C_{i+1,R}} \right) \right).
$$

The last two lines here are rational terms, with linear denominators, with their numerators both $\phi_{i,P}^3 \phi_{i+1,P}^3$ times a constant. There are 3 cases to consider here.

If the linear functions $A_{i+2,P}\big|_{e_{i,P}}$ and $A_{i+1,R}\big|_{e_{i-1,R}}$ are not constant multiples of each other, then there is no hope of any cancellation in (4.1.8). Therefore, if we want (4.1.8) to be zero, the coefficients on these rational terms must be zero. One possibility is to require that $C_{i-1,P} = C_{i+2,P}$ and $C_{i+1,R} = C_{i+2,R}$. Using the notation in Figure 3.4, this is equivalent to requiring that

$$
h_{i-1,P} = h_{i+2,P} \text{ and } h_{i+1,R} = h_{i+2,R}.
$$

Applied to an entire partition $\mathcal{P}$ of many quadrilaterals, this is equivalent to requiring that all quadrilaterals in $\mathcal{P}$ are parallelograms. Technically, this results in $A_{i+2,P}\big|_{e_{i,P}}$ and $A_{i+1,R}\big|_{e_{i-1,R}}$ remaining constant on the shared edge, which means they are of course constant multiples of each other, which is not in the spirit of this case. Therefore, we'll save this as our last case.

Otherwise, we'll need to require that the coefficients written at the end of the lines with rational terms in (4.1.8) are zero, so we require

$$K_{3,i} = (K_{1,i} - 20)\frac{C_{i+2}}{C_{i-1}} - 30\frac{C_{i+2}}{C_i} \text{ and}$$

$$K_{4,i} = (K_{2,i} - 20)\frac{C_{i+2}}{C_{i+1}} - 30\frac{C_{i+2}}{C_i},$$

which allows us to simplify (4.1.8) to retrieve

$$\left.\frac{\partial \psi_{i,P}^{(5)}}{\partial \vec{n}_{i,P}}\right|_{e_{i,P}} + \left.\frac{\partial \psi_{i,R}^{(5)}}{\partial \vec{n}_{i-1,R}}\right|_{e_{i-1,R}} = \tag{4.1.9}$$

$$\phi_{i,P}^3 \phi_{i+1,P}^2 \left(30 \left(\frac{|e_{i,P}|}{2C_{i,P}} - \frac{|e_{i-1,P}| \cos(\theta_{i,P})}{2C_{i,P}} + \frac{|e_{i-1,R}|}{2C_{i,R}} - \frac{|e_{i,R}| \cos(\theta_{i,R})}{2C_{i,R}} \right) \right.$$

$$\left. + (20 - K_{1,i,P})\frac{|e_{i,P}|C_{i+2,P}}{2C_{i-1,P}C_{i+1,P}} + (20 - K_{2,i,R})\frac{|e_{i-1,R}|C_{i+2,R}}{2C_{i-1,R}C_{i+1,R}} \right)$$

$$+ \phi_{i,P}^2 \phi_{i+1,P}^3 \left(30 \left(\frac{|e_{i+1,P}| \cos(\theta_{i+1,P})}{2C_{i+1,P}} + \frac{|e_{i,P}|C_{i+2,P}}{2C_{i,P}C_{i+1,P}} \right.\right.$$

$$\left. + \frac{|e_{i+2,R}| \cos(\theta_{i-1,R})}{2C_{i-1,R}} + \frac{|e_{i-1,R}|C_{i+2,R}}{2C_{i,R}C_{i-1,R}} \right)$$

$$\left. + (20 - K_{1,i,P})\frac{|e_{i,P}|C_{i+2,P}}{2C_{i-1,P}C_{i+1,P}} + (20 - K_{2,i,R})\frac{|e_{i-1,R}|C_{i+2,R}}{2C_{i-1,R}C_{i+1,R}} \right).$$

The terms involving $K_{1,i}$ and $K_{2,i}$ in (4.1.9) are identical in both coefficients, so both these coefficients can simultaneously be zero only if the remaining terms are equal; we need to enforce

$$\frac{|e_{i,P}|}{2C_{i,P}} \left(\frac{C_{i+1,P} - C_{i+2,P}}{C_{i+1,P}} \right) - \frac{|e_{i-1,P}| \cos(\theta_{i,P})}{2C_{i,P}} - \frac{|e_{i+1,P}| \cos(\theta_{i+1,P})}{2C_{i+1,P}}$$

$$= \frac{|e_{i-1,R}|}{2C_{i,R}} \left(\frac{C_{i+2,R} - C_{i-1,R}}{C_{i-1,R}} \right) + \frac{|e_{i,R}| \cos(\theta_{i,R})}{2C_{i,R}} + \frac{|e_{i+2,R}| \cos(\theta_{i-1,R})}{2C_{i-1,R}}.$$

While there are some geometric assumptions on $\mathcal{P}$ which can satisfy this, we weren't able to find anything intuitive or more minimal than the aforementioned possibility of forcing all quadrilaterals in $\mathcal{P}$ to be parallelograms. Therefore, we'll dismiss this

case.

We now consider the case that $A_{i+2,P}\big|_{e_{i,P}} = mA_{i+1,R}\big|_{e_{i-1,R}}$ for some constant m. We can solve for this constant m at each vertex:

$$A_{i+2,P}\big|_{v_{i,P}} = C_{i-1,P}, \quad A_{i+1,R}\big|_{v_{i,R}} = C_{i+1,R} \qquad \Rightarrow m = \frac{C_{i+1,R}}{C_{i-1,P}}$$

$$A_{i+2,P}\big|_{v_{i+1,P}} = C_{i+2,P}, \quad A_{i+1,R}\big|_{v_{i-1,R}} = C_{i+2,R} \qquad \Rightarrow m = \frac{C_{i+2,R}}{C_{i+2,P}}$$

Therefore, this case only occurs when

$$\frac{C_{i+2,P}}{C_{i-1,P}} = \frac{C_{i+2,R}}{C_{i+1,R}}$$

$$\Rightarrow \frac{|e_{i+1,P}|\sin(\theta_{i+2,P})}{|e_{i-1,P}|\sin(\theta_{i-1,P})} = \frac{|e_{i+2,R}|\sin(\theta_{i+2,R})}{|e_{i,R}|\sin(\theta_{i+1,R})}$$

$$\Rightarrow \frac{h_{i+2,P}}{h_{i-1,P}} = \frac{h_{i+2,R}}{h_{i+1,R}},$$

which is the same condition as we set in (3.2.17). As discussed there, we must require that the ratio of the heights shown in Figure 3.4 be the same in P and R. As before, this condition is too abstract and non-intuitive to enforce unless we require the ratio to be 1, which in general forces all quadrilaterals in $\mathcal{P}$ to be parallelograms.

All signs point us to require that $\mathcal{P}$ is a partition of parallelograms. While any geometric restriction is undesirable, this situation is at least more robust than the partitions which our degree-3 analysis permitted: with the absence of any requirement of collinearity of edges, we see far more robust behavior, and even admit *extraordinary points* - vertices on the interior of $\mathcal{P}$ which have a valence not equal to 4. An example of such a partition is shown in Figure 4.1.
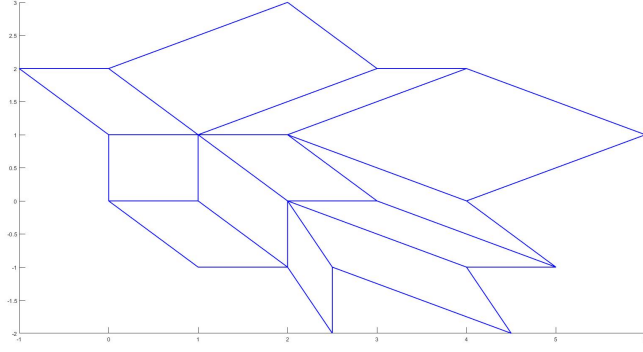
Figure 4.1: A partition of parallelograms

Exploiting parallelogram geometry, we are able to simplify (4.1.8) to

$$
\left.\frac{\partial \psi_{i,P}^{(5)}}{\partial \vec{n}_{i,P}}\right|_{e_{i,P}} + \left.\frac{\partial \psi_{i,R}^{(5)}}{\partial \vec{n}_{i-1,R}}\right|_{e_{i-1,R}} =
$$

$$
\phi_{i,P}^3 \phi_{i+1,P}^2 \left((50 - K_{1,i,P})\frac{|e_{i,P}|}{2C_P} + (50 - K_{2,i,R})\frac{|e_{i-1,R}|}{2C_R} \right.
$$

$$
\left. -30\left(\frac{|e_{i-1,P}|\cos(\theta_{i,P})}{2C_P} + \frac{|e_{i,R}|\cos(\theta_{i,R})}{2C_R} \right) \right)
$$

$$
+ \phi_{i,P}^2 \phi_{i+1,P}^3 \left(-30\left(\frac{|e_{i-1,P}|\cos(\theta_{i,P})}{2C_P} + \frac{|e_{i,R}|\cos(\theta_{i,R})}{2C_R} \right) \right.
$$

$$
\left. - K_{3,i,P}\frac{|e_{i,P}|}{2C_P} - K_{4,i,R}\frac{|e_{i-1,R}|}{2C_R} \right). \tag{4.1.10}
$$

We can make (4.1.10) zero by setting

$$
K_{1,i} = 50 - 30\frac{|e_{i-1}|}{|e_i|}\cos(\theta_i), \qquad K_{2,i} = 50 - 30\frac{|e_i|}{|e_{i-1}|}\cos(\theta_i),
$$

$$
K_{3,i} = -30\frac{|e_{i-1}|}{|e_i|}\cos(\theta_i), \qquad K_{4,i} = -30\frac{|e_i|}{|e_{i-1}|}\cos(\theta_i).
$$

In fact, these choices of coefficients will give us that $\left.\dfrac{\partial \psi_i^{(5)}}{\partial \vec{n}_i}\right|_{e_i} = \left.\dfrac{\partial \psi_i^{(5)}}{\partial \vec{n}_{i-1}}\right|_{e_{i-1}} = 0.$

The S coefficients can be found by computing the difference $1 - \sum_{j=1}^{4} \psi_j^{(5)}$, using the

fact that $1 = \left(\sum\limits_{j=1}^{4} \phi_j \right)^5$:

$$1 - \sum_{j=1}^{4} \psi_j^{(5)} = -B^2 C^4 \sum_{j=1}^{4} \phi_j \left(100 - S_{0,j} - S_{1,j+1} - S_{2,j-1} - S_{3,j+2} \right). \qquad (4.1.11)$$

Of course, there is not a unique set of values for the S coefficients to make (4.1.11) zero. We'll simply put everything into the $S_{0,i}$ coefficients, setting $S_{0,i} = 100$.

Then we retrieve the final result

$$\psi_i^{(5)} = \phi_i^2 \Bigg(\phi_i^3 + 5\phi_i^2 \left(\phi_{i+1} + \phi_{i-1} \right) + 10\phi_i \left(\phi_{i+1}^2 + \phi_{i-1}^2 \right)$$
$$+ \phi_{i+2} \Bigg(25\phi_i^2 + \phi_i \left(\left(50 - 30 \frac{|e_{i-1}|}{|e_i|} \cos(\theta_i) \right) \phi_{i+1} \right.$$
$$+ \left(50 - 30 \frac{|e_i|}{|e_{i-1}|} \cos(\theta_i) \right) \phi_{i-1} \Bigg)$$
$$- 30 \cos(\theta_i) \left(\frac{|e_{i-1}|}{|e_i|} \phi_{i+1}^2 + \frac{|e_i|}{|e_{i-1}|} \phi_{i-1}^2 \right) + 100\phi_i\phi_{i+2} \Bigg) \Bigg). \qquad (4.1.12)$$

As with our prior constructions, for every vertex v in $\mathcal{P}$, define the C^1 vertex splines $\psi_v^{(5)}$ by $\psi_{i,P}^{(5)}$ in each parallelogram $P \in \Omega_v$ where $v = v_i$ in P, and zero otherwise. The discussion in this section serves as a proof of the following:

Theorem 4.1.1. *Let Ω be a polygonal region in $\mathbb{R}^2$ which permits a partition by parallelograms as in Figure 4.1, and let $\mathcal{P}$ be such a parallelogram partition of Ω. For every vertex v in the partition $\mathcal{P}$, define a polygonal spline $\psi_v^{(5)}$ over Ω_v by*

$$\psi_v^{(5)}(\mathbf{x}) := \begin{cases} \psi_{i,P}^{(5)}(\mathbf{x}) & \mathbf{x} \in P \subseteq \Omega_v; \ v = v_{i,P} \\ 0 & \mathbf{x} \notin \Omega_v, \end{cases}$$

where $\psi_{i,P}^{(5)}$ is the function in (4.1.12).

Then $\psi_v^{(5)}$ satisfies the following properties:

(1) $\psi_v^{(5)}(w) = \delta_{v,w}$ for any vertex w of $\mathcal{P}$;

(2) $\nabla \psi_v^{(5)}(w) = 0$ *for any vertex w of $\mathcal{P}$;*

(3) $\nabla^2 \psi_v^{(5)}(w) = 0$ *for any vertex w of $\mathcal{P}$;*

(4) $\psi_v^{(5)} \in C^1(\Omega)$; *and*

(5) $\sum_{v \in \mathcal{P}} \psi_v^{(5)} = 1$.

The plot of a function $\psi_v^{(5)}$ over the paralellogram partition shown in Figure 4.1 is shown in Figure 4.2
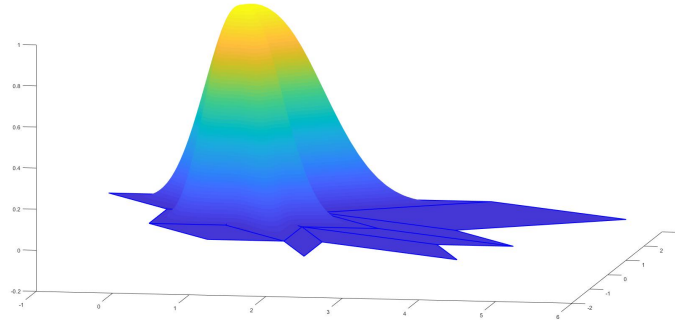
Figure 4.2: The plot of a function $\psi_v^{(5)}$

4.1.2 Construction of $\psi_{x,v}^{(5)}$ and $\psi_{y,v}^{(5)}$

As in the degree-3 case, we'll proceed from here to build functions $\psi_{x,v}^{(5)}$ and $\psi_{y,v}^{(5)}$ to extend the span of our C^1 vertex spline space to include linear polynomials. Just like before, we'll focus on $\psi_{x,v}^{(5)}$ first, and we'll begin by restricting our attention to a single parallelogram P in Ω_v, with $v = v_i$ in P and $\psi_{x,i,P}^{(5)} := \psi_{x,v}^{(5)}\big|_P$.

To remind the reader, we aim to satisfy the properties

$$\psi_{x,i}^{(5)}\big|_{v_j} = 0, \tag{4.1.13}$$

$$\nabla\psi_{x,i}^{(5)}\big|_{v_j} = \langle \delta_{ij}, 0\rangle, \tag{4.1.14}$$

$$\sum_{j=1}^{4} v_{j,x}\psi_j^{(5)} + \psi_{j,x}^{(5)} = x, \tag{4.1.15}$$

and we add the additional condition

$$\nabla^2\psi_{x,i}^{(5)}\big|_{v_j} = 0. \tag{4.1.16}$$

We can use the same template given in (4.1.1), and the condition (4.1.13) informs us that $J_{0,i} = 0$. We can compute the edge-direction derivatives at v_i by

$$\frac{\partial\psi_{x,i}^{(5)}}{\partial\tilde{e}_i}\bigg|_{v_i} = \frac{J_{1,i}}{|e_i|}; \qquad\qquad \frac{\partial\psi_{x,i}^{(5)}}{\partial\tilde{e}_{i-1}}\bigg|_{v_i} = \frac{-J_{2,i}}{|e_{i-1}|}.$$

By (4.1.14), we should have $\dfrac{\partial\psi_{x,i}^{(5)}}{\partial\tilde{e}_i}\bigg|_{v_i} = \dfrac{e_{i,x}}{|e_i|}$ and $\dfrac{\partial\psi_{x,i}^{(5)}}{\partial\tilde{e}_{i-1}}\bigg|_{v_i} = \dfrac{e_{i-1,x}}{|e_{i-1}|}$, so we'll set $J_{1,i} = e_{i,x}$ and $J_{2,i} = -e_{i-1,x}$.

To satisfy (4.1.16), we need to consider the second edge-direction derivatives at the vertices. First, notice that

$$\frac{\partial^2\psi_{x,i}^{(5)}}{\partial\tilde{e}_i^2}\bigg|_{v_{i+1}} = \frac{2J_{5,i}}{|e_i|^2}, \text{ and}$$

$$\frac{\partial^2\psi_{x,i}^{(5)}}{\partial\tilde{e}_{i-1}^2}\bigg|_{v_{i-1}} = \frac{2J_{6,i}}{|e_{i-1}|^2},$$

94

so we should set $J_{5,i} = J_{6,i} = 0$. Next, we compute

$$
\left. \frac{\partial^2 \psi_{x,i}^{(5)}}{\partial \tilde{e}_i^2} \right|_{v_i} = \frac{2J_{3,i} - 8e_{i,x}}{|e_i|^2},
$$

$$
\left. \frac{\partial^2 \psi_{x,i}^{(5)}}{\partial \tilde{e}_{i-1}^2} \right|_{v_i} = \frac{2J_{4,i} + 8e_{i-1,x}}{|e_{i-1}|^2},
$$

so we'll set $J_{3,i} = 4e_{i,x}$ and $J_{4,i} = -4e_{i-1,x}$.

Finally, we'll compute the mixed-direction derivative at v_i. After some simplification, we retrieve

$$
\left. \frac{\partial^2 \psi_{x,i}^{(5)}}{\partial \tilde{e}_i \partial \tilde{e}_{i-1}} \right|_{v_i} = \frac{5 \left(e_{i,x} - e_{i-1,x} \right) - K_{0,i}}{|e_i||e_{i-1}|},
$$

which is zero exactly when $K_{0,i} = 5 \left(e_{i,x} - e_{i-1,x} \right)$.

So far, then, we have

$$
\begin{aligned}
\psi_{x,i}^{(5)} = \phi_i^2 \Big(&\phi_i^2 (e_{i,x}\phi_{i+1} - e_{i-1,x}\phi_{i-1}) + 4\phi_i(e_{i,x}\phi_{i+1}^2 - e_{i-1,x}\phi_{i-1}^2) \\
&+ \phi_{i+2} \Big(5 \left(e_{i,x} - e_{i-1,x} \right) \phi_i^2 \\
&\qquad\qquad + \phi_i(K_{1,i}\phi_{i+1} + K_{2,i}\phi_{i-1}) + K_{3,i}\phi_{i+1}^2 + K_{4,i}\phi_{i-1}^2 \Big) \\
&+ \phi_{i+2}^2 (S_{0,i}\phi_i + S_{1,i}\phi_{i+1} + S_{2,i}\phi_{i-1} + S_{3,i}\phi_{i+2}) \Big). \quad\quad (4.1.17)
\end{aligned}
$$

As usual, we determine the rest of the K coefficients by enforcing smoothness across shared edges. We compute the outward normal derivatives of $\psi_{x,i}^{(5)}$ on edge e_i

and e_{i-1}, which can be simplified using parallelogram geometry and (3.2.25) to

$$\frac{\partial \psi_{x,i}^{(5)}}{\partial \vec{n}_i}\bigg|_{e_i} = \phi_i^5 \left(\frac{e_{i,y}}{|e_i|}\right)$$

$$+ 5\phi_i^4 \phi_{i+1} \left(\frac{e_{i,y}}{|e_i|}\right)$$

$$+ \phi_i^3 \phi_{i+1}^2 \left((20e_{i,x} - K_{1,i})\frac{|e_i|}{2C} - 8e_{i,x}\frac{|e_{i-1}|\cos(\theta_i)}{2C}\right)$$

$$+ \phi_i^2 \phi_{i+1}^3 \left(-K_{3,i}\frac{|e_i|}{2C} - 12e_{i,x}\frac{|e_{i-1}|\cos(\theta_i)}{2C}\right);$$

$$\frac{\partial \psi_{x,i}^{(5)}}{\partial \vec{n}_{i-1}}\bigg|_{e_{i-1}} = \phi_i^5 \left(\frac{e_{i-1,y}}{|e_{i-1}|}\right)$$

$$+ 5\phi_i^4 \phi_{i-1} \left(\frac{e_{i-1,y}}{|e_{i-1}|}\right)$$

$$+ \phi_i^3 \phi_{i-1}^2 \left((-20e_{i-1,x} - K_{2,i})\frac{|e_{i-1}|}{2C} + 8e_{i-1,x}\frac{|e_i|\cos(\theta_i)}{2C}\right)$$

$$+ \phi_i^2 \phi_{i-1}^3 \left(-K_{4,i}\frac{|e_{i-1}|}{2C} + 12e_{i-1,x}\frac{|e_i|\cos(\theta_i)}{2C}\right).$$

Considering two adjacent parallelograms P and R sharing an edge as before, we compute the sum of their outward normal derivatives on the shared edge by

$$\frac{\partial \psi_{x,i,P}^{(5)}}{\partial \vec{n}_{i,P}}\bigg|_{e_{i,P}} + \frac{\partial \psi_{x,i,R}^{(5)}}{\partial \vec{n}_{i-1,R}}\bigg|_{e_{i-1,R}} =$$

$$\phi_{i,P}^3 \phi_{i+1,P}^2 \left((20e_{i,x} - K_{1,i,P})\frac{|e_{i,P}|}{2C_P} - 8e_{i,x,P}\frac{|e_{i-1,P}|\cos(\theta_{i,P})}{2C_P}\right.$$

$$\left. + (-20e_{i-1,x,R} - K_{2,i,R})\frac{|e_{i-1,R}|}{2C_R} + 8e_{i-1,x,R}\frac{|e_{i,R}|\cos(\theta_{i,R})}{2C_R}\right)$$

$$+ \phi_{i,P}^2 \phi_{i+1,P}^3 \left(-K_{3,i,P}\frac{|e_{i,P}|}{2C_P} - 12e_{i,x,P}\frac{|e_{i-1,P}|\cos(\theta_{i,P})}{2C_P}\right.$$

$$\left. -K_{4,i,R}\frac{|e_{i-1,R}|}{2C_R} + 12e_{i-1,x,R}\frac{|e_{i,R}|\cos(\theta_{i,R})}{2C_R}\right). \tag{4.1.18}$$

There aren't unique choices for the K coefficients to make (4.1.18) zero, but with respect to the condition (4.1.15), which we'll discuss in more detail shortly as we find

the S coefficients, we'll set

$$K_{1,i} = \left(20 - 18\frac{|e_{i-1}|}{|e_i|}\cos(\theta_i)\right)e_{i,x} - 10e_{i-1,x}, \qquad K_{3,i} = -12\frac{|e_{i-1}|}{|e_i|}\cos(\theta_i)e_{i,x},$$

$$K_{2,i} = -\left(20 - 18\frac{|e_i|}{|e_{i-1}|}\cos(\theta_i)\right)e_{i-1,x} + 10e_{i,x}, \quad K_{4,i} = 12\frac{|e_i|}{|e_{i-1}|}\cos(\theta_i)e_{i-1,x}.$$

Finally, to find the remaining S coefficients, we expand

$$x = \left(\sum_{j=1}^{4} v_{j,x}\phi_j\right)\left(\sum_{k=1}^{4}\phi_k\right)^4$$

and compute the difference

$$x - \left(\sum_{j=1}^{4} v_{j,x}\psi_j^{(5)} + \psi_{x,j}^{(5)}\right) =$$

$$\sum_{j=1}^{4} B^2 C^4 \phi_j \left(40\left(e_{j-1,x} - e_{j,x}\right) - \left(S_{0,j} + S_{1,j-1} + S_{2,j+1} + S_{3,j+2}\right)\right).$$

Again, there is not a unique set of solutions, but we'll make a similar decision as we did for $\psi_i^{(5)}$, and set $S_{0,i} = 40\left(e_{i,x} - e_{i-1,x}\right)$, and $S_{1,i} = S_{2,i} = S_{3,i} = 0$.

Then we finally retrieve the lengthy expression

$$\psi_{x,i}^{(5)} = \phi_i^2\Bigg(\phi_i^2(e_{i,x}\phi_{i+1} - e_{i-1,x}\phi_{i-1}) + 4\phi_i(e_{i,x}\phi_{i+1}^2 - e_{i-1,x}\phi_{i-1}^2)$$

$$+ \phi_{i+2}\Bigg(5\left(e_{i,x} - e_{i-1,x}\right)\phi_i^2$$

$$+ \phi_i\left(\left(\left(20 - 18\frac{|e_{i-1}|}{|e_i|}\cos(\theta_i)\right)e_{i,x} - 10e_{i-1,x}\right)\phi_{i+1}\right.$$

$$\left.- \left(\left(20 - 18\frac{|e_i|}{|e_{i-1}|}\cos(\theta_i)\right)e_{i-1,x} - 10e_{i,x}\right)\phi_{i-1}\right)$$

$$-12\frac{|e_{i-1}|}{|e_i|}\cos(\theta_i)e_{i,x}\phi_{i+1}^2 + 12\frac{|e_i|}{|e_{i-1}|}\cos(\theta_i)e_{i-1,x}\phi_{i-1}^2\Bigg)$$

$$+ 40\left(e_{i,x} - e_{i-1,x}\right)\phi_i\phi_{i+2}^2\Bigg). \tag{4.1.19}$$

We can retrieve the expression for $\psi_{y,i}^{(5)}$ by simply replacing each x by y in (4.1.19), and for each vertex v in $\mathcal{P}$ we define $\psi_{x,v}^{(5)}$ and $\psi_{y,v}^{(5)}$ piecewise over Ω_v as usual. By construction, we have the following:

Theorem 4.1.2. *Let Ω be a polygonal region in $\mathbb{R}^2$ which permits a parallelogram partition as in Figure 4.1, and let $\mathcal{P}$ be such a parallelogram partition of Ω. For every vertex v in the partition $\mathcal{P}$, define polygonal splines $\psi_{x,v}^{(5)}$ and $\psi_{y,v}^{(5)}$ by*

$$\psi_{x,v}^{(5)}(\mathbf{x}) := \begin{cases} \psi_{x,i,P}^{(5)}(\mathbf{x}) & \mathbf{x} \in P \subseteq \Omega_v; \ v = v_{i,P} \\ 0 & \mathbf{x} \notin \Omega_v, \end{cases}$$

$$\text{and } \psi_{y,v}^{(5)}(\mathbf{x}) := \begin{cases} \psi_{y,i,P}^{(5)}(\mathbf{x}) & \mathbf{x} \in P \subseteq \Omega_v; \ v = v_{i,P} \\ 0 & \mathbf{x} \notin \Omega_v, \end{cases}$$

where $\psi_{x,i,P}^{(5)}$ is the function given in (4.1.26) and $\psi_{y,i,P}^{(5)}$ is the associated function retrieved by replacing every x in $\psi_{x,i,P}^{(5)}$ by y.

Then $\psi_{x,v}^{(5)}$ and $\psi_{y,v}^{(5)}$ satisfy the following properties:

(1) $\psi_{x,v}^{(5)}(w) = \psi_{y,v}^{(5)}(w) = 0$ for any vertex w of $\mathcal{P}$;

(2) $\nabla\psi_{x,v}^{(5)}(w) = \langle \delta_{v,w}, 0 \rangle$ and $\nabla\psi_{y,v}^{(5)} = \langle 0, \delta_{v,w} \rangle$ for any vertex w of $\mathcal{P}$;

(3) $\nabla^2\psi_{x,v}^{(5)}(w) = \nabla^2\psi_{y,v}^{(5)}(w) = 0$ for any vertex w of $\mathcal{P}$;

(4) $\psi_{x,v}^{(5)}, \psi_{y,v}^{(5)} \in C^1(\Omega)$; and

(5) $\sum_{v \in \mathcal{P}} v_x \psi_v^{(5)} + \psi_{x,v}^{(5)} = x$ and $\sum_{v \in \mathcal{P}} v_y \psi_v^{(5)} + \psi_{y,v}^{(5)} = y$.

Plots of these functions are shown in Figure 4.3.
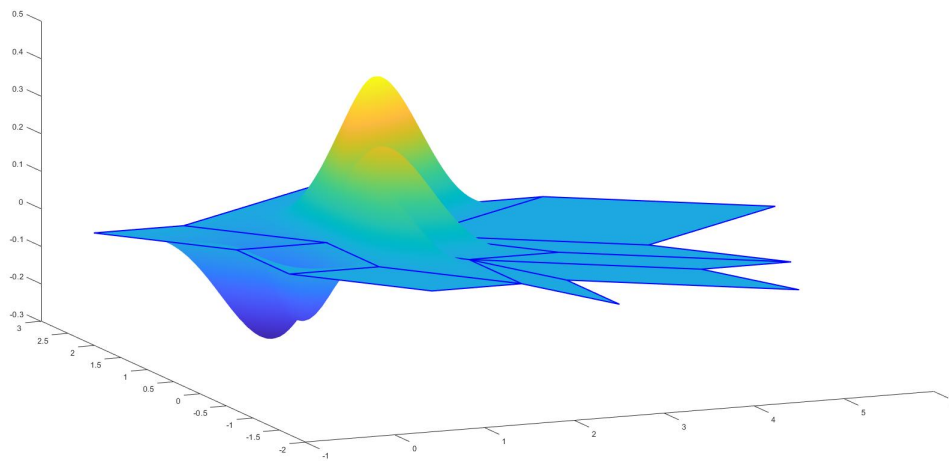
(a) The plot of a function $\psi_{x,v}^{(5)}$
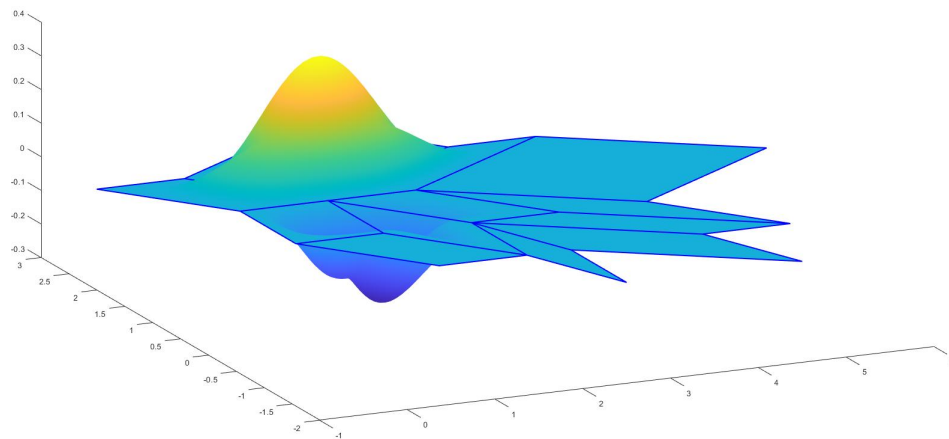
(b) The plot of a function $\psi_{y,v}^{(5)}$

Figure 4.3: Plots of degree-5 gradient-adjustment vertex splines

4.1.3   Construction of $\psi_{x^2,v}^{(5)}$, $\psi_{y^2,v}^{(5)}$, and $\psi_{xy,v}^{(5)}$

We'll extend the span of these vertex splines to include degree-2 polynomials. We'll do so by constructing new C^1 vertex splines to assert Hessian control. We'll construct functions $\psi_{x^2,v}^{(5)}, \psi_{y^2,v}^{(5)}$, and $\psi_{xy,v}^{(5)}$ which satisfy the following properties for every vertex w in $\mathcal{P}$:

$$\psi_{x^2,v}^{(5)}\big|_w = \psi_{y^2,v}^{(5)}\big|_w = \psi_{xy,v}^{(5)}\big|_w = 0; \tag{4.1.20}$$

$$\nabla\psi_{x^2,v}^{(5)}\big|_w = \nabla\psi_{y^2,v}^{(5)}\big|_w = \nabla\psi_{xy,v}^{(5)}\big|_w = 0; \tag{4.1.21}$$

$$\nabla^2\psi_{x^2,v}^{(5)}\big|_w = \begin{pmatrix} \delta_{v,w} & 0 \\ 0 & 0 \end{pmatrix}$$

$$\nabla^2\psi_{y^2,v}^{(5)}\big|_w = \begin{pmatrix} 0 & 0 \\ 0 & \delta_{v,w} \end{pmatrix}$$

$$\nabla^2\psi_{xy,v}^{(5)}\big|_w = \begin{pmatrix} 0 & \delta_{v,w} \\ \delta_{v,w} & 0 \end{pmatrix}, \tag{4.1.22}$$

along with the additional conditions that

$$\sum_{v\in\mathcal{P}} v_x^2\psi_v^{(5)} + 2v_x\psi_{x,v}^{(5)} + 2\psi_{x^2,v}^{(5)} = x^2;$$

$$\sum_{v\in\mathcal{P}} v_y^2\psi_v^{(5)} + 2v_y\psi_{y,v}^{(5)} + 2\psi_{y^2,v}^{(5)} = y^2;$$

$$\sum_{v\in\mathcal{P}} v_xv_y\psi_v^{(5)} + v_y\psi_{x,v}^{(5)} + v_x\psi_{y,v}^{(5)} + \psi_{xy,v}^{(5)} = xy. \tag{4.1.23}$$

We'll first construct the function $\psi_{xy,v}^{(5)}$. Again, we first restrict our attention to a single parallelogram P in Ω_v, with $v = v_i$ in P and define $\psi_{xy,i,P}^{(5)} := \psi_{xy,v}^{(5)}\big|_P$.

We begin with the same template given in (4.1.1), and note that conditions (4.1.20) and (4.1.21) imply that $J_{0,i} = J_{1,i} = J_{2,i} = 0$. Using the simplifications that come

with the restriction to parallelograms, it is not difficult to compute

$$\frac{\partial^2 \psi_{xy,i}^{(5)}}{\partial \tilde{e}_i}^2 \bigg|_{v_i} = \frac{2J_{3,i}}{|e_i|^2}, \qquad \frac{\partial^2 \psi_{xy,i}^{(5)}}{\partial \tilde{e}_{i-1}^2} \bigg|_{v_i} = \frac{2J_{4,i}}{|e_{i-1}|^2}, \qquad \frac{\partial \psi_{xy,i}^{(5)}}{\partial \tilde{e}_i \partial \tilde{e}_{i-1}} \bigg|_{v_i} = \frac{-K_{0,i}}{|e_i||e_{i-1}|},$$

$$\frac{\partial^2 \psi_{xy,i}^{(5)}}{\partial \tilde{e}_i^2} \bigg|_{v_{i+1}} = \frac{2J_{5,i}}{|e_i|^2}, \qquad \frac{\partial^2 \psi_{xy,i}^{(5)}}{\partial \tilde{e}_{i-1}^2} \bigg|_{v_{i-1}} = \frac{2J_{6,i}}{|e_{i-1}|^2},$$

$$\frac{\partial \psi_{xy,i}^{(5)}}{\partial \tilde{e}_i \partial \tilde{e}_{i+1}} \bigg|_{v_{i+1}} = 0, \qquad \frac{\partial \psi_{xy,i}^{(5)}}{\partial \tilde{e}_{i-1} \partial \tilde{e}_{i+2}} \bigg|_{v_{i-1}} = 0.$$

Using condition (4.1.22), we see that we should have

$$\frac{\partial^2 \psi_{xy,i}^{(5)}}{\partial \tilde{e}_i}^2 \bigg|_{v_i} = \frac{2e_{i,x}e_{i,y}}{|e_i|^2}, \qquad\qquad \frac{\partial^2 \psi_{xy,i}^{(5)}}{\partial \tilde{e}_{i-1}^2} \bigg|_{v_i} = \frac{2e_{i-1,x}e_{i-1,y}}{|e_{i-1}|^2},$$

$$\frac{\partial \psi_{xy,i}^{(5)}}{\partial \tilde{e}_i \partial \tilde{e}_{i-1}} \bigg|_{v_i} = \frac{e_{i,x}e_{i-1,y} + e_{i,y}e_{i-1,x}}{|e_i||e_{i-1}|},$$

$$\frac{\partial^2 \psi_{xy,i}^{(5)}}{\partial \tilde{e}_i^2} \bigg|_{v_{i+1}} = 0, \qquad\qquad \frac{\partial^2 \psi_{xy,i}^{(5)}}{\partial \tilde{e}_{i-1}^2} \bigg|_{v_{i-1}} = 0,$$

$$\frac{\partial \psi_{xy,i}^{(5)}}{\partial \tilde{e}_i \partial \tilde{e}_{i+1}} \bigg|_{v_{i+1}} = 0, \qquad\qquad \frac{\partial \psi_{xy,i}^{(5)}}{\partial \tilde{e}_{i-1} \partial \tilde{e}_{i+2}} \bigg|_{v_{i-1}} = 0.$$

Therefore, we'll set $J_{3,i} = e_{i,x}e_{i,y}$, $J_{4,i} = e_{i-1,x}e_{i-1,y}$, $J_{5,i} = J_{6,i} = 0$, and
$K_{0,i} = -(e_{i,x}e_{i-1,y} + e_{i,y}e_{i-1,x})$.

We determine the remaining K coefficients as usual, by enforcing C^1 smoothness on shared edges. We take outward normal derivatives of $\psi_{xy,i}^{(5)}$ on edges e_i and e_{i-1}.

Using (3.2.25) and some parallelogram geometry, we can simplify the derivatives to

$$
\left.\frac{\partial \psi_{xy,i}^{(5)}}{\partial \vec{n}_i}\right|_{e_i} = \phi_i^4 \phi_{i+1}\left(\frac{e_{i,y}^2 - e_{i,x}^2}{|e_i|}\right)
$$
$$
+ \phi_i^3 \phi_{i+1}^2\left((5e_{i,x}e_{i,y} - K_{1,i})\frac{|e_i|}{2C} - e_{i,x}e_{i,y}\frac{|e_{i-1}|\cos(\theta_i)}{2C}\right)
$$
$$
+ \phi_i^2 \phi_{i+1}^3\left(-K_{3,i}\frac{|e_i|}{2C} - 3e_{i,x}e_{i,y}\frac{|e_{i-1}|\cos(\theta_i)}{2C}\right),
$$
$$
\left.\frac{\partial \psi_{xy,i}^{(5)}}{\partial \vec{n}_{i-1}}\right|_{e_{i-1}} = \phi_i^4 \phi_{i-1}\left(\frac{e_{i-1,x}^2 - e_{i-1,y}^2}{|e_{i-1}|}\right)
$$
$$
+ \phi_i^3 \phi_{i-1}^2\left((5e_{i-1,x}e_{i-1,y} - K_{2,i})\frac{|e_{i-1}|}{2C} - e_{i-1,x}e_{i-1,y}\frac{|e_i|\cos(\theta_i)}{2C}\right)
$$
$$
+ \phi_i^2 \phi_{i-1}^3\left(-K_{4,i}\frac{|e_{i-1}|}{2C} - 3e_{i-1,x}e_{i-1,y}\frac{|e_i|\cos(\theta_i)}{2C}\right).
$$

If we consider two adjacent parallelograms P and R in $\mathcal{P}$ as we have before, we can add their outward normal derivatives on the shared edge to retrieve

$$
\left.\frac{\partial \psi_{xy,i,P}^{(5)}}{\partial \vec{n}_{i,P}}\right|_{e_{i,P}} + \left.\frac{\partial \psi_{xy,i,R}^{(5)}}{\partial \vec{n}_{i-1,R}}\right|_{e_{i-1,R}} =
$$
$$
\phi_{i,P}^3 \phi_{i+1,P}^2\left((5e_{i,x,R}e_{i,y,P} - K_{1,i,P})\frac{|e_{i,P}|}{2C_P} - e_{i,x,P}e_{i,y,P}\frac{|e_{i-1,P}|\cos(\theta_{i,P})}{2C_P}\right.
$$
$$
+ (5e_{i-1,x,R}e_{i-1,y,R} - K_{2,i,R})\frac{|e_{i-1,R}|}{2C_R} - e_{i-1,x,R}e_{i-1,y,R}\frac{|e_{i,R}|\cos(\theta_{i,R})}{2C_R}\Bigg)
$$
$$
\phi_{i,P}^2 \phi_{i+1,P}^3\left(-K_{3,i,P}\frac{|e_{i,P}|}{2C_P} - 3e_{i,x,P}e_{i,y,P}\frac{|e_{i-1,P}|\cos(\theta_{i,P})}{2C_P}\right.
$$
$$
-K_{4,i,R}\frac{|e_{i-1,R}|}{2C_R} - 3e_{i-1,x,R}e_{i-1,y,R}\frac{|e_{i,R}|\cos(\theta_{i,R})}{2C_R}\Bigg). \tag{4.1.24}
$$

As usual, there are not unique choices of coefficients to ensure that (4.1.24) is zero. However, just as when we were building $\psi_{x,i}^{(5)}$, we can refer to the condition (4.1.23)

to choose

$$K_{1,i} = 5e_{i,x}e_{i,y}\left(1 - \frac{|e_{i-1}|}{|e_i|}\cos(\theta_i)\right) - 2\left(e_{i,x}e_{i-1,y} + e_{i,y}e_{i-1,x}\right);$$

$$K_{2,i} = 5e_{i-1,x}e_{i-1,y}\left(1 - \frac{|e_i|}{|e_{i-1}|}\cos(\theta_i)\right) - 2\left(e_{i,x}e_{i-1,y} + e_{i,y}e_{i-1,x}\right);$$

$$K_{3,i} = e_{i,x}e_{i,y}\frac{|e_{i-1}|}{|e_i|}\cos(\theta_i) + 2\left(e_{i,x}e_{i-1,y} + e_{i,y}e_{i-1,x}\right);$$

$$K_{4,i} = e_{i-1,x}e_{i-1,y}\frac{|e_i|}{|e_{i-1}|}\cos(\theta_i) + 2\left(e_{i,x}e_{i-1,y} + e_{i,y}e_{i-1,x}\right).$$

Finally, we use the same condition (4.1.23) to find the S coefficients. We first expand

$$xy = \left(\sum_{j=1}^{4} v_{j,x}\phi_j\right)\left(\sum_{j=1}^{4} v_{j,y}\phi_j\right)\left(\sum_{j=1}^{4} \phi_j\right)^3$$

evaluate the difference

$$xy - \left(\sum_{j=1}^{4} v_{j,x}v_{j,y}\psi_i^{(5)} + v_{j,y}\psi_{x,i}^{(5)} + v_{j,x}\psi_{y,i}^{(5)} + \psi_{xy,i}^{(5)}\right) =$$

$$B^2C^4\left(\sum_{j=1}^{4} 10(e_{i,x}e_{i,y} + e_{i-1,x}e_{i-1,y}) - 16(e_{i,x}e_{i-1,y} + e_{i,y}e_{i-1,x}) - S_{0,i}\right),$$

so we'll set $S_{0,i} = 10(e_{i,x}e_{i,y} + e_{i-1,x}e_{i-1,y}) - 16(e_{i,x}e_{i-1,y} + e_{i,y}e_{i-1,x})$.

The result follows:

$$\psi_{xy,i}^{(5)} = \phi_i^2 \Bigg(\phi_i(e_{i,x}e_{i,y}\phi_{i+1}^2 + e_{i-1,x}e_{i-1,y}\phi_{i-1}^2)$$

$$+ \phi_{i+2}\Bigg(-(e_{i,x}e_{i-1,y} + e_{i,y}e_{i-1,x})\phi_i^2$$

$$+ \phi_i\Bigg(\bigg(5e_{i,x}e_{i,y}\bigg(1 - \frac{|e_{i-1}|}{|e_i|}\cos(\theta_i)\bigg) - 2(e_{i,x}e_{i-1,y} + e_{i,y}e_{i-1,x})\bigg)\phi_{i+1}$$

$$+ \bigg(5e_{i-1,x}e_{i-1,y}\bigg(1 - \frac{|e_i|}{|e_{i-1}|}\cos(\theta_i)\bigg) - 2(e_{i,x}e_{i-1,y} + e_{i,y}e_{i-1,x})\bigg)\phi_{i-1}\Bigg)$$

$$+ \bigg(e_{i,x}e_{i,y}\frac{|e_{i-1}|}{|e_i|}\cos(\theta_i) + 2(e_{i,x}e_{i-1,y} + e_{i,y}e_{i-1,x})\bigg)\phi_{i+1}^2$$

$$+ \bigg(e_{i-1,x}e_{i-1,y}\frac{|e_i|}{|e_{i-1}|}\cos(\theta_i) + 2(e_{i,x}e_{i-1,y} + e_{i,y}e_{i-1,x})\bigg)\phi_{i-1}^2\Bigg)$$

$$+ (10(e_{i,x}e_{i,y} + e_{i-1,x}e_{i-1,y}) - 16(e_{i,x}e_{i-1,y} + e_{i,y}e_{i-1,x}))\phi_i\phi_{i+2}^2\Bigg). \qquad (4.1.25)$$

In a similar manner to how we could retrieve $\psi_{y,i}^{(5)}$ from $\psi_{x,i}^{(5)}$ by simply replacing each x in (4.1.19) by y, we can retrieve $\psi_{y^2,i}^{(5)}$ and $\psi_{x^2,i}^{(5)}$ from (4.1.25) by replacing each x by y or each y by x, respectively, in addition to multiplying by a factor of $\frac{1}{2}$. Then we'll have

$$\psi_{x^2,i}^{(5)} = \frac{1}{2}\phi_i^2\Bigg(\phi_i(e_{i,x}^2\phi_{i+1}^2 + e_{i-1,x}^2\phi_{i-1}^2)$$

$$+ \phi_{i+2}\Bigg(-2e_{i,x}e_{i-1,x}\phi_i^2$$

$$+ \phi_i\Bigg(\bigg(5e_{i,x}^2\bigg(1 - \frac{|e_{i-1}|}{|e_i|}\cos(\theta_i)\bigg) - 4e_{i,x}e_{i-1,x}\bigg)\phi_{i+1}$$

$$+ \bigg(5e_{i-1,x}^2\bigg(1 - \frac{|e_i|}{|e_{i-1}|}\cos(\theta_i)\bigg) - 4e_{i,x}e_{i-1,x})\bigg)\phi_{i-1}\Bigg)$$

$$+ \bigg(e_{i,x}^2\frac{|e_{i-1}|}{|e_i|}\cos(\theta_i) + 4e_{i,x}e_{i-1,x}\bigg)\phi_{i+1}^2$$

$$+ \bigg(e_{i-1,x}^2\frac{|e_i|}{|e_{i-1}|}\cos(\theta_i) + 4e_{i,x}e_{i-1,x}\bigg)\phi_{i-1}^2\Bigg)$$

$$+ (10(e_{i,x}^2 + e_{i-1,x}^2) - 32e_{i,x}e_{i-1,x})\phi_i\phi_{i+2}^2\Bigg), \text{ and} \qquad (4.1.26)$$

$$\psi_{y^2,i}^{(5)} = \frac{1}{2}\phi_i^2\bigg(\phi_i(e_{i,y}^2\phi_{i+1}^2 + e_{i-1,y}^2\phi_{i-1}^2)$$

$$+ \phi_{i+2}\bigg(-2e_{i,y}e_{i-1,y}\phi_i^2$$

$$+ \phi_i\bigg(\bigg(\bigg(5e_{i,y}^2\bigg(1 - \frac{|e_{i-1}|}{|e_i|}\cos(\theta_i)\bigg) - 4e_{i,y}e_{i-1,y}\bigg)\phi_{i+1}$$

$$+ \bigg(5e_{i-1,y}^2\bigg(1 - \frac{|e_i|}{|e_{i-1}|}\cos(\theta_i)\bigg) - 4e_{i,y}e_{i-1,y}\bigg)\bigg)\phi_{i-1}\bigg)$$

$$+ \bigg(e_{i,y}^2\frac{|e_{i-1}|}{|e_i|}\cos(\theta_i) + 4e_{i,y}e_{i-1,y}\bigg)\phi_{i+1}^2$$

$$+ \bigg(e_{i-1,y}^2\frac{|e_i|}{|e_{i-1}|}\cos(\theta_i) + 4e_{i,y}e_{i-1,y}\bigg)\phi_{i-1}^2\bigg)$$

$$+ (10(e_{i,y}^2 + e_{i-1,y}^2) - 32e_{i,y}e_{i-1,y})\phi_i\phi_{i+2}^2\bigg). \tag{4.1.27}$$

For each vertex v in $\mathcal{P}$, we define the functions $\psi_{x^2,v}^{(5)}$, $\psi_{y^2,v}^{(5)}$, and $\psi_{xy,v}^{(5)}$ piecewise over Ω_v as usual. This section, combined with the 2 preceding it, serve as a proof of the following:

Theorem 4.1.3. *Let Ω be a polygonal region in $\mathbb{R}^2$ which permits a parallelogram partition as in Figure 4.1, and let $\mathcal{P}$ be such a parallelogram partition of Ω. For every vertex v in the partition $\mathcal{P}$, define polygonal splines $\psi_{x^2,v}^{(5)}$, $\psi_{y^2,v}^{(5)}$, and $\psi_{xy,v}^{(5)}$ over Ω_v by*

$$\psi_{x^2,v}^{(5)}(\mathbf{x}) := \begin{cases} \psi_{x^2,i,P}^{(5)}(\mathbf{x}) & \mathbf{x} \in P \subseteq \Omega_v; \ v = v_{i,P} \\ 0 & \mathbf{x} \notin \Omega_v, \end{cases}$$

$$\psi_{y^2,v}^{(5)}(\mathbf{x}) := \begin{cases} \psi_{y^2,i,P}^{(5)}(\mathbf{x}) & \mathbf{x} \in P \subseteq \Omega_v; \ v = v_{i,P} \\ 0 & \mathbf{x} \notin \Omega_v, \end{cases}$$

$$\psi_{xy,v}^{(5)}(\mathbf{x}) := \begin{cases} \psi_{xy,i,P}^{(5)}(\mathbf{x}) & \mathbf{x} \in P \subseteq \Omega_v; \ v = v_{i,P} \\ 0 & \mathbf{x} \notin \Omega_v, \end{cases}$$

where $\psi_{xy,i,P}^{(5)}$, $\psi_{x^2,i,P}^{(5)}$, and $\psi_{y^2,i,P}^{(5)}$ are the functions defined in (4.1.25), (4.1.26), and (4.1.27).

Then $\psi_{x^2,v}^{(5)}$, $\psi_{y^2,v}^{(5)}$, and $\psi_{xy,v}^{(5)}$ satisfy the following properties:

(1) $\psi_{x^2,v}^{(5)}(w) = \psi_{y^2,v}^{(5)}(w) = \psi_{xy,v}^{(5)}(w) = 0$ *for any vertex w of $\mathcal{P}$;*

(2) $\nabla\psi_{x^2,v}^{(5)}(w) = \nabla\psi_{y^2,v}^{(5)}(w) = \nabla\psi_{xy,v}^{(5)}(w) = 0$ *for any vertex w of $\mathcal{P}$;*

(3) $\nabla^2\psi_{x^2,v}^{(5)}(w) = \begin{pmatrix} \delta_{v,w} & 0 \\ 0 & 0 \end{pmatrix}, \nabla^2\psi_{y^2,v}^{(5)}(w) = \begin{pmatrix} 0 & 0 \\ 0 & \delta_{v,w} \end{pmatrix},$

   and $\nabla^2\psi_{xy,v}^{(5)}(w) = \begin{pmatrix} 0 & \delta_{v,w} \\ \delta_{v,w} & 0 \end{pmatrix}$ *for any vertex w of $\mathcal{P}$;*

(4) $\psi_{x^2,v}^{(5)}, \psi_{y^2,v}^{(5)}, \psi_{xy,v}^{(5)} \in C^1(\Omega)$;

(5) $\sum_v v_x^2\psi_v^{(5)} + 2v_x\psi_{x,v}^{(5)} + 2\psi_{x^2,v}^{(5)} = x^2, \sum_v v_y^2\psi_v^{(5)} + 2v_y\psi_{y,v}^{(5)} + 2\psi_{y^2,v}^{(5)} = y^2,$
   $\sum_v v_x v_y\psi_v^{(5)} + v_y\psi_{x,v}^{(5)} + v_x\psi_{y,v}^{(5)} + \psi_{xy,v}^{(5)} = xy$;

(6) *Where* $\Psi_{5,V}^1(\mathcal{P}) := span\left\{\psi_v^{(5)}, \psi_{x,v}^{(5)}, \psi_{y,v}^{(5)}, \psi_{x^2,v}^{(5)}, \psi_{y^2,v}^{(5)}, \psi_{xy,v}^{(5)}\right\}_{v\in\mathcal{P}}$,
   $dim(\Psi_{5,V}^1(\mathcal{P})) = 6|V|$;

(7) $\Pi_2 \subseteq \Psi_{5,V}^1(\mathcal{P})$.

Figure 4.4 shows plots of all three of these functions.

4.2   More degree-5 C^1 polygonal splines

4.2.1   Motivation to extend

Or course there is interest in maximizing the span of our C^1 polygonal spline space, and the linear span of degree-5 polynomials of Wachspress coordinates includes all bivariate polynomial functions of degree up to 5. Since polynomials are C^1, an ideal degree-5 C^1 polygonal spline space should include up to degree-5 polynomials, but so far we've only guaranteed inclusion of polynomials up to degree 2. We can check cubic polynomials manually; for example, if we have any hope of including x^3, it would be
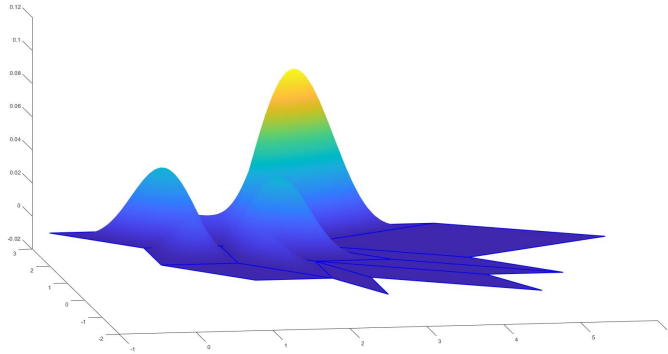
(a) The plot of a function $\psi_{x^2,v}^{(5)}$
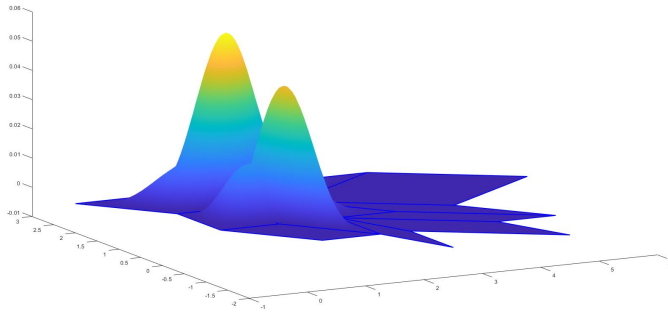
(b) The plot of a function $\psi_{y^2,v}^{(5)}$
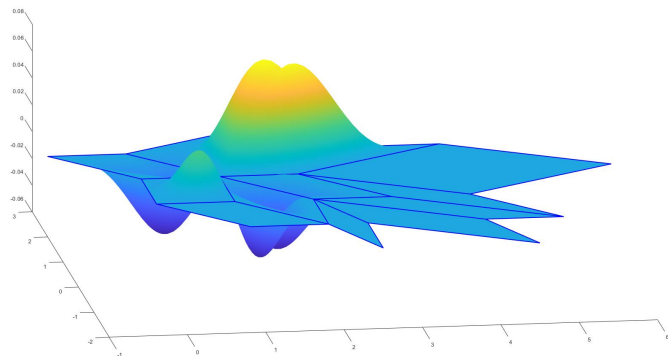
(c) The plot of a function $\psi_{xy,v}^{(5)}$

Figure 4.4: Plots of degree-5 Hessian-adjustment vertex splines

with the function

$$\sum_{v \in \mathcal{P}} v_x^3 \psi_v^{(5)} + 3v_x^2 \psi_{x,v}^{(5)} + 6v_x \psi_{x^2,v}^{(5)}. \tag{4.2.1}$$

Within a single parallelogram $P \in \mathcal{P}$, we can express x^3 by

$$x^3|_P = \left(\sum_{j=1}^{4} v_{j,x} \phi_j \right)^3 \left(\sum_{j=1}^{4} \phi_j \right)^2. \tag{4.2.2}$$

We can compute the difference of (4.2.2) and the restriction of (4.2.1) to P, and unfortunately, this difference is nonzero, which shows that the span of our vertex splines thus far does not include cubic polynomials:

$$x^3|_P - \sum_{j=1}^{4} v_{j,x}^3 \psi_j^{(5)} + 3v_{j,x}^2 \psi_{x,j}^{(5)} + 6v_{j,x} \psi_{x^2,j}^{(5)}$$

$$= C^2 B \sum_{j=1}^{4} 9\phi_j^2 \left(\phi_{j+1} e_{j,x}^2 \left(e_{j-1,x} + \frac{|e_{j-1}|}{|e_j|} \cos(\theta_j) e_{j,x} \right) \right.$$

$$\left. - \phi_{j-1} e_{j-1,x}^2 \left(e_{j,x} + \frac{|e_j|}{|e_{j-1}|} \cos(\theta_j) e_{j-1,x} \right) \right)$$

$$- 12 C^2 B \phi_j (e_{j,x} - e_{j-1,x}) e_{j,x} e_{j-1,x}.$$

A reasonable thought is to control third derivatives at each vertex, but not only are third derivatives cumbersome to compute, it is also questionable how useful third-derivative information is to an interpolation scheme - currently, we can define a quasi-interpolant $Q_V(f)$ for any function f which is C^2 at the vertices by

$$Q_V(f) = \sum_{v \in \mathcal{P}} f|_v \psi_v^{(5)} + \frac{\partial f}{\partial x}\bigg|_v \psi_{x,v}^{(5)} + \frac{\partial f}{\partial y}\bigg|_v \psi_{y,v}^{(5)}$$

$$+ \frac{\partial^2 f}{\partial x^2}\bigg|_v \psi_{x^2,v}^{(5)} + \frac{\partial^2 f}{\partial x \partial y}\bigg|_v \psi_{xy,v}^{(5)} + \frac{\partial^2 f}{\partial y^2}\bigg|_v \psi_{y^2,v}^{(5)}, \tag{4.2.3}$$

but it seems unlikely that third-derivative information would be available - it might

ϕ_4^5 $\phi_3\phi_4^4$ $\phi_3^2\phi_4^3$ $\phi_3^3\phi_4^2$ $\phi_3^4\phi_4$ ϕ_3^5

$\phi_1\phi_4^4$ $B\phi_4^3$ $B\phi_3\phi_4^2$ $B\phi_3^2\phi_4$ $B\phi_3^3$ $\phi_2\phi_3^4$

$\phi_1^2\phi_4^3$ $B\phi_1\phi_4^2$ $B^2\phi_4$ $B^2\phi_3$ $B\phi_2\phi_3^2$ $\phi_2^2\phi_3^3$

$\phi_1^3\phi_4^2$ $B\phi_1^2\phi_4$ $B^2\phi_1$ $B^2\phi_2$ $B\phi_2^2\phi_3$ $\phi_2^3\phi_3^2$

$\phi_1^4\phi_4$ $B\phi_1^3$ $B\phi_1^2\phi_2$ $B\phi_1\phi_2^2$ $B\phi_2^3$ $\phi_2^4\phi_3$

ϕ_1^5 $\phi_1^4\phi_2$ $\phi_1^3\phi_2^2$ $\phi_1^2\phi_2^3$ $\phi_1\phi_2^4$ ϕ_2^5
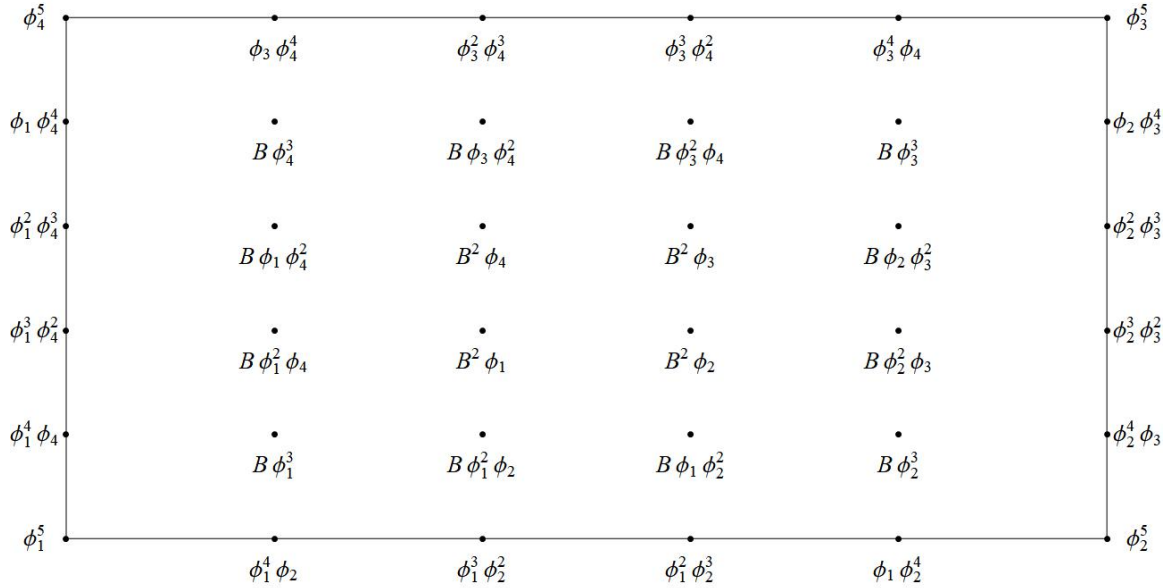
Figure 4.5: An illustration of the degree-5 polygonal spline basis functions with the associated domain points

be ambitious to even hope for second-derivative information. Moreover, even using polygonal splines of degree 5, we don't have enough flexibility to fully control third derivatives. At this point, it is helpful for us to consider the degree-5 monomials by their domain-point interpretation; see Figure 4.5.

In order to avoid disturbing the properties of our previous vertex splines - namely, the value, gradient, and Hessian at each vertex - we must be sure to avoid using the marked functions in Figure 4.6.

By Figure 4.6, we can see that the functions which would affect third derivatives at each vertex would include some which would interfere with the second derivatives of other vertices; for example, the functions which would affect the third derivatives at vertex v_1 include $\phi_1^2\phi_4^3, B\phi_1^2\phi_4, B\phi_1^2\phi_2$, and $\phi_1^2\phi_2^3$.

The functions associated with the unmarked points in Figure 4.6 are still free to manipulate without disrupting our previously established properties, but it is worthwhile to separate these into two classes. In particular, some of the functions are free
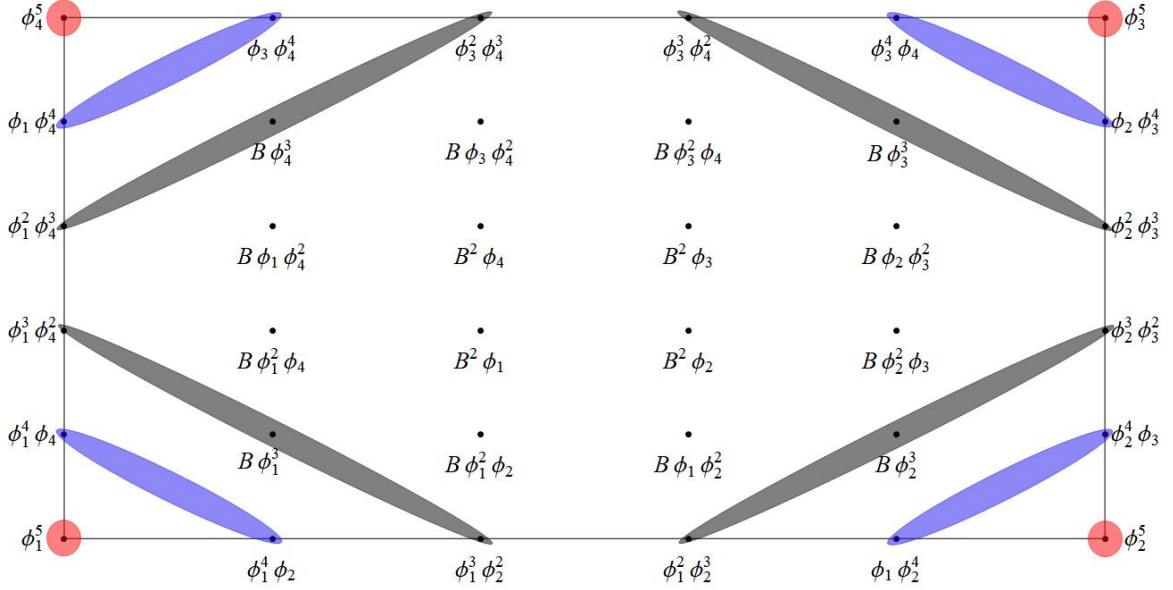
Figure 4.6: The functions marked in red affect values at each vertex; those marked in blue affect gradient, and those marked in grey affect the Hessian.

to manipulate without affecting C^1 smoothness on the edges, while some do affect the gradients on the edges. See Figure 4.7.

Finding some quantities we can use for quasi-interpolation in relation to the functions indicated in Figure 4.7 is worth considering. The functions marked in Figure 4.7a are more complex to consider on the scale of the entire partition $\mathcal{P}$, because we must ensure that they interact in a manner which maintains C^1 smoothness over shared edges.

From Figure 4.7a, consider particularly the functions $B\phi_1^2\phi_2$ and $B\phi_1\phi_2^2$. Since the function B is zero on every edge, and the product $\phi_1\phi_2$ is zero on every edge except e_1, these functions only affect the gradient on edge e_1. We can still make C^1 local basis splines using these, but instead of being based in the neighborhood Ω_v of a vertex v, these functions should be based in the neighborhood Ω_e of an edge e. For this reason, it would be inappropriate to call such functions vertex splines. Instead, we will call them edge splines.
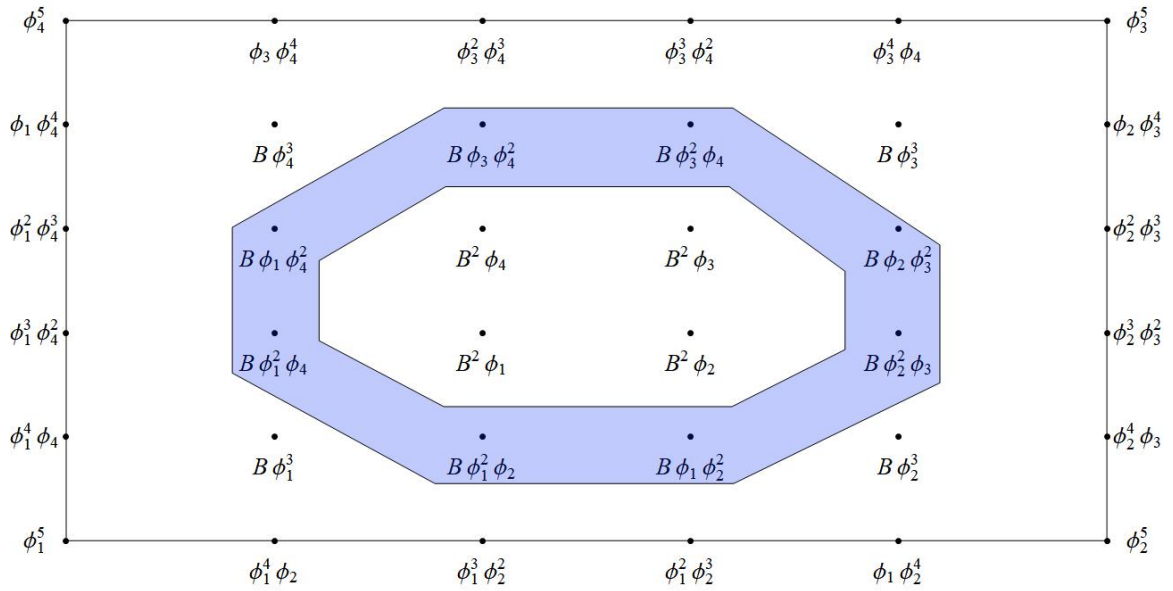
(a) Domain points associated with degree-5 functions which affect gradients on the edges
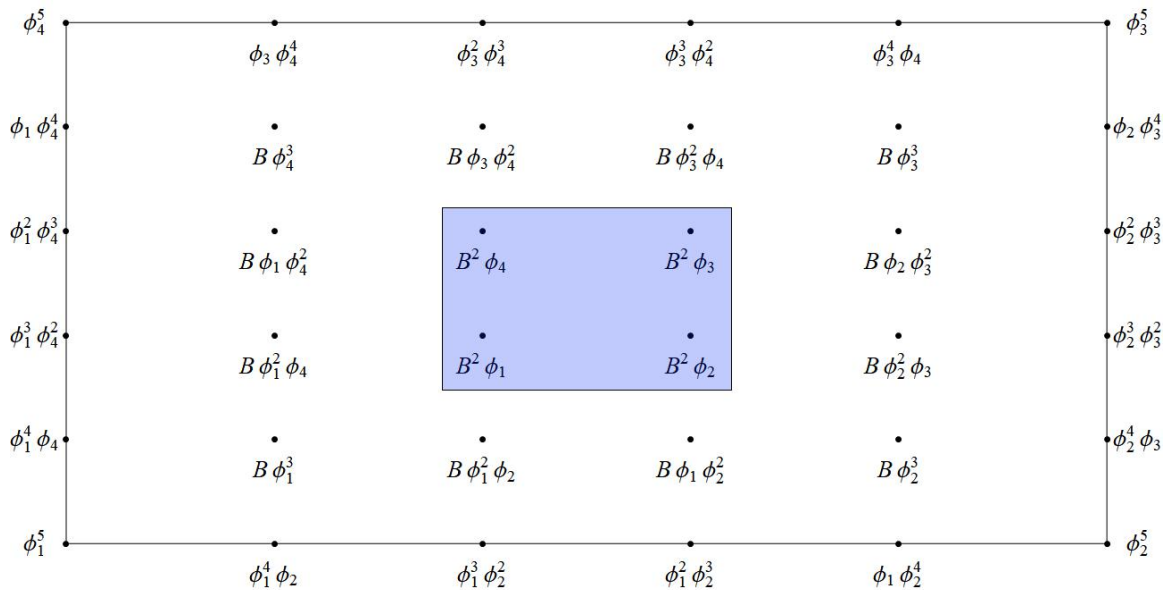
(b) Domain points associated with degree-5 basis functions which are free with respect to C^1 smoothness

Figure 4.7: A classification of remaining degree-5 functions into 2 classes illustrated by domain points

4.2.2 Degree-5 C^1 edge splines

We'll use the spline functions constructed in this section to control gradients on edges. Since the values along each edge are fully determined by the already-constructed vertex splines, the derivative in the edge directions can't be manipulated at all. We'll focus on the outward normal direction. However, if we're to use the outward normal derivative on the edges for quasi-interpolation, we should know how our other functions are affecting it. Fortunately, the functions $\psi_v^{(5)}$ have zero outward normal derivative on edges, but the other functions generally do not. Focusing on a single parallelogram P, the other vertex splines have the following normal derivatives on the edges:

$$\left.\frac{\partial \psi_{x,i}^{(5)}}{\partial \vec{n}_i}\right|_{e_i} = \frac{e_{i,y}}{|e_i|}\phi_i^3\left(\phi_i^2 + 5\phi_i\phi_{i+1} + 10\phi_{i+1}^2\right);$$

$$\left.\frac{\partial \psi_{x,i}^{(5)}}{\partial \vec{n}_{i-1}}\right|_{e_{i-1}} = \frac{e_{i-1,y}}{|e_{i-1}|}\phi_i^3\left(\phi_i^2 + 5\phi_i\phi_{i-1} + 10\phi_{i-1}^2\right);$$

$$\left.\frac{\partial \psi_{y,i}^{(5)}}{\partial \vec{n}_i}\right|_{e_i} = \frac{-e_{i,x}}{|e_i|}\phi_i^3\left(\phi_i^2 + 5\phi_i\phi_{i+1} + 10\phi_{i+1}^2\right);$$

$$\left.\frac{\partial \psi_{y,i}^{(5)}}{\partial \vec{n}_{i-1}}\right|_{e_{i-1}} = \frac{-e_{i-1,x}}{|e_{i-1}|}\phi_i^3\left(\phi_i^2 + 5\phi_i\phi_{i-1} + 10\phi_{i-1}^2\right);$$

$$\left.\frac{\partial \psi_{x^2,i}^{(5)}}{\partial \vec{n}_i}\right|_{e_i} = \frac{e_{i,x}e_{i,y}}{|e_i|}\phi_i^2\phi_{i+1}(\phi_i^2 + 2\phi_i\phi_{i+1} - 2\phi_{i+1}^2);$$

$$\left.\frac{\partial \psi_{x^2,i}^{(5)}}{\partial \vec{n}_{i-1}}\right|_{e_{i-1}} = \frac{e_{i-1,x}e_{i-1,y}}{|e_{i-1}|}\phi_i^2\phi_{i-1}(\phi_i^2 + 2\phi_i\phi_{i-1} - 2\phi_{i-1}^2);$$

$$\left.\frac{\partial \psi_{y^2,i}^{(5)}}{\partial \vec{n}_i}\right|_{e_i} = \frac{-e_{i,x}e_{i,y}}{|e_i|}\phi_i^2\phi_{i+1}(\phi_i^2 + 2\phi_i\phi_{i+1} - 2\phi_{i+1}^2);$$

$$\left.\frac{\partial \psi_{y^2,i}^{(5)}}{\partial \vec{n}_{i-1}}\right|_{e_{i-1}} = \frac{-e_{i-1,x}e_{i-1,y}}{|e_{i-1}|}\phi_i^2\phi_{i-1}(\phi_i^2 + 2\phi_i\phi_{i-1} - 2\phi_{i-1}^2);$$

$$\left.\frac{\partial \psi_{xy,i}^{(5)}}{\partial \vec{n}_i}\right|_{e_i} = \left(\frac{e_{i,y}^2 - e_{i,x}^2}{|e_i|}\right)\phi_i^2\phi_{i+1}(\phi_i^2 + 2\phi_i\phi_{i+1} - 2\phi_{i+1}^2);$$

$$\left.\frac{\partial \psi_{xy,i}^{(5)}}{\partial \vec{n}_{i-1}}\right|_{e_{i-1}} = \left(\frac{e_{i-1,y}^2 - e_{i-1,x}^2}{|e_{i-1}|}\right)\phi_i^2\phi_{i-1}(\phi_i^2 + 2\phi_i\phi_{i-1} - 2\phi_{i-1}^2);$$

and the functions which we will use to build our edge splines have the following normal derivatives on edge e_i:

$$\frac{\partial}{\partial \vec{n}_i}(\phi_{i+2}\phi_i^3\phi_{i+1})\bigg|_{e_i} = -\frac{|e_i|}{2C}\phi_i^3\phi_{i+1}^2; \qquad \frac{\partial}{\partial \vec{n}_i}(\phi_{i+2}\phi_i^2\phi_{i+1}^2)\bigg|_{e_i} = -\frac{|e_i|}{2C}\phi_i^2\phi_{i+1}^3.$$

We consider where these functions are maximized (in magnitude) on edge e_i. The former is maximized at the point $e_{i,i}^{(5)} := \frac{3}{5}v_i + \frac{2}{5}v_{i+1}$, while the latter is maximized at the point $e_{i,i+1}^{(5)} := \frac{2}{5}v_i + \frac{3}{5}v_{i+1}$.

We evaluate the outward normal derivative of the quasi-interpolatory vertex spline $Q_V(f)$ at the points $e_{i,i}$ and $e_{i,i+1}$:

$$\frac{\partial Q_V(f)}{\partial \vec{n}_i}\bigg|_{e_{i,i}} = 5^{-5}\vec{n}_i\left(\left(992\nabla f^T\big|_{v_{i+1}} + 2133\nabla f^T\big|_{v_i}\right)\right.$$

$$\left. +6\left(39\nabla^2 f\big|_{v_i} - 4\nabla^2 f\big|_{v_{i+1}}\right)\vec{e}_i^T\right);$$

$$\frac{\partial Q_V(f)}{\partial \vec{n}_i}\bigg|_{e_{i,i+1}} = 5^{-5}\vec{n}_i\left(\left(992\nabla f^T\big|_{v_i} + 2133\nabla f^T\big|_{v_{i+1}}\right)\right.$$

$$\left. +6\left(39\nabla^2 f\big|_{v_{i+1}} - 4\nabla^2 f\big|_{v_i}\right)\vec{e}_i^T\right).$$

Our goal is to find a revised quasi-interpolant $Q_E(f)$ such that

$$\frac{\partial Q_E(f)}{\partial \vec{n}_i}\bigg|_{e_{i,i}} = \frac{\partial f}{\partial \vec{n}_i}\bigg|_{e_{i,i}}, \text{ and } \frac{\partial Q_E(f)}{\partial \vec{n}_i}\bigg|_{e_{i,i+1}} = \frac{\partial f}{\partial \vec{n}_i}\bigg|_{e_{i,i+1}}.$$

Where the parallelograms P and R share the edge $e = e_{i,P} = e_{i-1,R}$, define the

functions

$$\psi_{e,i,P}^{(5)}(f) = \phi_{i+2,P}\phi_{i,P}^2\phi_{i+1,P}\left(K_{1,i,P}(f)\phi_{i,P} + K_{3,i,P}(f)\phi_{i+1,P}\right); \qquad (4.2.4)$$

$$\psi_{e,i-1,R}^{(5)}(f) = \phi_{i+2,R}\phi_{i,R}^2\phi_{i-1,R}^2\left(K_{2,i,R}(f)\phi_{i,R} + K_{4,i,R}(f)\phi_{i-1,R}\right);$$

$$\psi_e^{(5)}(f)(\mathbf{x}) = \begin{cases} \psi_{e,i,P}^{(5)}(f)(\mathbf{x}), & x \in P \\ \psi_{e,i-1,R}^{(5)}(f)(\mathbf{x}), & x \in R \end{cases}; \qquad (4.2.5)$$

$$Q_E(f) = Q_V(f) + \sum_{e \in \mathcal{P}} \psi_e^{(5)}(f). \qquad (4.2.6)$$

for constants $K_{1,i,P}(f), K_{2,i,R}(f), K_{3,i,P}(f)$ and $K_{4,i,R}(f)$ which depend on the function f. We compute the normal derivative of $\psi_{e,i,P}^{(5)}(f)$ at the points $e_{i,i;P}$ and $e_{i,i+1;P}$:

$$\left.\frac{\partial\psi_{e,i,P}^{(5)}(f)}{\partial\vec{n}_{i,P}}\right|_{e_{i,i;P}} = -\frac{|e_{i,P}|}{2C_P}36 \cdot 5^{-5}\left(2K_{1,i,P}(f) + 3K_{3,i,P}(f)\right);$$

$$\left.\frac{\partial\psi_{e,i,P}^{(5)}(f)}{\partial\vec{n}_{i,P}}\right|_{e_{i,i+1;P}} = -\frac{|e_{i,P}|}{2C_P}36 \cdot 5^{-5}\left(3K_{1,i,P}(f) + 2K_{3,i,P}(f)\right).$$

We want

$$\left.\frac{\partial\psi_{e,i,P}^{(5)}(f)}{\partial\vec{n}_{i,P}}\right|_{e_{i,i;P}} = \left.\left(\frac{\partial f}{\partial\vec{n}_{i,P}} - \frac{\partial Q_V(f)}{\partial\vec{n}_{i,P}}\right)\right|_{e_{i,i;P}}, \text{ and}$$

$$\left.\frac{\partial\psi_{e,i,P}^{(5)}(f)}{\partial\vec{n}_{i,P}}\right|_{e_{i,i+1;P}} = \left.\left(\frac{\partial f}{\partial\vec{n}_{i,P}} - \frac{\partial Q_V(f)}{\partial\vec{n}_{i,P}}\right)\right|_{e_{i,i+1;P}},$$

so we require that

$$2K_{1,i,P}(f) + 3K_{3,i,P}(f) = \frac{5^5}{36}\frac{2C_P}{|e_i|}\left(\left.\frac{\partial Q_V(f)}{\partial \vec{n}_{i,P}}\right|_{e_{i,i;P}} - \left.\frac{\partial f}{\partial \vec{n}_{i,P}}\right|_{e_{i,i;P}}\right), \text{ and}$$

$$3K_{1,i,P}(f) + 2K_{3,i,P}(f) = \frac{5^5}{36}\frac{2C_P}{|e_i|}\left(\left.\frac{\partial Q_V(f)}{\partial \vec{n}_{i,P}}\right|_{e_{i,i+1;P}} - \left.\frac{\partial f}{\partial \vec{n}_{i,P}}\right|_{e_{i,i+1;P}}\right); \text{ so}$$

$$\begin{pmatrix} 2 & 3 \\ 3 & 2 \end{pmatrix}\begin{pmatrix} K_{1,i,P}(f) \\ K_{3,i,P}(f) \end{pmatrix} = \frac{5^5}{36}\frac{2C_P}{|e_{i,P}|}\left(\begin{array}{c} \left(\frac{\partial Q_V(f)}{\partial \vec{n}_{i,P}} - \frac{\partial f}{\partial \vec{n}_{i,P}}\right)\Big|_{e_{i,i;P}} \\ \left(\frac{\partial Q_V(f)}{\partial \vec{n}_{i,P}} - \frac{\partial f}{\partial \vec{n}_{i,P}}\right)\Big|_{e_{i,i+1;P}} \end{array}\right)$$

$$\begin{aligned} \Rightarrow K_{1,i,P}(f) &= \frac{5^4}{36}\frac{2C_P}{|e_{i,P}|}\left(3\left(\left(\frac{\partial Q_V(f)}{\partial \vec{n}_{i,P}} - \frac{\partial f}{\partial \vec{n}_{i,P}}\right)\Big|_{e_{i,i+1;P}}\right.\right.\\ &\qquad\qquad\left.\left. - 2\left(\frac{\partial Q_V(f)}{\partial \vec{n}_{i,P}} - \frac{\partial f}{\partial \vec{n}_{i,P}}\right)\Big|_{e_{i,i;P}}\right)\right)\\ &= \frac{2C_P}{36|e_{i,P}|}\vec{n}_{i,P}\Big(\left(883\nabla f\big|_{v_{i,P}} - 258\nabla f\big|_{v_{i+1,P}}\right)\\ &\qquad\qquad\qquad + 6\left(25\nabla^2 f\big|_{v_{i,P}} - 18\nabla^2 f\big|_{v_{i+1,P}}\right)\vec{e}_{i,P}^T\Big)\\ &\quad + \frac{5^4}{36}\frac{2C_P}{|e_{i,P}|}\left(2\frac{\partial f}{\partial \vec{n}_{i,P}}\Big|_{e_{i,i;P}} - 3\frac{\partial f}{\partial \vec{n}_{i,P}}\Big|_{e_{i,i+1;P}}\right); \end{aligned}$$

$$\begin{aligned} K_{3,i,P}(f) &= \frac{5^4}{36}\frac{2C_P}{|e_{i,P}|}\left(3\left(\frac{\partial Q_V(f)}{\partial \vec{n}_{i,P}} - \frac{\partial f}{\partial \vec{n}_{i,P}}\right)\Big|_{e_{i,i;P}}\right.\\ &\qquad\qquad\left. - 2\left(\frac{\partial Q_V(f)}{\partial \vec{n}_{i,P}} - \frac{\partial f}{\partial \vec{n}_{i,P}}\right)\Big|_{e_{i,i+1;P}}\right)\\ &= \frac{2C_P}{36|e_{i,P}|}\vec{n}_{i,P}\Big(\left(883\nabla f\big|_{v_{i+1,P}} - 258\nabla f\big|_{v_{i,P}}\right)\\ &\qquad\qquad\qquad + 6\left(25\nabla^2 f\big|_{v_{i+1,P}} - 18\nabla^2 f\big|_{v_{i,P}}\right)\vec{e}_{i,P}^T\Big)\\ &\quad + \frac{5^4}{36}\frac{2C_P}{|e_{i,P}|}\left(2\frac{\partial f}{\partial \vec{n}_{i,P}}\Big|_{e_{i,i+1;P}} - 3\frac{\partial f}{\partial \vec{n}_{i,P}}\Big|_{e_{i,i;P}}\right). \end{aligned}$$

Similarly, we must set

$$
K_{2,i,R}(f) = \frac{2C_R}{36|e_{i-1,R}|}\left(\left(883\nabla f\big|_{v_{i,R}} - 258\nabla f\big|_{v_{i-1,R}}\right)\right.
$$
$$
\left. + 6\left(25\nabla^2 f\big|_{v_{i,R}} - 18\nabla^2 f\big|_{v_{i-1,R}}\right)\vec{e}_{i-1,R}^{\,T}\right)
$$
$$
+ \frac{5^4}{36}\frac{2C_R}{|e_{i-1,R}|}\left(2\frac{\partial f}{\partial\vec{n}_{i-1,R}}\bigg|_{e_{i-1,i;R}} - 3\frac{\partial f}{\partial\vec{n}_{i-1,R}}\bigg|_{e_{i-1,i-1;R}}\right), \text{ and}
$$
$$
K_{4,i,R}(f) = \frac{2C_R}{36|e_{i-1,R}|}\left(\left(883\nabla f\big|_{v_{i-1,R}} - 258\nabla f\big|_{v_{i,R}}\right)\right.
$$
$$
\left. + 6\left(25\nabla^2 f\big|_{v_{i-1,R}} - 18\nabla^2 f\big|_{v_{i,R}}\right)\vec{e}_{i-1,R}^{\,T}\right)
$$
$$
+ \frac{5^4}{36}\frac{2C_R}{|e_{i-1,R}|}\left(2\frac{\partial f}{\partial\vec{n}_{i-1,R}}\bigg|_{e_{i-1,i-1;R}} - 3\frac{\partial f}{\partial\vec{n}_{i-1,R}}\bigg|_{e_{i-1,i;R}}\right).
$$

Conveniently, this does give us that the functions $\psi^{(5)}_{e,i,P}(f)$ and $\psi^{(5)}_{e,i-1,R}(f)$ join C^1-smoothly over the shared edge $e_{i,P} = e_{i-1,R}$. The plot of an edge spline $\psi^{(5)}_e$ is shown in Figure 4.8.
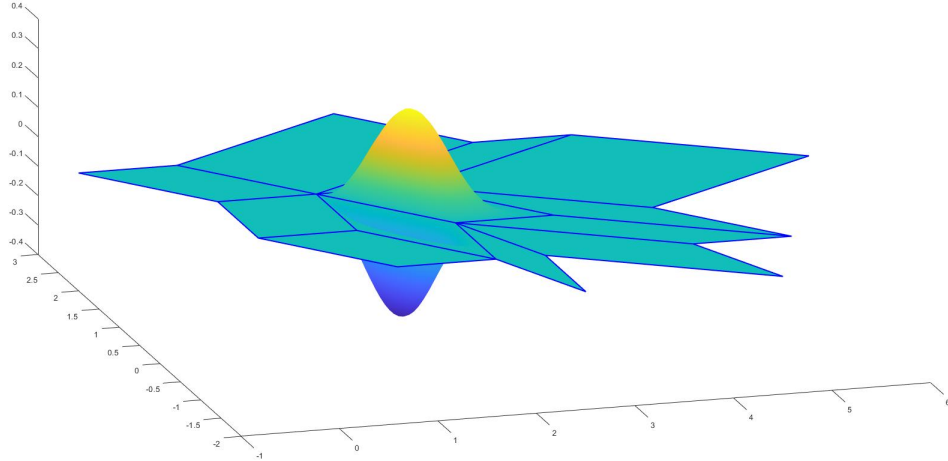
Figure 4.8: The plot of an edge spline $\psi^{(5)}_e$

We can create an improved quasi-interpolatory spline which utilizes both vertex

and edge splines, defined by

$$Q_E(f) = Q_V(f) + \sum_{e \in \mathcal{P}} \psi_e^{(5)}(f). \tag{4.2.7}$$

We should make some comments about degrees of freedom gained to incorporate this improved method. We first define some special edge splines which can act as basis functions. Where e is an edge in $\mathcal{P}$ with $P \in \Omega_e$ and $e = e_{i,P}$, denote by $\psi_{e,1}^{(5)}$ the edge spline which results from the conditions

$$Q_V(f) = 0; \qquad \left.\frac{\partial f}{\partial \vec{n}_{i,P}}\right|_{e_{i,i;P}} = 1; \qquad \left.\frac{\partial f}{\partial \vec{n}_{i,P}}\right|_{e_{i,i+1;P}} = 0,$$

and denote by $\psi_{e,2}^{(5)}$ the edge spline which results from the similar conditions

$$Q_V(f) = 0; \qquad \left.\frac{\partial f}{\partial \vec{n}_{i,P}}\right|_{e_{i,i;P}} = 0; \qquad \left.\frac{\partial f}{\partial \vec{n}_{i,P}}\right|_{e_{i,i+1;P}} = 1.$$

The dimension of the C^1 vertex spline space $\Psi_{5,V}^1(\mathcal{P})$ defined in Theorem 4.1.3 is $6|V|$, where $|V|$ is the number of vertices in $\mathcal{P}$. We can define an augmented space $\Psi_{5,E}^1(\mathcal{P}) := \Psi_{5,V}^1(\mathcal{P}) \bigoplus \text{span}\{\psi_{e,1}^{(5)}, \psi_{e,2}^{(5)}\}_{e \in \mathcal{P}}$ which has all the degrees of freedom of $\Psi_{5,V}^1(\mathcal{P})$, along with 2 additional degrees of freedom for each edge in $\mathcal{P}$, so that $\dim(\Psi_{5,E}^1(\mathcal{P})) = 6|V| + 2|E|$, where $|E|$ is the number of edges in $\mathcal{P}$. Unfortunately, in general the space $\Psi_{5,E}^1(\mathcal{P})$ does not in general contain a polynomial space of a degree higher than 2 - in particular, even degree 3 polynomials incur errors associated with the functions indicated in Figure 4.7b, and in fact these functions don't affect C^1 smoothness at all. For this reason, we can manipulate them freely in each parallelogram, and so we will create another class of new polygonal splines which could be called face splines.

117

4.2.3 Degree-5 face splines

For a given parallelogram P, define the function

$$\psi_{F,i,P}^{(5)} = \phi_i^3 \phi_{i+2}^2.$$

We'll construct a quasi-interpolatory face spline over P by

$$\psi_P^{(5)}(f) = \sum_{i=1}^{4} S_{i,P}(f)\psi_{F,i,P}^{(5)} \tag{4.2.8}$$

for some constants $S_{i,P}(f)$.

We'll determine the constants $S_{i,P}(f)$ as follows. First, we find points $p_{P,i} \in P$ which maximize the functions $\psi_{F,i,P}^{(5)}$. Exploiting parallelogram geometry, we can compute a nice expression of $\nabla\psi_{F,i,P}^{(5)}$:

$$
\begin{aligned}
\nabla\psi_{F,i,P}^{(5)} &= \phi_i^2 \phi_{i+2}\left(3\phi_{i+2}\nabla\phi_i + 2\phi_i\nabla\phi_{i+2}\right)\\
&= \frac{\phi_i^2 \phi_{i+2}}{C^4}\big(A_i(C-A_i)(2C-5A_{i-1})\nabla A_{i-1}\\
&\qquad\qquad + A_{i-1}(C-A_{i-1})(2C-5A_i)\nabla A_i\big).
\end{aligned}
$$

Since ∇A_i and ∇A_{i-1} are linearly independent, it's necessary that we enforce both of the following:

$$A_i(C-A_i)(2C-5A_{i-1}) = 0$$
$$A_{i-1}(C-A_{i-1})(2C-5A_i) = 0.$$

We can ignore the cases when $A_i = 0$, $A_i = C$, $A_{i-1} = 0$, or $A_{i-1} = C$, as these all

happen on ∂P, where $\psi_{F,i,P}^{(5)} = 0$. Thus, we really should enforce

$$\frac{A_i}{C} = \frac{A_{i-1}}{C} = \frac{2}{5}.$$

Since $A_{i+1} = C - A_{i-1}$ and $A_{i+2} = C - A_i$, we can also see that we'll have

$$\frac{A_{i+1}}{C} = \frac{A_{i+2}}{C} = \frac{3}{5}.$$

Then we'll have

$$\phi_i = \frac{A_{i+1}A_{i+2}}{C^2} = \frac{9}{25}; \qquad\qquad \phi_{i+1} = \frac{A_{i+2}A_{i-1}}{C^2} = \frac{6}{25};$$
$$\phi_{i-1} = \frac{A_iA_{i+1}}{C^2} = \frac{6}{25}; \qquad\qquad \phi_{i+2} = \frac{A_{i-1}A_i}{C^2} = \frac{4}{25}.$$

Thus, for $i = 1, 2, 3, 4$, we'll define the points

$$p_{P,i} = \frac{1}{25}\left(9v_i + 6v_{i+1} + 6v_{i-1} + 4v_{i+2}\right),$$

and we'll interpolate the values of f at these points. We have the following values of face spline functions at these points:

$$\psi_{F,i,P}^{(5)}\Big|_{p_{P,i}} = \frac{3^6\,2^4}{5^{10}}; \qquad\qquad \psi_{F,i,P}^{(5)}\Big|_{p_{P,i+1}} = \frac{3^5\,2^5}{5^{10}};$$
$$\psi_{F,i,P}^{(5)}\Big|_{p_{P,i+1}} = \frac{3^5\,2^5}{5^{10}}; \qquad\qquad \psi_{F,i,P}^{(5)}\Big|_{p_{P,i+2}} = \frac{3^4\,2^6}{5^{10}}.$$

Then, for each i, we'll have

$$\psi_{F,P}^{(5)}\Big|_{p_{P,i}} = \frac{3^4\,2^4}{5^{10}}\left(9S_{i,P}(f) + 6S_{i+1,P}(f) + 6S_{i-1,P}(f) + 4S_{i+2,P}(f)\right).$$

We aim to construct a new quasi-interpolant $Q_F(f)$ such that

$$Q_F(f) = Q_E(f) + \sum_{P \in \mathcal{P}} \psi_{F,P}^{(5)}, \qquad (4.2.9)$$

so for each P and $i = 1, 2, 3, 4$, we'll need

$$\psi_{F,P}^{(5)}\big|_{p_{P,i}} = (f - Q_E(f))\big|_{p_{P,i}}.$$

Then we can solve for the coefficients $S_{j,P}(f)$ by the following linear system:

$$\frac{3^4 \, 2^4}{5^{10}} \begin{pmatrix} 9 & 6 & 4 & 6 \\ 6 & 9 & 6 & 4 \\ 4 & 6 & 9 & 6 \\ 6 & 4 & 6 & 9 \end{pmatrix} \begin{pmatrix} S_{1,P}(f) \\ S_{2,P}(f) \\ S_{3,P}(f) \\ S_{4,P}(f) \end{pmatrix} = \begin{pmatrix} (f - Q_E(f))\big|_{p_{P,1}} \\ (f - Q_E(f))\big|_{p_{P,2}} \\ (f - Q_E(f))\big|_{p_{P,3}} \\ (f - Q_E(f))\big|_{p_{P,4}} \end{pmatrix}$$

While it might be preferable to compute some closed form of $Q_E(f)\big|_{p_{P,j}}$ (and, indeed, it can be done), the expression is perhaps best described as abominable. Instead, since this is only value-based, we can simply construct $Q_E(f)$ in full as an intermediate step in the construction of $Q_F(f)$, and then evaluate $Q_E(f)$ at the relevant points. In fact, in numerical trials, direct evaluation of $Q_E(f)$ has proven to be faster than evaluation of various simplifications of the closed form due to the large number of operations in its expression.

After solving the linear system above for the coefficients $S_{j,P}(f)$, we complete the construction of the face spline $\psi_P^{(5)}$ in (4.2.8), and the quasi-interpolatory spline $Q_F(f)$ in (4.2.9). The plot of a face spline $\psi_P^{(5)}$ is shown in Figure 4.9.

We have exhausted all degrees of freedom, and it is easy to show the following result, especially using a computer algebra system like Mathematica:

Theorem 4.2.1. $Q_F(f) = f$ *for any bivariate polynomial f of total degree 5 or less.*
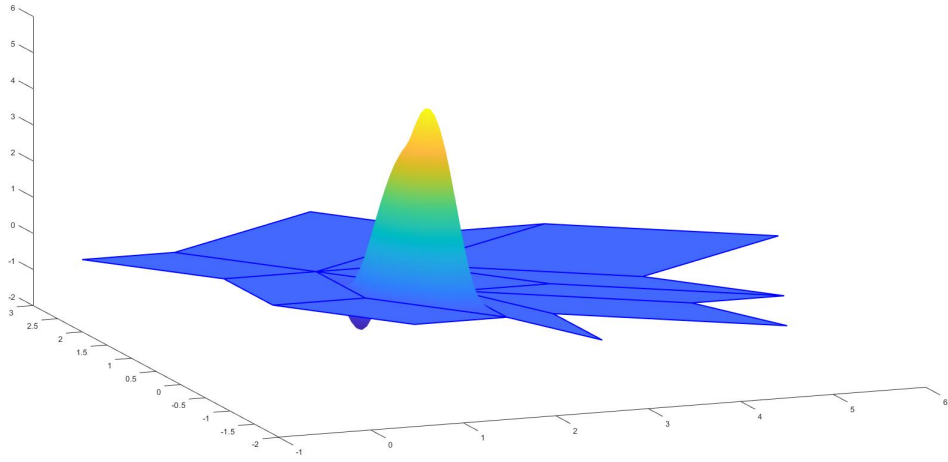
Figure 4.9: The plot of a face spline $\psi_P^{(5)}$

Our final result is an easy corollary of the theorem.

Corollary 4.2.1. *Let $\Omega \subset \mathbb{R}^2$ be a region which permits a parallelogram partition, and let $\mathcal{P}$ be such a parallelogram partition of Ω.*

Define $\Psi_{5,F}^1(\mathcal{P}) := \Psi_{5,E}^1(\mathcal{P}) \bigoplus span\{\psi_{F,i,P}^{(5)}; i = 1, 2, 3, 4\}_{P \in \mathcal{P}}$.

Then $dim(\Psi_{5,F}^1(\mathcal{P})) = 6|V| + 2|E| + 4|F|$, where $|F|$ is the number of parallelograms in $\mathcal{P}$, and $\Pi_5 \subset \Psi_{5,F}^1(\mathcal{P}) \subset C^1(\Omega)$.

4.3 Approximation properties and numerical results

Using the same notation and techniques as mentioned in Chapter 3 Section 3.3, we can show the following result on the approximation power of degree-5 C^1 polygonal vertex splines:

Theorem 4.3.1. *For any function $f \in C^3(\Omega)$, the quasi-interpolatory C^1 polygonal*

vertex spline $Q_{V,k}(f) \in \Psi^1_{5,V}(\mathcal{P}_k)$ *satisfies*

$$||f - Q_{V,k}(f)||_{\infty,\Omega} \le C|f|_{3,\infty,\Omega}2^{-3k}$$

where C is a positive constant independent of f.

For any function $u \in H^3(\Omega)$, *the quasi-interpolatory C^1 polygonal vertex spline* $Q_{V,k}(u) \in \Psi^1_{5,V}(\mathcal{P}_k)$ *satisfies*

$$||u - Q_{V,k}(u)||_{2,\Omega} \le C|u|_{3,2,\Omega}2^{-3k}$$

and

$$|u - Q_{V,k}(u)|_{1,2,\Omega} \le C|u|_{3,2,\Omega}2^{-2k}$$

where C is a positive constant independent of u, but which may depend on the boundary of Ω if Ω is nonconvex.

If we use the full degree-5 C^1 polygonal spline space $\Psi^1_{5,F}(\mathcal{P})$, we can similarly show the following:

Theorem 4.3.2. *For any function $f \in H^6(\Omega)$, the quasi-interpolatory polygonal spline $Q_{F,k}(f) \in \Psi^1_{5,F}(\mathcal{P}_k)$ satisfies*

$$||f - Q_{F,k}(f)||_{2,\Omega} \le C|f|_{6,2,\Omega}2^{-6k}$$

and

$$|f - Q_{F,k}(f)|_{1,2,\Omega} \le C|f|_{6,2,\Omega}2^{-5k}$$

where C is a positive constant independent of f, but which may depend on the boundary of Ω is Ω is nonconvex.

We devote the rest of this section to showing numerical examples of quasi-interpolation by the degree-5 C^1 polygonal splines developed in this chapter.
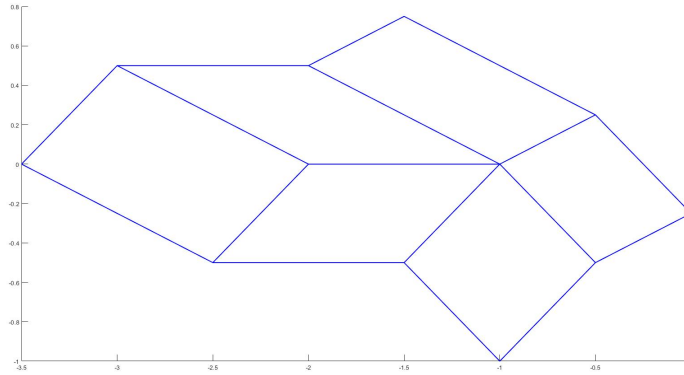
Figure 4.10: A parallelogram partition used to numerically test the degree-5 polygonal spline quasi-interpolation schemes

Let $\mathcal{P}$ be the partition shown in Figure 4.10, and let h be the largest diameter of any parallelogram in $\mathcal{P}$. For each example, we'll report the root mean square error $||\cdot||_{RMS}$ of the quasi-interpolants computed over approximately 500×500 points on the interior of the partition, along with the convergence rate in terms of h. We denote the errors by $E_V(u) := ||u - Q_V(u)||_{RMS}$ and $E_F(u) := ||u - Q_F(u)||_{RMS}$. We expect that the degree-5 C^1 polygonal vertex spline quasi-interpolants $Q_V(u)$ should converge in the L^2 norm at order $O(h^3)$, while the degree-5 C^1 polygonal spline quasi-interpolants $Q_F(u)$ should converge in the L^2 norm at order $O(h^6)$.

We display the numerical error of the quasi-interpolants in the tables below. We first attempt quasi-interpolation of a few trigonometric functions; in order of increasing frequency, we set $u_1(x, y) = \sin(x)\sin(y)$, $u_2(x, y) = \sin(\pi x)\sin(\pi y)$, and $u_3(x, y) = \sin(2\pi x)\sin(2\pi y)$. We measure the error of the quasi-interpolants constructed over the partition in Figure 4.10 along with 3 of its uniform refinements.

Table 4.1: Degree-5 C^1 polygonal vertex spline quasi-interpolation of the function $u_1(x, y) = \sin(x)\sin(y)$

# Quads	h	$E_V(u_1)$	rate
6	2.06e+00	1.14e-03	0.00
24	1.03e+00	1.38e-04	3.05
96	5.15e-01	1.67e-05	3.05
384	2.58e-01	2.03e-06	3.04

Table 4.2: Degree-5 C^1 polygonal spline quasi-interpolation of the function $u_1(x, y) = \sin(x)\sin(y)$

# Quads	h	$E_F(u_1)$	rate
6	2.06e+00	1.89e-05	0.00
24	1.03e+00	3.07e-07	5.94
96	5.15e-01	4.86e-09	5.98
384	2.58e-01	7.68e-11	5.98

Table 4.3: Degree-5 C^1 polygonal vertex spline quasi-interpolation of the function $u_2(x, y) = \sin(\pi x)\sin(\pi y)$

# Quads	h	$E_V(u_2)$	rate
6	2.06e+00	4.37e-02	0.00
24	1.03e+00	3.42e-03	3.68
96	5.15e-01	4.59e-04	2.89
384	2.58e-01	5.20e-05	3.14

Table 4.4: Degree-5 C^1 polygonal spline quasi-interpolation of the function $u_2(x, y) = \sin(\pi x)\sin(\pi y)$

# Quads	h	$E_F(u_2)$	rate
6	2.06e+00	1.31e-02	0.00
24	1.03e+00	3.07e-04	5.41
96	5.15e-01	4.93e-06	5.96
384	2.58e-01	7.88e-08	5.97

Table 4.5: Degree-5 C^1 polygonal vertex spline quasi-interpolation of the function $u_3(x, y) = \sin(2\pi x)\sin(2\pi y)$

# Quads	h	$E_V(u_3)$	rate
6	2.06e+00	5.02e-01	0.00
24	1.03e+00	4.55e-02	3.46
96	5.15e-01	3.41e-03	3.74
384	2.58e-01	4.51e-04	2.92

Table 4.6: Degree-5 C^1 polygonal spline quasi-interpolation of the function $u_3(x, y) = \sin(2\pi x)\sin(2\pi y)$

# Quads	h	$E_F(u_3)$	rate
6	2.06e+00	2.51e-01	0.00
24	1.03e+00	1.44e-02	4.13
96	5.15e-01	2.87e-04	5.64
384	2.58e-01	4.84e-06	5.89

Notice that, for functions which oscillate more quickly, we require a finer mesh before any convergence can be observed. In the cases of u_1 and u_2, we see convergence immediately, but in the case of u_3, we do not see the appropriate convergence using the full quasi-interpolant $Q_F(u_3)$ until the partition has been refined an additional time or two.

We interpolate a few more examples of different function types: set $u_4(x, y) = \sin(\pi(x^2 + y^2))$, $u_5(x, y) = (10 + x + y)^{-1}$, and $u_6(x, y) = (1 + x^2 + y^2)^{-1}$. In the case of u_4, we see again that, since the frequency rises quickly away from zero, we require a fine mesh before we can observe the asymptotic convergence. This function would be well-suited to using an adaptively-refined mesh, but we are not aware of such methods for parallelogram meshes.

Table 4.7: Degree-5 C^1 polygonal vertex spline quasi-interpolation of the function $u_4(x, y) = \sin(\pi(x^2 + y^2))$

# Quads	h	$E_V(u_4)$	rate
6	2.06e+00	3.83e+00	0.00
24	1.03e+00	7.71e-01	2.31
96	5.15e-01	7.95e-02	3.28
384	2.58e-01	4.66e-03	4.09

Table 4.8: Degree-5 C^1 polygonal spline quasi-interpolation of the function $u_4(x, y) = \sin(\pi(x^2 + y^2))$

# Quads	h	$E_F(u_4)$	rate
6	2.06e+00	2.04e+00	0.00
24	1.03e+00	3.61e-01	2.50
96	5.15e-01	1.73e-02	4.38
384	2.58e-01	3.37e-04	5.68

Table 4.9: Degree-5 C^1 polygonal vertex spline quasi-interpolation of the function $u_5(x, y) = (10 + x + y)^{-1}$

# Quads	h	$E_V(u_5)$	rate
6	2.06e+00	1.81e-06	0.00
24	1.03e+00	2.10e-07	3.11
96	5.15e-01	2.56e-08	3.04
384	2.58e-01	3.11e-09	3.04

Table 4.10: Degree-5 C^1 polygonal spline quasi-interpolation of the function $u_5(x, y) = (10 + x + y)^{-1}$

# Quads	h	$E_F(u_5)$	rate
6	2.06e+00	2.91e-09	0.00
24	1.03e+00	4.57e-11	5.99
96	5.15e-01	7.18e-13	5.99
384	2.58e-01	1.13e-14	5.98

Table 4.11: Degree-5 C^1 polygonal vertex spline quasi-interpolation of the function $u_6(x, y) = (1 + x^2 + y^2)^{-1}$

# Quads	h	$E_V(u_6)$	rate
6	2.06e+00	1.01e-03	0.00
24	1.03e+00	8.28e-05	3.61
96	5.15e-01	8.85e-06	3.23
384	2.58e-01	1.03e-06	3.10

Table 4.12: Degree-5 C^1 polygonal spline quasi-interpolation of the function $u_6(x, y) = (1 + x^2 + y^2)^{-1}$

# Quads	h	$E_F(u_6)$	rate
6	2.06e+00	1.46e-04	0.00
24	1.03e+00	2.51e-06	5.86
96	5.15e-01	4.34e-08	5.85
384	2.58e-01	7.78e-10	5.80

4.4 An application toward surface construction

We can use these polygonal splines to construct C^1 surfaces so long as we avoid self-intersection. Of course, if we can express such a surface as the plot of a function, we can simply interpolate that function with our C^1 polygonal splines. On the other hand, we can also create parametric surfaces by choosing a region $\Omega \subset \mathbb{R}^2$ which permits a parallelogram partition, and constructing three C^1 polygonal splines $x(u, v)$, $y(u, v)$, and $z(u, v)$ over $\mathcal{P}$, which we use as parameters. Below are some examples of some strange tori we can create over a grid partition of the unit square. To be clear: the torus surfaces plotted are parametric, where all parameters x, y, z are C^1 polygonal splines over the partitions shown.

First we quasi-interpolate a plain torus, parameterized over the square $[-\pi, \pi]^2$ in the plane which has parameters $x_1(u, v) = (1.5 + \cos(v)) \cos(u)$,
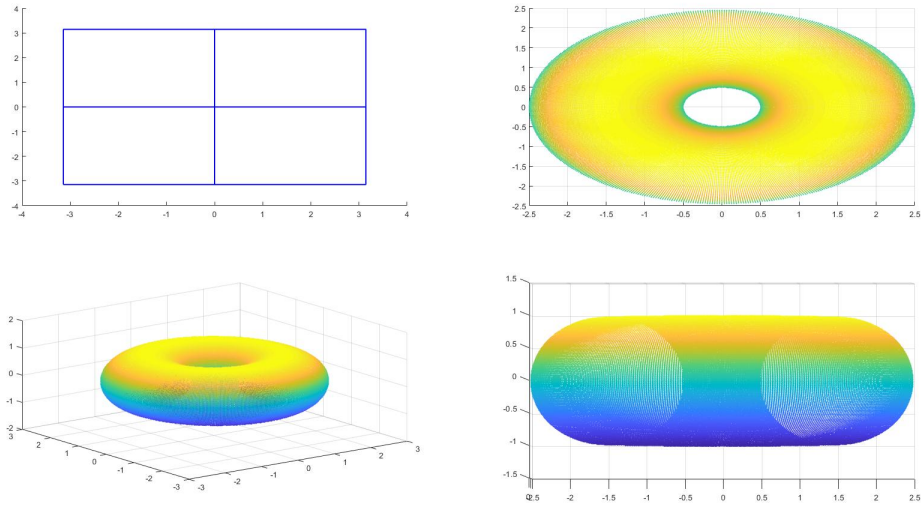
Figure 4.11: Views of a degree-5 C^1 polygonal spline quasi-interpolant of a torus parameterized by (x_1, y_1, z_1) over the partition shown in the upper-left

$y_1(u, v) = (1.5 + \cos(v)) \sin(u)$, and $z_1(u, v) = \sin(v)$. We show three views of the interpolated surface, which has parameters $Q_F(x_1), Q_F(y_1)$, and $Q_F(z_1)$. Note that, in this case, we only use 4 patches and still retrieve a nice, smooth quasi-interpolant. See Figure 4.11.

Now we'll quasi-interpolate some modified tori. The torus shown in Figure 4.12 is parameterized over the same square $[-\pi, \pi]^2$ in the plane, this time with parameters $x_2(u, v) = (\sin(v) + \cos(v) + 2) \cos(u)$, $y_2(u, v) = (\sin(v) + \cos(v) + 2) \sin(u)$, and $z_2(u, v) = \sin(v)$. The interpolated surface with parameters $Q_F(x_2)$, $Q_F(y_2)$, and $Q_F(z_2)$ is constructed over 16 patches this time, shown in Figure 4.12.

The torus shown in Figure 4.13 is again parameterized over the same square, this time with parameters $x_3(u, v) = (\sin(u) + 2 + 0.5(2 + \sin(u)) \cos(v)) \cos(u)$, $y_3(u, v) = (\sin(u) + 2 + 0.5(2 + \sin(u)) \cos(v)) \sin(u)$, and $z_3(u, v) = 0.5(2 + \sin(u)) \sin(v)$. The interpolated surface with parameters $Q_F(x_3)$, $Q_F(y_3)$, and $Q_F(z_3)$ is again constructed over 16 patches, shown in Figure 4.13.

127
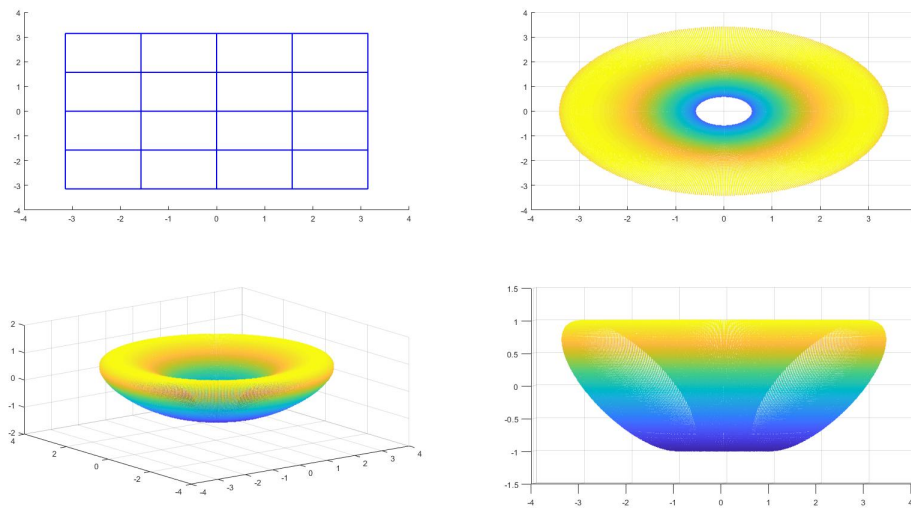
Figure 4.12: Views of a degree-5 C^1 polygonal spline quasi-interpolant of a modified torus parameterized by (x_2, y_2, z_2) over the partition shown in the upper-left
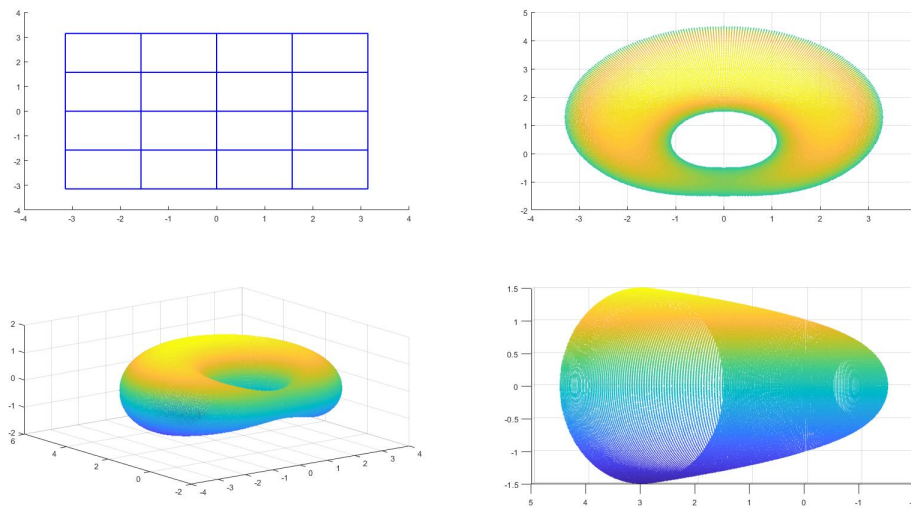
Figure 4.13: Views of a degree-5 C^1 polygonal spline quasi-interpolant of a modified torus parameterized by (x_3, y_3, z_3) over the partition shown in the upper-left
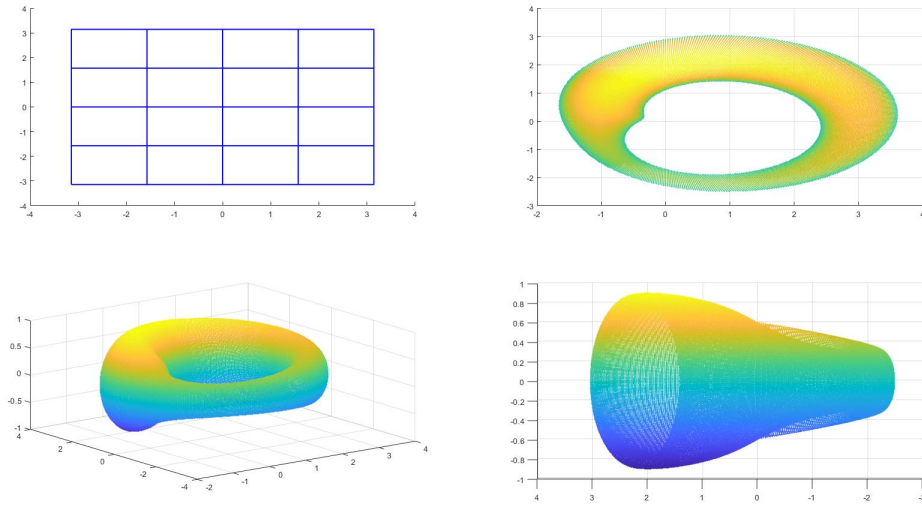
Figure 4.14: Views of a degree-5 C^1 polygonal spline quasi-interpolant of a modified torus parameterized by (x_4, y_4, z_4) over the partition shown in the upper-left

The torus shown in Figure 4.14 is parameterized over the same square with parameters $x_4(u, v) = (\cos(u) + 2 + 0.3(2 + \sin(u)) \cos(v)) \cos(u)$,

$y_4(u, v) = (\cos(u) + 2 + 0.3(2 + \sin(u)) \cos(v)) \sin(u)$, and

$z_4(u, v) = 0.3(2 + \sin(u)) \sin(v)$. The interpolated surface with parameters $Q_F(x_4)$, $Q_F(y_4)$, and $Q_F(z_4)$ is again constructed over 16 patches, shown in Figure 4.14.

The torus shown in Figure 4.15 is parameterized by

$x_5(u, v) = (\sin(v) + 2 + 0.5(2 + \sin(u)) \cos(v)) \cos(u)$,

$y_5(u, v) = (\sin(v) + 2 + 0.5(2 + \sin(u)) \cos(v)) \sin(u)$, and

$z_5(u, v) = 0.5(2 + \sin(u)) \sin(v)$. The interpolated surface with parameters $Q_F(x_5)$, $Q_F(y_5)$, and $Q_F(z_5)$ is again constructed over 16 patches, shown in Figure 4.15.
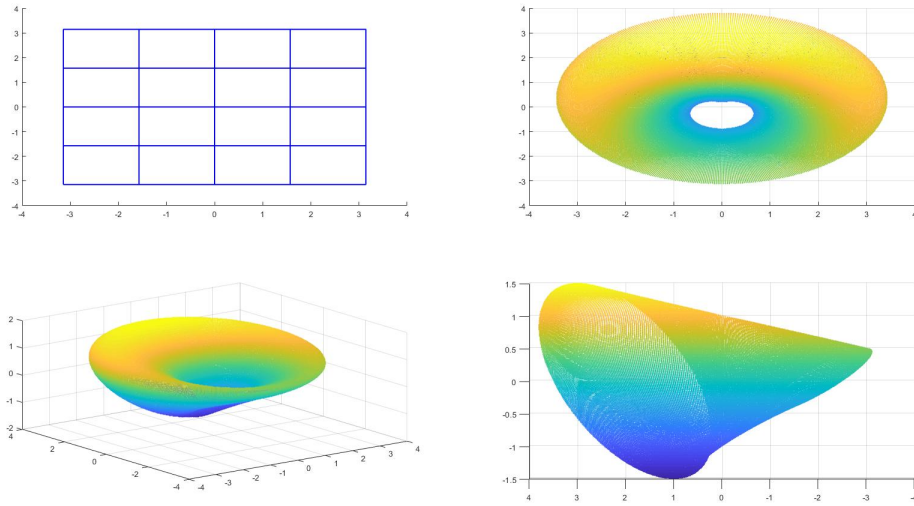
Figure 4.15: Views of a degree-5 C^1 polygonal spline quasi-interpolant of a modified torus parameterized by (x_5, y_5, z_5) over the partition shown in the upper-left

4.5 Increasing to degree 6

Again we try increasing the degree in order to further loosen the restrictions on the underlying partition, but we encounter a similar situation as when increasing from degree 3 to degree 4: the space $\Psi_6(\mathcal{P})$ is not a C^1 linear space over any more general partitions $\mathcal{P}$ than the space $\Psi_5(\mathcal{P})$. For this reason, we move on to construct some vertex splines in degree 7.

Chapter 5

A Degree-7 Construction of C^1 Polygonal Splines on Arbitrary Quadrilateral Partitions

5.1 Degree-7 polygonal vertex splines

5.1.1 Construction of $\psi_v^{(7)}$

We will now build a degree-7 polygonal spline function $\psi_v^{(7)}$ which is analogous to $\psi_v^{(5)}$ and $\psi_v^{(3)}$, but we'll see that the flexibility we gain by using this high degree allows us to construct quasi-interpolatory vertex spline functions which do not impose any additional conditions on the underlying partition of quadrilaterals $\mathcal{P}$.

As usual, we'll restrict our attention to a single quadrilateral P in Ω_v, and write $\psi_v^{(7)}\big|_P = \psi_{i,P}^{(7)}$ where $v = v_i$ in P. In this degree-7 case, a (lengthy) template for our

function is given by

$$
\psi_i^{(7)} = \phi_i^2 \Big(J_{0,i}\phi_i^5 + \phi_i^4(J_{1,i}\phi_{i+1} + J_{2,i}\phi_{i-1}) + \phi_i^3(J_{3,i}\phi_{i+1}^2 + J_{4,i}\phi_{i-1}^2)
$$

$$
+ \phi_i^2(J_{5,i}\phi_{i+1}^3 + J_{6,i}\phi_{i-1}^3) + \phi_i\left(J_{7,i}\phi_{i+1}^4 + J_{8,i}\phi_{i-1}^4\right) + J_{9,i}\phi_{i+1}^5 + J_{10,i}\phi_{i-1}^5
$$

$$
+ \phi_{i+2}\big(K_{0,i}\phi_i^4 + \phi_i^3(K_{1,i}\phi_{i+1} + K_{2,i}\phi_{i-1}) + \phi_i^2(K_{3,i}\phi_{i+1}^2 + K_{4,i}\phi_{i-1}^2)
$$

$$
+ \phi_i(K_{5,i}\phi_{i+1}^3 + K_{6,i}\phi_{i-1}^3) + K_{7,i}\phi_{i+1}^4 + K_{8,i}\phi_{i-1}^4\big)
$$

$$
+ \phi_{i+2}^2\big(S_{0,i}\phi_i^3 + \phi_i^2(S_{1,i}\phi_{i+1} + S_{2,i}\phi_{i-1}) + \phi_i(S_{3,i}\phi_{i+1}^2 + S_{4,i}\phi_{i-1}^2)
$$

$$
+ S_{5,i}\phi_{i+1}^3 + S_{6,i}\phi_{i-1}^3\big)
$$

$$
+ \phi_{i+2}^3\big(L_{0,i}\phi_i^2 + \phi_i(L_{1,i}\phi_{i+1} + L_{2,i}\phi_{i-1}) + L_{3,i}\phi_{i+1}^2 + L_{4,i}\phi_{i-1}^2\big)
$$

$$
+ \phi_{i+2}^4\big(N_{0,i}\phi_i + N_{1,i}\phi_{i+1} + N_{2,i}\phi_{i-1} + N_{3,i}\phi_{i+2}\big)\Big). \tag{5.1.1}
$$

Before beginning our analysis to solve for the coefficients in (5.1.1), it's worth considering its terms from a domain point perspective. As we can see from Figure 5.1, there is much overlap.

To be able to exert Hessian control locally at each vertex as we did in degree 5, we'll need to set $J_{9,i} = J_{10,i} = 0$. We'll leave all the K coefficients intact, as these allow us to ensure C^1 smoothness over the edges, but since the functions with $S, L,$ and N coefficients are more or less free, we choose to set as zero all the remaining coefficients except $S_{0,i}, S_{1,i}, S_{2,i}$ and $L_{0,i}$. We retrieve the following simplified template:

$$
\psi_i^{(7)} = \phi_i^2 \Big(J_{0,i}\phi_i^5 + \phi_i^4(J_{1,i}\phi_{i+1} + J_{2,i}\phi_{i-1}) + \phi_i^3(J_{3,i}\phi_{i+1}^2 + J_{4,i}\phi_{i-1}^2)
$$

$$
+ \phi_i^2(J_{5,i}\phi_{i+1}^3 + J_{6,i}\phi_{i-1}^3) + \phi_i\left(J_{7,i}\phi_{i+1}^4 + J_{8,i}\phi_{i-1}^4\right)
$$

$$
+ \phi_{i+2}\big(K_{0,i}\phi_i^4 + \phi_i^3(K_{1,i}\phi_{i+1} + K_{2,i}\phi_{i-1}) + \phi_i^2(K_{3,i}\phi_{i+1}^2 + K_{4,i}\phi_{i-1}^2)
$$

$$
+ \phi_i(K_{5,i}\phi_{i+1}^3 + K_{6,i}\phi_{i-1}^3) + K_{7,i}\phi_{i+1}^4 + K_{8,i}\phi_{i-1}^4\big)
$$

$$
+ \phi_{i+2}^2\big(S_{0,i}\phi_i^3 + \phi_i^2(S_{1,i}\phi_{i+1} + S_{2,i}\phi_{i-1})\big) + L_{0,i}\phi_{i+2}^3\phi_i^2\Big). \tag{5.1.2}
$$

132
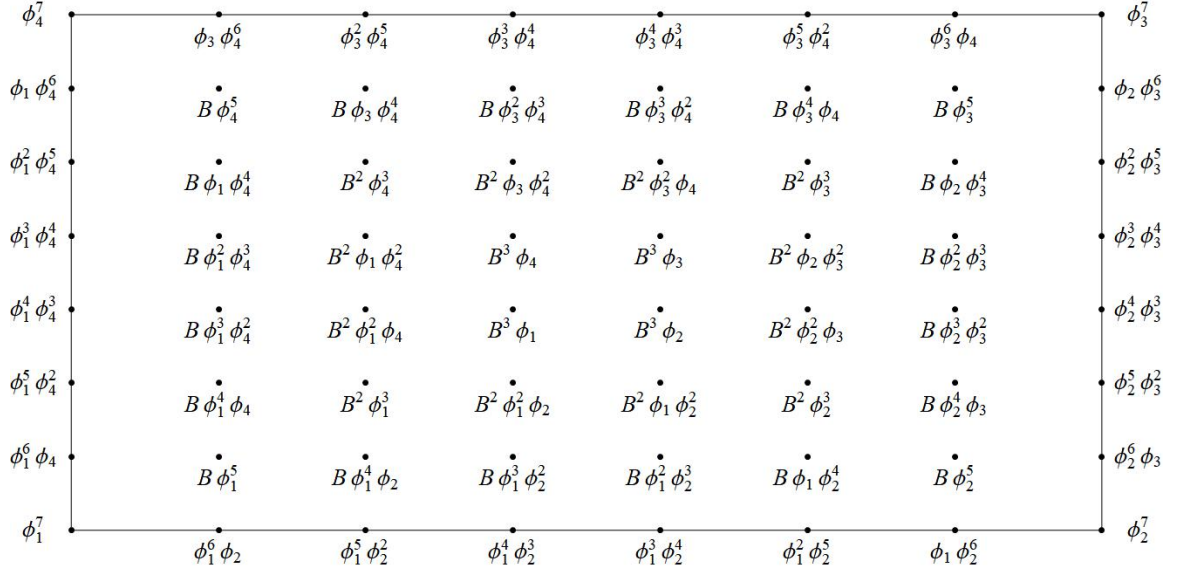
(a) Domain points associated with degree-7 basis functions
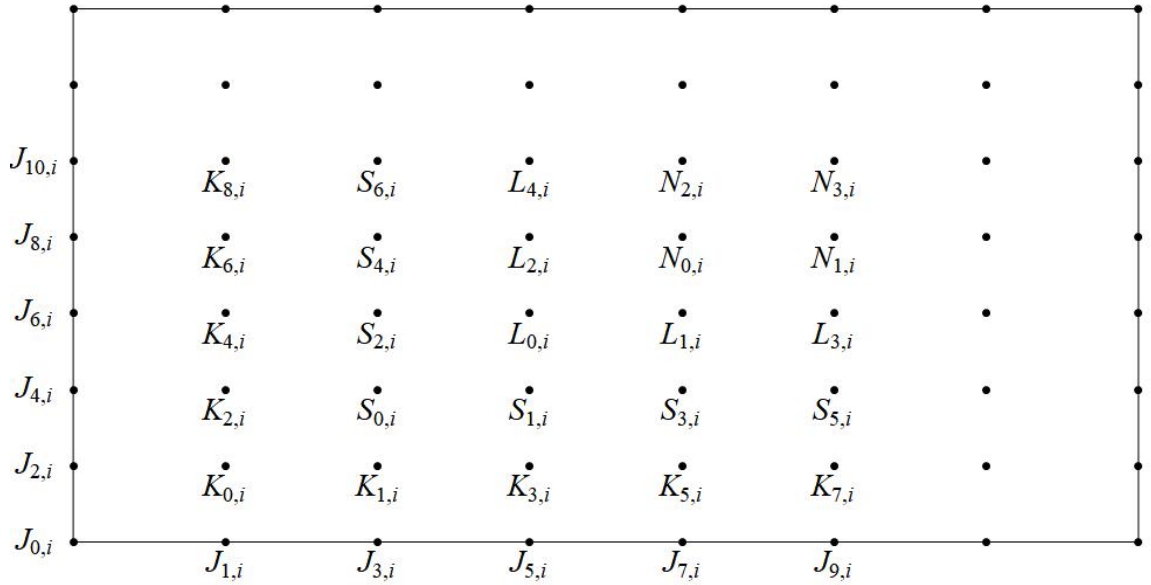
(b) Domain points and the associated coefficients in (5.1.1)

Figure 5.1: A domain point illustration of the redundancy of the terms used in the template (5.1.1

133

The function $\psi_i^{(7)}$ should satisfy $\psi_i^{(7)}\big|_{v_j} = \delta_{ij}$, so we'll need $\psi_i^{(7)}\big|_{v_i} = J_{0,i} = 1$. We'll also need that $\nabla\psi_i^{(7)}\big|_{v_i} = 0$, so we'll compute the edge direction derivatives at v_i:

$$\frac{\partial\psi_i^{(7)}}{\partial\tilde{e}_i}\bigg|_{v_i} = 7\frac{\partial\phi_i}{\partial\tilde{e}_i} + J_{1,i}\frac{\partial\phi_{i+1}}{\partial\tilde{e}_i}$$

$$= \frac{J_{1,i} - 7}{|e_i|};$$

$$\frac{\partial\psi_i^{(7)}}{\partial\tilde{e}_{i-1}}\bigg|_{v_i} = 7\frac{\partial\phi_i}{\partial\tilde{e}_{i-1}} + J_{2,i}\frac{\partial\phi_{i-1}}{\partial\tilde{e}_{i-1}}$$

$$= \frac{7 - J_{2,i}}{|e_{i-1}|};$$

so we'll set $J_{1,i} = J_{2,i} = 7$.

To enforce the condition $\nabla^2\psi_i^{(7)}\big|_{v_i} = 0$, we'll take the second edge-direction derivatives:

$$\frac{\partial^2\psi_i^{(7)}}{\partial\tilde{e}_i^2}\bigg|_{v_i} = 42\left(\frac{\partial\phi_i}{\partial\tilde{e}_i}\right)^2 + 84\frac{\partial\phi_i}{\partial\tilde{e}_i}\frac{\partial\phi_{i+1}}{\partial\tilde{e}_i} + 2J_{3,i}\left(\frac{\partial\phi_{i+1}}{\partial\tilde{e}_i}\right)^2$$

$$= \frac{2J_{3,i} - 42}{|e_i|^2};$$

$$\frac{\partial^2\psi_i^{(7)}}{\partial\tilde{e}_{i-1}^2}\bigg|_{v_i} = 42\left(\frac{\partial\phi_i}{\partial\tilde{e}_{i-1}}\right)^2 + 84\frac{\partial\phi_i}{\partial\tilde{e}_{i-1}}\frac{\partial\phi_{i+1}}{\partial\tilde{e}_{i-1}} + 2J_{4,i}\left(\frac{\partial\phi_{i-1}}{\partial\tilde{e}_{i-1}}\right)^2$$

$$= \frac{2J_{4,i} - 42}{|e_{i-1}|^2};$$

$$\frac{\partial^2\psi_i^{(7)}}{\partial\tilde{e}_i\partial\tilde{e}_{i-1}}\bigg|_{v_i} = 7\left(\frac{\partial^2\phi_i}{\partial\tilde{e}_i\partial\tilde{e}_{i-1}} + \frac{\partial^2\phi_{i+1}}{\partial\tilde{e}_i\partial\tilde{e}_{i-1}} + \frac{\partial^2\phi_{i-1}}{\partial\tilde{e}_i\partial\tilde{e}_{i-1}}\right)$$

$$+ 42\left(\frac{\partial\phi_i}{\partial\tilde{e}_i}\frac{\partial\phi_i}{\partial\tilde{e}_{i-1}} + \frac{\partial\phi_i}{\partial\tilde{e}_i}\frac{\partial\phi_{i-1}}{\partial\tilde{e}_{i-1}} + \frac{\partial\phi_i}{\partial\tilde{e}_{i-1}}\frac{\partial\phi_{i+1}}{\partial\tilde{e}_i}\right)$$

$$+ K_{0,i}\frac{\partial^2\phi_{i+2}}{\partial\tilde{e}_i\partial\tilde{e}_{i-1}}$$

$$= \frac{1}{|e_i||e_{i-1}|}\left(42 + \frac{C_iC_{i+2}}{C_{i+1}C_{i-1}}(7 - K_{0,i})\right);$$

so we'll set $J_{3,i} = J_{4,i} = 21$ and $K_{0,i} = 7 + 42\dfrac{C_{i+1}C_{i-1}}{C_iC_{i+2}}$.

At this point, we have the following:

$$\psi_i^{(7)} = \phi_i^2 \Bigg(\phi_i^5 + 7\phi_i^4(\phi_{i+1} + \phi_{i-1}) + 21\phi_i^3(\phi_{i+1}^2 + \phi_{i-1}^2)$$

$$+ \phi_i^2(J_{5,i}\phi_{i+1}^3 + J_{6,i}\phi_{i-1}^3) + \phi_i \left(J_{7,i}\phi_{i+1}^4 + J_{8,i}\phi_{i-1}^4 \right)$$

$$+ \phi_{i+2}\Bigg(\left(7 + 42\frac{C_{i+1}C_{i-1}}{C_iC_{i+2}} \right)\phi_i^4 + \phi_i^3(K_{1,i}\phi_{i+1} + K_{2,i}\phi_{i-1})$$

$$+ \phi_i^2(K_{3,i}\phi_{i+1}^2 + K_{4,i}\phi_{i-1}^2) + \phi_i(K_{5,i}\phi_{i+1}^3 + K_{6,i}\phi_{i-1}^3)$$

$$+ K_{7,i}\phi_{i+1}^4 + K_{8,i}\phi_{i-1}^4 \Bigg)$$

$$+ \phi_{i+2}^2\left(S_{0,i}\phi_i^3 + \phi_i^2(S_{1,i}\phi_{i+1} + S_{2,i}\phi_{i-1}) \right) + L_{0,i}\phi_{i+2}^3\phi_i^2 \Bigg). \qquad (5.1.3)$$

We are still missing some of the J coefficients. A reasonable first thought is to consider the sum condition $\sum_{j=1}^{4}\psi_i^{(7)} = 1$ on a single edge; say e_i:

$$\left(1 - \sum_{j=1}^{4}\psi_i^{(7)} \right)\Bigg|_{e_i} = \left((\phi_i + \phi_{i+1})^7 - \psi_i^{(7)} + \psi_{i+1}^{(7)} \right)\Big|_{e_i}$$

$$= (35 - (J_{5,i} + J_{7,i+1}))\phi_i^4\phi_{i+1}^3 + (35 - (J_{5,i+1} + J_{7,i}))\phi_i^3\phi_{i+1}^4.$$

Since the J coefficients are absolute constants in $\psi_i^{(3)}, \psi_i^{(5)}$, and thus far in $\psi_i^{(7)}$, we assume that $J_{5,i}$ and $J_{7,i}$ shouldn't break this trend, so that $J_{5,i} = J_{5,j}$ and $J_{7,i} = J_{7,j}$ for any i, j. Then we set $J_{7,i} = 35 - J_{5,i}$. Unfortunately, we aren't yet able to determine a set value for $J_{5,i}$ - we'll have to leave it for now, but we can solve for the K coefficients in terms of $J_{5,i}$ by enforcing C^1 smoothness over shared edges.

First, we need to take the outward normal derivatives on edges e_i and e_{i-1}. These expressions are long and complicated. Fortunately, we are still able to force that $\dfrac{\partial\psi_i^{(7)}}{\partial\vec{n}_i}\bigg|_{e_i} = \dfrac{\partial\psi_i^{(7)}}{\partial\vec{n}_{i-1}}\bigg|_{e_{i-1}} = 0$, as we did for $\psi_i^{(3)}$ and $\psi_i^{(5)}$. We'll show the computation

for the normal derivative on the edge e_i:

$$
\begin{aligned}
\frac{\partial \psi_i^{(7)}}{\partial \vec{n}_i}\bigg|_{e_i} = \frac{1}{2A_{i+2}}\bigg(& \phi_i^6 \phi_{i+1}^2 \bigg((105e_i + (3J_{5,i} - 105)|e_{i-1}|\cos(\theta_i)) \frac{C_{i-1}}{C_i} \\
& + (42 - K_{1,i})|e_i| \frac{C_{i+2}}{C_{i+1}} \bigg) \\
+ \phi_i^5 \phi_{i+1}^3 \bigg(& (147 - K_{1,i} - K_{3,i})|e_i| \frac{C_{i+2}}{C_{i+1}} \\
& + (7J_{5,i}e_i + (140 - 8J_{5,i})|e_{i-1}|\cos(\theta_i)) \frac{C_{i-1}}{C_i} \\
& + (3J_{5,i} - 105)|e_{i-1}|\cos(\theta_i) \frac{C_{i+2}}{C_i} \\
& + (105 - 3J_{5,i})|e_{i+1}|\cos(\theta_{i+1}) \frac{C_{i-1}}{C_{i+1}} \bigg) \\
+ \phi_i^4 \phi_{i+1}^4 \bigg(& ((7J_{5,i} - K_{3,i} - K_{5,i})|e_i| + (105 - 3J_{5,i})|e_{i+1}|\cos(\theta_{i+1})) \frac{C_{i+2}}{C_{i+1}} \\
& + ((245 - 7J_{5,i})|e_i| + (3J_{5,i} - 105)|e_{i-1}|\cos(\theta_i)) \frac{C_{i-1}}{C_i} \\
& + (140 - 8J_{5,i})|e_{i-1}|\cos(\theta_i) \frac{C_{i+2}}{C_i} \\
& + (8J_{5,i} - 140)|e_{i+1}|\cos(\theta_{i+1}) \frac{C_{i-1}}{C_{i+1}} \bigg) \\
+ \phi_i^3 \phi_{i+1}^5 \bigg(& ((245 - 7J_{5,i} - K_{5,i} - K_{7,i})|e_i| \\
& + (8J_{5,i} - 140)|e_{i+1}|\cos(\theta_{i+1})) \frac{C_{i+2}}{C_{i+1}} \\
& + (3J_{5,i} - 105)|e_{i-1}|\cos(\theta_i) \frac{C_{i+2}}{C_i} \\
& + (105 - 3J_{5,i})|e_{i+1}|\cos(\theta_{i+1}) \frac{C_{i-1}}{C_{i+1}} \bigg) \\
+ \phi_i^2 \phi_{i+1}^6 \bigg(& (-K_{7,i}|e_i| + (105 - 3J_{5,i})|e_{i+1}|\cos(\theta_{i+1})) \frac{C_{i+2}}{C_{i+1}} \bigg) \bigg). \quad (5.1.4)
\end{aligned}
$$

Moving from bottom to top, we can choose the following choices of K coefficients to

set each term zero one at a time:

$$K_{7,i} = (105 - 3J_{5,i})\frac{|e_{i+1}|}{|e_i|}\cos(\theta_{i+1});$$

$$K_{5,i} = 245 - 7J_{5,i} + \left(11J_{5,i} - 245 + (105 - 3J_{5,i})\frac{C_{i-1}}{C_{i+2}}\right)\frac{|e_{i+1}|}{|e_i|}\cos(\theta_{i+1})$$
$$+ (3J_{5,i} - 105)\frac{|e_{i-1}|}{|e_i|}\frac{C_{i+1}}{C_i}\cos(\theta_i);$$

$$K_{3,i} = 14J_{5,i} - 245 + \left(350 - 14J_{5,i} + (11J_{5,i} - 245)\frac{C_{i-1}}{C_{i+2}}\right)\frac{|e_{i+1}|}{|e_i|}\cos(\theta_{i+1})$$
$$+ \left(245 - 11J_{5,i} + (140 - 4J_{5,i})\frac{C_{i-1}}{C_{i+2}}\right)\frac{C_{i+1}}{C_i}\frac{|e_{i-1}|}{|e_i|}\cos(\theta_i);$$

$$K_{1,i} = 392 - 14J_{5,i} + \left(14J_{5,i} - 350 + (350 - 14J_{5,i})\frac{C_{i-1}}{C_{i+2}}\right)\frac{|e_{i+1}|}{|e_i|}\cos(\theta_{i+1})$$
$$+ \left(14J_{5,i} - 350 + 3J_{5,i}\frac{C_{i-1}}{C_{i+2}}\right)\frac{C_{i+1}}{C_i}\frac{|e_{i-1}|}{|e_i|}\cos(\theta_i).$$

With these choices, we can simplify (5.1.4) to

$$\left.\frac{\partial\psi_i^{(7)}}{\partial\vec{n}_i}\right|_{e_i} = \frac{\phi_i^6\phi_{i+1}^2}{2A_{i+2}}(350 - 14J_{5,i})\left(\left(|e_i| - |e_{i-1}|\cos(\theta_i)\right)\frac{C_{i-1}}{C_i} - |e_{i+1}|\cos(\theta_{i+1})\frac{C_{i-1}}{C_{i+1}}\right.$$
$$\left. - \left(|e_i| - |e_{i+1}|\cos(\theta_{i+1})\right)\frac{C_{i+2}}{C_{i+1}} + |e_{i-1}|\cos(\theta_i)\frac{C_{i+2}}{C_i}\right),$$

which is zero when $J_{5,i} = 25$. Then we deduce the following:

$$J_{7,i} = 10;$$
$$K_{1,i} = 42 + 15\left(7 - 2\frac{|e_{i-1}|}{|e_i|}\cos(\theta_i)\right)\frac{C_{i-1}C_{i+1}}{C_iC_{i+2}};$$
$$K_{3,i} = 5\left(21 + \left(14 - 6\frac{|e_{i-1}|}{|e_i|}\cos(\theta_i)\right)\frac{C_{i-1}C_{i+1}}{C_iC_{i+2}}\right.$$
$$\left. + 6\left(\frac{|e_{i+1}|}{|e_i|}\frac{C_{i-1}}{C_{i+2}}\cos(\theta_{i+1}) - \frac{|e_{i-1}|}{|e_i|}\frac{C_{i+1}}{C_i}\cos(\theta_i)\right)\right);$$
$$K_{5,i} = 10\left(7 - 3\left(\frac{|e_{i-1}|}{|e_i|}\frac{C_{i+1}}{C_i}\cos(\theta_i) - \left(1 + \frac{C_{i-1}}{C_{i+2}}\right)\frac{|e_{i+1}|}{|e_i|}\cos(\theta_{i+1})\right)\right);$$
$$K_{7,i} = 30\frac{|e_{i+1}|}{|e_i|}\cos(\theta_{i+1}).$$

A similar analysis on edge e_{i-1} provides us with the remaining J and K coefficients:

$$J_{6,i} = 25; \; J_{8,i} = 10;$$

$$K_{2,i} = 42 + 15 \left(7 - 2 \frac{|e_i|}{|e_{i-1}|} \cos(\theta_i) \right) \frac{C_{i+1} C_{i-1}}{C_i C_{i+2}};$$

$$K_{4,i} = 5 \left(21 + \left(14 - 6 \frac{|e_i|}{|e_{i-1}|} \cos(\theta_i) \right) \frac{C_{i+1} C_{i-1}}{C_i C_{i+2}} \right.$$
$$\left. + 6 \left(\frac{|e_{i+2}|}{|e_{i-1}|} \frac{C_{i+1}}{C_{i+2}} \cos(\theta_{i-1}) - \frac{|e_i|}{|e_{i-1}|} \frac{C_{i-1}}{C_i} \cos(\theta_i) \right) \right);$$

$$K_{6,i} = 10 \left(7 - 3 \left(\frac{|e_i|}{|e_{i-1}|} \frac{C_{i-1}}{C_i} \cos(\theta_i) - \left(1 + \frac{C_{i+1}}{C_{i+2}} \right) \frac{|e_{i+2}|}{|e_{i-1}|} \cos(\theta_{i-1}) \right) \right);$$

$$K_{8,i} = 30 \frac{|e_{i+2}|}{|e_{i-1}|} \cos(\theta_{i-1}).$$

We now have the following expression for $\psi_i^{(7)}$:

$$\psi_i^{(7)} = \phi_i^2\bigg(\phi_i^5 + 7\phi_i^4(\phi_{i+1} + \phi_{i-1}) + 21\phi_i^3(\phi_{i+1}^2 + \phi_{i-1}^2)$$

$$+ 25\phi_i^2(\phi_{i+1}^3 + \phi_{i-1}^3) + 10\phi_i\left(\phi_{i+1}^4 + \phi_{i-1}^4\right)$$

$$+ \phi_{i+2}\bigg(\left(7 + 42\frac{C_{i+1}C_{i-1}}{C_iC_{i+2}}\right)\phi_i^4$$

$$+ \phi_i^3\bigg(\left(42 + 15\left(7 - 2\frac{|e_{i-1}|}{|e_i|}\cos(\theta_i)\right)\frac{C_{i+1}C_{i-1}}{C_iC_{i+2}}\right)\phi_{i+1}$$

$$+ \left(42 + 15\left(7 - 2\frac{|e_i|}{|e_{i-1}|}\cos(\theta_i)\right)\frac{C_{i+1}C_{i-1}}{C_iC_{i+2}}\right)\phi_{i-1}\bigg)$$

$$+ 5\phi_i^2\bigg(\left(21 + \left(14 - 6\frac{|e_{i-1}|}{|e_i|}\cos(\theta_i)\right)\frac{C_{i-1}C_{i+1}}{C_iC_{i+2}}\right.$$

$$+ 6\left(\frac{|e_{i+1}|}{|e_i|}\frac{C_{i-1}}{C_{i+2}}\cos(\theta_{i+1}) - \frac{|e_{i-1}|}{|e_i|}\frac{C_{i+1}}{C_i}\cos(\theta_i)\right)\bigg)\phi_{i+1}^2$$

$$+ \left(21 + \left(14 - 6\frac{|e_i|}{|e_{i-1}|}\cos(\theta_i)\right)\frac{C_{i+1}C_{i-1}}{C_iC_{i+2}}\right.$$

$$+ 6\left(\frac{|e_{i+2}|}{|e_{i-1}|}\frac{C_{i+1}}{C_{i+2}}\cos(\theta_{i-1}) - \frac{|e_i|}{|e_{i-1}|}\frac{C_{i-1}}{C_i}\cos(\theta_i)\right)\bigg)\phi_{i-1}^2\bigg)$$

$$+ 10\phi_i\bigg(\left(7 - 3\left(\frac{|e_{i-1}|}{|e_i|}\frac{C_{i+1}}{C_i}\cos(\theta_i)\right) - \left(1 + \frac{C_{i-1}}{C_{i+2}}\right)\frac{|e_{i+1}|}{|e_i|}\cos(\theta_{i+1})\right)\phi_{i+1}^3$$

$$+ \left(7 - 3\left(\frac{|e_i|}{|e_{i-1}|}\frac{C_{i-1}}{C_i}\cos(\theta_i)\right) - \left(1 + \frac{C_{i+1}}{C_{i+2}}\right)\frac{|e_{i+2}|}{|e_{i-1}|}\cos(\theta_{i-1})\right)\phi_{i-1}^3\bigg)$$

$$+ 30\left(\frac{|e_{i+1}|}{|e_i|}\cos(\theta_{i+1})\phi_{i+1}^4 + \frac{|e_{i+2}|}{|e_{i-1}|}\cos(\theta_{i-1})\phi_{i-1}^4\right)\bigg)$$

$$+ \phi_{i+2}^2\big(S_{0,i}\phi_i^3 + \phi_i^2(S_{1,i}\phi_{i+1} + S_{2,i}\phi_{i-1}) + L_{0,i}\phi_{i+2}^3\phi_i^2\bigg). \qquad (5.1.5)$$

The remaining coefficients can be determined by the condition $\sum_{j=1}^{4} \psi_i^{(7)} = 1$. The technique is identical to that used in the degree-3 and degree-5 cases; we write $1 = \left(\sum_{j=1}^{4} \phi_i\right)^7$, simplify the difference between this and the sum of the functions $\psi_i^{(7)}$, and isolate terms with S and L coefficients. The actual expression of this difference is not particularly illuminating, so we merely report the deduced values of

the coefficients:

$$S_{0,i} = 3\left(7 + 10\frac{C_{i+1}C_{i-1}}{C_iC_{i+2}}\left(7 + 5\frac{C_{i+1}C_{i-1}}{C_iC_{i+2}}\right)\right);$$

$$S_{1,i} = S_{2,i} = 105\left(1 + 2\frac{C_{i+1}C_{i-1}}{C_iC_{i+2}}\left(2 + \frac{C_{i+1}C_{i-1}}{C_iC_{i+2}}\right)\right);$$

$$L_{0,i} = 35\left(1 + 2\frac{C_{i+1}C_{i-1}}{C_iC_{i+2}}\left(6 + \frac{C_{i+1}C_{i-1}}{C_iC_{i+2}}\left(9 + 2\frac{C_{i+1}C_{i-1}}{C_iC_{i+2}}\right)\right)\right).$$

The final expression of $\psi_i^{(7)}$, then, is

$$
\begin{aligned}
\psi_i^{(7)} = \phi_i^2 \Bigg(&\phi_i^5 + 7\phi_i^4(\phi_{i+1} + \phi_{i-1}) + 21\phi_i^3(\phi_{i+1}^2 + \phi_{i-1}^2) \\
&+ 25\phi_i^2(\phi_{i+1}^3 + \phi_{i-1}^3) + 10\phi_i\left(\phi_{i+1}^4 + \phi_{i-1}^4\right) \\
&+ \phi_{i+2}\Bigg(\left(7 + 42\frac{C_{i+1}C_{i-1}}{C_iC_{i+2}}\right)\phi_i^4 \\
&\quad + \phi_i^3\Bigg(\left(42 + 15\left(7 - 2\frac{|e_{i-1}|}{|e_i|}\cos(\theta_i)\right)\frac{C_{i+1}C_{i-1}}{C_iC_{i+2}}\right)\phi_{i+1} \\
&\qquad + \left(42 + 15\left(7 - 2\frac{|e_i|}{|e_{i-1}|}\cos(\theta_i)\right)\frac{C_{i+1}C_{i-1}}{C_iC_{i+2}}\right)\phi_{i-1}\Bigg) \\
&\quad + 5\phi_i^2\Bigg(\left(21 + \left(14 - 6\frac{|e_{i-1}|}{|e_i|}\cos(\theta_i)\right)\frac{C_{i-1}C_{i+1}}{C_iC_{i+2}}\right. \\
&\qquad + 6\left(\frac{|e_{i+1}|}{|e_i|}\frac{C_{i-1}}{C_{i+2}}\cos(\theta_{i+1}) - \frac{|e_{i-1}|}{|e_i|}\frac{C_{i+1}}{C_i}\cos(\theta_i)\right)\Bigg)\phi_{i+1}^2 \\
&\qquad + \left(21 + \left(14 - 6\frac{|e_i|}{|e_{i-1}|}\cos(\theta_i)\right)\frac{C_{i+1}C_{i-1}}{C_iC_{i+2}}\right. \\
&\qquad + 6\left(\frac{|e_{i+2}|}{|e_{i-1}|}\frac{C_{i+1}}{C_{i+2}}\cos(\theta_{i-1}) - \frac{|e_i|}{|e_{i-1}|}\frac{C_{i-1}}{C_i}\cos(\theta_i)\right)\Bigg)\phi_{i-1}^2\Bigg) \\
&\quad + 10\phi_i\Bigg(\left(7 - 3\left(\frac{|e_{i-1}|}{|e_i|}\frac{C_{i+1}}{C_i}\cos(\theta_i) - \left(1 + \frac{C_{i-1}}{C_{i+2}}\right)\frac{|e_{i+1}|}{|e_i|}\cos(\theta_{i+1})\right)\right)\phi_{i+1}^3 \\
&\qquad + \left(7 - 3\left(\frac{|e_i|}{|e_{i-1}|}\frac{C_{i-1}}{C_i}\cos(\theta_i) - \left(1 + \frac{C_{i+1}}{C_{i+2}}\right)\frac{|e_{i+2}|}{|e_{i-1}|}\cos(\theta_{i-1})\right)\right)\phi_{i-1}^3\Bigg) \\
&\quad + 30\left(\frac{|e_{i+1}|}{|e_i|}\cos(\theta_{i+1})\phi_{i+1}^4 + \frac{|e_{i+2}|}{|e_{i-1}|}\cos(\theta_{i-1})\phi_{i-1}^4\right)\Bigg) \\
&+ 3\phi_{i+2}^2\Bigg(\left(7 + 10\frac{C_{i+1}C_{i-1}}{C_iC_{i+2}}\left(7 + 5\frac{C_{i+1}C_{i-1}}{C_iC_{i+2}}\right)\right)\phi_i^3 \\
&\qquad + 35\left(1 + 2\frac{C_{i+1}C_{i-1}}{C_iC_{i+2}}\left(2 + \frac{C_{i+1}C_{i-1}}{C_iC_{i+2}}\right)\right)\phi_i^2(\phi_{i+1} + \phi_{i-1})\Bigg) \\
&+ 35\left(1 + 2\frac{C_{i+1}C_{i-1}}{C_iC_{i+2}}\left(6 + \frac{C_{i+1}C_{i-1}}{C_iC_{i+2}}\left(9 + 2\frac{C_{i+1}C_{i-1}}{C_iC_{i+2}}\right)\right)\right)\phi_{i+2}^3\phi_i^2\Bigg). \quad (5.1.6)
\end{aligned}
$$

As usual, we define the vertex spline $\psi_v^{(7)}$ piecewise in Ω_v by $\psi_{i,P}^{(7)}$ within each quadrilateral P in Ω_v, where $v = v_i$ in P.

Since any polygonal region can be triangulated, and any triangle can be partitioned by convex quadrilaterals, the polygonal splines built in this section are useful over extremely general regions. The discussion in this section serves as a proof of the

following:

Theorem 5.1.1. *Let Ω be any polygonal region in $\mathbb{R}^2$, and let $\mathcal{P}$ be a partition of Ω by quadrilaterals. For every vertex v in the partition $\mathcal{P}$, define a polygonal spline $\psi_v^{(7)}$ over Ω_v by*

$$\psi_v^{(7)} := \begin{cases} \psi_{i,P}^{(7)}(\mathbf{x}) & \mathbf{x} \in P \subseteq \Omega_v; \ v = v_{i,P} \\ 0 & \mathbf{x} \notin \Omega_v, \end{cases}$$

where $\psi_{i,P}^{(7)}$ is the function in (5.1.6).

  Then $\psi_v^{(7)}$ satisfies the following properties:

(1) $\psi_v^{(7)}(w) = \delta_{v,w}$ for any vertex w of $\mathcal{P}$;

(2) $\nabla \psi_v^{(7)}(w) = 0$ for any vertex w of $\mathcal{P}$;

(3) $\nabla^2 \psi_v^{(7)}(w) = 0$ for any vertex w of $\mathcal{P}$;

(4) $\psi_v^{(7)} \in C^1(\Omega)$; and

(5) $\sum_{v \in \mathcal{P}} \psi_v^{(7)} = 1$.

Figure 5.2 shows an unstructured quadrilateral partition, and Figure 5.3 shows the plot of a function $\psi_v^{(7)}$ over this partition.

5.1.2   Construction of $\psi_{x,v}^{(7)}$ and $\psi_{y,v}^{(7)}$

We now construct the gradient adjustment polygonal vertex splines $\psi_{x,v}^{(7)}$ and $\psi_{y,v}^{(7)}$. As before, we'll explicitly construct $\psi_{x,v}^{(7)}$, and we'll start by focusing on a single quadrilateral P in Ω_v, where $v = v_i$ in P, and define $\psi_{x,v}^{(7)}\big|_P = \psi_{x,i,P}^{(7)}$.

While most of the following calculations will be familiar, we'll need the following lemma:
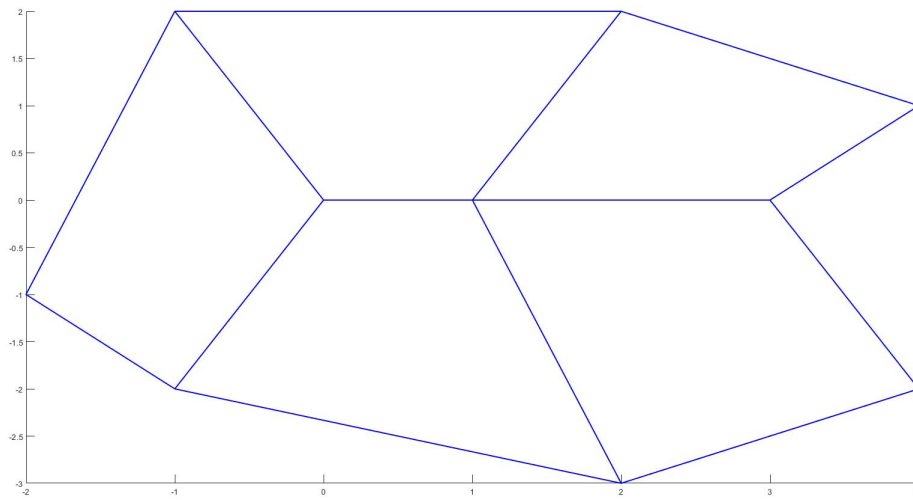
Figure 5.2: An unstructured quadrilateral partition
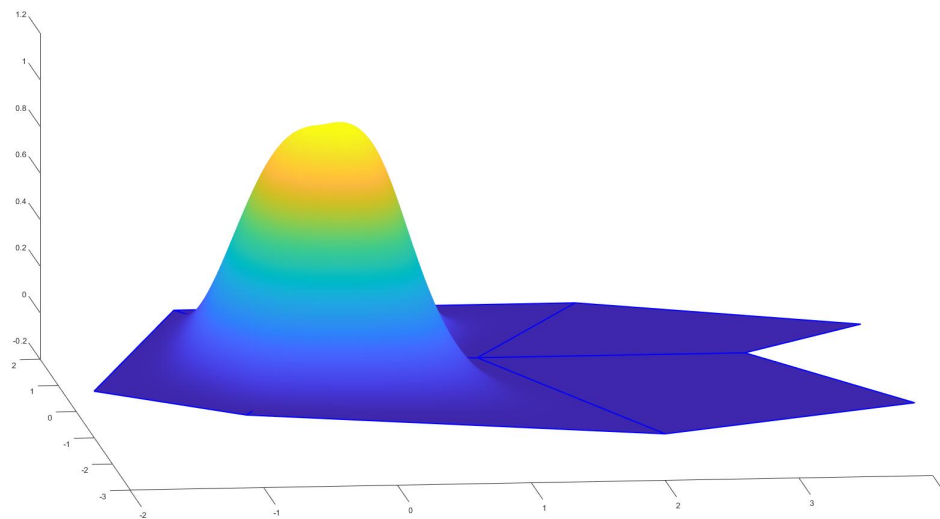
Figure 5.3: The plot of a function $\psi_v^{(7)}$

Lemma 5.1.1.

$$C_i \vec{e}_{i+1} + C_{i+1} \vec{e}_{i-1} + (C_{i+1} - C_{i+2}) \vec{e}_i = 0$$

Proof. Using two-dimensional vector cross products to express triangle areas, one can write

$$2C_j = \vec{e}_{j-1} \times \vec{e}_j$$
$$= \vec{e}_j \times (\vec{e}_{j+1} + \vec{e}_{j+2}).$$

Using this expression, along with the fact that $\vec{e}_i + \vec{e}_{i+2} = -(\vec{e}_{i-1} + \vec{e}_{i+1})$, we have

$$2\big(C_i \vec{e}_{i+1} + C_{i+1} \vec{e}_{i-1} + (C_{i+1} - C_{i+2}) \vec{e}_i\big)$$
$$= (\vec{e}_{i-1} \times \vec{e}_i)\, \vec{e}_{i+1} + (\vec{e}_i \times \vec{e}_{i+1})\, \vec{e}_{i-1} + (\vec{e}_i \times \vec{e}_{i+1} - \vec{e}_{i+1} \times \vec{e}_{i+2})\, \vec{e}_i$$
$$= (\vec{e}_{i-1} \times \vec{e}_i)\, \vec{e}_{i+1} + (\vec{e}_i \times \vec{e}_{i+1})\, \vec{e}_{i-1} + ((\vec{e}_i + \vec{e}_{i+2}) \times \vec{e}_{i+1})\, \vec{e}_i$$
$$= (\vec{e}_{i-1} \times \vec{e}_i)\, \vec{e}_{i+1} + (\vec{e}_i \times \vec{e}_{i+1})\, \vec{e}_{i-1} - ((\vec{e}_{i-1} + \vec{e}_{i+1}) \times \vec{e}_{i+1})\, \vec{e}_i$$
$$= (\vec{e}_{i-1} \times \vec{e}_i)\, \vec{e}_{i+1} + (\vec{e}_i \times \vec{e}_{i+1})\, \vec{e}_{i-1} - (\vec{e}_{i-1} \times \vec{e}_{i+1})\, \vec{e}_i.$$

Expanding the x and y components of this vector sum along with easy simplification immediately yields that the sum is zero. $\qquad\square$

We're now ready to construct the function $\psi_{x,i}^{(7)}$. We'll use the template from (5.1.2), and start by computing the J coefficients. Since we want $\psi_{x,i}^{(7)}\big|_{v_i} = 0$, we set $J_{0,i} = 0$. We require that $\nabla \psi_{x,i}^{(7)} = \langle 1, 0 \rangle$, so we compute the edge-direction derivatives:

$$\left.\frac{\partial \psi_{x,i}^{(7)}}{\partial \tilde{e}_i}\right|_{v_i} = \frac{J_{1,i}}{|e_i|};$$
$$\left.\frac{\partial \psi_{x,i}^{(7)}}{\partial \tilde{e}_{i-1}}\right|_{v_i} = \frac{-J_{2,i}}{|e_{i-1}|};$$

so we'll set $J_{1,i} = e_{i,x}$, $J_{2,i} = -e_{i-1,x}$. We can determine $J_{3,i}$, $J_{4,i}$, and $K_{0,i}$ by the

requirement that $\nabla^2 \psi_{x,i}^{(7)}\big|_{v_i} = 0$. We compute the second edge-direction derivatives:

$$\frac{\partial^2 \psi_{x,i}^{(7)}}{\partial \tilde{e}_i^2} = \frac{2J_{3,i} - 12e_{i,x}}{|e_i|^2};$$

$$\frac{\partial^2 \psi_{x,i}^{(7)}}{\partial \tilde{e}_{i-1}^2} = \frac{2J_{4,i} + 12e_{i-1,x}}{|e_{i-1}|^2};$$

$$\frac{\partial^2 \psi_{x,i}^{(7)}}{\partial \tilde{e}_i \partial \tilde{e}_{i-1}} = \frac{1}{|e_i||e_{i-1}|}\left(\left(6 + \frac{C_{i+2}}{C_{i+1}}\right)e_{i,x} - \left(6 + \frac{C_{i+2}}{C_{i-1}}\right)e_{i-1,x} - K_{0,i}\frac{C_{i+1}C_{i-1}}{C_i C_{i+2}}\right);$$

which are all zero precisely when

$$J_{3,i} = 6e_{i,x};$$

$$J_{4,i} = -6e_{i-1,x};$$

$$K_{0,i} = \left(1 + 6\frac{C_{i+1}}{C_{i+2}}\right)\frac{C_{i-1}}{C_i}e_{i,x} - \left(1 + 6\frac{C_{i-1}}{C_{i+2}}\right)\frac{C_{i+1}}{C_i}e_{i-1,x}.$$

As was the case when we constructed $\psi_i^{(7)}$, we can't determine the remaining J terms directly yet. However, it seems safe to assume that $J_{5,i} = j_5 e_{i,x}, J_{6,i} = j_6 e_{i-1,x}, J_{7,i} = j_7 e_{i,x}$, and $J_{8,i} = j_8 e_{i-1,x}$ for some constants j_5, j_6, j_7, and j_8. We can use the sum condition

$$\sum_{j=1}^{4} v_{j,x}\psi_j^{(7)} + \psi_{x,j}^{(7)} = x \tag{5.1.7}$$

restricted to edges e_i and e_{i-1} to conclude that $j_5 + j_8 = 5$ and $j_6 + j_7 = 5$. We'll make an additional assumption, based on our previous results: $j_5 = -j_6$, and $j_7 = -j_8$.

Then, if we put all of these in terms of j_7, we'll have

$$
\begin{aligned}
\psi_{x,i}^{(7)} = \phi_i^2 \Bigg(& \phi_i^4 (e_{i,x}\phi_{i+1} - e_{i-1,x}\phi_{i-1}) + 6\phi_i^3 (e_{i,x}\phi_{i+1}^2 - e_{i-1,x}\phi_{i-1}^2) \\
& + (j_7 + 5)\phi_i^2 (e_{i,x}\phi_{i+1}^3 - e_{i-1,x}\phi_{i-1}^3) + j_7\phi_i \left(e_{i,x}\phi_{i+1}^4 - e_{i-1,x}\phi_{i-1}^4\right) \\
& + \phi_{i+2}\left(\left(\left(1 + 6\frac{C_{i+1}}{C_{i+2}}\right)\frac{C_{i-1}}{C_i}e_{i,x} - \left(1 + 6\frac{C_{i-1}}{C_{i+2}}\right)e_{i-1,x}\right)\phi_i^4 \right. \\
& + \phi_i^3 (K_{1,i}\phi_{i+1} + K_{2,i}\phi_{i-1}) + \phi_i^2 (K_{3,i}\phi_{i+1}^2 + K_{4,i}\phi_{i-1}^2) \\
& \left. + \phi_i (K_{5,i}\phi_{i+1}^3 + K_{6,i}\phi_{i-1}^3) + K_{7,i}\phi_{i+1}^4 + K_{8,i}\phi_{i-1}^4 \right) \\
& + \phi_{i+2}^2 \left(S_{0,i}\phi_i^3 + \phi_i^2 (S_{1,i}\phi_{i+1} + S_{2,i}\phi_{i-1})\right) + L_{0,i}\phi_{i+2}^3\phi_i^2 \Bigg). \qquad (5.1.8)
\end{aligned}
$$

We can determine the K constants by enforcing C^1 smoothness over shared edges. We'll first compute the outward normal derivative of $\psi_{x,i}^{(7)}$ on edge e_i. Using the fact that $A_{i+2} = C_{i-1}\phi_i + C_{i+2}\phi_{i+1}$, along with (3.2.25) and $C_j = |e_{j-1}||e_j|\sin(\theta_j)$, we compute the following normal derivative:

146

$$\left.\frac{\partial \psi_{x,i}^{(7)}}{\partial \vec{n}_i}\right|_{e_i} = \phi_i^7 \frac{e_{i,y}}{|e_i|}$$

$$+ \phi_i^6 \phi_{i+1}\left(7\frac{e_{i,y}}{|e_i|} + \frac{|e_i|}{2C_i C_{i+1}}\left(C_i e_{i+1,x} + C_{i+1}e_{i-1,x} + (C_{i+1} - C_{i+2})e_{i,x}\right)\right)$$

$$+ \phi_i^5 \phi_{i+1}^2\left(3(j_7 - 5)\frac{e_{i,x}\cos(\theta_i)}{|e_i|\sin(\theta_i)} - 6\frac{e_{i,x}\cos(\theta_{i+1})}{|e_i|\sin(\theta_{i+1})}\right)$$

$$+ \phi_i^4 \phi_{i+1}^3\left(3(5 - j_7)\frac{e_{i,x}\cos(\theta_{i+1})}{|e_i|\sin(\theta_{i+1})} - 20\frac{e_{i,x}\cos(\theta_i)}{|e_i|\sin(\theta_i)}\right)$$

$$+ \phi_i^3 \phi_{i+1}^4\left(20\frac{e_{i,x}\cos(\theta_{i+1})}{|e_i|\sin(\theta_{i+1})} - 3j_7\frac{e_{i,x}\cos(\theta_i)}{|e_i|\sin(\theta_i)}\right)$$

$$+ \phi_i^2 \phi_{i+1}^5\left(3j_7\frac{e_{i,x}\cos(\theta_{i+1})}{|e_i|\sin(\theta_{i+1})} - \frac{|e_i|}{2C_{i+1}}K_{7,i}\right)$$

$$+ \frac{|e_i|}{2A_{i+2}}\left(\phi_i^6 \phi_{i+1}^2\left(6\frac{C_{i-1}}{C_i}(6e_{i,x} + e_{i-1,x}) - \frac{C_{i+2}}{C_i}(6e_{i-1,x} + e_{i,x})\right.\right.$$

$$\left. + \frac{C_{i+2}}{C_{i+1}}(7e_{i,x} - K_{1,i}) + \frac{C_{i+2}}{C_i C_{i+1}}(C_{i+2} - C_{i-1})e_{i,x}\right)$$

$$+ \phi_i^5 \phi_{i+1}^3\left(\frac{C_{i+2}}{C_{i+1}}(42e_{i,x} - K_{1,i} - K_{3,i}) + 7(5 + j_7)\frac{C_{i-1}}{C_i}e_{i,x}\right)$$

$$+ \phi_i^4 \phi_{i+1}^4\left(\frac{C_{i+2}}{C_{i+1}}(7(5 + j_7)e_{i,x} - K_{3,i} - K_{5,i}) + 7j_7\frac{C_{i-1}}{C_i}e_{i,x}\right)$$

$$\left. + \phi_i^3 \phi_{i+1}^5\left(\frac{C_{i+2}}{C_{i+1}}(7j_7 e_{i,x} - K_{5,i} - K_{7,i}) + \frac{C_{i-1}}{C_{i+1}}K_{7,i}\right)\right).$$

It seems best to consider this in parts: the top few lines correspond to polynomials of Wachspress coordinates, but the latter part is rational in Wachspress coordinates due to the linear function A_{i+2} in the denominator. When considering smoothness, these Wachspress-rational terms are especially concerning, as the function A_{i+2} depends on the geometry of the quadrilateral within which it is defined. Our focus, then, is to "move" these terms into the Wachspress-polynomial realm (in fact, if the reader is attempting to reproduce the result above, it should be noted that we have actually "moved" two sets of terms); more on this later.

The Wachspress-polynomial terms are those which we are looking to cooperate across shared edges, and we ought to only allow dependence on the geometry of the

shared edge itself. The first term satisfies this, but the second term does not at first glance, and (as we'll elaborate on soon), there aren't any more Wachspress-rational terms which can interact. This is where we'll need our result from Lemma 5.1.1, which tells us that all terms on this line except $7\frac{e_{i,y}}{|e_i|}$ are zero.

Focus now on the last Wachspress-polynomial term:

$$\phi_i^2\phi_{i+1}^5\left(3j_7\frac{e_{i,x}\cos(\theta_{i+1})}{|e_i|\sin(\theta_{i+1})} - \frac{|e_i|}{2C_{i+1}}K_{7,i}\right)$$
$$= \phi_i^2\phi_{i+1}^5\left(3j_7\frac{e_{i,x}\cos(\theta_{i+1})}{|e_i|\sin(\theta_{i+1})} - \frac{K_{7,i}}{|e_{i+1}|\sin(\theta_{i+1})}\right).$$

Now we really aim for this to be in terms of $\frac{e_{i,y}}{|e_i|}$, the x-coordinate of the vector $\vec{n}_i$. With (3.2.25) in mind, we let $K_{7,i}$ remain unsolved, but we allow it to take the form $K_{7,i} = -3j_7e_{i+1,x} + k_7\frac{|e_{i+1}|}{|e_i|}\sin(\theta_{i+1})e_{i,y}$ for some constant k_7, so we retrieve

$$\begin{aligned}
\frac{\partial\psi_{x,i}^{(7)}}{\partial\vec{n}_i}\Big|_{e_i} &= \frac{e_{i,y}}{|e_i|}\left(\phi_i^7 + 7\phi_i^6\phi_{i+1} - (3j_7 + k_7)\phi_i^2\phi_{i+1}^5\right) \\
&+ \phi_i^5\phi_{i+1}^2\left(3(j_7-5)\frac{e_{i,x}\cos(\theta_i)}{|e_i|\sin(\theta_i)} - 6\frac{e_{i,x}\cos(\theta_{i+1})}{|e_i|\sin(\theta_{i+1})}\right) \\
&+ \phi_i^4\phi_{i+1}^3\left(3(5-j_7)\frac{e_{i,x}\cos(\theta_{i+1})}{|e_i|\sin(\theta_{i+1})} - 20\frac{e_{i,x}\cos(\theta_i)}{|e_i|\sin(\theta_i)}\right) \\
&+ \phi_i^3\phi_{i+1}^4\left(20\frac{e_{i,x}\cos(\theta_{i+1})}{|e_i|\sin(\theta_{i+1})} - 3j_7\frac{e_{i,x}\cos(\theta_i)}{|e_i|\sin(\theta_i)}\right) \\
&+ \frac{|e_i|}{2A_{i+2}}\left(\phi_i^6\phi_{i+1}^2\left(6\frac{C_{i-1}}{C_i}(6e_{i,x} + e_{i-1,x}) - \frac{C_{i+2}}{C_i}(6e_{i-1,x} + e_{i,x})\right.\right. \\
&\qquad\left.+ \frac{C_{i+2}}{C_{i+1}}(7e_{i,x} - K_{1,i}) + \frac{C_{i+2}}{C_iC_{i+1}}(C_{i+2} - C_{i-1})e_{i,x}\right) \\
&+ \phi_i^5\phi_{i+1}^3\left(\frac{C_{i+2}}{C_{i+1}}(42e_{i,x} - K_{1,i} - K_{3,i}) + 7(5+j_7)\frac{C_{i-1}}{C_i}e_{i,x}\right) \\
&+ \phi_i^4\phi_{i+1}^4\left(\frac{C_{i+2}}{C_{i+1}}(7(5+j_7)e_{i,x} - K_{3,i} - K_{5,i}) + 7j_7\frac{C_{i-1}}{C_i}e_{i,x}\right) \\
&+ \phi_i^3\phi_{i+1}^5\left(\frac{C_{i+2}}{C_{i+1}}(7j_7e_{i,x} - K_{5,i} - K_{7,i}) + \frac{C_{i-1}}{C_{i+1}}K_{7,i}\right), \qquad (5.1.9)
\end{aligned}$$

where we don't substitute for every instance of $K_{7,i}$ yet to save space.

Now we'll elaborate on "moving" terms from the Wachspress-rational realm to the Wachspress-polynomial. Start by focusing on the first Wachspress-rational term. Using the fact that $C_{i+2} - C_{i-1} = C_{i+1} - C_i$, we will retrieve a factor of A_{i+2} from this term, and have a polynomial remainder

$$
\phi_i^6 \phi_{i+1}^2 \left(6 \frac{C_{i-1}}{C_i} (6e_{i,x} + e_{i-1,x}) - \frac{C_{i+2}}{C_i} (6e_{i-1,x} + e_{i,x}) \right.
$$
$$
\left. + \frac{C_{i+2}}{C_{i+1}} (7e_{i,x} - K_{1,i}) + \left(\frac{C_{i+2}}{C_i} - \frac{C_{i+2}}{C_i} \right) e_{i,x} \right)
$$
$$
= A_{i+2} \phi_i^5 \phi_{i+1}^2 \left(6 \frac{1}{C_i} (6e_{i,x} + e_{i-1,x}) - 6 \frac{C_{i+2}}{C_i C_{i-1}} e_{i-1,x} + \frac{C_{i+2}}{C_{i+1} C_{i-1}} (6e_{i,x} - K_{1,i}) \right)
$$
$$
- \phi_i^5 \phi_{i+1}^3 \left(6 \frac{C_{i+2}}{C_i} (6e_{i,x} + e_{i-1,x}) - 6 \frac{C_{i+2}^2}{C_i C_{i-1}} e_{i-1,x} + \frac{C_{i+2}^2}{C_{i+1} C_{i-1}} (6e_{i,x} - K_{1,i}) \right).
$$

Using this result, we can rewrite (5.1.9) by

$$
\left. \frac{\partial \psi_{x,i}^{(7)}}{\partial \vec{n}_i} \right|_{e_i} = \frac{e_{i,y}}{|e_i|} \left(\phi_i^7 + 7\phi_i^6 \phi_{i+1} - (3j_7 + k_7)\phi_i^2 \phi_{i+1}^5 \right)
$$
$$
+ \phi_i^5 \phi_{i+1}^2 \left(3(j_7 - 5) \frac{e_{i,x} \cos(\theta_i)}{|e_i| \sin(\theta_i)} - 6 \frac{e_{i,x} \cos(\theta_{i+1})}{|e_i| \sin(\theta_{i+1})} + 6 \frac{e_{i-1,x}}{|e_{i-1}| \sin(\theta_i)} + 36 \frac{|e_i|}{2C_i} e_{i,x} \right.
$$
$$
\left. + \frac{C_{i+2}}{C_{i-1}} \left(\frac{|e_i|}{2C_{i+1}} (6e_{i,x} - K_{1,i}) - 6 \frac{|e_i|}{2C_i} e_{i-1,x} \right) \right)
$$
$$
+ \phi_i^4 \phi_{i+1}^3 \left(3(5 - j_7) \frac{e_{i,x} \cos(\theta_{i+1})}{|e_i| \sin(\theta_{i+1})} - 20 \frac{e_{i,x} \cos(\theta_i)}{|e_i| \sin(\theta_i)} \right)
$$
$$
+ \phi_i^3 \phi_{i+1}^4 \left(20 \frac{e_{i,x} \cos(\theta_{i+1})}{|e_i| \sin(\theta_{i+1})} - 3j_7 \frac{e_{i,x} \cos(\theta_i)}{|e_i| \sin(\theta_i)} \right)
$$
$$
+ \frac{|e_i|}{2A_{i+2}} \left(\phi_i^5 \phi_{i+1}^3 \left(\frac{C_{i+2}}{C_{i+1}} (42e_{i,x} - K_{1,i} - K_{3,i}) - 6 \frac{C_{i+2}}{C_i} (6e_{i,x} + e_{i-1,x}) \right. \right.
$$
$$
\left. + 7(5 + j_7) \frac{C_{i-1}}{C_i} e_{i,x} - 6 \frac{C_{i+2}^2}{C_i C_{i-1}} e_{i-1,x} + \frac{C_{i+2}^2}{C_{i+1} C_{i-1}} (6e_{i,x} - K_{1,i}) \right)
$$
$$
+ \phi_i^4 \phi_{i+1}^4 \left(\frac{C_{i+2}}{C_{i+1}} (7(5 + j_7)e_{i,x} - K_{3,i} - K_{5,i}) + 7j_7 \frac{C_{i-1}}{C_i} e_{i,x} \right)
$$
$$
\left. + \phi_i^3 \phi_{i+1}^5 \left(\frac{C_{i+2}}{C_{i+1}} (7j_7 e_{i,x} - K_{5,i} - K_{7,i}) + \frac{C_{i-1}}{C_{i+1}} K_{7,i} \right) \right).
$$

Now focus on the Wachspress-polynomial terms divisible by $\phi_i^5\phi_{i+1}^2$:

$$\phi_i^5\phi_{i+1}^2\left(3(j_7-5)\frac{e_{i,x}\cos(\theta_i)}{|e_i|\sin(\theta_i)} - 6\frac{e_{i,x}\cos(\theta_{i+1})}{|e_i|\sin(\theta_{i+1})} + 6\frac{e_{i-1,x}}{|e_{i-1}|\sin(\theta_i)} + 36\frac{|e_i|}{2C_i}e_{i,x}\right.$$

$$\left. + \frac{C_{i+2}}{C_{i-1}}\left(\frac{|e_i|}{2C_{i+1}}(6e_{i,x}-K_{1,i}) - 6\frac{|e_i|}{2C_i}e_{i-1,x}\right)\right)$$

$$= \phi_i^5\phi_{i+1}^2\left(3(j_7-3)\frac{e_{i,y}}{|e_i|} + 3(7-j_7)\frac{|e_i|}{2C_i}e_{i-1,x} + 6\frac{|e_i|}{2C_{i+1}}e_{i+1,x} + 36\frac{|e_i|}{2C_i}e_{i,x}\right.$$

$$\left. + \frac{C_{i+2}}{C_{i-1}}\left(\frac{|e_i|}{2C_{i+1}}(6e_{i,x}-K_{1,i}) - 6\frac{|e_i|}{2C_i}e_{i-1,x}\right)\right); \tag{5.1.10}$$

we can retrieve a satisfactory result if we set

$$K_{1,i} = 6\left(e_{i,x} - \frac{C_{i+1}}{C_i}e_{i-1,x} + \frac{C_{i-1}}{C_{i+2}}e_{i+1,x}\right)$$

$$+ \frac{C_{i+1}C_{i-1}}{C_iC_{i+2}}\left(36e_{i,x} + 3(7-j_7)e_{i-1,x} + k_1\frac{|e_{i-1}|}{|e_i|}\sin(\theta_i)e_{i,y}\right)$$

for some constant k_1, which reduces (5.1.10) to

$$\phi_i^5\phi_{i+1}^2\left((3(j_7-3)-k_1)\frac{e_{i,y}}{|e_i|}\right).$$

Continuing in this manner, moving one set of terms from Wachspress-rational to Wachspress-polynomial at a time, we can set

$$K_{3,i} = 36e_{i,x} - 6e_{i+1,x} - \frac{C_{i+1}}{C_i}\left(72e_{i,x} + 3(7-j_7)e_{i-1,x} + k_1\frac{|e_{i-1}|}{|e_i|}\sin(\theta_i)e_{i,y}\right)$$

$$+ \frac{C_{i-1}}{C_{i+2}}\left(3(j_7-7)e_{i+1,x} + k_3\frac{|e_{i+1}|}{|e_i|}\sin(\theta_{i+1})e_{i,y}\right)$$

$$+ \frac{C_{i+1}C_{i-1}}{C_iC_{i+2}}\left((7j_7-1)e_{i,x} + (3j_7-1)e_{i-1,x} - k_1\frac{|e_{i-1}|}{|e_i|}\sin(\theta_i)e_{i,y}\right);$$

$$K_{5,i} = 7j_7e_{i,x} + (3j_7-20)e_{i+1,x} + (k_5-k_7)\frac{|e_{i+1}|}{|e_i|}\sin(\theta_{i+1})e_{i,y} + 3j_7\frac{C_{i+1}}{C_i}e_{i-1,x}$$

$$+ \frac{C_{i-1}}{C_{i+2}}\left(k_7\frac{|e_{i+1}|}{|e_i|}\sin(\theta_{i+1})e_{i,y} - 3j_7e_{i+1,x}\right)$$

for two more constants k_3 and k_5, which gives us

150

$$\frac{\partial \psi_{x,i}^{(7)}}{\partial \vec{n}_i}\bigg|_{e_i} = \frac{e_{i,y}}{|e_i|} \phi_i^2 \big(\phi_i^5 + 7\phi_i^4\phi_{i+1} + (3(j_7 - 3) - k_1)\phi_i^3\phi_{i+1}^2$$

$$+ (3j_7 - 35 - k_3)\phi_i^2\phi_{i+1}^3 - (3j_7 + k_5 + 20)\phi_i\phi_{i+1}^4 - (3j_7 + k_7)\phi_{i+1}^5 \big)$$

$$+ \frac{|e_i|}{2A_{i+2}} \phi_i^4\phi_{i+1}^4 \left(\frac{C_{i+2}}{C_{i+1}} \left(11e_{i+1,x} - e_{i,x} + (k_3 - k_5 + k_7)\frac{|e_{i+1}|}{|e_i|} \sin(\theta_{i+1})e_{i,y} \right) \right.$$

$$- \frac{C_{i+2}}{C_i} \left((6j_7 - 41)e_{i-1,x} - 72e_{i,x} - k_1\frac{|e_{i-1}|}{|e_i|} \sin(\theta_i)e_{i,y} \right)$$

$$+ \frac{C_{i-1}}{C_{i+1}} \left(e_{i+1,x} + (k_5 - k_3 - k_7)\frac{|e_{i+1}|}{|e_i|} \sin(\theta_{i+1})e_{i,y} \right)$$

$$\left. + \frac{C_{i-1}}{C_i} \left(e_{i,x} + e_{i-1,x} + k_1\frac{|e_{i-1}|}{|e_i|} \sin(\theta_i)e_{i,y} \right) \right).$$

Then we must find constants j_7, k_1, k_3, k_5, and k_7 that make the remaining Wachspress-rational term 0, will cooperate with the choices we'll make for the constants $K_{2,i}, K_{4,i}, K_{6,i}$, and $K_{8,i}$, and also satisfy (5.1.7). A similar analysis on edge e_{i-1} to that which we've just completed on edge e_i will result in choosing

$$K_{2,i} = -6\left(e_{i-1,x} - \frac{C_{i-1}}{C_i}e_{i,x} + \frac{C_{i+1}}{C_{i+2}}e_{i+2,x} \right)$$

$$- \frac{C_{i+1}C_{i-1}}{C_iC_{i+2}} \left(36e_{i-1,x} + 3(7 - j_7)e_{i,x} + k_2\frac{|e_i|}{|e_{i-1}|} \sin(\theta_i)e_{i-1,y} \right);$$

$$K_{4,i} = -36e_{i-1,x} + 6e_{i+2,x} + \frac{C_{i-1}}{C_i} \left(72e_{i-1,x} + 3(7 - j_7)e_{i,x} + k_2\frac{|e_i|}{|e_{i-1}|} \sin(\theta_i)e_{i-1,y} \right)$$

$$- \frac{C_{i+1}}{C_{i+2}} \left(3(j_7 - 7)e_{i+2,x} + k_4\frac{|e_{i+2}|}{|e_{i-1}|} \sin(\theta_{i-1})e_{i-1,y} \right)$$

$$- \frac{C_{i+1}C_{i-1}}{C_iC_{i+2}} \left((7j_7 - 1)e_{i-1,x} + (3j_7 - 1)e_{i,x} - k_2\frac{|e_i|}{|e_{i-1}|} \sin(\theta_i)e_{i-1,y} \right);$$

$$K_{6,i} = -7j_7e_{i-1,x} - (3j_7 - 20)e_{i+2,x} - (k_6 - k_8)\frac{|e_{i+2}|}{|e_{i-1}|} \sin(\theta_{i-1})e_{i-1,y} - 3j_7\frac{C_{i-1}}{C_i}e_{i,x}$$

$$- \frac{C_{i+1}}{C_{i+2}} \left(k_8\frac{|e_{i+2}|}{|e_{i-1}|} \sin(\theta_{i-1})e_{i-1,y} - 3j_7e_{i+2,x} \right);$$

$$K_{8,i} = 3j_7e_{i+2,x} - k_8\frac{|e_{i+2}|}{|e_{i-1}|} \sin(\theta_{i-1})e_{i-1,y};$$

for more constants k_2, k_4, k_6, and k_8, which will yield

$$\frac{\partial \psi_{x,i}^{(7)}}{\partial \vec{n}_{i-1}}\bigg|_{e_{i-1}} = \frac{e_{i-1,y}}{|e_{i-1}|}\phi_i^2\big(\phi_i^5 + 7\phi_i^4\phi_{i-1} + (3(j_7-3)-k_2)\phi_i^3\phi_{i-1}^2$$

$$+ (3j_7 - 35 - k_4)\phi_i^2\phi_{i-1}^3 - (3j_7 + k_6 + 20)\phi_i\phi_{i-1}^4 - (3j_7 + k_8)\phi_{i-1}^5\big)$$

$$- \frac{|e_{i-1}|}{2A_{i+1}}\phi_i^4\phi_{i-1}^4\Bigg(\frac{C_{i+2}}{C_{i-1}}\bigg(11e_{i+2,x} - e_{i-1,x}$$

$$+ (k_4 - k_6 + k_8)\frac{|e_{i+2}|}{|e_{i-1}|}\sin(\theta_{i-1})e_{i-1,y}\bigg)$$

$$- \frac{C_{i+2}}{C_i}\bigg((6j_7 - 41)e_{i,x} - 72e_{i-1,x} - k_2\frac{|e_i|}{|e_{i-1}|}\sin(\theta_i)e_{i-1,y}\bigg)$$

$$+ \frac{C_{i+1}}{C_{i-1}}\bigg(e_{i+2,x} + (k_6 - k_4 - k_8)\frac{|e_{i+2}|}{|e_{i-1}|}\sin(\theta_{i-1})e_{i-1,y}\bigg)$$

$$+ \frac{C_{i+1}}{C_i}\bigg(e_{i-1,x} + e_{i,x} + k_2\frac{|e_i|}{|e_{i-1}|}\sin(\theta_i)e_{i-1,y}\bigg)\Bigg).$$

We can refine our solutions of the K coefficients using the sum condition (5.1.7) along with the consideration that the coefficients of the single remaining rational terms in each of $\dfrac{\partial \psi_{x,i}^{(7)}}{\partial \vec{n}_i}$ and $\dfrac{\partial \psi_{x,i}^{(7)}}{\partial \vec{n}_{i-1}}$ must be zero. We can see from Figure 5.1b that, for example, $K_{1,i}$ and $K_{8,i+1}$ interact; the remaining terms will set up a linear system which we can solve for the constants k_j in terms of j_7. The following is the result:

$$K_{1,i} = 6\left(e_{i,x} - \frac{C_{i+1}}{C_i}e_{i-1,x} + \frac{C_{i-1}}{C_{i+2}}e_{i+1,x}\right)$$
$$+ 3\frac{C_{i+1}C_{i-1}}{C_iC_{i+2}}\left(\left(12 - 10\frac{|e_{i-1}|}{|e_i|}\cos(\theta_i)\right)e_{i,x} - (j_7+3)e_{i-1,x}\right);$$

$$K_{2,i} = -\left(6\left(e_{i-1,x} - \frac{C_{i-1}}{C_i}e_{i,x} + \frac{C_{i+1}}{C_{i+2}}e_{i+2,x}\right)\right.$$
$$\left. + 3\frac{C_{i+1}C_{i-1}}{C_iC_{i+2}}\left(\left(12 - 10\frac{|e_i|}{|e_{i-1}|}\cos(\theta_i)\right)e_{i-1,x} - (j_7+3)e_{i,x}\right)\right);$$

$$K_{3,i} = 35e_{i,x} + 5e_{i+1,x}$$
$$- \frac{C_{i+1}}{C_i}\left((3j_7+10)e_{i-1,x} + 30\frac{|e_{i-1}|}{|e_i|}\cos(\theta_i)e_{i,x}\right) + \frac{C_{i-1}}{C_{i+2}}(3j_7-20)e_{i+1,x}$$
$$+ \frac{C_{i+1}C_{i-1}}{C_iC_{i+2}}\left(\left(7j_7 - 30\frac{|e_{i-1}|}{|e_i|}\cos(\theta_i)\right)e_{i,x} + 3(j_7-10)e_{i-1,x}\right);$$

$$K_{4,i} = -\left(35e_{i-1,x} + 5e_{i+2,x}\right.$$
$$- \frac{C_{i-1}}{C_i}\left((3j_7+10)e_{i,x} + 30\frac{|e_i|}{|e_{i-1}|}\cos(\theta_i)e_{i-1,x}\right) + \frac{C_{i+1}}{C_{i+2}}(3j_7-20)e_{i+2,x}$$
$$\left. + \frac{C_{i+1}C_{i-1}}{C_iC_{i+2}}\left(\left(7j_7 - 30\frac{|e_i|}{|e_{i-1}|}\cos(\theta_i)\right)e_{i-1,x} + 3(j_7-10)e_{i,x}\right)\right);$$

$$K_{5,i} = 7j_7 e_{i,x} + (3j_7-20)e_{i+1,x}$$
$$+ 3\frac{C_{i+1}}{C_i}\left((j_7-10)e_{i-1,x} - 10\frac{|e_{i-1}|}{|e_i|}\cos(\theta_i)e_{i,x}\right) - 3j_7\frac{C_{i-1}}{C_{i+2}}e_{i+1,x};$$

$$K_{6,i} = -\left(7j_7 e_{i-1,x} + (3j_7-20)e_{i+2,x} + \right.$$
$$\left. + 3\frac{C_{i-1}}{C_i}\left((j_7-10)e_{i,x} - 10\frac{|e_i|}{|e_{i-1}|}\cos(\theta_i)e_{i-1,x}\right) - 3j_7\frac{C_{i+1}}{C_{i+2}}e_{i+2,x}\right);$$

$$K_{7,i} = -3j_7 e_{i+1,x};$$

$$K_{8,i} = 3j_7 e_{i+2,x}.$$

For two adjacent quadrilaterals P and R which share the edge $e_{i,P} = e_{i-1,R}$, it turns out that this set of K coefficients also satisfies that $\left.\dfrac{\partial\psi_{x,i,P}^{(7)}}{\partial\vec{n}_{i,P}}\right|_{e_{i,P}} + \left.\dfrac{\partial\psi_{x,i,R}}{\partial\vec{n}_{i-1,R}}\right|_{e_{i-1,R}} = 0$. In effect, then, j_7 is free. We choose to set $j_7 = 0$, which gives us that $J_{5,i} = 5e_{i,x}$, $J_{6,i} = -5e_{i-1,x}$, and, conveniently, that $J_{7,i} = J_{8,i} = K_{7,i} = K_{8,i} = 0$. Then we

retrieve the following final determinations of the other K coefficients:

$$K_{1,i} = 6\left(e_{i,x} - \frac{C_{i+1}}{C_i}e_{i-1,x} + \frac{C_{i-1}}{C_{i+2}}e_{i+1,x}\right)$$
$$+ 3\frac{C_{i+1}C_{i-1}}{C_iC_{i+2}}\left(\left(12 - 10\frac{|e_{i-1}|}{|e_i|}\cos(\theta_i)\right)e_{i,x} - 3e_{i-1,x}\right);$$

$$K_{2,i} = -\left(6\left(e_{i-1,x} - \frac{C_{i-1}}{C_i}e_{i,x} + \frac{C_{i+1}}{C_{i+2}}e_{i+2,x}\right)\right.$$
$$\left. + 3\frac{C_{i+1}C_{i-1}}{C_iC_{i+2}}\left(\left(12 - 10\frac{|e_i|}{|e_{i-1}|}\cos(\theta_i)\right)e_{i-1,x} - 3e_{i,x}\right)\right);$$

$$K_{3,i} = 5\left(7e_{i,x} + e_{i+1,x} - \frac{C_{i+1}}{C_i}\left(2e_{i-1,x} + 6\frac{|e_{i-1}|}{|e_i|}\cos(\theta_i)e_{i,x}\right)\right.$$
$$\left. - 4\frac{C_{i-1}}{C_{i+2}}e_{i+1,x} - 6\frac{C_{i+1}C_{i-1}}{C_iC_{i+2}}\left(\frac{|e_{i-1}|}{|e_i|}\cos(\theta_i)e_{i,x} + e_{i-1,x}\right)\right);$$

$$K_{4,i} = -5\left(7e_{i-1,x} + e_{i+2,x} - \frac{C_{i-1}}{C_i}\left(2e_{i,x} + 6\frac{|e_i|}{|e_{i-1}|}\cos(\theta_i)e_{i-1,x}\right)\right.$$
$$\left. - 4\frac{C_{i+1}}{C_{i+2}}e_{i+2,x} - 6\frac{C_{i+1}C_{i-1}}{C_iC_{i+2}}\left(\frac{|e_i|}{|e_{i-1}|}\cos(\theta_i)e_{i-1,x} + e_{i,x}\right)\right);$$

$$K_{5,i} = -20e_{i+1,x} - 30\frac{C_{i+1}}{C_i}\left(e_{i-1,x} + \frac{|e_{i-1}|}{|e_i|}\cos(\theta_i)e_{i,x}\right);$$

$$K_{6,i} = 20e_{i+2,x} + 30\frac{C_{i-1}}{C_i}\left(e_{i,x} + \frac{|e_i|}{|e_{i-1}|}\cos(\theta_i)e_{i-1,x}\right).$$

Finally, using the same sum condition (5.1.7), we determine the S and L coefficients:

$$S_{0,i} = 6\left(\left(1 + 5\frac{C_{i+1}C_{i-1}}{C_iC_{i+2}}\right)(e_{i,x} + e_{i+1,x})\right.$$
$$\left. + 5\frac{C_{i+1}C_{i-1}}{C_iC_{i+2}}\left(1 + 2\frac{C_{i+1}C_{i-1}}{C_iC_{i+2}}\right)(e_{i,x} - e_{i-1,x})\right);$$

$$S_{1,i} = 15\left(\left(1 + 2\frac{C_{i+1}C_{i-1}}{C_iC_{i+2}}\right)(3e_{i,x} + 2e_{i+1,x})\right.$$
$$\left. + 2\frac{C_{i+1}C_{i-1}}{C_iC_{i+2}}\left(1 + \frac{C_{i+1}C_{i-1}}{C_iC_{i+2}}\right)(3e_{i,x} - 2e_{i-1,x})\right);$$

$$S_{2,i} = -15\left(\left(1 + 2\frac{C_{i+1}C_{i-1}}{C_iC_{i+2}}\right)(3e_{i-1,x} + 2e_{i+2,x})\right.$$
$$\left. + 2\frac{C_{i+1}C_{i-1}}{C_iC_{i+2}}\left(1 + \frac{C_{i+1}C_{i-1}}{C_iC_{i+2}}\right)(3e_{i-1,x} - 2e_{i,x})\right);$$

$$L_{0,i} = 15\left(\left(1 + 2\frac{C_{i+1}C_{i-1}}{C_iC_{i+2}}\left(4 + 3\frac{C_{i+1}C_{i-1}}{C_iC_{i+2}}\right)\right)(e_{i,x} + e_{i+1,x})\right.$$
$$\left. + 4\frac{C_{i+1}C_{i-1}}{C_iC_{i+2}}\left(1 + \frac{C_{i+1}C_{i-1}}{C_iC_{i+2}}\left(3 + \frac{C_{i+1}C_{i-1}}{C_iC_{i+2}}\right)\right)(e_{i,x} - e_{i-1,x})\right).$$

With this, our construction of $\psi_{x,i}^{(7)}$ is complete. Unfortunately, the expression is so long that we will have to reduce the font size to have it fit on a single page.

$$\psi_{x,i}^{(7)} = \phi_i^2 \bigg(\phi_i^4 (e_{i,x}\phi_{i+1} - e_{i-1,x}\phi_{i-1}) + 6\phi_i^3 (e_{i,x}\phi_{i+1}^2 - e_{i-1,x}\phi_{i-1}^2)$$

$$+ 5\phi_i^2 (e_{i,x}\phi_{i+1}^3 - e_{i-1,x}\phi_{i-1}^3)$$

$$+ \phi_{i+2}\bigg(\bigg(\bigg(1 + 6\frac{C_{i+1}}{C_{i+2}}\bigg)\frac{C_{i-1}}{C_i}e_{i,x} - \bigg(1 + 6\frac{C_{i-1}}{C_{i+2}}\bigg)\frac{C_{i+1}}{C_i}e_{i-1,x} \bigg)\phi_i^4$$

$$+ 3\phi_i^3\bigg(\bigg(2\bigg(e_{i,x} - \frac{C_{i+1}}{C_i}e_{i-1,x} + \frac{C_{i-1}}{C_{i+2}}e_{i+1,x}\bigg)$$

$$+ \frac{C_{i+1}C_{i-1}}{C_iC_{i+2}}\bigg(\bigg(12 - 10\frac{|e_{i-1}|}{|e_i|}\cos(\theta_i)\bigg)e_{i,x} - 3e_{i-1,x}\bigg)\bigg)\phi_{i+1}$$

$$- \bigg(2\bigg(e_{i-1,x} - \frac{C_{i-1}}{C_i}e_{i,x} + \frac{C_{i+1}}{C_{i+2}}e_{i+2,x}\bigg)$$

$$+ \frac{C_{i+1}C_{i-1}}{C_iC_{i+2}}\bigg(\bigg(12 - 10\frac{|e_i|}{|e_{i-1}|}\cos(\theta_i)\bigg)e_{i-1,x} - 3e_{i,x}\bigg)\bigg)\phi_{i-1}\bigg)$$

$$+ 5\phi_i^2\bigg(\bigg(7e_{i,x} + \bigg(1 - 4\frac{C_{i-1}}{C_{i+2}}\bigg)e_{i+1,x} - \frac{C_{i+1}}{C_i}\bigg(2e_{i-1,x} + 6\frac{|e_{i-1}|}{|e_i|}\cos(\theta_i)e_{i,x}\bigg)$$

$$- 6\frac{C_{i+1}C_{i-1}}{C_iC_{i+2}}\bigg(e_{i-1,x} + \frac{|e_{i-1}|}{|e_i|}\cos(\theta_i)e_{i-1,x}\bigg)\bigg)\phi_{i+1}^2$$

$$- \bigg(7e_{i-1,x} + \bigg(1 - 4\frac{C_{i+1}}{C_{i+2}}\bigg)e_{i+2,x} - \frac{C_{i-1}}{C_i}\bigg(2e_{i,x} + 6\frac{|e_i|}{|e_{i-1}|}\cos(\theta_i)e_{i-1,x}\bigg)$$

$$- 6\frac{C_{i+1}C_{i-1}}{C_iC_{i+2}}\bigg(e_{i,x} + \frac{|e_i|}{|e_{i-1}|}\cos(\theta_i)e_{i-1,x}\bigg)\bigg)\phi_{i-1}^2\bigg)$$

$$- 10\phi_i\bigg(\bigg(2e_{i+1,x} + 3\frac{C_{i+1}}{C_i}\bigg(e_{i-1,x} + \frac{|e_{i-1}|}{|e_i|}\cos(\theta_i)e_{i,x}\bigg)\bigg)\phi_{i+1}^3$$

$$- \bigg(2e_{i+2,x} + 3\frac{C_{i-1}}{C_i}\bigg(e_{i,x} + \frac{|e_i|}{|e_{i-1}|}\cos(\theta_i)e_{i-1,x}\bigg)\bigg)\phi_{i-1}^3\bigg)\bigg)$$

$$+ 3\phi_{i+2}^2\bigg(2\bigg(\bigg(1 + 5\frac{C_{i+1}C_{i-1}}{C_iC_{i+2}}\bigg)(e_{i,x} + e_{i+1,x})$$

$$+ 5\frac{C_{i+1}C_{i-1}}{C_iC_{i+2}}\bigg(1 + 2\frac{C_{i+1}C_{i-1}}{C_iC_{i+2}}\bigg)(e_{i,x} - e_{i-1,x})\bigg)\phi_i^3$$

$$+ 5\phi_i^2\bigg(\bigg(\bigg(1 + 2\frac{C_{i+1}C_{i-1}}{C_iC_{i+2}}\bigg)(3e_{i,x} + 2e_{i+1,x})$$

$$+ 2\frac{C_{i+1}C_{i-1}}{C_iC_{i+2}}\bigg(1 + \frac{C_{i+1}C_{i-1}}{C_iC_{i+2}}\bigg)(3e_{i,x} - 2e_{i-1,x})\bigg)\phi_{i+1}$$

$$- \bigg(\bigg(1 + 2\frac{C_{i+1}C_{i-1}}{C_iC_{i+2}}\bigg)(3e_{i-1,x} + 2e_{i+2,x})$$

$$+ 2\frac{C_{i+1}C_{i-1}}{C_iC_{i+2}}\bigg(1 + \frac{C_{i+1}C_{i-1}}{C_iC_{i+2}}\bigg)(3e_{i-1,x} - 2e_{i,x})\bigg)\phi_{i-1}\bigg)\bigg)$$

$$15\bigg(\bigg(1 + 2\frac{C_{i+1}C_{i-1}}{C_iC_{i+2}}\bigg(4 + 3\frac{C_{i+1}C_{i-1}}{C_iC_{i+2}}\bigg)\bigg)(e_{i,x} + e_{i+1,x})$$

$$+ 4\frac{C_{i+1}C_{i-1}}{C_iC_{i+2}}\bigg(1 + \frac{C_{i+1}C_{i-1}}{C_iC_{i+2}}\bigg(3 + \frac{C_{i+1}C_{i-1}}{C_iC_{i+2}}\bigg)\bigg)(e_{i,x} - e_{i-1,x})\bigg)\phi_{i+2}^3\phi_i^2\bigg) \quad (5.1.11)$$

We can retrieve the function $\psi_{y,i}^{(7)}$ by replacing every x in (5.1.11) with y, and we can define the vertex splines $\psi_{x,v}^{(7)}$ and $\psi_{y,v}^{(7)}$ piecewise in Ω_v as usual: for each quadrilateral P in Ω_v, let $\psi_{x,v}^{(7)}\big|_P = \psi_{x,i}^{(7)}$, where $v = v_i$ in P. This section serves as a proof of the following:

Theorem 5.1.2. *Let Ω be a polygonal region in $\mathbb{R}^2$, and let $\mathcal{P}$ be a quadrilateral partition of Ω. For every vertex v in the partition $\mathcal{P}$, define polygonal splines $\psi_{x,v}^{(7)}$ and $\psi_{y,v}^{(7)}$ over Ω_v by*

$$
\psi_{x,v}^{(7)} := \begin{cases} \psi_{x,i,P}^{(7)}(\mathbf{x}) & \mathbf{x} \in P \subseteq \Omega_v; \ v = v_{i,P} \\ 0 & \mathbf{x} \notin \Omega_v \end{cases}
$$

$$
and \ \psi_{y,v}^{(7)} := \begin{cases} \psi_{y,i,P}^{(7)}(\mathbf{x}) & \mathbf{x} \in P \subseteq \Omega_v; \ v = v_{i,P} \\ 0 & \mathbf{x} \notin \Omega_v \end{cases}
$$

where $\psi_{x,i,P}^{(7)}$ is the function given in (5.1.11) and $\psi_{y,i,P}^{(7)}$ is the associated function retrieved by replacing every x in $\psi_{x,i,P}^{(7)}$ by y.

Then $\psi_{x,v}^{(7)}$ and $\psi_{y,v}^{(7)}$ satisfy the following properties:

(1) $\psi_{x,v}^{(7)}(w) = \psi_{y,v}^{(7)}(w) = 0$ for any vertex w of $\mathcal{P}$;

(2) $\nabla\psi_{x,v}^{(7)}(w) = \langle \delta_{v,w}, 0 \rangle$ and $\nabla\psi_{y,v}^{(7)}(w) = \langle 0, \delta_{v,w} \rangle$ for any vertex w of $\mathcal{P}$;

(3) $\nabla^2\psi_{x^2,v}^{(7)}(w) = \nabla^2\psi_{y,v}^{(7)}(w) = 0$ for any vertex w of $\mathcal{P}$;

(4) $\psi_{x,v}^{(7)}, \psi_{y,v}^{(7)} \in C^1(\Omega)$; and

(5) $\sum\limits_{v \in \mathcal{P}} v_x \psi_v^{(7)} + \psi_{x,v}^{(7)} = x$ and $\sum\limits_{v \in \mathcal{P}} v_y \psi_v^{(7)} + \psi_{y,v}^{(7)} = y$.

Figure 5.4 shows the plot of the functions $\psi_{x,v}^{(7)}$ and $\psi_{y,v}^{(7)}$ over the partition shown in Figure 5.2.
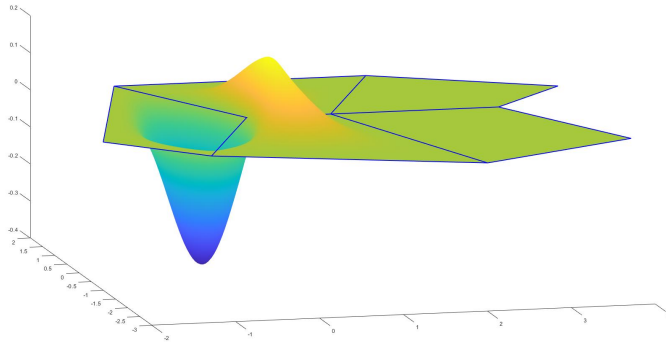
(a) The plot of a function $\psi_{x,v}^{(7)}$
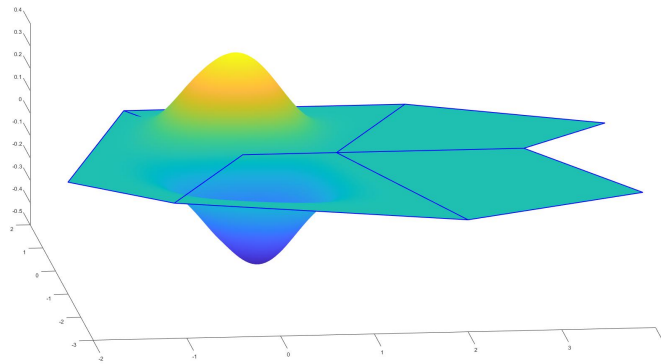
(b) The plot of a function $\psi_{y,v}^{(7)}$

Figure 5.4: Plots of degree-7 gradient-adjustment basis splines

5.1.3   Construction of $\psi_{x^2,v}^{(7)}$, $\psi_{y^2,v}^{(7)}$, and $\psi_{xy,v}^{(7)}$

Frankly, there's not much insight to be gained from the details of these computations which couldn't be gained from the computations in the previous section. The overall flavor and repertoire of techniques are nearly identical, merely applied to a different

set of constraints:

$$\psi^{(7)}_{x^2,v}\big|_w = \psi^{(7)}_{y^2,v}\big|_w = \psi^{(7)}_{xy,v}\big|_w = 0;$$

$$\nabla\psi^{(7)}_{x^2,v}\big|_w = \nabla\psi^{(7)}_{y^2,v}\big|_w = \nabla\psi^{(7)}_{xy,v}\big|_w = 0;$$

$$\nabla^2\psi^{(7)}_{x^2,v}\big|_w = \begin{pmatrix} \delta_{v,w} & 0 \\ 0 & 0 \end{pmatrix}; \quad \nabla^2\psi^{(7)}_{y^2,v}\big|_w = \begin{pmatrix} 0 & 0 \\ 0 & \delta_{v,w} \end{pmatrix}; \quad \nabla^2\psi^{(7)}_{xy,v}\big|_w = \begin{pmatrix} 0 & \delta_{v,w} \\ \delta_{v,w} & 0 \end{pmatrix};$$

along with the sum conditions

$$x^2 = \sum_{j=1}^{4} v_x^2 \psi_v^{(7)} + 2v_x\psi^{(7)}_{x,v} + 2\psi^{(7)}_{x^2,v};$$

$$y^2 = \sum_{j=1}^{4} v_y^2 \psi_v^{(7)} + 2v_y\psi^{(7)}_{y,v} + 2\psi^{(7)}_{y^2,v};$$

$$xy = \sum_{j=1}^{4} v_x v_y \psi_v^{(7)} + v_y\psi^{(7)}_{x,v} + v_x\psi^{(7)}_{y,v} + \psi^{(7)}_{xy,v}.$$

As in the construction of the three degree-5 Hessian manipulation functions, the general strategy is to explicitly construct the function $\psi^{(7)}_{xy,i}$ over a single quadrilateral P, then retrieve the functions $\psi^{(7)}_{x^2,i}$ and $\psi^{(7)}_{y^2,i}$ by replacing each x by y or y by x, respectively, and dividing the result by 2.

To construct $\psi^{(7)}_{xy,i}$, we follow nearly the same steps as in the previous section: we use the template given in (5.1.2), and we set $J_{0,i} = J_{1,i} = J_{2,i} = 0$ to satisfy the value and gradient conditions. We set $J_{3,i} = e_{i,x}e_{i,y}$, $J_{4,i} = e_{i-1,x}e_{i-1,y}$, and $K_{0,i} = -\dfrac{C_{i+1}C_{i-1}}{C_i C_{i+2}}(e_{i,x}e_{i-1,y} + e_{i,y}e_{i-1,x})$ to satisfy the Hessian conditions.

Even with the sum conditions, we still can't quite solve for the remaining J coefficients, but we can reduce the degrees of freedom with some symmetry assumptions - namely, that $J_{5,i} = j_5 e_{i,x}e_{i,y}$, $J_{6,i} = j_5 e_{i-1,x}e_{i-1,y}$, $J_{7,i} = j_7 e_{i,x}e_{i,y}$, and $J_{8,i} = j_7 e_{i-1,x}e_{i-1,y}$ for some constants j_5 and j_7, which the sum conditions tell us must satisfy $j_5 + j_7 = -5$.

From here, we can take outward normal derivatives on edges e_i and e_{i-1}, and follow the same kind of analysis as before, including using the sum condition, to retrieve:

$$J_{5,i} = -5e_{i,x}e_{i,y}; \quad J_{6,i} = -5e_{i-1,x}e_{i-1,y}; \quad J_{7,i} = 0; \quad J_{8,i} = 0;$$

$$K_{1,i} = \frac{C_{i-1}}{C_{i+2}}(e_{i,x}e_{i+1,y} + e_{i,y}e_{i+1,x}) - \frac{C_{i+1}}{C_i}(e_{i,x}e_{i-1,y} + e_{i,y}e_{i-1,x})$$

$$+ \frac{C_{i+1}C_{i-1}}{C_iC_{i+2}}\left(\left(7 - 30\frac{|e_{i-1}|}{|e_i|}\cos(\theta_i)\right)e_{i,x}e_{i,y} - 4(e_{i,x}e_{i-1,y} + e_{i,y}e_{i-1,x})\right);$$

$$K_{2,i} = \frac{C_{i+1}}{C_{i+2}}(e_{i-1,x}e_{i+2,y} + e_{i-1,y}e_{i+2,x}) - \frac{C_{i-1}}{C_i}(e_{i,x}e_{i-1,y} + e_{i,y}e_{i-1,x})$$

$$+ \frac{C_{i+1}C_{i-1}}{C_iC_{i+2}}\left(\left(7 - 30\frac{|e_i|}{|e_{i-1}|}\cos(\theta_i)\right)e_{i-1,x}e_{i-1,y} - 4(e_{i,x}e_{i-1,y} + e_{i,y}e_{i-1,x})\right);$$

$$K_{3,i} = 7e_{i,x}e_{i,y} + (e_{i,x}e_{i+1,y} + e_{i,y}e_{i+1,x}) + 22\frac{C_{i-1}}{C_{i+2}}\frac{|e_{i+1}|}{|e_i|}\cos(\theta_{i+1})e_{i,x}e_{i,y}$$

$$- \frac{C_{i+1}}{C_i}\left(4(e_{i,x}e_{i-1,y} + e_{i,y}e_{i-1,x}) + 30\frac{|e_{i-1}|}{|e_i|}\cos(\theta_i)e_{i,x}e_{i,y}\right)$$

$$- 42\frac{C_{i+1}C_{i-1}}{C_iC_{i+2}}\left(1 - \frac{|e_{i-1}|}{|e_i|}\cos(\theta_i)\right)e_{i,x}e_{i,y};$$

$$K_{4,i} = 7e_{i-1,x}e_{i-1,y} + (e_{i-1,x}e_{i+2,y} + e_{i-1,y}e_{i+2,x}) + 22\frac{C_{i+1}}{C_{i+2}}\frac{|e_{i+2}|}{|e_{i-1}|}\cos(\theta_{i-1})e_{i-1,x}e_{i-1,y}$$

$$- \frac{C_{i-1}}{C_i}\left(4(e_{i,x}e_{i-1,y} + e_{i,y}e_{i-1,x}) + 30\frac{|e_i|}{|e_{i-1}|}\cos(\theta_i)e_{i-1,x}e_{i-1,y}\right)$$

$$- 42\frac{C_{i+1}C_{i-1}}{C_iC_{i+2}}\left(1 - \frac{|e_i|}{|e_{i-1}|}\cos(\theta_i)\right)e_{i-1,x}e_{i-1,y};$$

160

$$K_{5,i} = -20\frac{|e_{i+1}|}{|e_i|}\cos(\theta_{i+1})e_{i,x}e_{i,y}; \quad K_{6,i} = -20\frac{|e_{i+2}|}{|e_{i-1}|}\cos(\theta_{i-1})e_{i-1,x}e_{i-1,y};$$

$$K_{7,i} = 0; \quad K_{8,i} = 0;$$

$$S_{0,i} = (e_{i,x} + e_{i+1,x})(e_{i,y} + e_{i+1,y}) + 5\frac{C_{i+1}C_{i-1}}{C_iC_{i+2}}\bigg((e_{i,x} - e_{i-1,x})(e_{i,y} + e_{i+1,y})$$

$$+ (e_{i,y} - e_{i-1,y})(e_{i,x} + e_{i+1,x}) - (e_{i,x}e_{i-1,y} + e_{i,y}e_{i-1,x})$$

$$+ 2\frac{C_{i+1}C_{i-1}}{C_iC_{i+2}}\bigg((e_{i,x} - e_{i-1,x})(e_{i,y} - e_{i-1,y}) - (e_{i,x}e_{i-1,y} + e_{i,y}e_{i-1,x})\bigg)\bigg);$$

$$S_{1,i} = 5\bigg(3e_{i,x}e_{i,y} + e_{i+1,x}e_{i+1,y} + 2(e_{i,x}e_{i+1,y} + e_{i,y}e_{i+1,y})$$

$$+ 2\frac{C_{i+1}C_{i-1}}{C_iC_{i+2}}\bigg(2(3e_{i,x}e_{i,y} + e_{i,x}(e_{i+1,y} - e_{i-1,y}) + e_{i,y}(e_{i+1,x} - e_{i-1,x}))$$

$$- (e_{i-1,x}(e_{i,y} + e_{i+1,y}) + e_{i-1,y}(e_{i,x} + e_{i+1,x}))$$

$$+ \frac{C_{i+1}C_{i-1}}{C_iC_{i+2}}(e_{i-1,x}e_{i-1,y} + 3(e_{i,x}e_{i,y} - (e_{i,x}e_{i-1,y} + e_{i,y}e_{i-1,y})))\bigg)\bigg);$$

$$S_{2,i} = 5\bigg(3e_{i-1,x}e_{i-1,y} + e_{i+2,x}e_{i+2,y} + 2(e_{i-1,x}e_{i+2,y} + e_{i-1,y}e_{i+2,x})$$

$$+ 2\frac{C_{i+1}C_{i-1}}{C_iC_{i+2}}\bigg(2(3e_{i-1,x}e_{i-1,y} + e_{i-1,x}(e_{i+2,y} - e_{i,y}) + e_{i-1,y}(e_{i+2,x} - e_{i,x}))$$

$$- (e_{i,x}(e_{i-1,y} + e_{i+2,y}) + e_{i,y}(e_{i-1,x} + e_{i+2,x}))$$

$$+ \frac{C_{i+1}C_{i-1}}{C_iC_{i+2}}(e_{i,x}e_{i,y} + 3(e_{i-1,x}e_{i-1,y} - (e_{i,x}e_{i-1,y} + e_{i,y}e_{i-1,x})))\bigg)\bigg);$$

$$L_{0,i} = 5\bigg((e_{i,x} + e_{i+1,x})(e_{i,y} + e_{i+1,y}) + 2\frac{C_{i+1}C_{i-1}}{C_iC_{i+2}}\bigg(6e_{i,x}e_{i,y} + 2e_{i+1,x}e_{i+1,y}$$

$$+ 4(e_{i,x}e_{i+1,y} + e_{i,y}e_{i+1,x}) - (e_{i-1,x}(3e_{i,y} + 2e_{i+1,y}) + e_{i-1,y}(3e_{i,x} + e_{i+1,x}))$$

$$+ \frac{C_{i+1}C_{i-1}}{C_iC_{i+2}}\bigg(3(3e_{i,x}e_{i,y} + e_{i-1,x}e_{i-1,y} + (e_{i,x}e_{i+1,y} + e_{i,y}e_{i+1,x})$$

$$- (e_{i-1,x}(3e_{i,y} + e_{i+1,y}) + e_{i-1,y}(3e_{i,x} + e_{i+1,x})))$$

$$+ \frac{C_{i+1}C_{i-1}}{C_iC_{i+2}}(2(e_{i,x}e_{i,y} + e_{i-1,x}e_{i-1,y}) - 3(e_{i,x}e_{i-1,y} + e_{i,y}e_{i-1,x}))\bigg)\bigg)\bigg).$$

There is no point in listing the full expression of the function $\psi_{xy,i}^{(7)}$. It is long enough that it would either span multiple pages, or we would have to reduce the font size so far as to be unreadable.

We define $\psi_{x^2,i}^{(7)}$ and $\psi_{y^2,i}^{(7)}$ by the aforementioned substitutions, and then define the polygonal vertex splines $\psi_{x^2,v}^{(7)}$, $\psi_{y^2,v}^{(7)}$, and $\psi_{xy,v}^{(7)}$ piecewise over Ω_v as usual. The chapter thus far serves as a proof of the following:

Theorem 5.1.3. *Let Ω be a polygonal region in $\mathbb{R}^2$, and let $\mathcal{P}$ be a partition of Ω by quadrilaterals. For every vertex v in the partition $\mathcal{P}$, define polygonal splines $\psi_{x^2,v}^{(7)}$, $\psi_{y^2,v}^{(7)}$, and $\psi_{xy,v}^{(7)}$ over Ω_v by*

$$
\psi_{x^2,v}^{(7)} := \begin{cases} \psi_{x^2,i,P}^{(7)}(\mathbf{x}) & \mathbf{x} \in P \subseteq \Omega_v; \ v = v_{i,P} \\ 0 & \mathbf{x} \notin \Omega_v, \end{cases}
$$

$$
\psi_{y^2,v}^{(7)} := \begin{cases} \psi_{y^2,i,P}^{(7)}(\mathbf{x}) & \mathbf{x} \in P \subseteq \Omega_v; \ v = v_{i,P} \\ 0 & \mathbf{x} \notin \Omega_v, \end{cases}
$$

$$
\psi_{xy,v}^{(7)} := \begin{cases} \psi_{x^2,i,P}^{(7)}(\mathbf{x}) & \mathbf{x} \in P \subseteq \Omega_v; \ v = v_{i,P} \\ 0 & \mathbf{x} \notin \Omega_v, \end{cases}
$$

where $\psi_{xy,i,P}^{(7)}$ is the function which follows the template given in (5.1.2) with the coefficients given in this section, $\psi_{x^2,i,P}^{(7)}$ is the function retrieved by replacing every y in $\psi_{xy,i,P}^{(7)}$ by x and then multiplying by $\frac{1}{2}$, and $\psi_{y^2,i,P}^{(7)}$ is the function retrieved by replacing every x in $\psi_{xy,i,P}^{(7)}$ by y and then multiplying by $\frac{1}{2}$.

Then $\psi_{x^2,v}^{(7)}$, $\psi_{y^2,v}^{(7)}$, and $\psi_{xy,v}^{(7)}$ satisfy the following properties:

(1) $\psi_{x^2,v}^{(7)}(w) = \psi_{y^2,v}^{(7)}(w) = \psi_{xy,v}^{(7)}(w) = 0$ *for any vertex w of $\mathcal{P}$;*

(2) $\nabla\psi_{x^2,v}^{(7)}(w) = \nabla\psi_{y^2,v}^{(7)}(w) = \nabla\psi_{xy,v}^{(7)}(w) = 0$ *for any vertex w of $\mathcal{P}$;*

(3) $\nabla^2\psi_{x^2,v}^{(7)}(w) = \begin{pmatrix} \delta_{v,w} & 0 \\ 0 & 0 \end{pmatrix}$, $\nabla^2\psi_{y^2,v}^{(7)}(w) = \begin{pmatrix} 0 & 0 \\ 0 & \delta_{v,w} \end{pmatrix}$,

and $\nabla^2\psi_{xy,v}^{(7)}(w) = \begin{pmatrix} 0 & \delta_{v,w} \\ \delta_{v,w} & 0 \end{pmatrix}$ *for any vertex w of $\mathcal{P}$;*

(4) $\psi_{x^2,v}^{(7)}, \psi_{y^2,v}^{(7)}, \psi_{xy,v}^{(7)} \in C^1(\Omega)$;

(5) $\sum\limits_{v\in\mathcal{P}} v_x^2\psi_v^{(7)}+2v_x\psi_{x,v}^{(7)}+2\psi_{x^2,v}^{(7)} = x^2, \ \sum\limits_{v\in\mathcal{P}} v_y^2\psi_v^{(7)}+2v_y\psi_{y,v}^{(7)}+2\psi_{y^2,v}^{(7)} = y^2, \ \sum\limits_{v\in\mathcal{P}} v_xv_y\psi_v^{(7)}+$
$v_y\psi_{x,v}^{(7)} + v_x\psi_{y,v}^{(7)} + \psi_{xy,v}^{(7)} = xy$;

(6) Where $\Psi_{7,V}^1(\mathcal{P}) := span\left\{\psi_v^{(7)}, \psi_{x,v}^{(7)}, \psi_{y,v}^{(7)}, \psi_{x^2,v}^{(7)}, \psi_{y^2,v}^{(7)}, \psi_{xy,v}^{(7)}\right\}_{v\in\mathcal{P}}$,
$dim(\Psi_{7,V}^1(\mathcal{P})) = 6|V|$;

(7) $\Pi_2 \subseteq \Psi_{7,V}^1(\mathcal{P})$.

Figure 5.5 shows plots of all three of these functions.
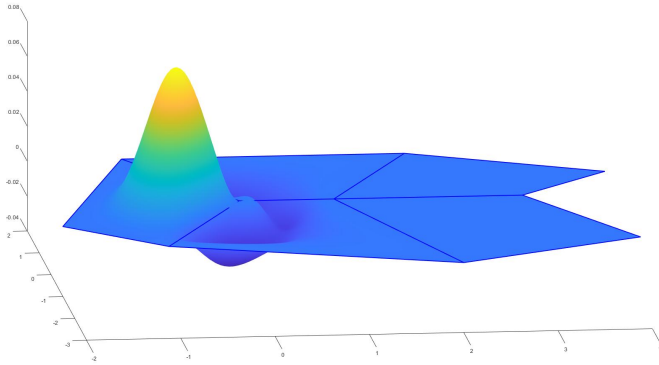
(a) The plot of a function $\psi_{x^2,v}^{(7)}$
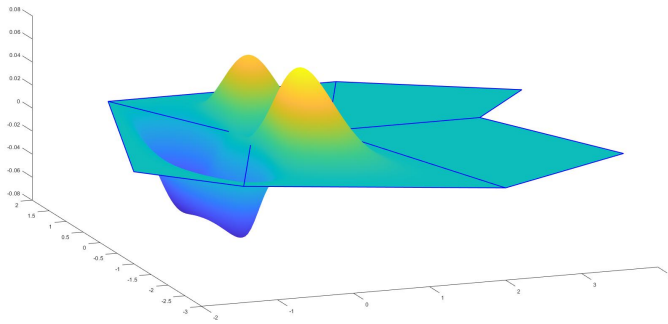
(b) The plot of a function $\psi_{y^2,v}^{(7)}$
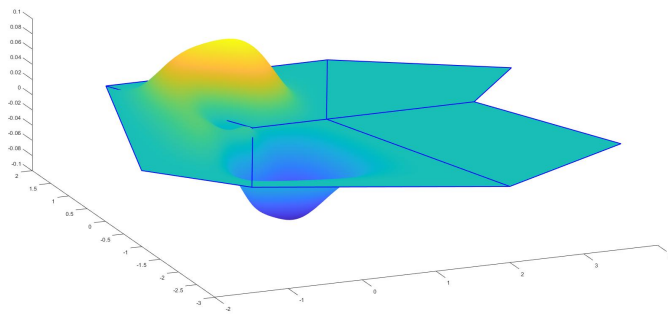
(c) The plot of a function $\psi_{xy,v}^{(7)}$

Figure 5.5: Plots of degree-7 Hessian-adjustment basis splines

5.2 Approximation properties and numerical results

As usual, let Ω be a polygonal region in $\mathbb{R}^2$ and let $\mathcal{P}$ be a partition of Ω by convex quadrilaterals. We (slightly abusively) reuse the notation $Q_V(f)$ in this section to mean the degree-7 quasi-interpolatory C^1 polygonal vertex spline given by

$$Q_V(f) = \sum_{v \in \mathcal{P}} f\big|_v \psi_v^{(7)} + \frac{\partial f}{\partial x}\bigg|_v \psi_{x,v}^{(7)} + \frac{\partial f}{\partial y}\bigg|_v \psi_{y,v}^{(7)}$$
$$+ \frac{\partial^2 f}{\partial x^2}\bigg|_v \psi_{x^2,v}^{(7)} + \frac{\partial^2 f}{\partial x \partial y}\bigg|_v \psi_{xy,v}^{(7)} + \frac{\partial^2 f}{\partial y^2}\bigg|_v \psi_{y^2,v}^{(7)}.$$

Using the notation and techniques referenced in Chapter 3 Section 3.3 and Chapter 4 Section 4.3, we can show the following result on the approximation power of degree-7 C^1 polygonal vertex splines:

Theorem 5.2.1. *For any function $f \in C^3(\Omega)$, the quasi-interpolatory C^1 polygonal vertex spline $Q_{V,k}(f) \in \Psi_{7,V}^1(\mathcal{P}_k)$ satisfies*

$$||f - Q_{V,k}(f)||_{\infty,\Omega} \le C|f|_{3,\infty,\Omega} 2^{-3k}$$

where C is a positive constant independent of f.

For any function $u \in H^3(\Omega)$, the quasi-interpolatory C^1 polygonal vertex spline $Q_{V,k}(u) \in \Psi_{7,V}(\mathcal{P}_k)$ satisfies

$$||u - Q_{V,k}(u)||_{2,\Omega} \le C|u|_{3,2,\Omega} 2^{-3k}$$

and

$$|u - Q_{V,k}|_{1,2,\Omega} \le C|u|_{3,2,\Omega} 2^{-2k}$$

where C is a positive constant independent of u, but which may depend on the bound-

ary of Ω if Ω is nonconvex.

We devote the rest of this section to numerical examples of quasi-interpolation by degree-7 C^1 polygonal vertex splines developed in this chapter. Let $\mathcal{P}$ be the quadrilateral partition shown in Figure 5.2, and see the notation in Chapter 4 Section 4.3. We expect that the quasi-interpolants should converge in the L^2 norm at rate $O(h^3)$.

We display the numerical error of the quasi-interpolants of the same functions as in Chapter 4 Section 4.3; for convenience, we restate the functions below:

$$u_1(x, y) = \sin(x)\sin(y), \qquad u_2(x, y) = \sin(\pi x)\sin(\pi y),$$

$$u_3(x, y) = \sin(2\pi x)\sin(2\pi y), \qquad u_4(x, y) = \sin(\pi(x^2 + y^2)),$$

$$u_5(x, y) = (10 + x + y)^{-1}, \qquad u_6(x, y) = (1 + x^2 + y^2)^{-1}.$$

Table 5.1: Degree-7 C^1 polygonal vertex spline quasi-interpolation of the function $u_1(x, y) = \sin(x)\sin(y)$

# Quads	h	$E_V(u_1)$	rate
5	2.00e+00	7.41e-03	0.00
20	1.44e+00	8.74e-04	3.08
80	7.21e-01	1.01e-04	3.11
320	3.61e-01	1.21e-05	3.06

Table 5.2: Degree-7 C^1 polygonal vertex spline quasi-interpolation of the function $u_2(x, y) = \sin(\pi x)\sin(\pi y)$

# Quads	h	$E_V(u_2)$	rate
5	2.00e+00	2.67e-01	0.00
20	1.44e+00	4.11e-02	2.70
80	7.21e-01	4.18e-03	3.30
320	3.61e-01	4.33e-04	3.27

Table 5.3: Degree-7 C^1 polygonal vertex spline quasi-interpolation of the function $u_3(x, y) = \sin(2\pi x)\sin(2\pi y)$

# Quads	h	$E_V(u_3)$	rate
5	2.00e+00	1.28e+00	0.00
20	1.44e+00	3.90e-01	1.72
80	7.21e-01	3.31e-02	3.56
320	3.61e-01	4.12e-03	3.00

Table 5.4: Degree-7 C^1 polygonal vertex spline quasi-interpolation of the function $u_4(x, y) = \sin(\pi(x^2 + y^2))$

# Quads	h	$E_V(u_4)$	rate
5	2.00e+00	2.39e+00	0.00
20	1.44e+00	4.71e-01	2.34
80	7.21e-01	5.71e-02	3.04
320	3.61e-01	4.98e-03	3.52

Table 5.5: Degree-7 C^1 polygonal vertex spline quasi-interpolation of the function $u_5(x, y) = (10 + x + y)^{-1}$

# Quads	h	$E_V(u_5)$	rate
5	2.00e+00	6.75e-06	0.00
20	1.44e+00	7.96e-07	3.08
80	7.21e-01	9.58e-08	3.05
320	3.61e-01	1.19e-08	3.01

Table 5.6: Degree-7 C^1 polygonal vertex spline quasi-interpolation of the function $u_6(x, y) = (1 + x^2 + y^2)^{-1}$

# Quads	h	$E_V(u_6)$	rate
5	2.00e+00	1.97e-02	0.00
20	1.44e+00	3.16e-03	2.64
80	7.21e-01	2.93e-04	3.43
320	3.61e-01	3.10e-05	3.24

As in the degree-5 cases, we see that, after achieving a sufficiently fine mesh, we observe the expected rate of convergence.

Chapter 6

Future Directions

6.1   More general polygons

The original aim for this work was to find a way to ensure smoothness for polygonal splines *in general*, but even restriction to quadrilaterals has been computationally intensive. Moving up to pentagons brings the primary challenge of determining linear independence of terms which vanish on edges. By Theorem 1 in [16], the number of linearly independent degree-2 Bernstein-Bezier functions of Wachspress coordinates on an n-gon is $2n + \binom{n-2}{2}$. There are $2n$ functions supported on the edge, so on the interior there are $\binom{n-2}{2}$ degrees of freedom; on a quadrilateral ($n = 4$), this gives us only one degree of freedom, which corresponds to the fact that $\phi_1\phi_3 = \dfrac{C_1C_3}{C_2C_4}\phi_2\phi_4$. However, on a pentagon ($n = 5$), we instead have 3 degrees of freedom - but there are 5 degree-2 Bernstein-Bezier functions which are zero on the boundary: $\phi_1\phi_3, \phi_1\phi_4, \phi_2\phi_4, \phi_2\phi_5$, and $\phi_3\phi_5$. In the same way that we used $\phi_1\phi_3$ and $\phi_2\phi_4$ interchangeably, it seems that the best strategy to construct C^1 vertex splines would be to choose a certain triple of these functions for each vertex, but it's not immediately clear if there is any advantage to any of them. Moreover, when moving up to degree 3, there are 20 Bernstein-Bezier functions which vanish on the boundary

of a pentagon. It is not clear how many of these can be chosen linearly independently, and at first glance it is perhaps even less clear how to choose them.

If the issue of linear independence was resolved, then the techniques used to determine C^1 local basis polygonal splines over quadrilaterals should be able to be extended to other polygonal partitions.

6.2   Higher smoothness

Higher smoothness could be desirable, and the techniques discussed in this work should suffice to construct C^r local basis polygonal splines over quadrilaterals at least. The primary issue in this direction is computational complexity: the computations done in this work were already extremely complex and cumbersome, but C^2 computations on the edges would obviously be much harder. First and foremost, while we only needed to compute one outward normal derivative per edge, $\dfrac{\partial}{\partial \vec{n}_i}$, to ensure C^1 smoothness, we would need to compute both $\dfrac{\partial^2}{\partial \vec{n}_i^2}$ and $\dfrac{\partial^2}{\partial \vec{n}_i \partial \tilde{e}_i}$ to ensure C^2 smoothness, both of which would be *extremely* cumbersome and lengthy.

6.3   Coefficient conditions

The derivation of coefficient conditions for varying levels of smoothness in traditional bivariate splines over triangles has allowed for development and successful implementation of arbitrarily smooth functions over triangulations. These conditions allow for construction of a smoothness matrix which can directly enforce a predetermined level of smoothness, and for anything higher than C^1-smoothness I think that finding similar coefficient conditions for polygonal splines is the right strategy. Implementing this over arbitrary polygonal partitions will still require some analysis of linear independence; for this reason, I think the primary task which should be accomplished

in order to extend polygonal splines further is to construct a "correct" basis for the span of the Bernstein-Bezier functions.

Bibliography

[1] L. B. ao da Veiga, K. Lipnikov, and G. Manzini. Arbitrary-order nodal mimetic discretizations of elliptic problems on polygonal meshes. *SIAM Journal on Numerical Analysis*, 49:1737–1760, 2011.

[2] G. Awanou, M.-J. Lai, and P. Wenston. The multivariate spline method for scattered data fitting and numerical solution of partial differential equations. In *Wavelets and Splines: Athens*, pages 24–74, 2006.

[3] L. Beirão da Veiga and G. Manzini. A virtual element method with arbitrary regularity. *IMA Journal of Numerical Analysis*, 34:759–781, 2014.

[4] L. Beirão da Veiga, F. Brezzi, A. Cangiani, G. Manzini, L. Marini, and A. Russo. Basic principles of virtual element methods. *Mathematical Models and Methods in Applied Sciences*, 23, 2013.

[5] K. Bey and J. Oden. hp-version discontinuous galerkin methods for hyperbolic conservation laws. *Computer Methods in Applied Mechanics and Engineering*, 133:259–286, 1996.

[6] D. Braess. *Finite elements*. Cambridge University Press, 1997.

[7] S. Brennet and L. Scott. *The mathematical theory of finite element methods*. Springer, 1994.

[8] T. J. Cashman, U. H. Augsdörfer, N. A. Dodgson, and M. A. Sabin. Nurbs with extraordinary points: high-degree, non-uniform, rational subdivision schemes. *ACM Transactions on Graphics*, 28, 2009.

[9] E. Catmull and J. Clark. Recursively generated b-spline surfaces on arbitrary topological meshes. *Computer-Aided Design*, 10:350–355, 1978.

[10] P. Ciarlet. *The finite element method for elliptic problems*. North-Holland, 1978.

[11] R. Courant, K. Friedrichs, and H. Lewy. Über die partiellen differenzengleichungen der mathematischen physik. *Mathematische Annalen*, 1928.

[12] L. Evans. *Partial differential equations*. American Math. Society, 1998.

[13] M. Floater. Generalized barycentric coordinates and applications. *Acta Numerica*, 24:161–214, 2015.

[14] M. Floater. The inverse of a rational bilinear mapping. *Comp. Aided Geom. Design*, 33:46–50, 2015.

[15] M. Floater, A. Gillette, and N. Sukumar. Gradient bounds for wachspress coordinates on polytopes. *SIAM Journal of Numerical Analysis*, 52:515–532, 2014.

[16] M. Floater and M.-J. Lai. Polygonal spline spaces and the numerical solution of the poisson equation. *SIAM Journal of Numerical Analysis*, 54:797–824, 2016.

[17] P. Grisvard. *Elliptic problems in nonsmooth domains*. Pitman Advanced Pub. Program, 1985.

[18] P. Houston, C. Schwab, and E. Suli. Stabilized hp-finite element methods for first-order hyperbolic problems. *SIAM J. Numerical Analysis*, 37:1618–1643, 2000.

[19] P. Houston, C. Schwab, and E. Suli. Discontinuous hp-finite element methods for advection-diffusion problems. *SIAM J. Numerical Analysis*, 39:2133–2163, 2002.

[20] M.-J. Lai and L. Schumaker. *Spline functions over triangulations*. Cambridge University Press, 2007.

[21] G. Manzini, A. Russo, and N. Sukumar. New perspectives on polygonal and polyhedral finite element methods. *Math. Models Methods Appl. Sci*, 24:1665–1699, 2014.

[22] L. Mu, J. Wang, Y. Wang, and X. Ye. A computational study of the weak galerkin method for second-order elliptic equations. *Numerical Algorithms*, 63:753–777, 2013.

[23] L. Mu, J. Wang, and X. Ye. Weak galerkin finite element methods on polytopal meshes. *International Journal of Numerical Analysis*, 12:31–53, 2015.

[24] H. Prautzsch. Smoothness of subdivision surfaces at extraordinary points. *Advances in Computational Mathematics*, 9:377–389, 1998.

[25] A. Rand, A. Gillette, and C. Bajaj. Quadratic serendipity finite elements on polygons using generalized barycentric coordinates. *Mathematics of computation*, 83:2691–2716, 2014.

[26] T. W. Sederberg, G. T. Finnigan, X. Li, H. Lin, and H. Ipson. Watertight trimmed nurbs. *ACM Transactions on Graphics*, 27, 2008.

[27] T. W. Sederberg, J. Zheng, A. Bakenov, and A. Nasri. T-splines and t-nurccs. *ACM Transactions on Graphics*, 22, 2003.

[28] E. Stein. *Singular integrals and differentiability properties of functions*. Princeton University Press, 1970.

[29] V. Thomée. From finite difference to finite elements: A short history of numerical analysis of partial differential equations. *J. Comp. Appl. Math.*, 128:1–54, 2001.

[30] J. Wang and X. Ye. A weak galerkin finite element method for second-order elliptic problems. *J. Comp. Appl. Math.*, 241:103–115, 2013.

[31] J. Wang and X. Ye. A weak galerkin finite element method for the stokes equations. *Advances in Computational Mathematics*, 42:155–174, 2016.